Vol. 60 JANUARY, 1956 No. 1

THE JOURNAL OF PHYSICAL CHEMISTRY

(Registered in U. S. Patent Office)

THE JOURNAL OF PHYSICAL CHEMISTRY

(Registered in U. S. Patent Office)

Published monthly by the American Chemical Society at 20th and Northampton Sts., Easton, Pa.

Entered as second-class matter at the Post Office at Easton, Pennsylvania.

The *Journal of Physical Chemistry* is devoted to the publication of selected symposia in the broad field of physical chemistry and to other contributed papers.

Manuscripts originating in the British Isles, Europe and Africa should be sent to F. C. Tompkins, The Faraday Society, 6 Gray's Inn Square, London W. C. 1, England.

Manuscripts originating elsewhere should be sent to W. Albert Noyes, Jr., Department of Chemistry, University of Rochester, Rochester 3, N. Y.

Correspondence regarding accepted copy, proofs and reprints should be directed to Assistant Editor, Allen D. Bliss, Department of Chemistry, Simmons College, 300 The Fenway, Boston 15, Mass.

Business Office: Alden H. Emery, Executive Secretary, American Chemical Society, 1155 Sixteenth St., N. W., Washington 6, D. C.

Advertising Office: Reinhold Publishing Corporation, 430 Park Avenue, New York 22, N. Y.

Articles must be submitted in duplicate, typed and double spaced. They should have at the beginning a brief Abstract, in no case exceeding 300 words. Original drawings should accompany the manuscript. Lettering at the sides of graphs (black on white or blue) may be pencilled in, and will be typeset. Figures and tables should be held to a minimum consistent with adequate presentation of information. Photographs will not be printed on glossy paper except by special arrangement. All footnotes and references to the literature should be numbered consecutively and placed in the manuscript at the proper places. Initials of authors referred to in citations should be given. Nomenclature should conform to that used in *Chemical Abstracts*, mathematical characters marked for italic, Greek letters carefully made or annotated, and subscripts and superscripts clearly shown. Articles should be written as briefly as possible consistent with clarity and should avoid historical background unnecessary for specialists.

Symposium papers should be sent in all cases to Secretaries of Divisions sponsoring the symposium, who will be responsible for their transmittal to the Editor. The Secretary of the Division by agreement with the Editor will specify a time after which symposium papers cannot be accepted. The Editor reserves the right to refuse to publish symposium articles, for valid scientific reasons. Each symposium paper may not exceed four printed pages (about sixteen double spaced typewritten pages) in length except by prior arrangement with the Editor.

Remittances and orders for subscriptions and for single copies, notices of changes of address and new professional connections, and claims for missing numbers should be sent to the American Chemical Society, 1155 Sixteenth St., N. W., Washington 6, D. C. Changes of address for the *Journal of Physical Chemistry* must be received on or before the 30th of the preceding month.

Claims for missing numbers will not be allowed (1) if received more than sixty days from date of issue (because of delivery hazards, no claims can be honored from subscribers in Central Europe, Asia, or Pacific Islands other than Hawaii), (2) if loss was due to failure of notice of change of address to be received before the date specified in the preceding paragraph, or (3) if the reason for the claim is "missing from files."

Subscription Rates (1956): members of American Chemical Society, $8.00 for 1 year; to non-members, $10.00 for 1 year. Postage free to countries in the Pan American Union; Canada, $0.40; all other countries, $1.20. $12.50 per volume, foreign postage $1.20, Canadian postage $0.40; special rates for A.C.S. members supplied on request. Single copies, current volume, $1.35; foreign postage, $0.15; Canadian postage $0.05. Back issue rates (starting with Vol. 56): $15.00 per volume, foreign postage $1.20, Canadian, $0.40; $1.50 per issue, foreign postage $0.15, Canadian postage $0.05.

The American Chemical Society and the Editors of the *Journal of Physical Chemistry* assume no responsibility for the statements and opinions advanced by contributors to This Journal.

The American Chemical Society also publishes *Journal of the American Chemical Society*, *Chemical Abstracts*, *Industrial and Engineering Chemistry*, *Chemical and Engineering News*, *Analytical Chemistry*, and *Journal of Agricultural and Food Chemistry*. Rates on request.

(Continued from first page of cover)

THE JOURNAL OF PHYSICAL CHEMISTRY

(Registered in U. S. Patent Office) (© Copyright, 1956, by the American Chemical Society)

VOLUME 60 JANUARY 20, 1956 NUMBER 1

THE UREA–HYDROCARBON ADDUCTS

BY P. H. CALDERBANK AND N. S. NIKOLOV

Department of Chemical Engineering, University of Toronto, Toronto, Canada

Received February 28, 1955

Three-component phase diagrams were constructed for complexes involving urea, straight and branched chain hydrocarbons and urea solvents. These diagrams confirmed the compositions previously reported for the adducts involved. They also showed that in some cases complete separation of straight and branched chain hydrocarbons is not possible. In addition it was found that the solvent for urea (water or methanol) has no other function than that of precipitating solid urea (when its solubility is lowered by mutual solvent action or decrease in temperature). The same separation is achieved when solid urea equal in amount to that precipitated from solution is used in the absence of solvent.

These facts indicated that adduct formation is a two-phase interaction involving solid urea.

Experiments with solid urea showed that adduct formation was observable only when the particle size was less than a certain critical value. This is due to the fact that a heat of adsorption is necessary to supply the energy for the transition from tetragonal to hexagonal solid urea. After the transition, diffusion of straight chain hydrocarbon into the crystal lattice occurs at measurable rates. The rate of this process was found to obey the normal laws of diffusion, and a value of the diffusivity of *n*-octane into urea is reported. From calorimetric measurements, some observations were made concerning the several energetic steps involved in adduct formation.

Introduction

Previous work on the urea adducts is almost entirely due to Schlenk[1] who showed from X-ray diagrams that the normal tetragonal urea crystal is transformed into a hexagonal structure in the presence of straight chain hydrocarbons and some of their derivatives. Such straight chain hydrocarbons penetrate the hexagonal structure and are imprisoned therein. Branched chain or other bulky molecules cannot enter the solid structure for spacial reasons and thus a means is afforded for separating molecules differing only in shape.

The practical application of this principle to industrially important separations has been discussed in a number of places.[2]

The work described here is an analysis of the phenomenon by means of the phase rule and calorimetric measurements.

Three-component Phase Diagrams Involving the Urea Adduct.—Urea adduct separations have generally been performed by adding a saturated solution of urea in water or methanol to the mixture of hydrocarbons. The adduct of the straight chain hydrocarbon component precipitates from the mixture on cooling in the case of water as solvent or as a result of the reduced solubility for urea of hydrocarbon–methanol solutions as compared to methanol alone.

In order to elucidate the function of the solvent, three-component equilibrium phase diagrams were constructed for complexes involving solvent, one hydrocarbon and urea as well as for two hydrocarbons (one branched chain, one straight) and solid urea.

The diagrams were prepared by a combination of wet-residue, synthetic complex and cloud-point methods where they proved most convenient. Urea was analyzed for by the "urease" method and mixtures of two hydrocarbons by their refractive indices.

Synthetic complexes were made up by weighing into a large test-tube which was subsequently placed in a thermostat and agitated for two hours before sampling. Frequent checks established that adequate time was allowed for equilibrium to be established. The phases were then allowed to separate and the supernatant liquid was removed for analysis by suction through a micro-filter stick. The wet residue was also analyzed as a check on the results obtained. Ternary solutions were extracted with water prior to analysis.

Figures 1 to 6 show some of the results obtained,

(1) W. Schlenk, Jr., *Ann. Chem.*, **565**, 204 (1949); *Angew. Chem.*, **62**, 299 (1950); *Experientia*, **6**, 292 (1950); *Ann. Chem.*, **573**, 142 (1951); C. Hermann and H. V. Lenne, *Naturwissenschaften*, **39**, 234 (1952).

(2) O. Redlich, C. M. Gable, A. K. Dunlop and R. W. Millar, *J. Am. Chem. Soc.*, **72**, 4153 (1950); E. V. Tatter, *Research (London)*, **6**, 320 (1953); D. Swern, *Ind. Eng. Chem.*, **47**, 216 (1955).

in which the axes represent weight proportions of the three components. Synthetic complex compositions are shown by open circles. In Figs. 1 to 4, two open circles appearing on a common tie-line indicate the two synthetic complexes of widely different composition which were made up and which should, if the accepted adduct composition were correct, give the same weight proportions in the mother liquor of the two immiscible liquid phases in equilibrium with the adduct.

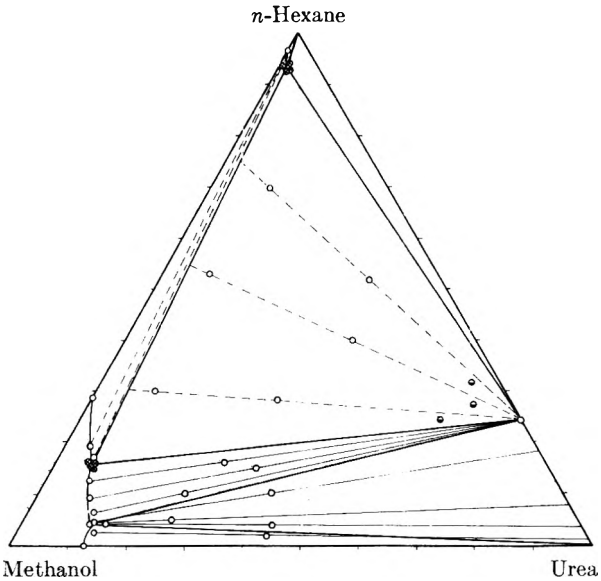

Fig. 1.—Urea–*n*-hexane–methanol system at 25°: ⊗, liquid phase composition; ◒, wet residue.

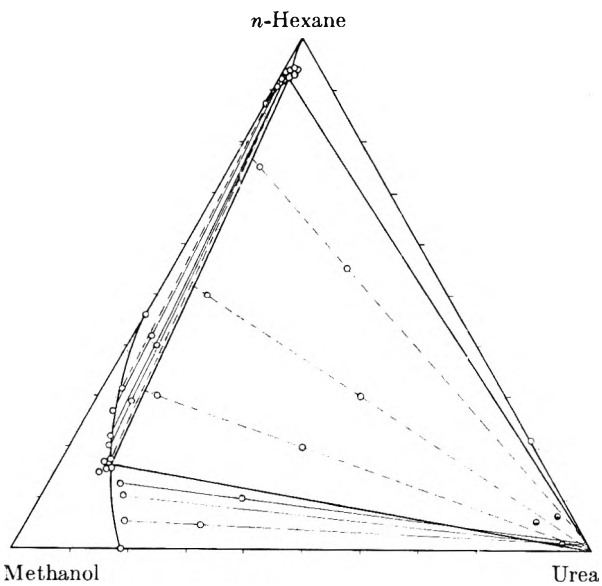

Fig. 2.—Urea–*n*-hexane–methanol system at 25°: ◒, wet residue.

The fact that these two synthetic complex points do in fact lie on a common tie-line indicates that this test, in all cases, gave results in agreement with the accepted adduct composition. The wet residue composition was only determined for one of the two synthetic complexes made up.

Urea–*n*-Hexane–Methanol Systems (Figs. 1 and 2).—Figure 1 clearly indicates that adduct formation occurs at 0° giving an adduct of composition 4.54 moles urea:1 mole *n*-hexane. Figure 2 shows that the *n*-hexane:urea adduct is not formed at 25°, if it is formed at all, its stability range is very narrow and experimentally indeterminate.

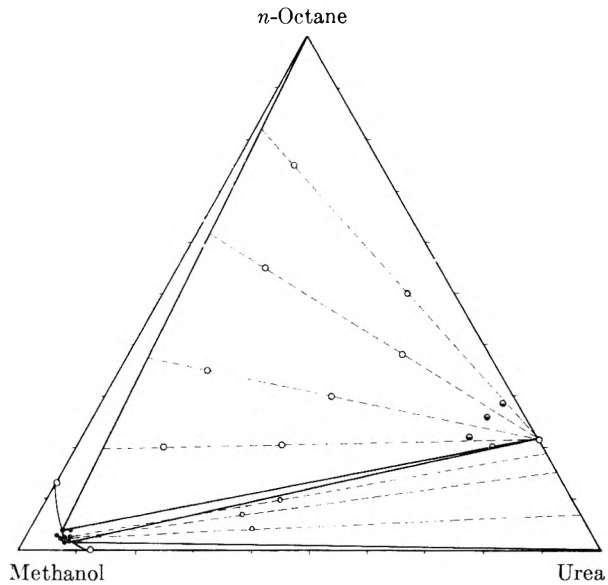

Fig. 3.—Urea–*n*-octane–methanol system at 0°: ⊗, liquid phase composition; ◒, wet residue.

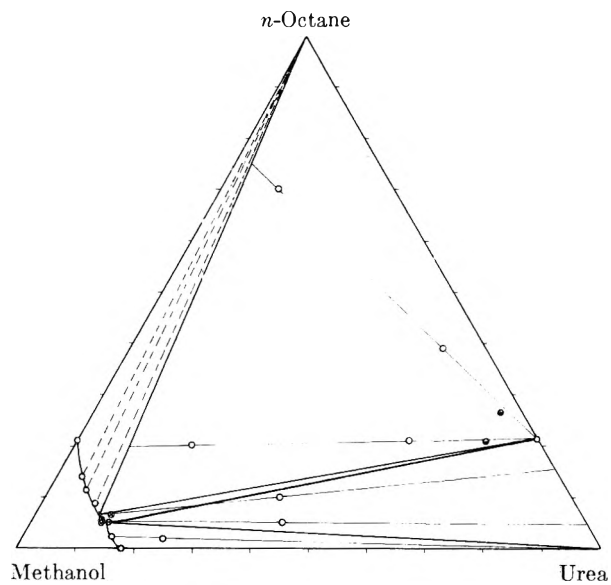

Fig. 4.—Urea–*n*-octane–methanol system at 25°: ⊗, liquid phase composition; ◒, wet residue.

Urea–*n*-Octane–Methanol System (Figs. 3 and 4).—Figures 3 and 4 show that the *n*-octane adduct is stable at a higher temperature than that of hexane and has a composition of 7 moles urea:1 mole *n*-octane. Certain very narrow phase regions shown in these figures have been drawn in because of thermodynamic requirements for their presence rather than because the data prove their existence.

Urea–*n*-Octane–Isooctane (Fig. 5).—It is apparent from Fig. 5 that separation of *n*- and isooctane is possible to about 4% octane. This separation limit perhaps explains the limited success achieved in improving the octane rating of gasoline by urea extraction.

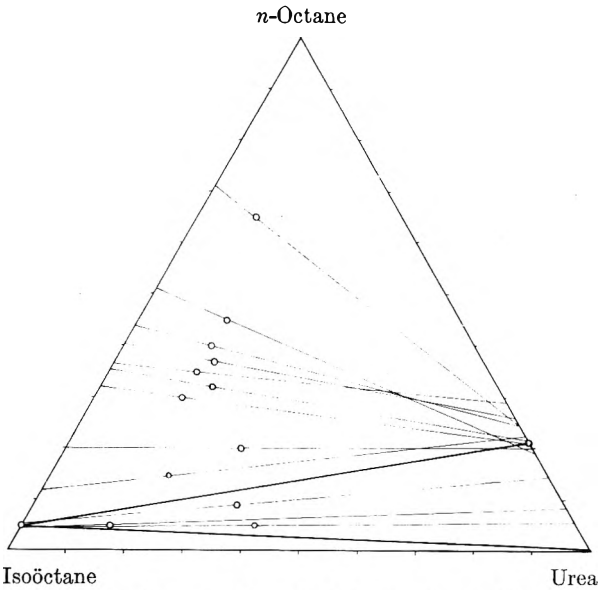

Fig. 5.—Urea–*n*-octane–isoöctane system at 25°.

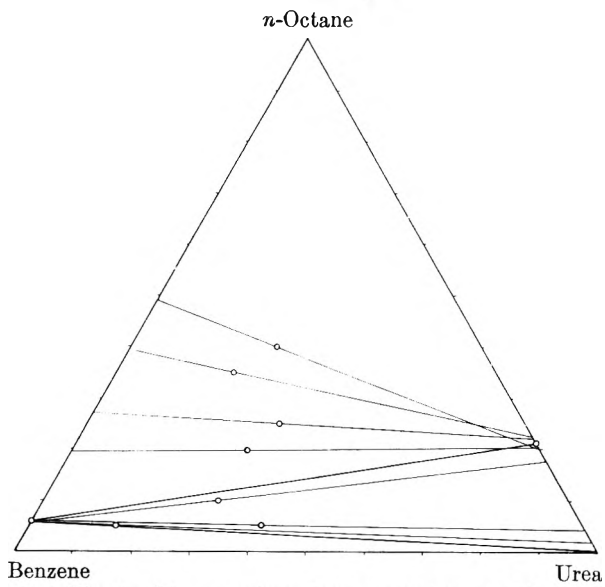

Fig. 6.—Urea–*n*-octane–benzene system at 25°.

A similar situation is apparent in Fig. 6 for the urea–benzene–*n*-octane system.

There has been some suggestion in the literature[1] that association of urea and straight chain hydrocarbon may occur in solution. To test this possibility the phase diagram of Fig. 6 was reproduced in the presence of water, the urea being added by cooling a hot saturated aqueous solution of urea. From the known solubilities of urea at the two temperatures involved, the amount of solid urea precipitated was calculated. Using this figure, it was found that Fig. 6 was exactly reproduced. This result indicates that the solvent plays no part in adduct formation and is simply a medium for the ultimate addition of solid urea.

The Kinetics of Adduct Formation.—In the determination of the foregoing phase diagrams it was observed that urea of particle size less than 150 mesh reacted with *n*-octane rapidly to form the adduct. Urea of 150 mesh size consequently was used in all the equilibrium phase diagram work; 35 mesh urea, on the other hand, had not reacted appreciably after 48 hours. Urea screened to between 115 and 150 mesh reacted with *n*-octane at a rate convenient for measurement.

Figure 7 shows the rate of adduct formation when solid urea of 115–150 mesh is added to a solution of benzene and *n*-octane as followed by refractive index measurements. The complex composition was chosen such that the initial *n*-octane concentration had decreased by 6% at equilibrium.

A mixture of urea, *n*-octane and benzene in the weight proportions 35:42:23 was made up and agitated in a thermostat. Small samples of the solution were withdrawn at 1-hr. intervals for periods up to 20 hr. and analyzed for *n*-octane by refractive index measurements. In this time the *n*-octane concentration fell from about 65 to about 59%.

The results were found to be reproducible and the same at 0° as at 25°, suggestive of a physically controlled process.

It was considered most probable that the rate process involved is that for diffusion of hydrocarbon into the urea lattice. If the equation for diffusion into a spherical body is assumed, diffusivities may be calculated from conversion–time observations during the progress of the addition reaction. If these diffusivities remain constant, strong confirmation for a diffusion controlled process is provided.

For material diffusion through a permeable spherical body the differential equation

$$D\left(\frac{\delta^2 c}{\delta r^2} + \frac{2}{r}\frac{\delta c}{\delta r}\right) = \frac{\delta c}{\delta T} \qquad (1)$$

applies where

c = concn. at radial position "r"
t = time
D = diffusivity

The solution to this equation for the case of constant interfacial concentration has been given by Newman[3] and others and results in the converging infinite Fourier series

$$E = \frac{c_0 - c_t}{c_0 - c_\infty} = 1 - \frac{6}{\pi^2}\sum_1^\infty \frac{1}{n^2} \times e^{-Dn^2\pi^2 t/R^2} \qquad (2)$$

where

E = fractional approach to equilibrium
c_0 = initial concn. of hydrocarbon in soln. at $t = 0$
c_t = concn. of hydrocarbon in soln. at time "t"
c_∞ = concn. of hydrocarbon in soln. at equil.
R = radius of sphere

The roots of equation 2 have been evaluated by Newman[3] who plots the dimensionless parameter $D\pi^2 t/R^2$ against the fractional approach to equilibrium (E).

From the experimental E/t relationship, resource may be made to the above plot and the diffusivity (D) evaluated, since the radius of the urea particle (R) is known from its screen size.

Results are shown in Table I for *n*-octane in benzene diffusing into urea of size (115–150) mesh.

Since the *n*-octane concentration in benzene fell by only 6% during the course of the addition, the condition for a constant solution concentration demanded by eq. 2 is reasonably well fulfilled.

(3) A. B. Newman, *Trans. Am. Inst. Chem. Engr.*, **27**, 311 (1931).

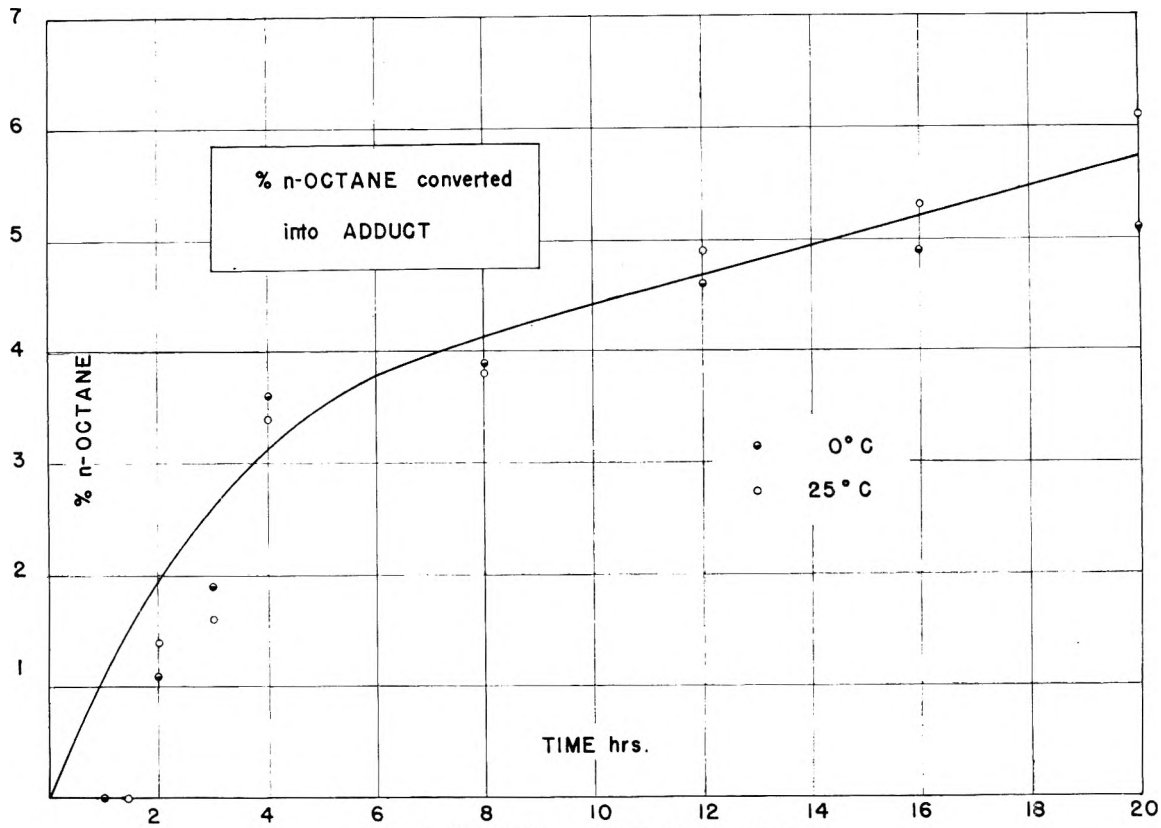

Fig. 7.—% *n*-octane converted into adduct.

It may be seen that the evaluated diffusivity is reasonably constant having an average value of 3.5 $\times 10^{-10}$ ft.^{2}/hr.

From the foregoing results, it seems probable therefore that urea undergoes the transition from tetragonal to hexagonal symmetry and that this process is followed by diffusion of hydrocarbon into the lattice. The problem then arises as to the source of the energy required for the crystal transformation. It seemed most likely that adsorption of the hydrocarbon on the surface of the urea particle provides such energy.

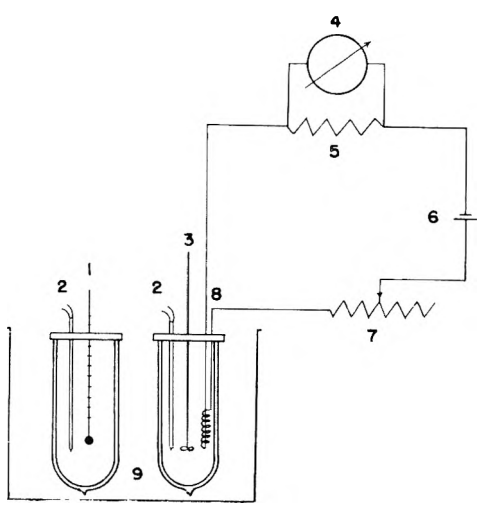

Fig. 8.—Heat of adsorption measurement: 1, thermometer; 2, thermocouples; 3, stirrer; 4, millivoltmeter; 5, rheostat (0.2 Ω); 6, batter (16 Ω.); 7, rheostat (26 Ω); 8, heater (47.76 Ω); 9, thermostat.

TABLE I

DIFFUSION OF *n*-OCTANE IN UREA

E	$\frac{D\pi^2 t}{R^2}$	t, hr.	D(ft.^{2}/hr.)
0.16	0.024	0.3	2.93×10^{-10}
.24	.056	0.7	2.93×10^{-10}
.32	.107	1.1	3.56×10^{-10}
.40	.177	1.75	3.70×10^{-10}
.48	.272	2.35	4.23×10^{-10}
.56	.398	3.50	4.16×10^{-10}
.64	.564	6.05	3.41×10^{-10}
.72	.799	9.25	3.16×10^{-10}
.80	1.12	13.10	3.13×10^{-10}
.88	1.63	18.05	3.30×10^{-10}

In the following section the existence of a heat of adsorption is confirmed and the energetics of adduct formation discussed.

The Energetics of Adduct Formation. The heats evolved when urea of various particle size is added to *n*-octane were measured. The calorimeter, depicted in Fig. 8 comprised twin vacuum flasks containing thermocouples which were connected to a d.c. amplifier and thence to a self-balancing strip chart potentiometer recorder. A full-scale deflection for 10 microvolts was obtainable with this arrangement.

A weighed quantity of urea was added to one flask, both initially containing *n*-octane, and temperature–time observations were recorded. A small heater was then used to determine the water equivalent of the calorimeter.

A typical result is shown in Fig. 9 in which curve "a" represents the temperature changes occurring

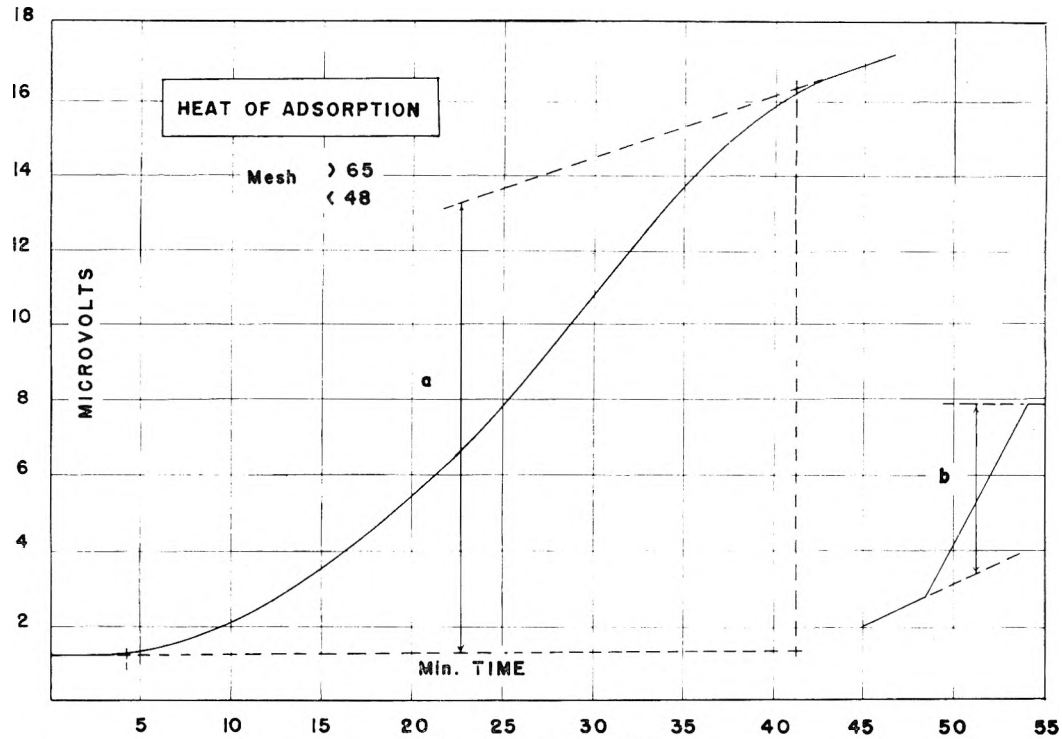

Fig. 9.—Heat of adsorption.

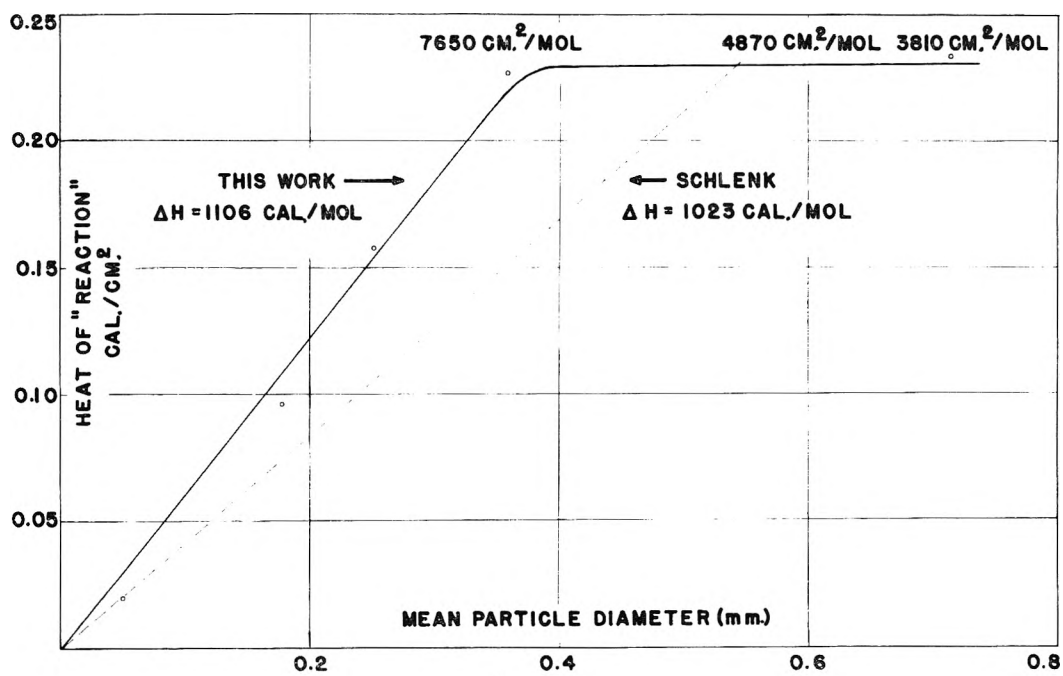

Fig. 10.

on addition of urea and curve "b" refers to the water equivalent determination.

Figure 10 shows the results obtained in this study.

Above a certain urea particle size, where no adduct formation was observed, the heat evolved per unit area of solid is constant, indicative of a heat of adsorption.

Below this critical size, the amount of heat evolved decreases since endothermic adduct formation also occurs.

The results obtained with the larger particles of urea (20–28 mesh) are thus believed to represent the heat of adsorption.

In the formation of the adduct, four distinct steps may be recognized as

n-octane (liq.) ⟶ *n*-octane (adsorbed)(Exothermic) $\Delta H_1 \cdot x$ (1)

urea (*tetragonal*) ⟶ urea(*hexagonal*)(Endothermic) ΔH_2 (2)

n-octane(*adsorbed*) ⟶ *n*-octane(*in lattice*)(Endothermic) ΔH_3 (3)

urea(*hexagonal*) + *n*-octane(*in lattice*) $\rightleftharpoons$ adduct (Exothermic) ΔH_4 (4)

Combining steps 1 and 2

n-Octane(*liq.*) + urea (*tetragonal*) $\longrightarrow$ *n*-octane(*adsorbed*) + urea(*hexagonal*) (5)

We see that this reaction has some unusual features since it cannot involve any condition of finite equilibrium. This is because one cannot imagine a single crystal of urea which is partly hexagonal and partly tetragonal. Thus reaction only occurs when the total energy available from the bonding of the adsorbate on a crystal of urea is sufficiently large to supply the energy for transition of the whole underlying crystal.

It appears then that there are two possibilities.

First, with large particles of urea, the adsorption process (step 1) only occurs since the energy available is insufficient to cause transition of the whole substrate. For this condition, the heat evolved per unit area of urea is constant. If enthalpy changes are computed on the basis of 1 mole of urea, ΔH_1 is the heat of adsorption per unit surface of urea and x is the surface area per mole of urea. From the horizontal portion of the line in Fig. 10, ΔH_1 = 0.234 cal./cm.^{2}.

Secondly, for smaller particles of urea, the energy of bonding of all the adsorbate molecules is sufficient to cause transition of the whole of the substrate. After transition of the substrate, penetration of *n*-octane into the crystal occurs, all entering octane molecules in turn experiencing the adsorption step so that the total heat of adsorption due to the entry of a stoichiometric amount of *n*-octane (7 urea: 1 *n*-octane) expressed as calories per mole of urea is constant. In fact from the point of view of the enthalpy changes involved, we may now ignore the adsorption step if we simply consider the change in enthalpy of a *n*-octane molecule in the liquid phase in being transferred to a position inside the crystal lattice.

Thus steps 1 to 4 may alternatively be represented as

n-octane(*liq.*) $\longrightarrow$ *n*-octane(*in lattice*) ΔH_6 (6)

urea(*tetragonal*) $\longrightarrow$ urea(*hexagonal*) ΔH_7 (7)

urea(*hexagonal*) + *n*-octane(*in lattice*) $\longrightarrow$ Adduct ΔH_8 (8)

ΔH_6 represents the energy involved in separating molecules of *n*-octane in the liquid phase so that they may penetrate as separate entities into the urea lattice and is taken as the latent heat of vaporization of *n*-octane. Thus ΔH_6 = 1,332 cal./mole urea. ΔH_7 = 914 cal./mole urea as measured by Schlenk.[1] Step 8 represents the equilibrium between adduct, hexagonal urea and molecules of *n*-octane having the same energy as they would have in the gaseous state. Schlenk[1] has measured the vapor pressure of the *n*-octane adduct and applying his data to the Clausius–Clapeyron or Van't Hoff equation, ΔH_8 is evaluated as −2,200 cal./mole urea.

Thus the over-all heat of "reaction" ΔH_T = −2,200 + 1,332 + 914 = 46 cal./mole urea.

A constant heat of "reaction" per mole of urea will be represented by a straight line of finite slope passing through the origin in Fig. 10 as is in fact found. The dotted line represents the heat of "reaction" reported by Schlenk (ΔH_T = −1,023 cal./mole urea). It is believed that the difference between Schlenk's value of ΔH_T and that indicated by the results in Fig. 10 is not necessarily a real one. This is because of the uncertainty involved in the calorimetric determinations where the reaction was slow. Where the reaction was fast, as with the smallest urea particles, good agreement with Schlenk's result was obtained (ΔH_T = −1,106 cal./mole urea). However, the discrepancy between the measured ΔH_T and that predicted by steps 6, 7 and 8 is serious and suggests some substantial error, most probably in the value assigned to ΔH_8.

It is fairly certain that the horizontal part of the curve of Fig. 10 is not due to adduct formation still occurring, only at a very slow rate, because no adduct was formed even after several days and the diffusion equation (equation 2) does not predict any such marked decrease in rate with increase in particle size. Moreover the heat liberated was developed rapidly on mixing the urea and *n*-octane.

These ideas then would appear to offer a plausible explanation for the observation that there is a maximum particle size of urea which readily undergoes adduct formation lying between the (35–48) mesh and the (20–28) mesh fractions having mean surface areas of 7,650 and 3,810 cm.^{2}/mole urea, respectively.

The function of a solvent for urea in adduct preparations is therefore most probably that of precipitating urea in a finely divided form such that interaction with the hydrocarbon is substantially instantaneous.

THE VOLUMES OF SOLUTE IN SOLUTION[1,2]

BY JOSEPH S. ROSEN

The University of Kansas City, Kansas City, Missouri

Received March 5, 1955

The volumes of a solute in solution are found by a method which was used previously to compute the volumes of solutions under pressure. These solute volumes have the same values as those computed by another investigator from crystallographic data and from certain assumptions as to the solution state. The method developed here for finding the solute volumes is generally applicable and does not require crystallographic data.

The causes for the change of volume during solution have received the attention of a number of investigators. Some writers have attributed the change in volume during solution to the change in volume of one or the other component alone, while in some cases both the solvent and solute have been assumed to participate in the volume change. By experiment it is possible to observe only the resultant contractions and expansions during solution and it is understandable that the values for the purported volumes in solution depend on the theories assumed. In this article we show that the solute volumes in solution may be found by a method which was used previously to compute the volumes of solutions under pressure, and that the volumes thus found have been obtained from other assumptions on the mechanism of solution.

In a forthcomfng article[3] we derived the equation

$$v_s = x_1 c^{\alpha} (v_w - b) + b x_1 + x_2 \psi_2 \qquad (1)$$

where v_s, v_w and ψ_2 are, respectively, the specific volumes at atmospheric pressure[4] of the solution, water and the volume of the solute in solution. x_1 and x_2 are the weight fractions of water and solute; α is the relative concentration of the solute and is the ratio of either the weight fraction of salt x_2 or of the volume concentration x_2/v_s.[5] In this article we shall use $\alpha = x_2/x_2^*$ (where the asterisk designates some arbitrary concentration) so that α is 1 for the solution which contains x_2^* g. of solute and c is a constant corresponding to this concentration and depends on the amount the water is compressed due to the presence of the solute. b is the constant in the equation

$$P_0 - P = a \log_{10} \left(\frac{v_w^{(P)} - b}{v_w^{(P_0)} - b} \right) \qquad (2)$$

which represents the variation of volumes of water with pressure. $v_w^{(P_0)}$ and $v_w^{(P)}$ are the specific volumes of water at the pressures P_0 and P and the two parameters a and b may be determined by adapting the compressibility data of water to the equation.[6]

In eq. 1 only c and ψ_2 are unknown (after α is appropriately defined and the value of b assumed) and these may be found by writing this equation for each concentration and determining by the method of least squares their best values.

In eq. 1, $c^{\alpha}(v_w - b) + b$ represents the specific volume of *water in solution*, and from these terms it is evident that only a portion of the water is compressed (since $c < 1$ for aqueous solutions of electrolytes). Thus b is the relatively incompressible portion of the volume of water, and because its value is not critically determined by eq. 2,[6] neither is ψ_2, the solute volume, in eq. 1.

Another condition is posed by eq. 1 before it describes the solution state: that is, that the exponent α, which involves the concentration of the solution, must be adequately defined. We have not in previous work resolved this question of concentration and we have used both the weight fraction, x_2, or the volume concentration, x_2/v_s. Thus, it is apparent that the choice between these definitions (or others, for that matter) would again commit us to some particular theory on the mechanism of the solute state.

These considerations are made apparent in Fig. 1 where we show how ψ_2, the volume of the solute in sodium chloride solutions, varies with b and with the two definitions of concentrations indicated.

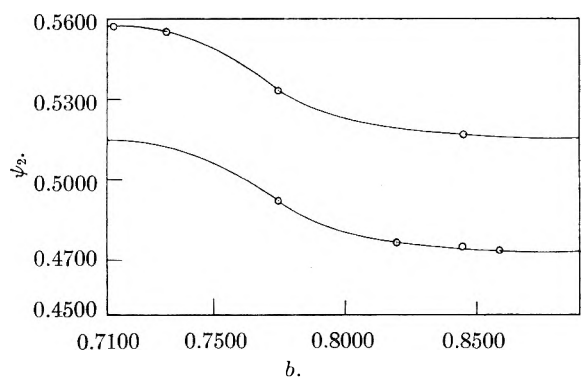

Fig. 1.—The variation of ψ_2, the volumes of the solute in sodium chloride solutions, with different values of b. In the upper curve α is the ratio of the volume concentration x_2/v_s, and in the lower curve it is the ratio of the weight fraction of salt x_2.

In this article we give an interpretation of the volumes of solute, ψ_2, which result from eq. 1 for a particular choice of α and b. If we take for the concentration of the solution its percentage by weight and set $b = 0.8591$,[7] we find that the volumes of solute given by eq. 1 are remarkably close to those derived by Scott by a method so different that, both the methods and the results invite careful consideration.

(1) Sponsored by the Office of Ordnance Research, U. S. Army.

(2) I am indebted to the Research Corporation for some assistance.

(3) J. S. Rosen, *J. Chem. Phys.*, in press (1956).

(4) In the original article eq. 1 is shown to hold for all pressures P; the equation was used to compute the volumes of a number of salts in solution to 10,000 bars.

(5) It may be noted that other expressions for the concentration in α might be used (*e.g.*, x_2/x_1, to correspond to molal concentration).

(6) The values of these parameters have been determined with the initial pressure P_0 taken at atmospheric pressure. b does not remain constant as the pressure range P is increased; see Rosen, ref. 3.

(7) This is the value of b in eq. 2 for water with $P_0 = 1$ and a pressure range of 1000 bars. See Tables I and II, Rosen, ref. 3. It should be apparent from Fig. 1 that ψ_2 remains essentially constant around the value of b assumed here.

TABLE I

THE MOLAL SOLUTE VOLUMES AND CRITICAL DISRUPTIVE VOLUMES OF THE ALKALI HALIDES AT 25°

Salt[a]	Max. x_2	c[b]	Molal solute vol., ϕ^* Scott[c]	Rosen[d]	Mol. vol. of solid[a]	Critical disruptive vol., V^* Scott	Rosen	Space-filling ratio, ϕ^*/V^* Scott	Rosen
LiCl	0.11	0 85880	25.3	27.09	20.5	32.4	21.75	0.78	1.246
LiBr	.20	.95873	30.0	30.00	25.1	39.1	38.33	.77	0.783
LiI	.19	.98325	39.2	39.19	33.0	51.2	51.95	.77	.755
NaCl	.25	.88968	26.9	27.65	27.05	41.6	36.63	.65	.755
NaBr	.40	.95313	31.5	31.53	32.13	49.0	48.04	.64	.657
NaI	.59	.97891	40.6	40.39	40.9	61.1	64.74	.66	.624
KCl	.22	.90803	36.3	38.11	37.5	56.6	40.31	.64	.945
KBr	.40	.95970	41.3	41.81	43.3	64.7	57.59	.64	.726
KI	.56	.97620	51.0	51.55	53.2	78.0	63.19	.65	.816
RbCl	.43	.95426	40.7	41.12	43.2	63.8	57.55	.64	.715
RbBr	.53	.97228	46.3	46.32	49.4	72.7	71.72	.64	.646
RbI	.41	.98422	55.9	55.94	59.8	86.7	81.47	.64	.687
CsCl	.66	.96831	48.0		42.3	62.4		77	
CsBr	.53	.98113	53.4		47.9	70.4		.76	
CsI	.48	.98846	63.2		57.6	83.3		.76	
CsCl[e]	.66	.96831	47.2	47.49	42.3	73.4	67.82	.64	.700
CsBr[e]	.53	.98113	52.8	52.69	47.9	82.6	85.53	.64	.616
CsI[e]	.48	.98846	62.7	62.70	57.6	97.5	101.35	.64	.619

[a] The constants of eq. 1 were obtained from the volumes of the aqueous solutions of the alkali halides using the data of G. P. Baxter and C. C. Wallace, *J. Am. Chem. Soc.*, **38**, 96 (1916). [b] This is the value of c when $x_2 = 0.1$, so that for other concentrations $\alpha = x_2/0.1$ in eq. 1. We have set $b = 0.8591$ in this equation. [c] A. F. Scott, THIS JOURNAL, **35**, 3386 (1931). [d] Obtained from ψ_2, the specific volume of the solute, in eq. 1. [e] Hypothetical rock-salt type lattice structure.

Scott, in a series of papers,[8] has considered the problem of the volumes of solute in solution from a number of view points. We will outline briefly one of his methods for computing the solute volumes of the alkali halides in water and show in Table I that his results are essentially reproduced with our eq. 1.

Scott[9] postulates that the hypothetical upper limit to the concentration of the solute in solution[10] is reached when the crystalline solid attains its "critical disruptive volume," V^*; and he establishes this volume from the following considerations. In the crystalline state, R, the normal interionic distance of the lattice, is determined from the condition of the equilibrium of the attractive and repulsive forces of the ions. When the crystal is expanded from its normal equilibrium volume to V^*, the resulting cohesive forces reach a maximum; and when this maximum force is exceeded, the crystal is pulled apart so that the volume V^* marks the transition from the regular lattice arrangement to the more irregular arrangement in solution.

In the formula

$$\frac{R^*}{R} = \left(\frac{n+3}{m+3}\right)^{\frac{1}{n-m}} \qquad (3)$$

derived by Joffe,[11] R^* is the interionic distance in the critical disruptive state, m is the attractive exponent (and is unity for the alkali halides), and n is the repulsive exponent for which the values given by Pauling[12] are used.

From the "critical disruptive volume," V^*, calculated from R^*, the hypothetical upper limit to the concentration of the solute in solution is obtained and is $1000/V^*$ (moles per 1000 cc. solution).

Scott then introduces Masson's empirical equation[10]

$$\phi = a\sqrt{m} + b \qquad (4)$$

where ϕ is the apparent molal volume of the solute, m the concentration (moles per 1000 cc. solution), and where a and b are constants characteristic of each salt.[13] Scott identifies the hypothetical maximum value of the apparent volume, given by

$$\phi^* = a\sqrt{1000/V^*} + b \qquad (5)$$

with the molal volume of the solute in solution.

In Table I we give the constants of eq. 1 for the aqueous solutions of the alkali halides fitted to the same data[14] used by Scott to determine the constants of eq. 4 and 5. In Table I are shown also the volumes of the solute obtained by Scott and those given by eq. 1. The agreement of these results is remarkable, considering the dissimilar methods used in finding these volumes. It should, however, be noted that our solute volumes for the chlorides are consistently higher than those of Scott. In this table the "critical disruptive volumes," V^*, are also compared[15]; the corresponding values in the two sets often differ considerably. This is due to the fact that in the two methods ϕ^* (equated to the molal solute volume) and V^* are obtained in different order from eq. 5, and that in this equation a small change in ϕ^* produces a large change in V^*.

For the interpretation of the molal solute volumes, ϕ^*, the "disruptive critical volumes," V^*,

(8) (a) A. F. Scott, THIS JOURNAL, **35**, 2315 (1931); (b) **35**, 3379 (1931); (c) A. F. Scott and R. W. Wilson, *ibid.*, **38**, 951 (1934).

(9) See ref. 8a. A summary of Scott's work is also given in H. S. Harned and B. B. Owen, "The Physical Chemistry of Electrolytic Solutions," Reinhold Publ. Corp., New York, N. Y., 1950, p. 257 ff.

(10) D. O. Masson had previously suggested that this hypothetical upper limit was reached when the concentration of the electrolyte became that of the pure crystalline salt. See *Phil. Mag.*, [7] **8**, 218 (1929).

(11) A. F. Joffe, "The Physics of Crystals," McGraw-Hill Book Co., New York, N. Y., 1928.

(12) L. Pauling, "Nature of the Chemical Bond," Cornell University Press, Ithaca, N. Y., 1948, p. 341.

(13) These constants for the alkali halides are given in ref. 8a, p. 2317. See also Harned and Owen, ref. 9, p. 253.

(14) G. P. Baxter and C. C. Wallace, *J. Am. Chem. Soc.*, **38**, 96 (1916).

(15) Our "critical disruptive volume" was found by setting ϕ^* in eq. 5 equal to our molal solute volume and solving for V^*; the reverse order is necessary for finding these quantities by Scott's method.

and the space-filling ratio, ϕ^*/V^*, the reader should consult the literature cited.[8,9]

If these solute volumes have any intrinsic meaning, some special merit in the method developed here (as well as the fact that it may throw additional light on the complex factors involved in the solution state), is that it requires only the specific volumes of the solutions and can be applied also where the crystallographic data used by Scott are lacking.

THE EFFECT OF BUFFER AND ELECTROLYTE ON THE DIFFUSION OF AN ACID DYE IN GELATIN

By R. B. Pontius, M. L. Kaplan and R. M. Husney

Communication No. 1717 from the Kodak Research Laboratories, Research Laboratories, Eastman Kodak Company, Rochester, N. Y.

Received March 24, 1955

A freeze-drying technique for measuring diffusion of dyes in gelatin on a microscopic scale has been used to study the diffusion of an acid dye in plain gelatin. The method consists in dyeing a sample of a thin gelatin coating, arresting diffusion by rapidly freezing the sample, dehydrating it while frozen, sectioning the dry sample, and making micro-densitometer measurements of dye density as a function of penetration. The effect of the addition of buffer and electrolyte to the dye-bath has been studied. It is shown that the maximum concentration of dye in the gelatin, which is very much greater than that in the dye-bath, apparently is not reached at the gelatin surface immediately at the start of dyeing. Difficulties in the computation of numerical values of the diffusion coefficients resulting from the time-dependent surface concentration are discussed.

Introduction

A useful method of measuring diffusion of dyes in gelatin in a simplified system and on a microscopic scale was originally suggested by E. E. Jelley,[1] of these Laboratories. The method consists in dyeing a sample of thin gelatin coating for a definite time, arresting the diffusion by rapidly freezing it in a low temperature bath of alcohol and solid carbon dioxide, and drying the sample while frozen by sublimation of the ice. Drying is accomplished by sweeping a high-velocity stream of dry nitrogen precooled below $-6°$ across the sample. Finally, the dried sample is sectioned and examined under the microscope. The method resembles the freeze-drying technique frequently used in the preparation of biological specimens for microscopical observation. A similar method also has been used for studying the dyeing of textile fibers.[2] In the present case, the penetration distance of the dye for a given condition of dyeing is of primary interest.

An improvement in the method, which greatly facilitates interpretation of the results, was achieved by constructing a new type of high-resolution micro-densitometer. In this instrument, the stage of a microscope holds stationary a thin section of gelatin which has been cut and mounted in balsam after dye diffusion has been arrested. Scanning is carried out by moving the light source and the slit on a micrometer screw perpendicular to the optical axis at a distance of 50 cm. from the objective. Focusing is accomplished by an arrangement of mirrors for projecting the image of the section backward through the optical system onto a screen which is par-focal with the slit. In operation, the moving image of the slit, reduced 930 times by means of a 10X Leitz coated ocular and a 4.3-mm. Bausch and Lomb coated oil-immersion fluorite objective, scans the section. The central portion of the cone of light transmitted is collected by an 8-mm. Bausch and Lomb coated objective and transmitted to the cathode of an RCA photomultiplier tube. By means of an amplifier and a Brown recorder, traces of the variations in density across the section are made automatically.

As the construction of the micro-densitometer and the technique of dyeing, freezing and drying have been described previously,[3] these details will not be discussed further here. In the present paper will be shown some of the results obtained by the new technique, particularly the differences in the manner of dye diffusion which result when gelatin is dyed from baths with and without buffer and with and without neutral electrolyte.

Diffusion Measurement.—The measurements of diffusion distance are obtained from micro-densitometer traces, such as those in Fig. 1, where the y-axis represents dye density in the section, and the x-axis represents distance in microns from the front surface of the gelatin coating. The sections are cut approximately 5 μ thick, and the dry coating has a width, in sections, of about 11.5 μ. In interpreting the micro-densitometer traces, it should be noted that, although the geometrical width of the scanning beam is 0.22 μ, the effective width is larger, owing to diffraction. As a consequence of the finite scanning width, the micro-densitometer can never reproduce a sharp edge as a vertical line. The location of the exact geometrical edge of the sample is somewhat uncertain. In practice, it is necessary to fix the geometrical edge by drawing a vertical line at the point where the rising density trace becomes linear, a position known to be approximately correct, both on the basis of theory and of experience. The traces of the diffusion curves may be extrapolated back to the geometrical edge of the section, as shown by the broken lines. It will be recognized that extrapolations such as these are arbitrary and do not reduce the uncertainty of the exact maximum density.

(1) Reported in R. B. Pontius, *Phys. Rev.*, **80**, 927 (1950) (abstract only).

(2) B. Olofsson, *Medd. Sv. Textilforskningsinst.*, **4**, 1 (1953).

(3) E. E. Jelley and R. B. Pontius, *J. Phot. Sci.*, **2**, 15 (1954).

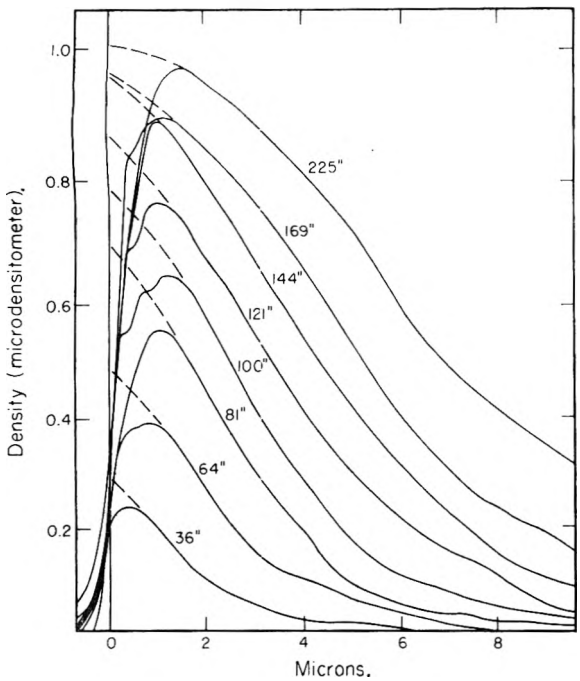

Fig. 1.—Diffusion of Brilliant Alizarine Light Red B in unhardened gelatin, the case of dyeing from unbuffered dye-bath at *p*H 4.0. The numbers beside the individual curves are dyeing times in seconds.

Experimental Data.—In all diffusion measurements, the sample, before being placed in the dye-bath, was swollen for ten minutes in a presoak bath of *p*H 4.0, similar to the dye-bath, except that it did not contain the dye. Brilliant Alizarine Light Red B (free acid *pK* 1.8) was used for dyeing at a concentration of 0.298 g. per liter in the dye-bath at *p*H 4.0 at 20°. Samples of plain, unhardened gelatin coating of isoelectric point approximately 4.8 were dyed for definite periods of time by means of a rotating camel's-hair brush moving across the surface of the sample. The dye-bath was vigorously agitated, and it was of sufficient size to maintain a virtually constant concentration.

Sets of diffusion curves (micro-densitometer traces) resulting from dyeing in an unbuffered dye-bath are shown in Fig. 1. Similar curves for dyeing from a phthalate-buffered dye-bath are shown in Fig. 2. The compositions of these and two other different dye-baths used are given in Table I.

TABLE I

COMPOSITION OF DYE-BATHS[a] OF *p*H 4.0

	Buffered with acetate–citrate	Buffered with acetate–citrate and containing NaCl	Buffered with acid potassium phthalate	Unbuffered
Dye (as free acid), g.	0.298	0.298	0.298	0.298
Sodium acetate, anhydrous, g.	1.44	1.44		
Sodium citrate, crystals, g.	1.27	1.27		
Glacial acetic acid, g.	7.5	7.5		
Sodium chloride, g.		10.2		
Acid potassium phthalate, g.			10.2	
Distilled water to, ml.	1000	1000	1000	1000

[a] The dye-baths were finally adjusted to *p*H 4.0 by means of either acetic acid or sodium hydroxide.

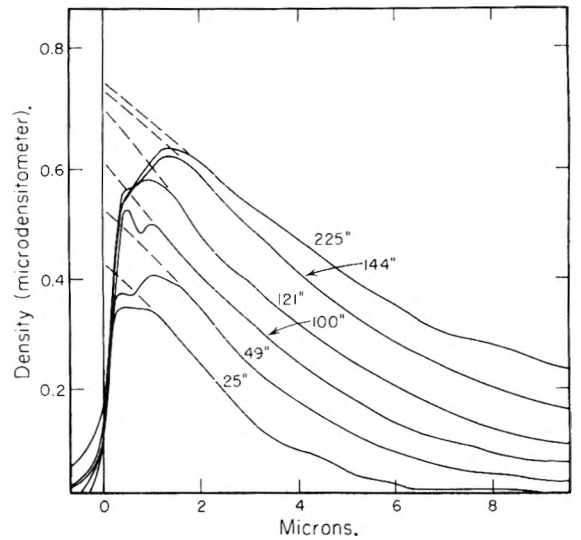

Fig. 2.—Diffusion of Brilliant Alizarine Light Red B in unhardened gelatin, the case of dyeing at *p*H 4.0 in dye-bath buffered with 10.2 g. per liter of acid potassium phthalate.

The micro-densitometer curves in Figs. 1 and 2 have not been corrected for section thickness. As the sections cut on the microtome may vary about 20% in thickness from one section to another, it is necessary, for quantitative work, to measure the thickness under the microscope, and to make a correction to the density indicated. Also, it should be noted that the density–distance curves shown are in the dried gelatin. Diffusion actually took place in the swollen gelatin so that an independent determination of swelling ratio is needed for measurements of absolute diffusion distances.

The curves for dyeing in the unbuffered dye-bath (Fig. 1) and in the acetate–citrate–acetic acid buffered dye-bath are somewhat similar. Both sets of curves are considerably different from those of Fig. 2, which shows the results of using phthalate as the buffer. The addition of 10.2 g. per liter of sodium chloride to the lightly buffered acetate–citrate–acetic acid dye-bath yielded a set of curves similar to those of Fig. 2 resulting from the use of phthalate buffer.

Concentration of Dye.—In all that follows, the concentration of dye in sections, as a first approximation, is assumed to be linearly proportional to the density as measured with the micro-densitometer.

An unexpected result of the measurements is that the concentration of dye at the surface of the gelatin, from which diffusion inward occurs, appears to increase with the time of dyeing. It cannot be excluded, of course, that from the very first instant of dyeing some dye of the maximum concentration does appear at the surface. However, even with the present high resolution in the micro-densitometer, it is impossible to measure the concentration closer to the surface than 0.5 to 1 μ. Therefore, in the present work, the surface densities will be taken as those given by measured curves extrapolated arbitrarily to the surface in the manner shown by the dotted lines in Figs. 1 and 2. These surface densities, corrected for section thickness, are shown in Fig. 3 as a function of dyeing time.

From Fig. 3, it can be seen that the apparent rate of increase of surface concentration shows a different time-dependence in each of the four cases, depending upon the composition of the dye-bath.

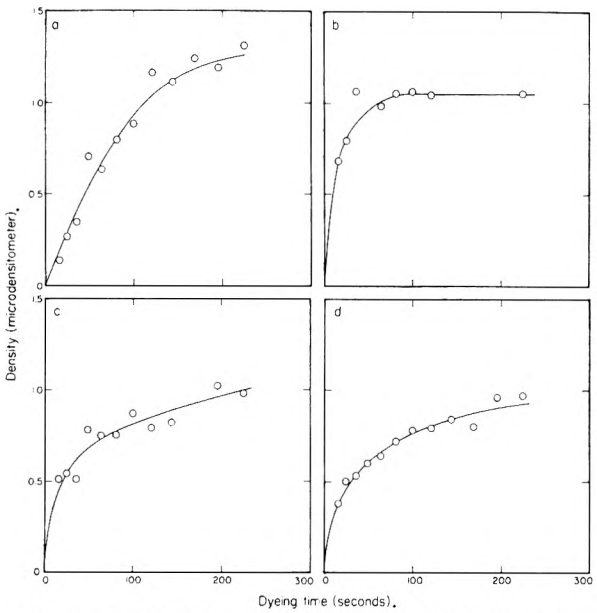

Fig. 3.—Increase in surface density with length of time in the dye-bath. Density measured in sections with microdensitometer: a, unbuffered dye-bath; b, acetate–citrate–acetic acid buffered dye-bath; c, acid potassium phthalate buffered dye-bath; d, acetate–citrate–acetic acid buffered dye-bath with added sodium chloride.

In the unbuffered dye-bath, the rate of increase is initially the slowest, but the final dye concentration is the highest. The rapid rate of increase of surface density when dyeing from the acetate–citrate–acetic acid buffered dye-bath is greatly reduced by the addition of sodium chloride.

Differences in the dyeing behavior in the four cases can also be shown by ordinary densitometer measurements of the dyed samples before sectioning. These ordinary density values are proportional to the total amount of dye in the sample. The ordinary densitometer measurements are plotted against the square root of the dyeing time in Fig. 4. Dyeing curves plotted as in Fig. 4 may be called *transport curves*, since the slope of the straight-line portion is related to the rate at which dye is transported into the gelatin through the surface from the dye-bath. In each case, there is a time delay before the transport curve becomes linear. The time delay is the greatest when dyeing from the unbuffered dye-bath. Were diffusion taking place from a constant surface concentration with diffusion coefficient independent of concentration, these transport curves would be linear with origin at time zero.

Magnitude of the Dye Concentration.—The absolute magnitude of the surface concentration, even a few seconds after the start of dyeing, is very considerably greater than the dye concentration in the dye-bath.

In Figs. 1 to 3, optical density has been plotted on the y-axis. In the measurement of diffusion, it is more desirable to work with actual concentration. The equivalence between density and concentration was determined by extracting the dye and measuring the amount present colorimetrically. It was found that one unit of density for the present dye, measured in the section with the microdensitometer, using a Kodak Wratten Filter No. 61, represents 0.54×10^{-4} g. of dye per square centimeter. This density in a 5 μ thick dry section is a concentration of 0.108 g. per cubic centimeter. In order to obtain the absolute magnitudes during dyeing, the factor of swelling must be applied.

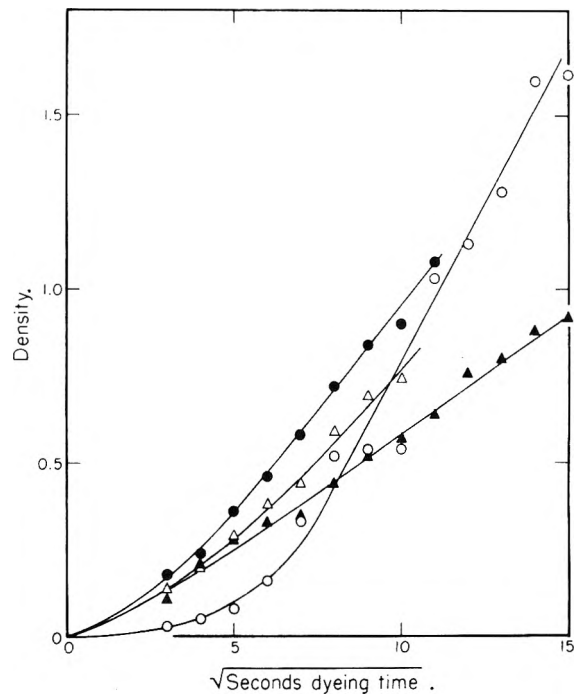

Fig. 4.—Transport curves showing the rate of dyeing of unhardened gelatin by Brilliant Alizarine Light Red B at *p*H 4.0. Density of samples measured with Eastman Transmission Densitometer before sectioning: ○, unbuffered dye-bath; ●, acetate–citrate–acetic acid buffered dye-bath; △, acid potassium phthalate buffered dye-bath; ▲, acetate–citrate–acetic acid buffered dye-bath with added sodium chloride.

The swelling can be measured in a variety of ways. The method which has been used here consists in making micrometer measurements on a large number of samples, dry gelatin plus support (film base), support alone, and gelatin plus support, swollen to equilibrium in the same dye and buffer baths used for diffusion measurements. The swelling of the gelatin alone is found by difference after a small correction has been made for the swelling of the support. The average dry thickness of all the gelatin sections studied is 11.46 ± 0.16 μ. The swollen thicknesses are shown in Table II.

TABLE II

THICKNESSES OF UNHARDENED GELATIN COATING SWOLLEN 10 MINUTES AT 20° AND *p*H 4.0

Type of swelling employed	Swollen thickness, μ
Unbuffered bath	91.1 ± 1.6
Phthalate buffer	82.3 ± 0.8
Acetate–citrate–acetic acid buffer	95.7 ± 1.4
Acetate–citrate–acetic acid buffer containing sodium chloride	90.0 ± 1.1

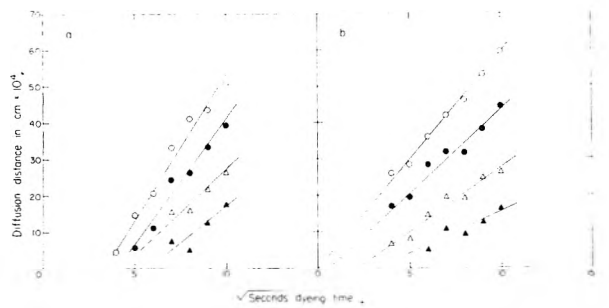

Fig. 5.—Distance of diffusion of Brilliant Alizarine Light Red B in unhardened gelatin at *p*H 4.0 as a function of square root of dyeing time and of concentration: (a) dyeing from unbuffered dye-bath; ○, concn. 1.36×10^{-3} g. cm.$^{-3}$; ●, concn. 2.72×10^{-3} g. cm.$^{-3}$; △, concn. 5.44×10^{-3} g. cm.$^{-3}$; ▲, concn. 8.16×10^{-3} g. cm.$^{-3}$. (b) dyeing from dye-bath buffered with acid potassium phthalate; ○, concn. 1.50×10^{-3} g. cm.$^{-3}$; ●, concn. 3.00×10^{-3} g. cm.$^{-3}$; △, concn. 6.00×10^{-3} g. cm.$^{-3}$; ▲, concn. 9.00×10^{-3} g. cm.$^{-3}$.

If the factor of swelling is taken into account, a density of 0.5, measured in the dry section, with the micro-densitometer, represents a concentration of dye, in the case of maximum swelling, of 0.0065 g. cm.$^{-3}$. Since the concentration of dye in the dye-bath is 0.298×10^{-3} g. ml.$^{-1}$, the dye concentration within the gelatin is approximately 22 times that in the dye-bath. In the dry gelatin, the concentration is actually 180 times that in the dye-bath.

Dyeing Mechanism.—In the swollen state, gelatin is a colloidal gel consisting of an aqueous phase and a solid or protein phase. Since the solid phase carries a net positive charge at *p*H 4.0, it would be expected, on the basis of the Donnan membrane theory,[4,5] that the equilibrium dye concentration would be greater than that in the dye-bath. The Donnan concentration refers to concentration in the aqueous phase at the gel surface. On a molecular scale, the gel surface cannot be anything so simple as a definite geometrical plane. The solid structure of the gel, which one may picture as a tangled mat of polypeptide chains, is completely permeated by water. It seems reasonable to expect that the Donnan equilibrium must apply to the concentration of ions in the aqueous phase within the gel.

The micro-densitometer traces are made of the dry sections. Were it possible to make a trace of the swollen section during dyeing, the instrument would still not be able to distinguish between dye in the aqueous phase within the gel and dye which may be associated with the solid phase of the gel through the action of binding forces between the dye molecules and the protein, such as, for example, hydrogen bonds. Were any binding between dye anions and charged protein to occur, the membrane potential would be modified, perhaps even before equilibrium could be established. The concentration of dye at any instant within the gelatin near the surface is probably determined by competition between the tendency of the gelatin to take up dye molecules from the dye-bath, and the tendency for the dye already present to diffuse down the concentration gradient toward the interior of the gelatin layer.

Diffusion Coefficient.—The data obtained from the micro-densitometer traces of samples in which dye diffusion has been arrested consist of measurements of concentration as a function of diffusion time and distance. The data should, in principle, make possible the determination of diffusion coefficients.

In order to investigate the applicability of the present data to the determination of the dye-diffusion coefficient in the gelatin, the penetration distances for definite concentrations are plotted against the square roots of the dyeing times, as in Fig. 5, making use of data for the unbuffered dye bath, Fig. 5a, and data for the phthalate-buffered dye-bath, Fig. 5b. The experimental points define straight lines which do not, except in one case of low concentration, extrapolate linearly to zero at zero time. This unfortunate circumstance makes it impossible to deal with the problem by representing the concentration as a function of $x/\sqrt{t}$,[6] and may be taken as corroborative evidence of a time-dependent surface concentration. Inasmuch as it is not clear what significance is to be attached to these results, no further steps will be taken here to compute numerical values of the dye-diffusion coefficients.

Conclusion

The use of the freeze-drying technique for arresting dye diffusion in gelatin, with the measurement of concentration gradients by means of the micro-densitometer, leads to qualitative evidence regarding several aspects of diffusion in the colloid. The information so far obtained points to the existence of a time-dependent surface concentration, which factor in turn leads to difficulties in attempts to determine numerical values of the diffusion coefficients.

In the present paper, only changes in diffusion behavior caused by the addition of two types of buffer and of one type of neutral electrolyte to the dye bath have been dealt with. Many other factors affect the diffusion rate and the concentration profile. Among these factors are the effects of *p*H, of temperature, of dye structure, of type of gelatin, of mordant, and of dye solvent. Some of the factors have been discussed briefly in earlier papers,[1,3] and some of the others, it is hoped, will be reported on later. In addition to the study of these many effects, there remains for the future the important problem of expressing and solving the diffusion equation in such a way as to take account of Donnan phenomena, adsorption phenomena, and variable boundary conditions.

(4) S. E. Sheppard, R. C. Houck and C. Dittmar, THIS JOURNAL, **46**, 158 (1942).

(5) T. R. Bolam, "The Donnan Equilibrium," G. Bell and Sons, London, 1932.

(6) L. Boltzmann, *Ann. physik. Chem.*, **53**, 959 (1894).

THE LITHIUM–SODIUM LIQUID METAL SYSTEM

BY O. N. SALMON AND D. H. AHMANN

Knolls Atomic Power Laboratory,[1] *Schenectady, N. Y.*

Received March 24, 1955

A brief investigation of the lithium–sodium liquid metal system was made using thermal analysis plus chemical analysis of the immiscible phases sampled at temperature. Addition of 3.8 atomic % sodium to lithium lowers its freezing point from 179.4 to 171°. At 171° sodium and lithium form two immiscible liquid phases of composition 3.8 and 86.9 atomic % sodium. The estimated critical temperature and composition are 380° and 35 atomic % sodium, respectively. The composition at the eutectic point is 3.7 atomic % lithium and the temperature is 93.4°.

A brief investigation of the binary system sodium–lithium was made as a part of the program on liquid metals. The system had been investigated previously[2–4] but no measurements were made of the mutual solubility of the two molten phases.

The system was studied using thermal and chemical analysis, the melting point of lithium and the temperature at which a solid lithium phase is in equilibrium with two liquid phases being determined thermally and the composition of the immiscible liquid phases being determined chemically. The limits of the miscibility gap were estimated from the data by use of the equations relating the activity to the mole volume and the solubility parameters.[5]

Materials.—Reagent grade brick sodium from the du Pont Company was used. Impurities were potassium 250 p.p.m., calcium 330 p.p.m., lithium 90 p.p.m., sulfur 50 p.p.m., chlorine 30 p.p.m., and phosphorus 20 p.p.m.

Lithium was obtained from the Maywood Chemical Company. The purity claimed was 99.8% with the major impurities being Na 0.02, Ca 0.06, Fe 0.03, Si 0.015, and heavy metals 0.09%. The alkali metals were separated from oxides formed during handling by drip casting in an argon atmosphere into the crucible; the oxide remained as a *skin* in the casting crucible.

Apparatus.—Mild steel crucibles (10-10 low carbon steel, 3″ tall × $^{15}/_{16}$″ i.d. × .015″ thick wall) were used to contain the alkali metals. Examination of crucibles exposed to lithium and sodium at 170–200° for ten days showed no evidence of corrosion.

The temperatures were measured with a Leeds and Northrup Type K2 potentiometer using a chromel–alumel thermocouple spot welded to the side of a mild steel crucible. The thermocouple was calibrated using an ice-bath, boiling water and a Bureau of Standards calibrated mercury thermometer. The temperatures, as reported, are considered accurate to within 0.5°.

The samples were heated under an inert atmosphere or vacuum inside a Pyrex chamber by a resistance furnace.

Experimental Method.—The thermal arrests were determined by heating and cooling curves run on a melt containing 7.4 g. of lithium and 12.5 g. of sodium. The mixture was heated to 280° to ensure adequate mutual solution of the two phases, a static argon atmosphere was maintained over the melt to reduce sodium distillation. After equilibration the furnace current was turned off, and when the melt had cooled to 200° the argon was evacuated to isolate the sample thermally and thereby increase the sensitivity of the arrest. The heating curve was obtained by setting the furnace to heat from room temperature to an ultimate temperature of 210°. All arrests were pronounced, varying in duration from 15 to 60 minutes. The heating and cooling arrests agreed to within 1°.

Before determining the composition of the two liquid phases, the lithium–sodium alloy was equilibrated by holding at temperature for 24 hours or more. Comparison of samples taken at times greater than 24 hours showed no variation beyond the errors of the analytical method; hence equilibrium was assumed. The liquid layers were sampled by breaking the tip of an evacuated glass sample bulb under the molten metal. Contamination of the melt with glass from the break off tip was avoided by wrapping the tip with 0.010 inch iron wire. When sampling the light metal phase, the break off tip was broken by pulling against the tip with an extension of the wrapping wire. The heavy phase was sampled by pushing the break off tip against the bottom of the crucible. The light phase was always sampled first to avoid contamination of the light phase sample by the heavy phase. By quickly cooling the sample in a jet of argon, 2-ml. glass sampling bulbs can be used to sample lithium up to temperatures of 240° without initiating the vigorous exothermic reaction between the Pyrex and lithium.

The samples were dissolved in water and neutralized with a standard hydrochloric acid solution. The lithium and sodium in these neutral solutions were determined using a Beckman Flame Photometer, Model DU. The relative accuracy of the analytical results is considered to be within 5% of the minor constituent for each sample.

Experimental Results.—The data obtained by thermal analysis include the melting point of 179.4° for lithium, the temperature of 171.0° at the base of the miscibility gap and the temperature of 93.4° at the eutectic point. The melting point of sodium was not determined but was assumed to be 97.8°.[6]

The analytical results on the phases sampled after equilibrating at temperature are listed in Table I. The results are plotted in Fig. 1.

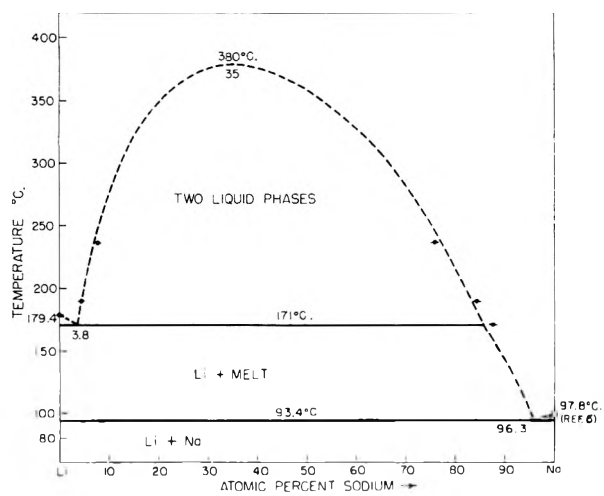

Fig. 1.

In a subsequent experiment a sodium–lithium

(1) Operated by the General Electric Company for the Atomic Energy Commission. Work carried out under contract No. W-31-109 Eng-52.

(2) C. T. Heycock and F. H. Neville, *J. Chem. Soc.*, **55**, 675 (1889).

(3) G. Masing and G. Tammann *Z. anorg. allgem. Chem.*, **67**, 187 (1910).

(4) B. Bohm and W. Klemm, *ibid.*, **243**, 89 (1939).

(5) J. H. Hildebrand and R. L. Scott, "Solubility of Non-electrolytes," Third Edition, Reinhold Publ. Corp., New York, N. Y., 1950, p. 131, eq. 47.

(6) "Liquid Metals Handbook," Second Edition, Atomic Energy Commission, Department of the Navy, Washington, D. C., 1952, p. 42.

TABLE I

COMPOSITION OF LIQUID PHASES (Sampled at temperature)

Equil. temp., °C.	Treatment of melt preceding sampling	Anal. of phases (wt. %) Top layer Li	Top layer Na	Bottom layer Li	Bottom layer Na	Av. compn. (at. %) Top layer Li	Top layer Na	Bottom layer Li	Bottom layer Na
171	3 hr. above 235°	..	..	4.0	96.0	...	...	12.4	87.6
	2 hr. at 171°								
	3 hr. above 235°	..	..	4.2	95.8				
	3 hr. at 171°								
190	24 hr. at 190°	86	14	5.3	94.7	95.7	4.3	15.6	84.4
	96 hr. at 190°	88	12	5.4	94.6				
237	48 hr. at 237°	78	22	8.8	91.2	92.2	7.8	24.2	75.8

melt was sampled at the thermal arrest of 93.4° during cooling. At this temperature a solid lithium phase and a solid sodium phase are in equilibrium with a single liquid phase. The composition of the melt was 3.7 atomic % lithium.

Discussion.—Since it was expected that lithium–sodium solutions would be simple mixtures of monatomic atoms, an attempt was made to use solution theory to extrapolate the experimental results and to predict the critical temperature and composition. A modification of regular solution theory as given by Hildebrand and Scott[5] which relates the activity of individual components to the molar volumes, the solubility parameters and the composition was used for this system. From the densities and heats of vaporization[6] the parameters $(V_1/V_2) = 0.528$ and $V_2(\delta_1 - \delta_2) = 9090$ were calculated, where V_1 and V_2 = mole volumes of Li and Na, respectively, and $\delta_1 = (\Delta E_1^V/V_1)^{1/2}$ and $\delta_2 = (\Delta E_2^V/V_2)^{1/2}$ the solubility parameters of Li and Na, respectively. The calculated critical temperature was 1350° and the composition at the critical point was 28 atomic % sodium. These results are in marked disagreement with the graphical extrapolation of the data which indicates a critical temperature of 350 to 450° at approximately the same composition. One reason for the large discrepancy is that heat of mixing may be much smaller than that calculated from the solubility parameters as a result of a somewhat ionic character of the bonding between sodium and lithium.[7]

An equation of the same form, but where the two parameters, (V_1/V_2) and $V_2(\delta_1 - \delta_2)^2$, were treated as empirical constants, was fitted to experimental compositions determined in the two liquid phase region. For the value of the constants which were obtained

$$(V_1/V_2)^* = 0.67 \text{ and } V_2(\delta_1 - \delta_2)^{2*} = 3200 \pm 50$$

a critical temperature and composition of 380° and 35 atomic % Na were calculated. The calculated immiscibility loop is given as a broken curve in Fig. 1. Experimental values are shown as large dots.

The heat of fusion of both sodium and lithium which can be calculated from the liquidus of the sodium-rich and lithium-rich alloys, respectively, are high by a factor of two to three over the accepted values of 717.1 cal./mole for lithium[8] and 622.2 cal./mole for sodium.[6] A possible explanation for such discrepancies could be limited solid solution regions on each side of the phase diagram.

Acknowledgment.—We wish to thank Mr. W. C. Judd for carrying out the analyses of sodium and lithium and Dr. L. F. Epstein for his helpful comments.

(7) Ref. 5, p. 322.

(8) "The Heat Capacity of Lithium from 25 to 900°," T. B. Douglas, L. F. Epstein, J. L. Dever and W. H. Howland, National Bureau of Standards Report 2879.

SELF-DIFFUSION IN LIQUIDS. I. CONCENTRATION DEPENDENCE IN IDEAL AND NON-IDEAL BINARY SOLUTIONS[1,2]

BY P. A. JOHNSON AND A. L. BABB

Department of Chemical Engineering, University of Washington, Seattle, Washington

Received May 19, 1955

A capillary diffusion-cell technique combined with radioactivity measurements has been used to measure self-diffusion rates in ideal and non-ideal binary liquid mixtures at 25° with an accuracy of 5%. In the ideal systems studied there was a generally linear variation of the self-diffusion coefficient with molar composition and the values for mutual and self-diffusion agreed within 10% over the entire composition range. In the non-ideal systems, however, the self-diffusion coefficient differed from the mutual diffusion coefficient by a factor of two or more except at low concentrations of the diffusing component where the agreement was within 5 to 10%. A general relationship between the mutual and self-diffusion coefficients recently proposed by Lamm and based on the existence of two frictional forces in the system was shown to be approximately true for the ideal system. The behavior of the non-ideal systems may be rationalized with this theory if the forces are considered to vary with solution composition.

Introduction

In the past few years some consideration has been given to possible relationships between mutual and self-diffusion coefficients. Several theoretical relationships have been proposed[3-5] and experimental evidence of differences between mutual and self-

(1) This work was supported in part by the Office of Ordnance Research, U. S. Army.

(2) Based in part on a Dissertation submitted by Paul Amos Johnson in partial fulfillment of the requirements for the degree of Doctor of Philosophy, University of Washington, Seattle, Washington.

(3) A. W. Adamson, THIS JOURNAL, **58**, 514 (1954).

(4) O. Lamm, *Acta Chem. Scand.*, **6**, 1331 (1952).

(5) S. Prager, *J. Chem. Phys.*, **21**, 1344 (1953).

diffusion coefficients in liquids and solids have been presented by Wang[6] and Johnson,[7] respectively. The results on solids have been discussed by Darken[8] and Seitz[9] who suggest that corrections for non-ideality would have to be made in the case of self-diffusion in the gold–silver alloys studied by Johnson.[7] Since few experimental data for components of binary non-electrolytic solutions are available to adequately compare the mutual and self-diffusion coefficients, this study was undertaken to measure the self-diffusion coefficients for components in both ideal and non-ideal binary solutions for which mutual diffusion data were available over the entire composition range.

The systems studied were selected on the basis of availability of mutual diffusion data[10, 11] and liquids suitably tagged with radioactive atoms. The ideal systems selected were benzene–carbon tetrachloride and ethanol–methanol; the non-ideal systems selected were ethanol–benzene and methanol–benzene.

Experimental

Materials.—The following compounds labeled with carbon-14 were purchased from the Nuclear Instrument and Chemical Corporation: 0.4 mc. uniformly labeled benzene, 0.5 mc. ethanol-1-C^{14}, 0.5 mc. methanol-C^{14}. The radioactivity of the liquids as purchased was approximately 1 mc./mmole.

The benzene and methanol used to dilute the tracer liquids and to make up the required non-tracer solutions were C.P. grade, analyzed reagent, obtained from the J. T. Baker Chemical Co., and the ethanol was of anhydrous grade, obtained from U. S. Industrial Chemical Co.

The radioactive liquids as purchased were initially diluted to stock solutions with an approximate activity of either 0.25 mc./cc. or 0.025 mc./cc. and stored at 5° in glass bottles. The desired tagged solution for a diffusion experiment was prepared by diluting the stock radioactive liquid with appropriate non-radioactive liquids until a solution with a radioactivity of approximately 0.004 to 0.008 mc./cc. was obtained. When a binary solution was being studied, the desired tracer solution was prepared volumetrically, but the actual composition was determined gravimetrically with an analytical balance after each solution addition. The non-radioactive solution of the same chemical composition was also prepared on a volumetric basis and the liquid additions checked gravimetrically.

Apparatus and Procedure.—The self-diffusion coefficients were determined by a capillary cell technique similar to that used by Wang.[12] The capillaries were made from nominal 1.5 mm. i.d. thick-walled capillary tubing with a precision bore tolerance of ±0.01 mm. The lengths, nominally 6 cm., were measured with a traveling microscope to ±0.01 cm.

During the diffusion process the capillaries were filled with the radioactive solution and immersed in approximately 350 cc. of non-radioactive solution contained in glass vessels sealed with screwed lids and aluminum gaskets. The capillaries were held upright by aluminum stands wedged against the cell wall to maintain rigidity. The diffusion cells were maintained at a temperature constant within ±0.03°.

The radioactivity of the solution within the capillaries was measured with a thin mica-window (1.4 mg./cm.^{2}) Geiger–Mueller tube connected to a scalar manufactured by Nuclear Instrument and Chemical Corporation. The liquid sample to be counted was placed in a cylindrical brass cell approximately one centimeter in diameter and one centimeter high. The bottom of the cell consisted of a sheet of mica, with a density of either 1.4 or 1.5 mg./cm.^{2}, sealed to the brass cell wall with Araldite cold-setting cement. After the liquid sample was placed in the cell, evaporation was prevented by sealing a brass lid to the cell wall with a thin film of silicone grease. Tests indicated that with 0.1-cc. liquid samples the counting rate remained constant for periods of several hours. This method is similar to that used by Hughes and Maloney,[13] but achieves greater simplicity at a sacrifice in counting efficiency as only approximately 0.2% of the disintegrations register as counts in the scalar.

Since the β-decay energy from carbon-14 is only 0.154 Mev., a liquid depth of approximately 0.4 to 0.2 mm. is adequate to shield completely this radiation as the liquid density varies from 0.7 to 1.5. In all cases the size of the sample was such that the liquid depth was greater than the shielding depth of the liquid in the cell so small variations in liquid had no effect on the observed counting rate.

The diffusion coefficients were calculated from the solution to Fick's second law given by Carslaw and Jaeger[14] for the particular geometry of the capillary diffusion cell use.

Results and Discussion

The statistical error introduced in the observed diffusion coefficients by the radioactive counting method employed was less than 2%, but a more conservative estimate of the error based on reproducibility of data for given concentrations and the general smoothness of the final diffusion isotherms is 5%. The results also compare favorably with those reported previously by Graupner and Winter,[15] and Partington, Hudson and Bagnall[16] for the pure liquids as shown in Table I. The agreement for methanol is within 4% and for ethanol and benzene is within the stated precision of the previous work. Although the previous investigators used deuterium to label the molecules, there should be reasonable agreement with the results of this study unless unexpected bonding changes occur when deuterium is substituted for hydrogen.

Although radioactive carbon tetrachloride was not available for this study, diffusion coefficients for the pure liquid have been recently reported by Hildebrand, *et al.*,[17] and the value at 25° is given in Table I.

TABLE I

SELF-DIFFUSION COEFFICIENTS OF PURE LIQUIDS AT 25°

Liquid	$D \times 10^5$, cm.^{2}/sec.	Reference	Stated precision of ref. work
Benzene	2.18	This work	±0.05
	2.15	Graupner and Winter	
Carbon tetrachloride	1.41	Watts, Alder and Hildebrand	± .06
Ethanol	1.02	This work	
	1.01	Partington, Hudson, and Bagnall	± .01
	1.05	Graupner and Winter	+ .05
Methanol	2.36	This work	
	2.27	Partington, Hudson and Bagnall	± .03

Ideal Systems.—The results for the benzene–carbon tetrachloride system are shown in Fig. 1,

(6) J. H. Wang, *J. Am. Chem. Soc.*, **75**, 2777 (1953).

(7) W. A. Johnson, *Tr. Am. Inst. Mining Met. Engrs.*, **147**, 331 (1942).

(8) L. S. Darken, *Am. Inst. Mining Met. Engrs., Inst. Met. Div. Metals Technol., Techn. Publ.*, 2311 (1948).

(9) F. Seitz, *Phys. Rev.*, **74**, 1509 (1948).

(10) C. S. Caldwell and A. L. Babb, THIS JOURNAL, **59**, 1113 (1955).

(11) C. S. Caldwell, Ph.D. Thesis, University of Washington, 1955.

(12) J. H. Wang, *J. Am. Chem. Soc.*, **73**, 510 (1951).

(13) H. E. Hughes and J. O. Maloney, *Chem. Eng. Progr.*, **48**, 192 (1952).

(14) H. S. Carslaw and J. C. Jaeger, "Conduction of Heat in Solids," Clarendon Press, Oxford, England, 1947.

(15) K. Graupner and E. R. S. Winter, *J. Chem. Soc.*, 1145 (1952).

(16) J. R. Partington, R. F. Hudson and K. W. Bagnall, *Nature*, **169**, 583 (1952).

(17) H. Watts, B. J. Alder and J. H. Hildebrand, *J. Chem. Phys.*, **23**, 659 (1955).

and for the ethanol–methanol system in Fig. 2. A common feature to both systems is the linearity of the self-diffusion data, the variation from a straight line being at most 10%. The linearity of mutual diffusion in ideal systems has been shown by Caldwell and Babb[10] where deviations were at most four and generally less than 2% from linearity for the three systems studied.

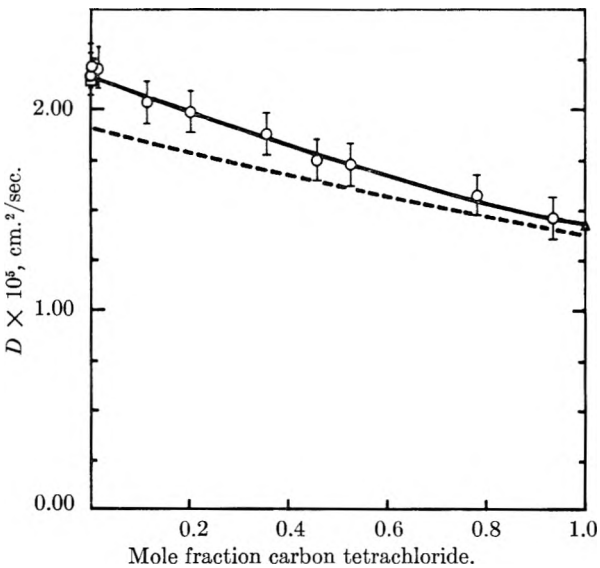

Fig. 1.—Diffusion in the carbon tetrachloride–benzene system: ○, □, self-diffusion of benzene (the authors, and Graupner and Winter, respectively); ▲, self-diffusion of carbon tetrachloride (Watts, Alder and Hildebrand); dotted line, mutual diffusion (Caldwell and Babb).

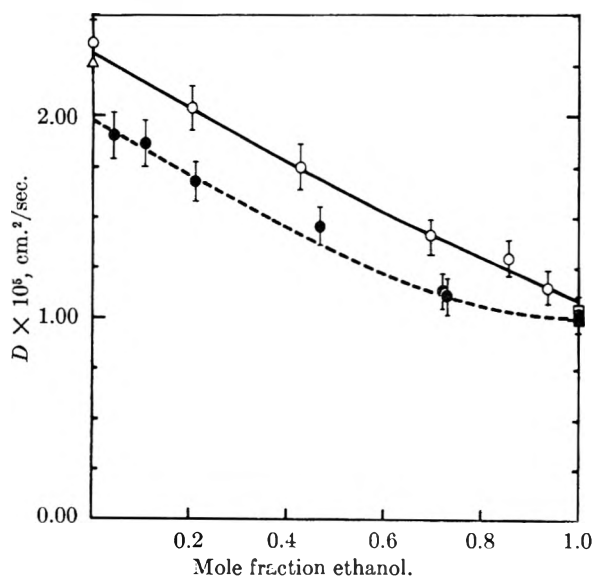

Fig. 2.—Diffusion in the ethanol–methanol system: ○,△ self-diffusion of methanol (the authors, and Partington, *et al.*, respectively); ●,□,■, self-diffusion of ethanol (the authors, Graupner and Winter, and Partington, *et al.*, respectively).

The comparison of the self-diffusion rates of benzene with the mutual diffusion rates in the benzene–carbon tetrachloride system shows that there is a significant difference between the two types of coefficients except in very dilute solution. Such behavior is not unexpected, however, if diffusion in a binary system of A and B is considered to occur by interchange of molecules. In mutual diffusion an observable transport occurs only when A and B molecules move relative to each other, but in self-diffusion this transport as well as the relative motion of like molecules is observed. In the case of concentrated solutions significantly different values of the diffusion coefficients may be observed if the molecules have greatly different tendencies to move out of position. In a dilute solution of A in B, on the other hand, A molecules are usually surrounded by B molecules and any motion of A is essentially relative to B, thus the mutual and self-diffusion coefficients will be nearly identical.

Since no mutual diffusion data were available for the methanol–ethanol system, it would be of interest to predict such coefficients from the observed self-diffusion data. From the above observations the mutual diffusion isotherm would have a value of 1.10 cm.²/sec. $\times 10^{-5}$ for pure ethanol and a value of 1.98 $\times 10^{-5}$ for pure methanol with the end values joined by a curve deviating several percentage from linearity in a negative sense.

Non-ideal Systems.—Inspection of Figs. 3 and 4 shows that the differences between mutual and self-diffusion in the non-ideal benzene–alcohol sys-

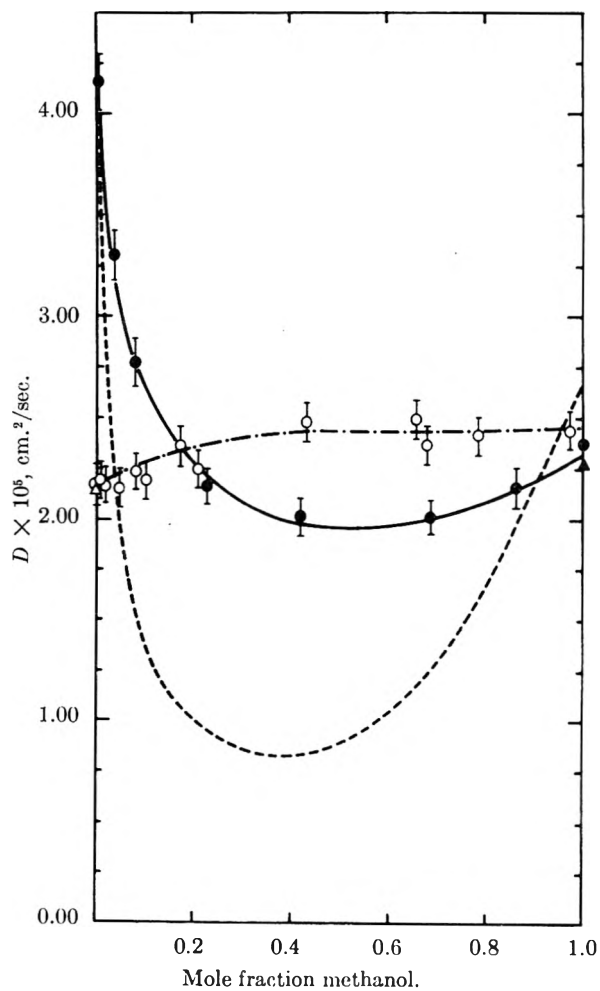

Fig. 3.—Diffusion in the methanol–benzene system: ○, △, self-diffusion of benzene (the authors and Graupner and Winter, respectively); ●, ▲, self-diffusion of methanol (the authors and Partington, *et al.*, respectively); dotted line, mutual diffusion (Caldwell and Babb).

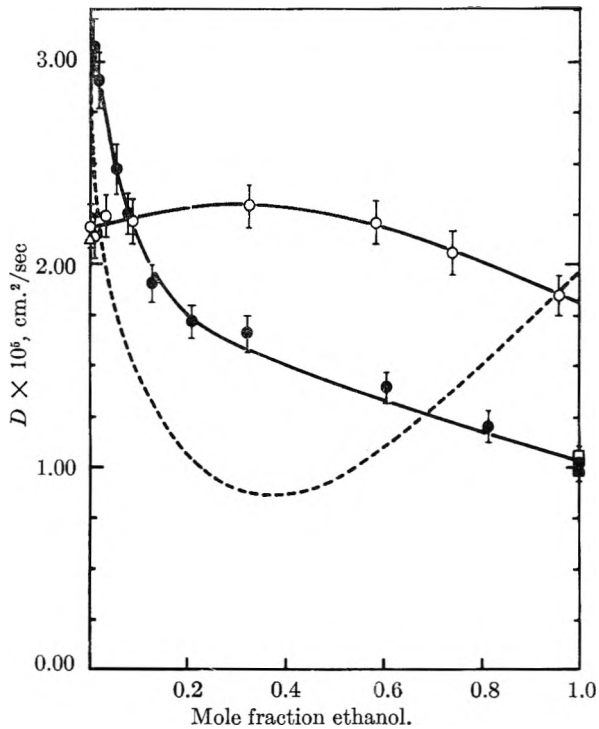

Fig. 4.—Diffusion in the ethanol–benzene system: ○, △, self-diffusion of benzene (the authors and Graupner and Winter, respectively); ●, □, ■, self-diffusion of ethanol (the authors, Graupner and Winter, and Partington, *et al.*, respectively); dotted line, mutual diffusion (Caldwell and Babb).

tems are marked, being as great as twofold or more over much of the concentration range. In general the variation of the self-diffusion coefficients was less extreme than that of mutual diffusion, particularly for benzene, which indicates that the behavior of the alcohol molecules in each system is primarily responsible for the large variations in the mutual diffusion rate with concentration. Only at low concentrations of the diffusing substance do the mutual and self-diffusion coefficients agree within 5 to 10%. While this is admittedly close to the experimental error of these measurements, it is noted that at high benzene concentrations the self-diffusion rates of the alcohols are higher and at high alcohol concentrations the self-diffusion rates of benzene are lower in both systems. This consistency in results indicates that in non-ideal systems there may be differences in the coefficients even at low concentrations of the diffusing molecule, notwithstanding the fact that simple analysis of the diffusion problem would indicate the two coefficients should agree in dilute solution. Although it was not possible to determine the self-diffusion coefficients at lower concentrations, closer agreement would not be expected in view of the behavior of the coefficients in the observed range of concentrations.

The observed self-diffusion rates of the alcohols were higher than the corresponding mutual diffusion rates and a relative decrease in the self-diffusion rate of the alcohols in very dilute solution is not expected as there is conclusive evidence that the alcohols dissociate into monomers in very low alcohol concentrations in benzene which would tend to continue to increase the diffusion rate. The self-diffusion rate of benzene, on the other hand, was changing slowly with composition at low benzene concentrations and a sudden increase in rate as the benzene concentration approaches zero is not expected.

The self-diffusion behavior of the benzene–alcohol systems appears rational in view of information on alcohol association. At high alcohol concentrations there are no sharp variations in association and hence the diffusion rates vary in a slow ordered manner. At low alcohol concentrations, however, when the dissociation into smaller aggregates begins, the self-diffusion rates of the alcohols increase sharply. The self-diffusion rate of benzene, on the other hand, is much less influenced by this behavior of the alcohol molecules because in the region where the change in association of the alcohols is most marked, the benzene is in such a high concentration that the influence of the small proportion of surrounding alcohol molecules is slight.

Application of the Prager Equation.—Prager[5] has shown that if the solution non-ideality alters the random motion of the molecules, the effect will be different if ordinary or self-diffusion is occurring with the result that the two coefficients will be related as

$$\frac{D_{12}}{D_{11}} = \frac{D_{12}}{D_{22}} = (1 + \partial \ln \gamma_i / \partial \ln x_i) \qquad (1)$$

where D_{12} is the mutual diffusion coefficient, D_{11} and D_{22} are the self-diffusion coefficients of components 1 and 2, respectively, at mole fraction x. This same result can be developed by assuming the driving force for diffusion is the gradient of chemical potential for both mutual and self-diffusion and that the hydrodynamic resisting force is the same for each type of diffusion.

Figs. 5, 6 and 7 show the mutual diffusion coefficients for the carbon tetrachloride–benzene, methanol–benzene and ethanol–benzene systems, corrected for solution activity in accordance with equation 1. Although the first system is nearly ideal

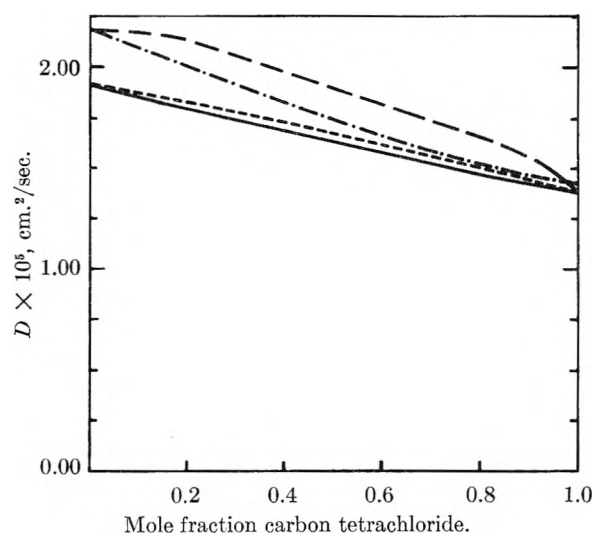

Fig. 5.—Diffusion coefficients in the system carbon tetrachloride–benzene: — · —, — —, self-diffusion of benzene (the authors, and calculated by the Lamm equation, respectively); ——, – – –, mutual diffusion (Caldwell and Babb, and corrected for solution activity, respectively).

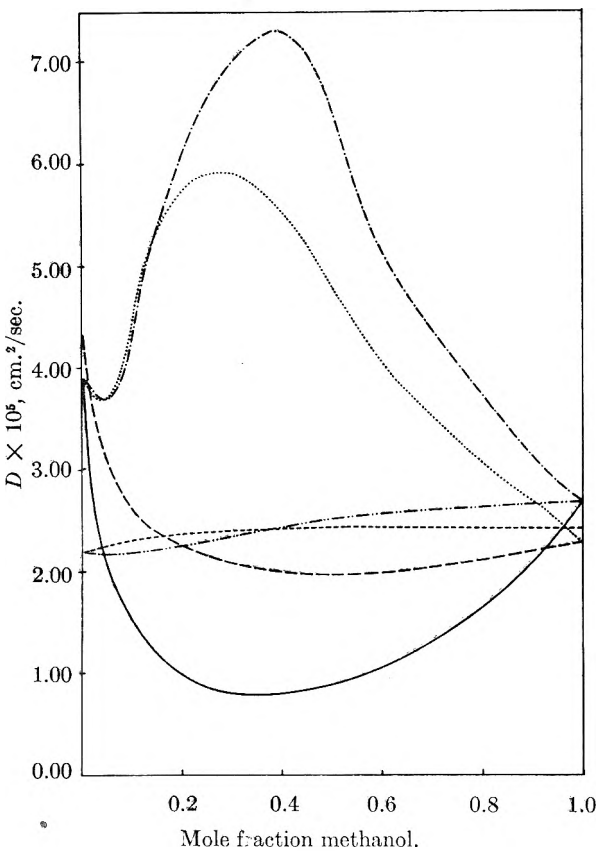

Fig. 6.—Diffusion coefficients in the system methanol–benzene: – – – –, — ·· —, self-diffusion of benzene (the authors, and calculated by the Lamm equation, respectively); — —, ... , self-diffusion of methanol (the authors, and calculated by the Lamm equation, respectively); ——, —·—, mutual diffusion (Caldwell and Babb and corrected for solution activity, respectively).

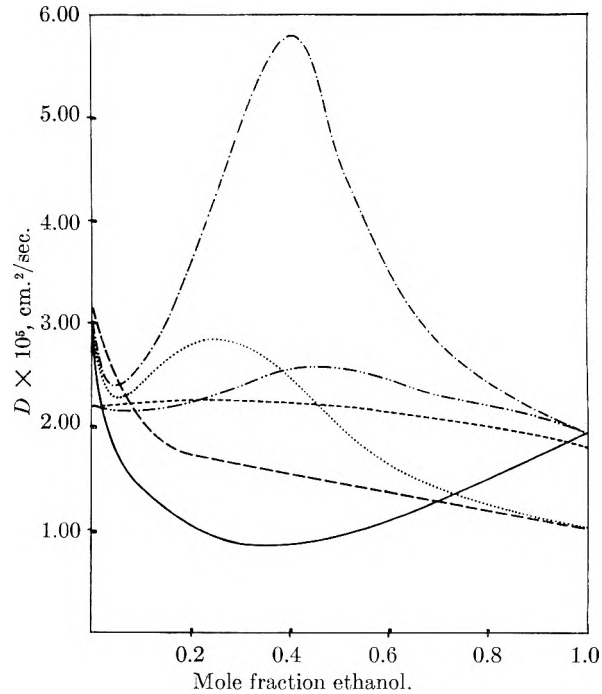

Fig. 7.—Diffusion coefficients in the system ethanol–benzene: – – –, — ·· —, self-diffusion of benzene (the authors, and calculated by the Lamm equations, respectively); — —, ... , self-diffusion of ethanol (the authors, and calculated by the Lamm equation, respectively); ——, —·—, mutual diffusion (Caldwell and Babb and corrected for solution activity, respectively).

the slight corrections noted were calculated from the total vapor pressure data of Edwards[18] at 20° assuming symmetrical constants in a Van Laar type equation. While no vapor pressure data were available to calculate activity corrections for the alcohol–benzene systems at 25°, sufficient data were available at 35° to estimate the corrections. The usual variation of activity with temperature is sufficiently small that any general observations should be valid with the estimated corrections. The activities of the methanol–benzene system were determined graphically from a plot of the partial pressure data of Scatchard, *et al.*,[19] at 35° and the corrections for the ethanol–benzene system were computed from Van Laar constants calculated from the azeotropic composition data at 34.8°.

The plotted data clearly show that correcting the observed mutual diffusion coefficients for solution activity does little to make the mutual and self-diffusion coefficients comparable, as suggested by Prager. In the ideal system the two coefficients agree within 10 to 15%, but in non-ideal systems the discrepancies become greater than threefold when the appropriate activity corrections are applied. The tendency to "over-correct" the mutual diffusion rate is perhaps not surprising as Eyring[20] indicated this same phenomenon occurred for systems with positive vapor pressure deviations from ideality when attempts were made to linearize the diffusivity–viscosity product by correcting it for solution activity.

Application of the Lamm Equation.—It is of considerable interest to verify the relation between mutual and self-diffusion coefficients proposed by Lamm.[4] This relation between the two types of coefficients is based on the concept that there is a different mechanism acting between the interchange of A molecules as compared with the exchange of A and B molecules in a binary solution of A and B. Since self-diffusion is a measure of both types of molecular exchange, it is apparent that the same phenomenological factors may not be involved. The development by Lamm has a hydrodynamic basis with one force acting between the tagged molecules and the chemically identical non-tagged molecules and another force acting between the tagged molecules and the chemically dissimilar molecules. In its more general form, however, the theory cannot be readily tested if the two frictional forces considered are not linearly concentration dependent. Since there is ordinarily no positive way of determining whether such linear concentration dependence exists Lamm has proposed a simplified equation based on a volume dependence of the frictional forces involved

$$\frac{1}{D_{11}} - \frac{x_1 v_1^{\circ}}{D_{11}^{\circ}} \cong \frac{x_2}{D_{12}} \left\{ 1 + \frac{\partial \ln \gamma_2}{\partial \ln x_2} \right\} \qquad (2)$$

(18) A. L. Edwards, B.S. Thesis, Univ. of Washington, 1954.

(19) G. Scatchard, S. E. Wood and J. M. Mochel, *J. Am. Chem. Soc.*, **68**, 1957 (1946).

(20) J. A. Kincaid, H. Eyring and E. A. Stearn, *Chem. Revs.*, **28**, 301 (1941).

where D_{12} and D_{11} are the respective mutual and self-diffusion coefficients at mole fraction x_2, v_1^0 is the molar volume of pure 1, n_1^0 is the molar concentration of 1, and D_{11}^0 is the self-diffusion coefficient of pure 1.

The conformance of the benzene–carbon tetrachloride system to this simplified equation is shown in Fig. 5, where the observed and calculated self-diffusion coefficients agree within 10%.

The observed and calculated diffusion coefficients for the non-ideal systems studied are shown in Figs. 6 and 7. Although the agreement with the Lamm equation of such systems would not be expected to be as consistent as in ideal systems, the results for self-diffusion of benzene in both systems are surprisingly accurate, the calculated values agreeing within 15% at all times and usually within 10%. This agreement might be interpreted to mean that the forces between the benzene molecules are adequately handled by assuming the benzene is non-associated in the solution. While the alcohols are associated to varying degrees dependent on the solution composition, this behavior may not greatly influence the interaction of the benzene molecules and the mutual interaction effects are included in the observed mutual diffusion coefficient.

There is little agreement between the calculated and observed self-diffusion coefficients of the alcohols. The calculated values are much too large, reaching a variation of twofold with methanol. Some of this difficulty may be due to the use of a molar volume for an associated liquid, a quantity which would vary considerably from the usual definition of the volume occupied by a formula weight of a compound. Use of a larger molar volume would have decreased the values for self-diffusion and improved the agreement. It is possible to rationalize the disagreement of the alcohols with the agreement for benzene as the interaction of alcohol molecules would be influenced by the extent of alcohol association. The effect would not then be completely included in the mutual coefficient. It has been previously noted that for systems with positive vapor pressure deviations from Raoult's law, the use of solution activity corrections does not seem to transform diffusion data into the linear concentration variation predicted by simple theory. It is reasonable that in this treatment corrections are required, either to the molar volume or by other means, to allow for some of the interactions that occur in the solution.

Acknowledgment.—One of the authors, P. A. Johnson, gratefully acknowledges the financial assistance of the National Science Foundation.

X-RAY POWDER PATTERN AND UNIT CELL DIMENSIONS OF K_2ReI_6

BY J. C. MORROW

Contribution from the Department of Chemistry, University of North Carolina, Chapel Hill, North Carolina

Received May 27, 1955

Diffraction of X-rays by powdered crystals of K_2ReI_6 indicates an orthorhombic unit cell with $a = 11.07 \pm 0.05$ Å., $b = 13.48 \pm 0.07$ Å., $c = 10.19 \pm 0.05$ Å. Density determinations indicate four molecules in the unit cell.

Introduction.—The rather peculiar behavior of K_2ReI_6 partitioned between H_2SO_4 solution[1] and ether suggested the existence of $HReI_5$ in solution. Sidgwick[2] pointed out the possibility of having in solid K_2ReI_6 a KI–$KReI_5$ mixed crystal which could correspond to the suggested parent acid. Studies of the other members of the series, K_2ReF_6,[3] K_2ReCl_6[4] and K_2ReBr_6,[5] have demonstrated that these crystals are all of the cubic K_2PtCl_6 type (space group O_h^5-Fm3m) with the halogens F, Cl and Br forming regular octahedra about Re(IV), so that for these salts the formula representation can be $K_2(ReX_6)$. The regularity of these structures and the reported solution chemistry irregularity of K_2ReI_6 made the determination of some properties of crystalline K_2ReI_6 desirable.

Experimental.—Preparation of K_2ReI_6 as suggested by Briscoe and co-workers[6] involved the reduction of potassium perrhenate with potassium iodide in hydriodic acid solution. The potassium perrhenate was certified as spectroscopically free of heavy metal impurities and containing some light metals in trace amounts only. Mr. C. E. Coffey analyzed the K_2ReI_6 and found 18.13% Re (18.16% calculated); 74.20% I (74.22% calculated); rhenium was determined as tetraphenylarsonium perrhenate and iodine as silver iodide. In the isolation of K_2ReI_6, extensive evaporation of the solvent was avoided so that unreacted potassium iodide would not contaminate the product.

Samples of K_2ReI_6 ground to pass 300 mesh screen were placed in capillary tubes and exposed to Cu Kα X-radiation, the typical Debye–Scherrer diffraction pattern being recorded on photographic film in a cylindrical camera with diameter 114.59 mm. Both collodion and glass capillary tubes were employed. Exposures with and without nickel foil filtration of the X-radiation made possible the distinction of Kα and Kβ lines. Intensities of the powder lines were estimated visually. The patterns were checked carefully for lines characteristic of potassium iodide, but none were detected.

The ease of hydrolysis of K_2ReI_6 made interaction of moist air and the finely divided samples a matter of some concern. Three weak lines which could not be assigned indices were observed. Powder diffraction studies were made of mate-

(1) W. Biltz, F. W. Wrigge, E. Prange and G. Lange, *Z. anorg. Chem.*, **234**, 142 (1937).

(2) N. V. Sidgwick, "The Chemical Elements and Their Compounds," Vol. II, The Clarendon Press, Oxford, 1950, p. 1310.

(3) O. Ruff and W. Kwasnik, *Z. anorg. Chem.*, **219**, 78 (1934).

(4) B. Aminoff, *Z. Krist.*, **A94**, 246 (1936).

(5) D. H. Templeton and C. H. Dauben, *J. Am. Chem. Soc.*, **73**, 4492 (1951).

(6) H. V. A. Briscoe, P. L. Robinson and A. J. Rudge, *J. Chem. Soc.*, 3218 (1931).

rial deliberately subjected to extensive hydrolysis. Spacings for the three strong lines of the resulting complex pattern were indeed the same as those noticed as impurity lines in the main photographs.

Density determinations for the K_2ReI_6 crystals made by the sink-float method gave as approximate value of the density 4.4 g./cm.^{3}.

Unit Cell Dimensions.—Rapid survey of the interplanar spacings shows that, unlike the other members of the K_2ReX_6 series, the hexaiodorhenate(IV) is not isometric at room temperature. Use of difference diagrams and tables for $\sin^2\theta$ as described by Henry, Lipson and Wooster[7] led to successful indexing of the pattern on the basis of an orthorhombic unit cell with dimensions: a = 11.07 ± 0.05 Å., b = 13.48 ± 0.07 Å., c = 10.19 ± 0.05 Å.; $a:b:c$ = 1.086:1.323:1. The unit cell volume is 1520 Å.^{3}, and the density is 1.121n g./cm.^{3} where n is the number of molecules in the unit cell. The rough density of 4.4 g./cm.^{3} indicates n = 4, and the X-ray value of the density is, then, 4.484 g./cm.^{3}. Table I contains interplanar spacings and *hkl* values for the observed lines.

The existence of general reflections establishes the lattice as primitive. The *hOl* and *hkO* spectra suggest glide planes c and n perpendicular, respectively, to the axes b and c. The possible space groups, then, are Pmcn (D_{2h}^{16}), $P2_1cn$ (C_{2v}^{9}), Pncn (D_{2h}^{6}), Pbcn (D_{2h}^{14}) and Pccn (D_{2h}^{10}).

(7) N. F. M. Henry, H. Lipson, and W. A. Wooster, "The Interpretation of X-Ray Diffraction Photographs," Macmillan and Co., Ltd., London, 1951, p. 182.

TABLE I

X-RAY RESULTS FOR K_2ReI_6

hkl	Interplanar spacing, Å.	Obsd. rel. int.[a]	*hkl*	Interplanar spacing, Å.	Obsd. rel. int.[a]
111	6.48	s	440	2.162	(bl)ms
200	5.56	s	115	1.980	mw
310	3.56	w	244	1.907	w
311	3.36	m	404	1.875	w
113	3.11	vs	263	1.771	vw
302	2.98	vw	006	1.698	vw
330	2.86	vw	372	1.616	vw
400	2.77	s	226	1.580	vw
313	2.462	m	654	1.307	vw
214	2.281	vw	536	1.290	vw

[a] vs = very strong; s = strong; ms = medium strong; m = medium; mw = medium weak; w = weak; vw = very weak; bl = broad line.

Acknowledgment.—The author is grateful to Dr. Roy Ingram for opportunity to use Debye–Scherrer equipment of the Department of Geology and Geography and to the du Pont Company which provided generous financial assistance.

TERNARY SYSTEMS WITH THREE SEPARATE BINODAL CURVES[1]

BY ALFRED W. FRANCIS

Contribution from Socony Mobil Laboratories (A Division of Socony Mobil Oil Co., Inc.), Research and Development Department, Paulsboro, N. J.

Received May 31, 1956

Examples have been studied of several novel types of ternary liquid systems. In certain temperature ranges (near room temperature and at atmospheric pressure) these systems have three separate binodal curves. With decreasing temperature two of the curves usually merge at their plait points (the col) to form a band. At a still lower temperature the third curve may merge with the band at a "subcol" to form a triangle indicating three liquid phases. In one system the two mergers take place in reverse order; while another system has two cols and a subcol between them in temperature. These two systems have unusual relations, which are discussed. The components of the four systems studied giving these relations are ethylene glycol, nitromethane or nitroethane, and decyl or lauryl alcohol.

Several systems with two separate binodal curves have been described recently.[2,3] Some systems with three separate binodal curves also were shown.[3] It was suggested that the phenomenon was favored by the proximity of the critical temperature of one of the components, carbon dioxide, to the temperature of the observations. Such a component has a mixing action with moderate concentrations and a demixing or precipitating action at high concentrations. However, the phenomenon can result from other conditions.

It was shown[2,3] that two wholly convex binodal curves meeting externally must do so at both plait points. If one binodal area is a band, and so lacks a plait point, its border just before contact must be concave. The shapes of these curves at and near these contacts have been schematic in physical chemistry text books since no examples of external contact had been observed. It was impractical to observed these shapes with adequate precision in the carbon dioxide systems[3] because of the high pressure, about 65 atmospheres. The systems now described were observed at ordinary pressures and temperatures.

About forty ternary systems having compositions separating into three liquid phases have been published.[3,4] These systems have three binodal areas, but the latter are not isolated by areas of homogeneous composition. None of these systems changes to one with three separate binodal curves on raising the temperature, as might be supposed. Instead, one component becomes miscible with at least one of the other two components, giving even-

(1) Presented before the Division of Physical and Inorganic Chemistry at the 128th Meeting of the American Chemical Society, Minneapolis, Minn., Sept. 1955. In this paper "separate" means isolated by areas of homogeneous composition.

(2) A. W. Francis, *J. Am. Chem. Soc.*, **76**, 393 (1954).

(3) A. W. Francis, THIS JOURNAL, **58**, 1099 (1954).

(4) Compiled by A. W. Francis in "Solubilities of Inorganic and Organic Compounds," A. Seidell and W. F. Linke, eds., D. Van Nostrand Co., New York, N. Y., Suppl. to the 3rd. ed., 1952, pp. 847, 977, 1009, 1015, 1029–1031, 1035–1036, 1070.

tually a single binodal area, either a band or a bite.[5] On lowering the temperature again, the three phase area results from the eruption of one of the extra binodal curves from *within* the first one. One binodal area already reaches a side line, and the other two extend toward the other side lines.

For three separate binodal curves to result, the components must be selected so that the three binary critical solution temperatures (C.S.T.) are not too greatly different. This requirement is not commonly met. The two least miscible of three liquids normally must be very dissimilar and immiscible in order that the third one be incompletely miscible with either. The C.S.T. of the first pair is then extremely high; or it may not even exist. Thus, in *each* of the published[3,4] three-liquid phase systems one of the binary C.S.T. cannot be observed because it is above the critical temperature of one of the liquid phases. Such a C.S.T. is imaginary.

The 44 solvents tested by Drury[6] were rearranged into an order of mutual miscibility. The first one in the new arrangement, glycerol, is miscible with the first 14 but with no others. The last one, "benzin," is miscible with 32 of the last 33. Pyridine and ethyl and butyl alcohols are miscible with all 44 solvents. In descending the series the members have a decreasing number of solvents immiscible with them near the bottom of the list and an increasing number near the top. (*Cf.* the "octagon figure."[7]) A few changes were made in the listed miscibilities as a result of experiments. Some slight inconsistencies remain which cannot be eliminated by rearrangement. For two of the solvents, adiponitrile and nitromethane, no places can be found in the list which even approach consistency. Their antagonistic solvents are distributed throughout the list. This incongruity helped in the search for reagents in the present investigation, since these two solvents were promising as "intermediate" components. An analogous listing[8] of a much larger number of solvents with respect to hydrocarbon miscibilities showed no inconsistencies.

The requirement of three neighboring C.S.T. is satisfied by systems of ethylene glycol, nitromethane or nitroethane, and some aliphatic alcohols of nine to twelve carbon atoms. The C.S.T. of glycol with eight-carbon alcohols are too low, and those with alcohols containing more than twelve carbons are too high. Four systems were studied in detail. Each shows a novel feature in type of diagram not shared by the others.

Acetonitrile and adiponitrile show miscibility relations with glycol and decyl alcohol similar to those found for the nitroalkanes, giving three free binodal curves on the three sides of the triangle, but not in any single temperature range. They mix with ethylene glycol at -13.5 and $+27°$, respectively (C.S.T.), below the cols or merging temperatures of the other two curves, which are at -1 and $41°$, respectively.

It is recognized in several physical chemistry text books that as a system with three separate binodal curves is cooled, the curves should expand and eventually overlap, forming an internal triangle, which would indicate compositions separating into

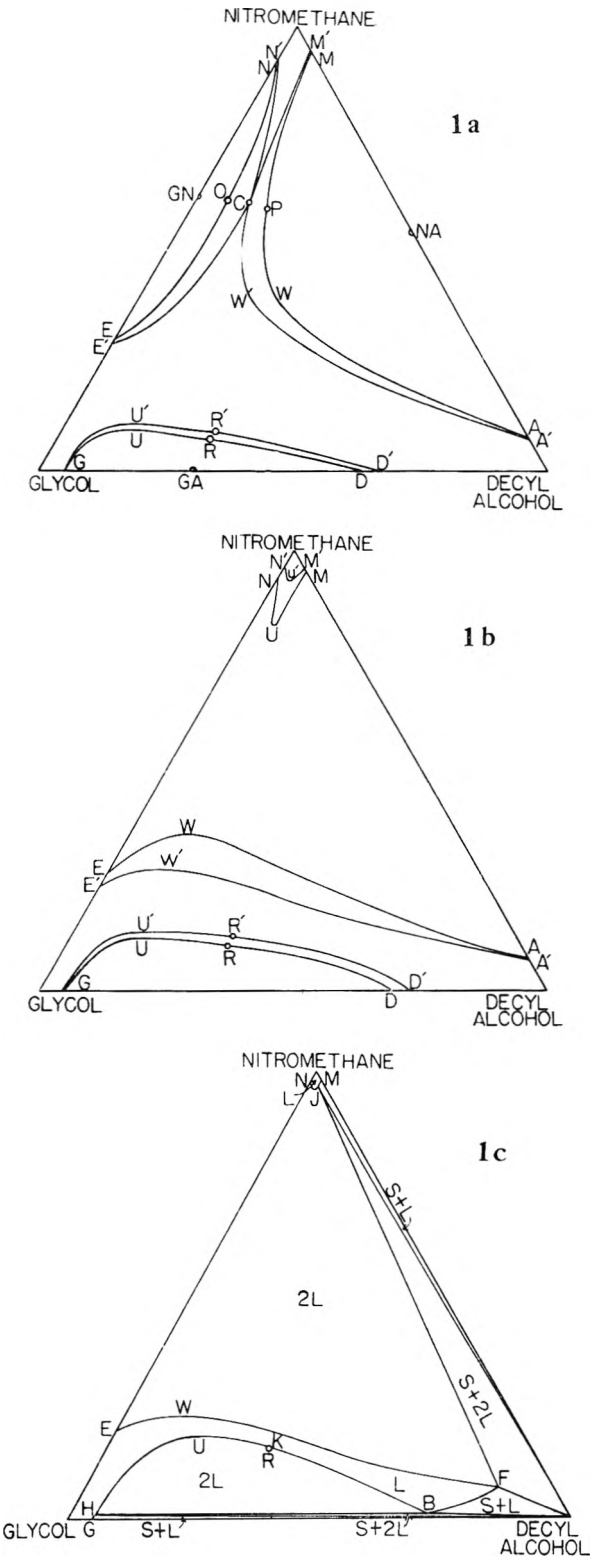

Fig. 1.—Isotherms of system ethylene glycol–nitromethane–*n*-decyl alcohol (*cf.* Table III): graph 1a, 26° (curves closer to side lines) and 23.4° (col temperature); graph 1b, 20° and 10° (curves with prime letters); graph 1c, 0°.

(5) A. W. Francis in "Chemistry of Petroleum Hydrocarbons," B. T. Brooks and others, eds., Reinhold Publ. Corp., New York, N. Y., 1954, pp. 207, 210–211.

(6) J. S. Drury, *Ind. Eng. Chem.*, **44**, 2744 (1952).

(7) A. W. Francis, *ibid.*, **36**, 1102 (1944), Fig. 4.

(8) Ref. 3, Table II, column 3.

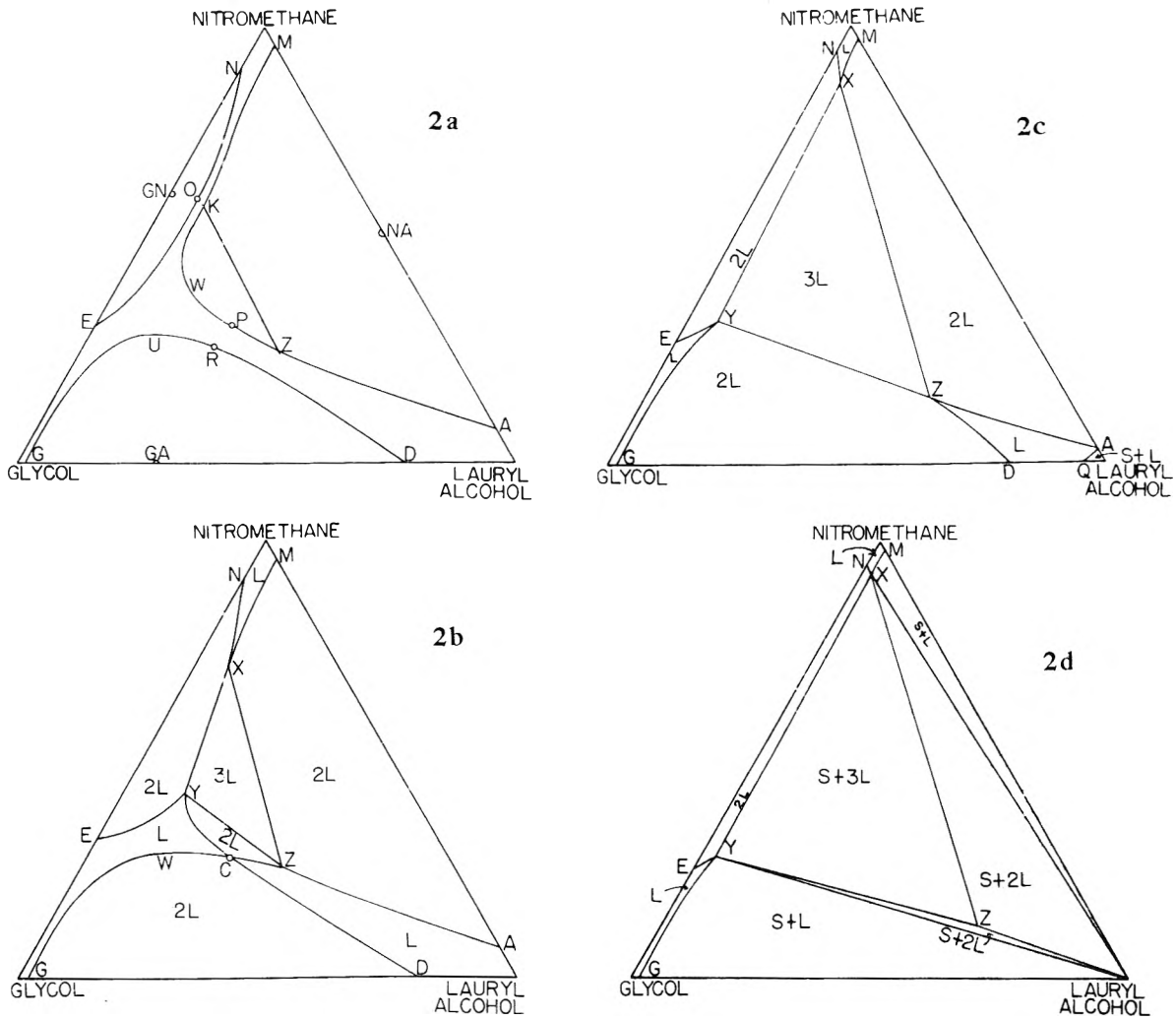

Fig. 2.—Isotherms of system ethylene glycol–nitromethane–lauryl alcohol (*cf.* Table IV): graph 2a, 29°; graph 2b, 28° (col temperature); graph 2c, 22°; graph 2d, 16° (quadruple point temperature).

three liquid phases. It would be a rare coincidence if the three curves met at the same point. Such a contact would require the curves to be sharply pointed at their plait points, a very unusual though perhaps not impossible shape. Instead, the overlapping takes place in at least two steps. In the simplest form the steps are presented by Wetmore and LeRoy[9] in schematic agreement with the present observations. The points of contact of the curves are here called for convenience the "col"[2] and the "subcol," since they are distinctly different relations.

Col and Subcol.—A col is a point in a ternary system where two separate binodal curves meet at their respective plait points (on lowering the temperature) forming a band (C in Graphs 1a, 2b, 3b, 4a). In a triangular prism diagram with temperature as the vertical coördinate the col is the low point of a ridge (Figs. 5 and 6) like that in a mountain range (from which the name col is derived). There is an appreciable area on the binodal surface near the col which is nearly flat and level. At the col $dt/dx = 0$ in each direction, but d^2t/dx^2 is positive in one direction and negative in a direction at right angles to it. There is no cusp or angular intersection of surfaces as a result of the meeting, either on the top or sides of the ridge formed. Just above the col in temperature the tie lines in the two curves approach parallelism, and the curves seem to reach toward each other, as by appointment. At the col the isotherm resembles curves intersecting at a finite angle, not curves with a common tangent.

Location of a col requires direct observations of the plait points of both curves at progressively lower temperatures and approaching compositions. This is tedious since settling of the layers is slow near the plait points, and changes in composition must be in small increments to avoid uncertainty as to which binodal curve is involved when two layers appear. However, the col temperature can usually be verified easily by observing the cloud point of a mixture of composition between those of neighboring plait points.

Observation of the upper col (at 21°) of the system glycol–nitroethane–lauryl alcohol (Graph 4a), presents a peculiar difficulty because the refractive indices of the two phases are identical. A heterogeneous composition in this region is as clear as a homogeneous one. Even the usual structural col-

(9) F. E. W. Wetmore and D. J. LeRoy, "Principles of Phase Equilibria," McGraw-Hill Book Co., New York, N. Y., 1951, pp. 126–127.

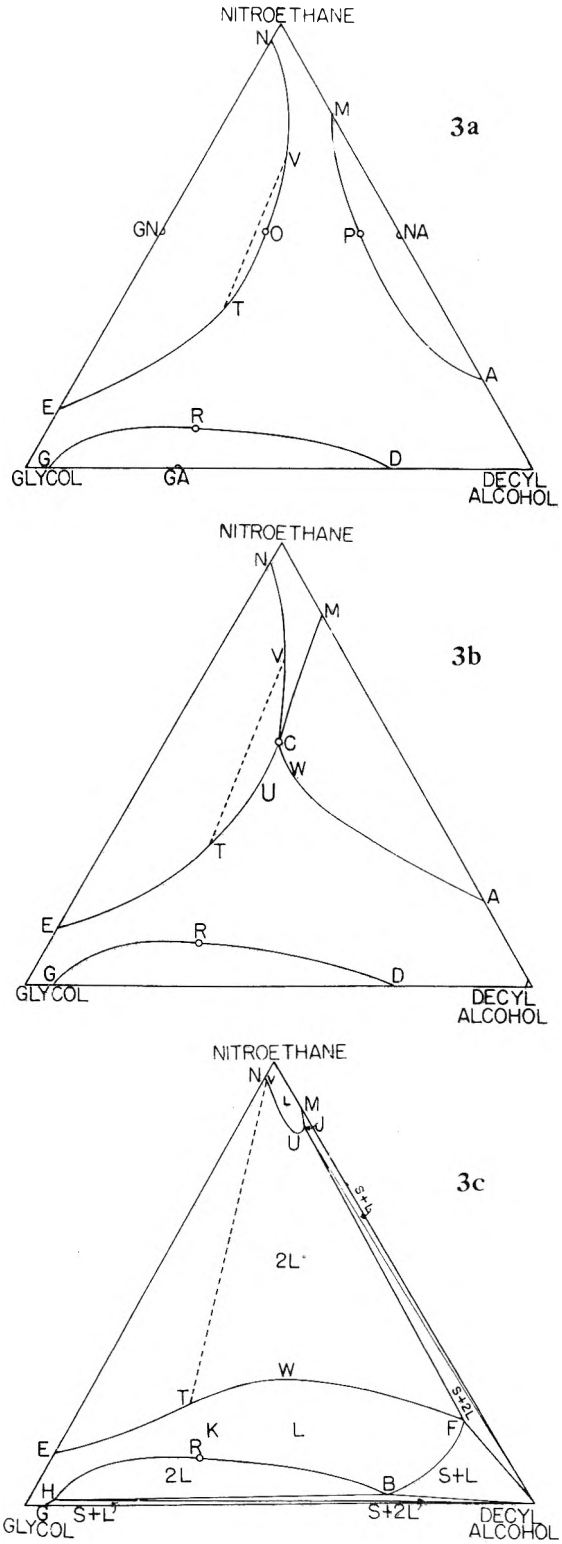

Fig. 3.—Isotherms of system ethylene glycol–nitroethane–*n*-decyl alcohol (*cf.* Table V): graph 3a, 10°; graph 3b, 6° (col temperature); graph 3c, 0°.

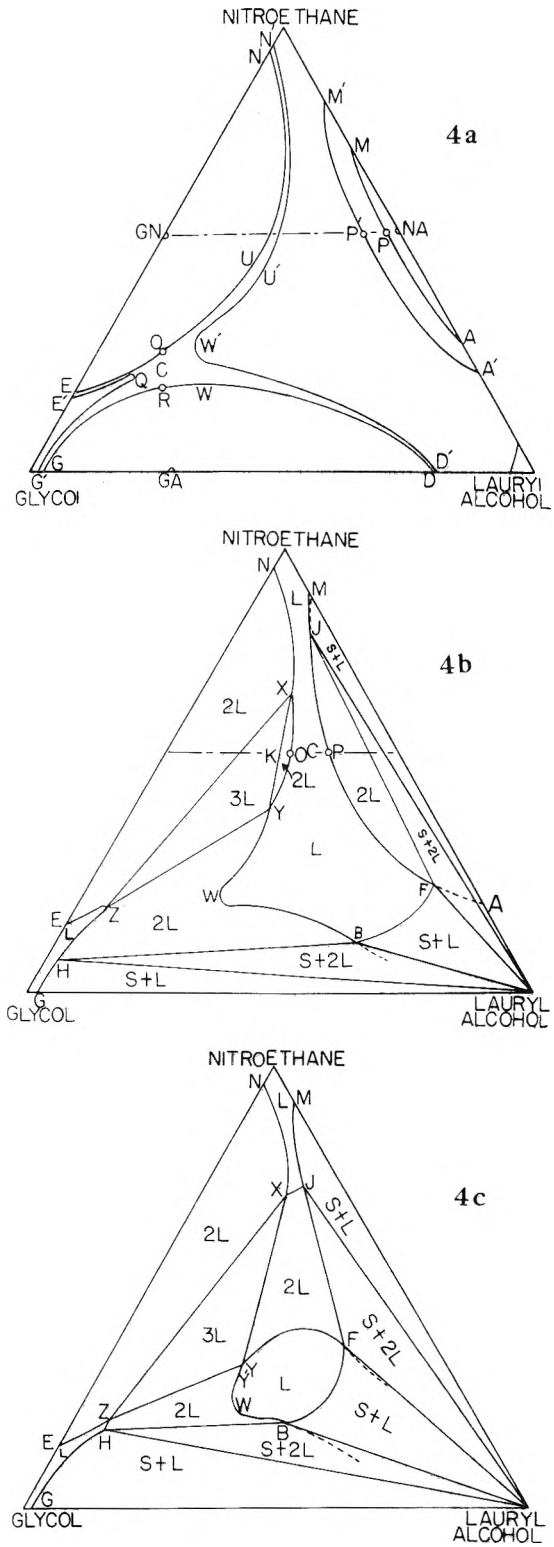

Fig. 4.—Isotherms of system ethylene glycol–nitroethane–lauryl alcohol (*cf.* Table VI): graph 4a, 24° and 20° (curves with prime letters); graph 4b, 16° (the dashed dot lines on graphs 4a, 4b indicate the vertical section shown in Fig. 6); graph 4c, 14°.

ors[10] are almost lacking because the identity of the refractive indices extends in this case practically throughout the spectrum. It was necessary to add a trace of an insoluble powder, which after several minutes collected at the interface to make it visible.

(10) A. W. Francis, THIS JOURNAL, **56**, 510 (1952).

A subcol is a point in a ternary system where a third binodal curve meets with its plait point (internally or externally) an isotherm of a ridge such as that mentioned above (K in Graphs 1c, 2a and 4b and Figs. 5, 6). The two curves lie on the same side

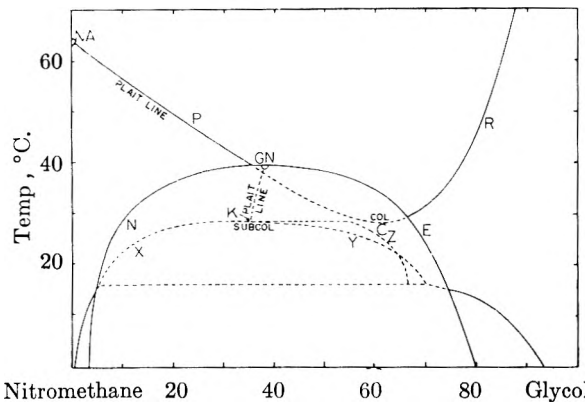

Fig. 5.—Projection on plane, ethylene glycol–nitromethane—temperature of system, ethylene glycol–nitromethane–lauryl alcohol (*cf.* Table VII).

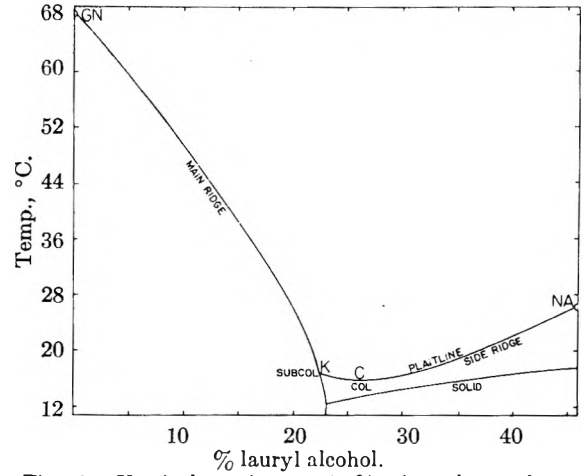

Fig. 6.—Vertical section at 54% nitroethane through triangular prism diagram of system, ethylene glycol–nitroethane–lauryl alcohol (*cf.* Table VI and Fig. 4).

of a common tangent so that if the contact is external (Graphs 1c and 2a), the border of one of the areas just before contact is concave at that point. The tie lines in the two binodal areas as the curves meet are at a sharp angle, sometimes almost perpendicular. One of them, the "subcol tie line" (KZ in Graph 2a) splits to form a triangle (XYZ in Graphs 2b, 2c, 2d, 4b, 4c) whose corners indicate the compositions of the three liquid phases.

The subcol is at the maximum temperature for coexistence of three liquid phases in equilibrium. It can also be considered as the critical solution point of two phases, X and Y, when the system is saturated with the third phase Z, of substantially different composition. In a solid diagram it is the inner end of the plait line or crest of a side ridge as it meets the main ridge below its crest. There is no flat or level spot on the binodal surface near the subcol; and below the subcol in temperature there are cusps X, Y and Z, on each side of each ridge, three in all (Fig. 5 and Table VII), corresponding to the corners of the triangles on isothermal diagrams. A system with two intersecting or crossing ridges is probably impossible because it would seem to involve four liquid phases in equilibrium in a univariant ternary system.

In most cases, probably, the col is higher than the subcol in temperature and near the subcol tie line in composition. In one system studied, however, that of ethylene glycol–nitromethane–lauryl alcohol, the col is about 0.5° lower than the subcol (Graphs 2a and 2b). This means that with descending temperature the first contact of separate curves is at the side of one of them instead of at its plait point. Such a contact, with its resulting triangular area indicating three liquid phases was unexpected.

In view of Schreinemakers' rule[11] the relation is not possible[3,5,12,13] unless the binodal curve contacted at its side is concave at that point (Graph 2a), an unusual shape for a free binodal curve in a ternary system.[14] This relation is unlikely to occur except in systems which have three separate binodal curves. In a triangular prism diagram this system shows no essential difference in type from the other three studied, since the side ridge still meets at the subcol (Fig. 5) the main ridge below its crest although at a point higher than the col. The side ridge usually slopes downward when it meets the main ridge.

In another system, ethylene glycol–nitroethane–lauryl alcohol, the side ridge contains a second col (C, Graph 4b and Fig. 6) or low point at 15.6°, and meets the main ridge on the up grade. This results in a subcol, K, at 16.5° between the two cols in temperature. The 16° isotherm (Graph 4b) shows a new binodal curve, XOY, which in effect has erupted from within the binodal band at K, forming a three phase area, XYZ, in the same manner as are those in the classical three phase systems.[4,5] Graph 4b resembles in this respect the graph of formic acid–carbon dioxide–*n*-tetradecane[15]; and isotherms at lower temperatures resemble that with *n*-hexadecane.[15] Advantage was taken of the near equality in percentage of nitroethane for the points GN, NA, P, P′ on graph 4a and K, O, C, P on graph 4b to show these relations by a vertical section in Fig. 6.

In each of the four systems here described all three ridge ends reach the side lines on the up grade. Probably systems can be found with meeting ridges (resulting in three liquid phases) in which one ridge end is on the down grade. These would have only two separate binodal curves. Each of the published three-liquid phase systems[4] has two ridge ends on the down grade. A system with all three ridge ends on the down grade is less probable. An isotherm of it might have an island triangle with binodal loops on each side of it. In the carbon dioxide systems[3] some of the ridges are inverted.

Materials and Procedure.—The properties of the reagents are listed in Table I. In view of the high freezing point of

(11) F. A. H. Schreinemakers; "Die heterogenen Gleichgewichte," H. Roozeboom, ed., Friedr. Viewig u. Sohn, Braunschweig, Germany, 1911, Drittes Heft, Zweiter Teil, pp. 6–17.

(12) A. W. Francis in "Physical Chemistry of Hydrocarbons," A. Farkas, ed., Academic Press, Inc., New York, N. Y., 1950, pp. 252–253.

(13) Ref. 4, p. 830.

(14) The conspicuous concavities in published free binodal curves are due to the presence of a fourth component (impurity or diluent), or to a fourth type of molecule resulting from reversible interaction of two of the components. (Ref. 4, pp. 895, 941, 988–989, 1003–1004, 1065, 1072, 1077, 1080–1081, 1116).

(15) Ref. 3, Graphs C10, C24.

TABLE I

PROPERTIES OF REAGENTS

Reagent		Density (temp., °C.)	$n^{20}D$	M.p., °C.	B.p., °C.	C.S.T.	With
Ethylene glycol	Obsd.	1.1101 (25)	1.4315	−13.3	...	56.5	EtOAc
	Lit.[a]	1.1099 (25)	1.4319	−12.6	197.6	57[b]	
Nitromethane	Obsd.	1.1298 (25)	1.3820	−30.5	100.5–101.5	62.5	CS_2
	Lit.[a]	1.1312 (25)	1.3820	−28.6	101.25	63.3	
Nitroethane	Obsd.	1.0469 (20)	1.3920	<−78	114–5	See below ($EtNO_2$)	
	Lit.[c]	1.050 (20)	1.392	<−50	114.8		
n-Decyl alcohol	Obsd.	0.8318 (20)	1.4372	6.8	...	22.7	MeCN
						18.4	$EtNO_2$
	Lit.	0.8292[d] (20)	1.43682[d]	6.88[e]	231[d]	22[e]	MeCN
						20[e]	$EtNO_2$
n-Dodecyl alcohol (Lauryl alcohol)	Obsd.	0.832 (24)	1.4410 at 24°	22.7	...	35.2	MeCN
						26.5	$EtNO_2$
	Lit.	0.831[c] (24)	...	23.95[e]	259[c]	35.2[e]	MeCN
						29[e]	$EtNO_2$

[a] J. Timmermans, "Physico-Chemical Constants of Pure Organic Compounds," Elsevier Pub. Co., Inc., New York, N. Y., 1950, pp. 335, 577–8. [b] G. E. Mukhin and A. A. Mukhina, *Chem. Zentr.*, **102, I,** 3434 (1931). [c] "International Critical Tables," Vol. I, McGraw-Hill Book Co., New York, N. Y., 1926, pp. 180, 248, 276. [d] C. H. Kao and S. Y. Ma, *Chem. Zentr.*, **103, II,** 3076 (1932). [e] C. W. Hoerr, H. J. Harwood and A. W. Ralston, *J. Org. Chem.*, 9, 268, 277 (1944); critical solution temperatures scaled from their graphs.

ethylene glycol as obtained, and its low critical solution temperature with ethyl acetate, both indicating low water content, it was not purified further. The nitroalkanes (Eastman Kodak Co., white label) were distilled at atmospheric pressure through a 30-cm. column with reflux, removing a trace of water; and those portions, about 75%, boiling within 1° were saved. The nitromethane was further purified by decanting that portion not frozen at −30.5°. The alcohols were purified similarly by filtering off liquid at the melting points listed.

Mutual critical solution temperatures of pairs of these and several other reagents before purification were observed as partial qualifications of the reagents for the present paper. Observations of the eight C.S.T. listed in Table II were repeated on purified material. The glycol–alcohol C.S.T. are isoöptic,[10,16] showing no turbidity but only a faint purple color below the actual C.S.T. because of identity of refractive indices of the two phases.

TABLE II

SIGNIFICANT TEMPERATURES (IN °C.) IN TERNARY SYSTEMS OF ETHYLENE GLYCOL GIVING THREE SEPARATE BINODAL CURVES

Nitroalkane	Nitromethane		Nitroethane	
Table	III	IV, VII	V	VI
Figure	1	2, 5	3	4, 6
Alcohol	Decyl	Lauryl	Decyl	Lauryl
Melting point, °C.	6.8	22.7	6.8	22.7
Critical soln. temp.				
Glycol–nitroalkane	39.7		68	
Glycol–alcohol	60	135	60	135
Nitroalkane–alcohol	56.3	63	18.4	26.5
Col	23.4	28.0	6	21, 15.6
Subcol	−1	28.5	<−10[b]	16.5
Quadruple point[a]	−1	16	None	12
Straddled component[c]	$MeNO_2$	Lauryl	$EtNO_2$	Glycol

[a] Equilibrium of three liquid phases and crystals of alcohol. [b] Metastable. Subcooled below crystallization temperature of −4°. [c] This component is on one side of the main ridge; the other two components are on the other side.

After numerous exploratory observations the temperatures indicated in the isothermal graphs were selected as those best illustrating the new liquid phase relations. The observations were made after vigorous shaking in glass stoppered graduated tubes of about 15 ml. capacity immersed in water-baths in large Dewar flasks. The water was agitated with a rapid stream of air bubbles. Temperature was read with a calibrated thermometer reading in fifths of degrees from −38 to +42°. The temperature was adjusted by adding small amounts of cooler or warmer water occasionally as required. Equilibrium temperatures in these systems were much less sensitive to moisture content than in the system of the earlier study.[2]

A filling started with 5 ml. of one reagent followed by small additions of the other two, usually alternately, to maintain a trace of lower or upper layer, until the composition of a plait point was reached, or until the tube was nearly full. Each isotherm thus required at least six fillings. When a triangular area was encountered, there were two small lower layers or two upper layers or one of each. Settling of an hour or more was sometimes required to assure presence of both trace layers.

At the lower temperatures the appearance of crystals was often delayed enough to permit some observations on metastable liquid phase relations (dashed lines in Graphs 4b and 4c), but not enough to leave uncertainty about the solid phase relations. The latter did not interfere seriously with the new liquid relations, which are the chief interest of this paper. They might have been eliminated by using a lower melting branched chain decyl alcohol.

Results are presented in the figures and in Tables II to VII. Table II is a summary of the important temperatures involved in the four systems studied. It is also an index to the graphs and to the other tables, which give the detailed compositions. The last line of Table II indicates which two binodal curves merge to form the main ridge.

Only a few of the nearly 2000 observations made are listed. Weight percentages were calculated from the volumes of reagents used and their densities, with slight adjustments based on the composition and volume of the trace layer, which was always less than 0.25 ml. (except for compositions close to plait points). In most cases integral percentages are listed. Higher accuracy would have required about twice as many observations. For clarity the graphs are lettered in a uniform manner, with the letters included in the tables. A few intermediate points are listed to permit plotting. The percentage of ethylene glycol is 100% minus the sum of the percentages listed (except in Table VII).

Each of graphs 1a, 1b and 4a illustrates two isotherms, partly to save space, but also to show more clearly the development with change in temperature. In other cases such doubling up would be too confusing.

The dashed tie lines (TV) in Graphs 3a, b, c indicate isopycnics or lines connecting compositions of equal density in equilibrium.[16] An isopycnic across a band is inevitable when the density of the straddled component (nitroethane in these graphs) is intermediate between those of the other two components, unless as in Graph 4c a three phase area is involved. The quadruple points are the temperatures of equilibrium of alcohol crystals with three liquid phases. They can be considered as the freezing points of the alcohol rich phases.

(16) A. W. Francis, *Ind. Eng. Chem.*, **45**, 2789 (1953).

TABLE III

ETHYLENE GLYCOL–NITROMETHANE–*n*-DECYL ALCOHOL[a]

(Plotted in Fig. 1. Ternary compositions in weight per cent.)

Graph 1a

Point, temp., °C.	$MeNO_2$	Decyl alcohol
GN, 39.7	62	0
GA, 60	0	30
NA, 56.3	54	46
N, 26	92	0
	75	5
O, pp.	61	6.5
	50	6
	40	5
E	30	0
G	0	5
	6	6
U	9.5	12
	9	20
R, pp.	7.5	31
	4.3	45
D	0	63
M	94	6
	76	9
P, pp.	59	14.5
W	36	30
	24	55
A	8	92
N′, 23.4	93	0
	75	7
C, col.	61	11
	45	10
	35	6
′	29	0
G	0	5
	7	8
U′	10.5	15
R′, pp.	8.5	31.5
	5	46
D′	0	66
M′	94.5	5.5
	78	8
C, col.	61	11
W′	40	20
	24	50
A′	7.5	92.5

Graph 1b

Point, temp., °C.	$MeNO_2$	Decyl alcohol
N, 20	94	0
U	82	5
M	95	5
E	27	0
W	35.5	12
	20	52
	10	80
A	7	93
G	0	5
	8	7
U	12	13
R, pp.	10	32
	7	50
D	0	69
N′, 10	96	0
U′	92.5	3
M′	96	4
E′	23	0
W′	27.5	8
	17	49
A′	7	93
G	0	5
	11	7
U′	13	16
R′, pp.	12	32
	9	50
D′	0	73

Graph 1c

N, 0	97	0
J	96	2
M	98	2
E	20	0
W	23	12
	15	45
F	6.5	82
G	0	4.5
H	1	5
	15	9
U	18.5	18
R, pp.	16	32
	10	48
B	1	71
K, −1	18	32
Subcol, also quadruple pt.		

[a] C, col (even if slightly off the isotherm in temperature, as shown in tables); K, subcol (same); O, P and R (and pp. in tables and circles on binodal curves), plait points; half circles on side lines, with double letters, binary critical solution points (at higher temperatures, as shown in tables); X, Y and Z, three liquid phases in equilibrium. (X and Y are the two phases which merge at the subcol); T, V, extremities of isopycnics; E, G, glycol rich phases in binary systems; N, M, nitroalkane rich phases in binary systems; D, A, alcohol rich phases in binary systems; B, F, H and J, liquid phases in equilibrium with crystals of alcohol and another liquid phase; U, W, maximum concentration of some component; S, L, 2L, 3L, solid and liquid phases in equilibrium in an area. (Omitted on Graphs 1a, 1b, 2a, 3a, 3b, 4a and Figs. 5 and 6); Q, miscellaneous; prime after a letter. Corresponding point at a lower temperature.

TABLE IV

ETHYLENE GLYCOL–NITROMETHANE–LAURYL ALCOHOL

(Plotted in Fig. 2. Ternary compositions in weight per cent. *Cf.* Fig. 5 and Table VII)

Graph 2a

Point, temp., °C.	$MeNO_2$	Lauryl alcohol
GN, 39.7	62	0
GA, 135	0	28
NA, 63	53	47
N, 29	90	0
	75	4
O, pp.	61	6
	42	5
E	31	0
M	96	4
	80	5
	60	8
	50	9
W	40	14
P, pp.	31.5	28
	20	55
A	8	92
G	0	2
	20	3
	25	5
U	28.5	15
R, pp.	26.5	27
	15.5	50
D	0	78
K,[a] 28.5 subcol	60	7
Z[a]	25	40

Graph 2b, 28°

N	91	0
M	96	4
X	71	7
Y	42	12
Z	25	40
E	32	0
C, col	27.5	28
G	0	2
	20	3
W	28.5	18
	16	50
D	0	79
	15	69
A	7	93

Graph 2c, 22°

Point	$MeNO_2$	Lauryl alcohol
N	94	0
M	97	3
X	87	4
Y	33	6
Z	15	57
E	28	0
G	0	2
	25	3
D	0	81
A	3	97
Q	0	96
(equil. with crystals)		

Graph 2d, 16°
Quadruple points
(all points except N and E in equil. with crystals)

N	95	0
M	98	2
X	92.5	2.5
Y	28	3
Z	12	64
E	25	0
G	0	1.5

[a] KZ is the subcol tie line. It extends slightly beyond the binodal curve in the graph at 29° since it is at 28.5°.

TABLE V

ETHYLENE GLYCOL–NITROETHANE–*n*-DECYL ALCOHOL

(Plotted in Fig. 3. Ternary compositions in weight per cent.)

Graph 3a

Point, temp., °C.	$EtNO_2$	Decyl alcohol
GN, 68	53	0
GA, 60	0	30
NA, 18.4	53	47
N, 10°	96	0
	82	10
V	69	16
O, pp.	54	20
T	36	21
	25	15
E	13.5	0
M	80	20

Graph 3b, 6°

Point	$EtNO_2$	Decyl alcohol
N	96	0
V	73	14
C, col	54	22
U	45	22.5
T	32	20
	19	10
E	13	0
M	84	16
W	50	26
	34	50
A	19	81

TABLE V (*Continued*)

Graph 3a

Point, temp., °C.	$EtNO_2$	Decyl alcohol
P, pp.	53	39
	35	57
A	21	79
G	0	5
	8	12
R, pp.	9	29
	7.5	45
D	0	73

Graph 3b, 6°

Point	$EtNO_2$	Decyl alcohol
G	0	5
	8	12
R, pp.	10	29
	7.5	45
D	0	74

Graph 3c, 0°

Point temp., °C.	$EtNO_2$	Decyl alcohol
N	96.5	0
V	95	1
U	84	12
J	86	13
M	90	10
E	12	0
T	23	22
W	28.5	37
F	19	77
G	0	4
H	1.5	5
	9	11
R, pp.	11	29
	8.5	45
B	2	70
	10	77
−4° (equil. with crystals)	20	28
K, < −10° subcol	20	28

TABLE VI

ETHYLENE GLYCOL–NITROETHANE–LAURYL ALCOHOL

(Plotted in Fig. 4. Ternary compositions in weight per cent. *Cf.* Fig. 6.)

Graph 4a

Point, temp., °C.	$EtNO_2$	Lauryl alcohol
GN, 68	53	0
GA, 135	0	28
NA, 26.5	55	45
N, 24°	94	0
	75	13
U	50	20.5
	40	19
O, pp.	32	13
E	18.5	0
M	75	25
P, pp.	54	43
A	30	70
G	0	3
	13	7
R, pp.	19	17
W	19.5	25
	16	48
	12	60
D	0	80
C, 21 col	24	15
N′, 20	96	0
	75	13
U′	46	23
	35	20
W′	27	20
	20	40
	10	65
D′	0	81
M′	84	16
P′	54	39
A′	23	77
E′	16.5	0
Q	22	10
	15	5
G′	0	2
(equil. with crystals)	0	94.5
	6	94

Graph 4b

Point, temp., °C.	$EtNO_2$	Lauryl alcohol
K, 16.5 subcol	54	22.5
N, 16	96	0
	82	10
X	68	18
O, pp.	54	24
Y	41	27
	30	28
W	22	27
	19	36
B	11	60
E	15	0
Z	19	7
H	7	3
G	0	2
M	90	10
J	82	14
P, pp.	54	32
	40	45
F	24	68
A (metastable)	20	80
C, 15.6 col	54	27

Graph 4c

	$EtNO_2$	Lauryl alcohol
N, 14	96	4
	83	11
X	71	17
Y	32	28
Z	21	7
E	14	0
H	18	7
G	0	2
M	92	8
J	73	19
F	38	45
(metastable)	29	57.5
	12	60
	18	48
B	19.5	43
U	26	48
W	23	30
Y′, 12 (quadruple point temp.)	30	30

TABLE VII

PROJECTION ON ETHYLENE GLYCOL–NITROMETHANE–TEMPERATURE PLANE IN ETHYLENE GLYCOL–NITROMETHANE–LAURYL ALCOHOL SYSTEM

(Plotted in Fig. 5. Compositions in weight percentages of ethylene glycol on a lauryl alcohol free basis. Nitromethane is 100% minus figures given. Letters at heads of columns and on curves are those of points in isotherms 2a to 2d and in Table IV.)

Plait lines[a] (Crest of main ridge)

Temp., °C.	P	Glycol	R
135 (GA)	..		100[b]
63	0[c]	(NA)	86
50	20		82
40	35		77
30	52		67.5
28 (C)	61		Col

Binary binodal curve nitromethane–glycol (End of side ridge)

Temp., °C.	N	Glycol E
0	3	80
10	4	77
16	5	75
20	6	73
22	7	72
26	8	70
28	9	68
35	18	60
39.7 (GN)	38[d]	C.S.T.

(Crest of side ridge)

	O	
39.7 (GN)	38[d]	C.S.T.
35	37	
28.5 (K)	35	Subcol

Cusps[e]

Temp., °C.	X	Y	Z
28.5	35	35	56
	(Subcol tie line)		
28	24	47	57
25	13	58	62
22	9	65	65
16	5	71	66

[a] Each point on a plait line shows compositions exhibiting the characteristics of a plait point in an isothermal system. These plait lines follow the crests of the ridges, unlike the plait line of an isothermal quaternary system (A. W. Francis, *Ind. Eng. Chem.*, 46, 205 (1954)) either on its tetrahedron or triangular prism models. [b] Critical solution point, ethylene glycol–lauryl alcohol. [c] Critical solution point, nitromethane–lauryl alcohol. [d] Critical solution point, ethylene glycol–nitromethane. [e] X and Y are the curves of meeting of the two ridges. Z is on the lauryl alcohol side of the main ridge. The curves below 16° for equilibrium with lauryl alcohol crystals are only schematic.

THE MECHANISM OF THE INHIBITION OF CORROSION BY THE PERTECHNETATE ION.[1] II. THE REVERSIBILITY OF THE INHIBITING MECHANISM

BY G. H. CARTLEDGE

Contribution from the Chemistry Division of the Oak Ridge National Laboratory, Oak Ridge, Tennessee

Received May 21, 1955

An attempt has been made to determine the extent to which the process responsible for the inhibition of corrosion by the pertechnetate ion is reversible. It has been found that the disturbance of inhibition by added electrolytes involves a specific action and not merely an increase in electrical conductivity of the solution phase. The electrode potential of electrolytic iron was measured both in potassium pertechnetate and in mixtures of this with other electrolytes. The potential was found to respond quickly to changes in the composition of the solution in a manner that clearly represented kinetic influences at the interface. It is concluded that the potential and the inhibition alike depend upon a labile state at the interface that is quickly responsive to changes in the composition of the solution.

In the theories of inhibitor action that assume an adsorption of the inhibitor[2-6] there is considerable uncertainty concerning the degree of reversibility of the adsorption. The most recent work has made use of radioactive Cr^{51}, and the difficulty in interpreting the results arises from the fact that no distinction has been made between firmly bound, unreduced chromate and insoluble or strongly held reaction products. Chromates stimulate the corrosion of carbon steel in acidic solution,[7-9] and some reduction inevitably occurs under such conditions. It is also likely that precipitated chromium(III) oxide carries with it some chromium(VI). Thus, Uhlig and Geary[10] found 3×10^{16} atoms of chromium per cm.^{2} on Armco iron, half of which was removed by long soaking in distilled water. Hackerman and Powers[6] were unable to remove the Cr^{51} adsorbed on chromium, and found no activity at *p*H 11. The interpretation of the results at high *p*H's, however, is complicated by the fact that corrosion is inhibited in sufficiently alkaline aerated solutions even without the chromate.[11]

If the inhibition were due to a film-repair mechanism[12] then the deleterious effect of hydrogen ions and chloride ions would require *ad hoc* assumptions to account for their action, such as dissolution, penetration or peptization of the protective film by the antagonistic agent. In such a case, the inhibiting mechanism itself would be completely irreversible. The experiments presented in the preceding paper[13] made it apparent that no extensive reduction of the inhibitor necessarily occurs when the inhibition is due to the pertechnetate ion. The present experiments were therefore directed to an attempt to determine, by some means not dependent upon the activity deposited on the metal, whether the inhibitory process in this case is reversible or irreversible.

Two types of experiments were conducted, involving the effect of added electrolytes upon (a) the inhibiting property of the pertechnetate ion and (b) the electrode potential of electrolytic iron in a pertechnetate solution. As shown previously,[14] inhibition by the pertechnetate was lost in the presence of sufficient concentrations of hydrogen ions or other electrolytes. For the present study, the sulfate ion was selected, since it is an excellent flocculating agent for hydrous iron oxide and could hardly be suspected of peptizing a protective film. For a second non-inhibiting ion of different charge type the perrhenate ion was chosen because of its close similarity to the pertechnetate ion in most respects.

Inhibition in the Presence of Added Electrolytes.—The inhibiting concentrations of potassium pertechnetate are so small (from 5×10^{-5} *f* up) that the solutions have a low electrical conductivity. Even 10 p.p.m. of added chloride ion is only 2.8×10^{-4} *f*. Since added electrolytes were shown to weaken or destroy the inhibiting power of the pertechnetate, this effect might be ascribed to the increase in conductivity of the solution as well as to any specific action on the metal–solution interface, such as the competitive displacement of an adsorbed inhibitor. Because of the minute amounts of reaction film formed in the presence of the pertechnetate ion it would not be likely that the effect of added electrolytes could be ascribed to a decrease in film resistance. Parallel inhibition tests were therefore conducted in two solutions of essentially equal conductivities but of different ionic types. One solution was 0.01 *f* potassium perrhenate, $KReO_4$, and the other was 0.005 *f* sodium sulfate. At 25°, the equivalent conductance of 0.010284 *f* $KReO_4$ is 119.15 mho cm.^{2} [15] and that of 0.005 *f* Na_2SO_4 is 117.28 mho cm.^{2} [16] Neither solution by itself inhibits corrosion.[17]

Each solution was made 3.6×10^{-6} *f* in techne-

(1) This work was done for the U. S. Atomic Energy Commission.

(2) Norman Hackerman and A. A. Makrides, *Ind. Eng. Chem.*, **46**, 523 (1954).

(3) E. Cook and Norman Hackerman, THIS JOURNAL, **55**, 549 (1951).

(4) H. H. Uhlig, "Metal Interfaces" A Symposium, Am. Soc. Metals, Cleveland, Ohio, 1951, p. 312.

(5) R. A. Powers and N. Hackerman, *J. Electrochem. Soc.*, **100**, 314 (1953).

(6) N. Hackerman and R. A. Powers, THIS JOURNAL, **57**, 139 (1953).

(7) T. P. Hoar and U. R. Evans, *J. Chem. Soc.*, 2476 (1932).

(8) U. R. Evans, *Trans. Electrochem. Soc.*, **69**, 213 (1936).

(9) E. Chyzewski and U. R. Evans, *ibid.*, **76**, 215 (1939).

(10) H. H. Uhlig and A. Geary, *J. Electrochem. Soc.*, **101**, 215 (1954).

(11) J. E. O. Mayne, J. W. Menter and M. J. Pryor, *J. Chem. Soc.*, 3229 (1950).

(12) T. P. Hoar and U. R. Evans, *J. Electrochem. Soc.*, **99**, 212 (1952).

(13) G. H. Cartledge, THIS JOURNAL, **59**, 979 (1955).

(14) G. H. Cartledge, *Corrosion*, **11**, 335t (1955).

(15) J. H. Jones, *J. Am. Chem. Soc.*, **68**, 240 (1946).

(16) "International Critical Tables," Vol. VI, McGraw-Hill Book Co., New York, N. Y., 1929, p. 236.

(17) Negative results with the perrhenate ion will be presented in the next paper in this series.

tium and 1 × 2 cm. emeried specimens of carbon steel (sample no. 102) were exposed at 100° (23° overnight). The metal in the sulfate solution became heavily smudged almost immediately, the solution became turbid, and rusting soon followed. The specimen in the perrhenate mixture remained bright during the first hour at 100° except for a few small blue-grey spots. After four days at 23° there were a few small areas of localized rusting in the rhenium specimen, whereas the sulfate specimen showed much rust. After three weeks, the specimen in the TcO_4^-–ReO_4^- mixture had much bright metal, some interference film, and a few very small pits. The specimen in the TcO_4^-–$SO_4^=$ mixture was dark all over, except for a large bare area that was deeply corroded and numerous other areas less deeply corroded. There was much more loose rust in suspension in this tube than in the one containing the perrhenate mixture. It was evident that whereas the presence of the perrhenate interfered to some extent with the pertechnetate inhibition, such effect was far less prominent than that observed in the sulfate solution. It appears, then, that the disturbance caused by the presence of electrolytes is not due merely to the increase in conductivity, but also involves specific effects such as competition between different ionic species in adsorption at the interface. This result is in agreement with the data of Hackerman and Powers,[6] who showed that there is a corresponding competition between chromate and sulfate ions adsorbed on chromium.

Electrode Potentials.—In another series of experiments the electrode potential of iron was measured in dilute solutions of potassium pertechnetate, potassium perrhenate, sodium sulfate and mixtures of these.[18] Measurements were made in aerated solutions and also in solutions through which nitrogen was bubbled. The temperature was 23–24°. Strips of very pure electrolytic iron 10 mil sheet about 5 mm. wide were emeried and covered with an insulating lacquer except at the ends. After the lacquer had been dried overnight at 110° the exposed end was again lightly emeried just before use. The cell consisted of the experimental half-cell bridged to a saturated calomel half-cell (S.C.E.). The measurements were made by means of a vibrating-reed electrometer and Brown recorder. Table I shows the results of a preliminary experiment. (In this table and in Figs. 1–4 the potential corresponds to the polarity of the iron electrode, *i.e.*, the European Convention for signs is followed.)

TABLE I

ELECTRODE POTENTIALS OF ELECTROLYTIC IRON (AERATED SOLUTIONS)

Electrolyte, *f*	Potential *vs.* S.C.E. (mv.)	Observations
$KTcO_4$, 10^{-3}	+ 10	No corrosion
$KTcO_4$ + Na_2SO_4, 10^{-3}	+ 5 to 8	No corrosion
$KTcO_4$ + Na_2SO_4, 10^{-2}	−290	No corrosion; *p*H 6.37 after 3 hr.[a]
Na_2SO_4, 5 × 10^{-4}	−520, drifting negative	Corroding; *p*H 6.60 after 2 hr.

[a] Slight corrosion overnight.

(18) The author is indebted to Mr. F. A. Posey for assistance in certain of these measurements.

In potassium pertechnetate alone (100 p.p.m. Tc) the potential became essentially constant at +10 mv. S.C.E. After 2.6 hours from the time of immersion, sufficient 0.05 *f* sodium sulfate was added to bring its concentration to 1 × 10^{-3} *f*. The addition caused an immediate negative shift of the potential which did not exceed 5 mv.; the potential drifted slowly back to +8 mv. S.C.E. during the next 24 minutes. At this time additional sodium sulfate was added to raise its concentration to 10^{-2} *f*. Immediately the potential debased rapidly and attained a nearly steady value of −290 mv. within about 20 minutes. The following day this value had debased further to −380 mv., *p*H had changed to 7.40, and slight corrosion had occurred.

A second specimen was measured in 5 × 10^{-4} *f* sodium sulfate alone. Corrosion set in at once; the potential went to −400 mv. almost at once and drifted steadily to lower values. After 2 hours it was −520 mv. and the following day it measured −570 mv.; corrosion was very extensive.

A similar experiment was done in which the potentials were recorded over a two-day period and the electrode was carried through two complete cycles of being ennobled in pertechnetate alone and debased by addition of sulfate. Figure 1 shows the

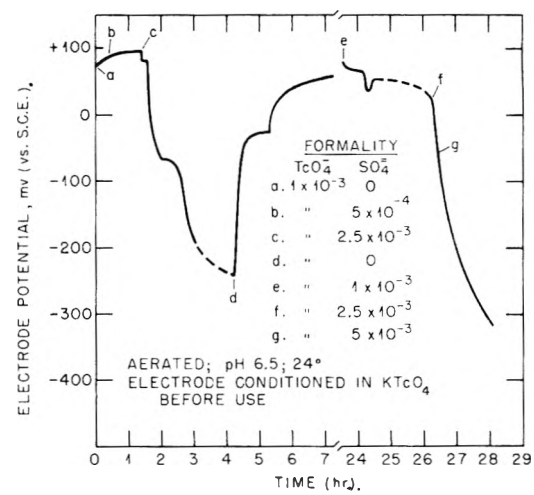

Fig. 1.—Effect of added sulfate ion upon the electrode potential of electrolytic iron in aerated potassium pertechnetate.

complete history of the experiment. Although this specimen became somewhat more noble in the pertechnetate solution than the electrode used in the first experiment and actually continued ennobling somewhat in the presence of 5 × 10^{-4} *f* Na_2SO_4, the addition of sodium sulfate up to 2.5 × 10^{-3} *f* induced immediate and extensive debasing. It is especially to be noted that the specimen returned to a noble potential rapidly when the sulfate–pertechnetate mixture was replaced by pertechnetate alone. When sulfate was next added to only 1 × 10^{-3} *f*, the electrode became unsteady and debased slightly, but the potential dropped extensively only when the sulfate concentration was again increased to 2.5 × 10^{-3} *f* and finally to 5 × 10^{-3} *f*. The debasing and re-ennobling cycle was confirmed in still a third experiment (Fig. 2). The measurements leave no doubt that the potential-determining interface is in a labile state which involves an antagonis-

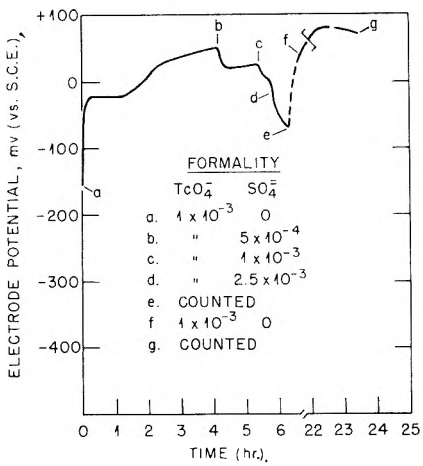

Fig. 2.—Effect of added sulfate upon the electrode potential of electrolytic iron in aerated potassium pertechnetate.

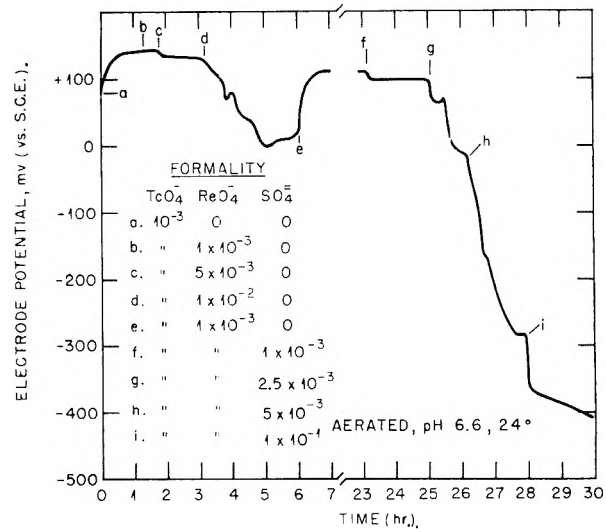

Fig. 3.—Effect of added perrhenate and sulfate upon the electrode potential of electrolytic iron in aerated potassium pertechnetate.

tic action between the sulfate and pertechnetate ions. The variation in potential corresponds precisely to the observed behavior with respect to corrosion.

These changes in potential were shown not to be associated with corresponding changes in the beta activity of the thoroughly washed electrode. Thus, in the experiment summarized in Fig. 2, the electrode was removed and counted after it had debased by 125 mv. (point e). It was then returned to the aerated pertechnetate without sulfate and left overnight. A recount was made at point g, the electrode being held as nearly in the same position in the counter as possible. The total activities found were 49 and 58 counts per minute at points e and g, respectively. Because of the uncertain geometry, absolute values of the technetium content can be only approximately estimated as in the range of 10^{13}–10^{14} atoms per cm.^{2}, but the magnitudes are seen to be very similar under both conditions. This observation again demonstrates that the counted activity is of only secondary importance for the inhibitory process itself. Had the debasing been allowed to proceed to still lower potentials, corrosion would have ensued in spite of the fact that the beta activity would then have increased greatly.

In a similar series of measurements, the debasing effect of the perrhenate ion was determined. Figure 3 shows the results of one experiment, which indicate that the noble potential reached in 10^{-3} *f* $KTcO_4$ was not appreciably debased even by 5×10^{-3} *f* $KReO_4$. An immediate and rapid debasing occurred when the concentration was raised to 10^{-2} *f*, but this soon leveled off and was rapidly reversed when the electrolyte was changed back to 10^{-3} *f* in each component (point e). Here again, the comparative effects of perrhenate and sulfate ions are similar to their effects in weakening the inhibition due to the pertechnetate ion.

The electrode potentials have a great advantage over measurements of contact potentials in demonstrating the rapid and extensive changes in the interface associated with changes in the composition of the solution, in that there is no necessity of disturbing this state by removal of the electrode from its environment. The quick and reversible responses observed demonstrate clearly the labile state prevailing at the interface. Nevertheless, the changes in potential amounting to several tenths of a volt caused by low concentrations of foreign ions correspond to relatively large free-energy differences at the active interface. This energy therefore represents, not the energy of adsorption, but the internal energy of the system made available or unavailable according to the kinetic effects due to the antagonistic components of the environment.

It was found that oxygen plays an important part in the processes responsible for this electrochemically labile interfacial state. In all the experiments described in the preceding paragraphs a stream of air bubbled through the solutions. Similar measurements were made with purified nitrogen in place of air. In aerated 1×10^{-3} *f* $KTcO_4$ at a *p*H of approximately 6.5 the different electrodes attained potentials of from +10 to 100 mv. *vs.* S.C.E. In one case, an electrode that had remained in the solution for nearly a month had a potential of +150 mv. When freshly emeried specimens were immersed in 1×10^{-3} *f* $KTcO_4$ through which nitrogen was bubbling, the potential ennobled only to −50 mv. in two experiments. Addition of sodium sulfate again caused debasing at 1–2 $\times 10^{-3}$ *f*, and subsequent admission of air in place of nitrogen led to rapid ennobling by 230 mv. (Fig. 4). The reversibility of the process with respect to the pertechnetate ion also was shown in this experiment at point g, at which an increase in the concentration of this ion caused an immediate temporary ennobling.

The Effect of Cupric Sulfate.—The reversibility of the inhibitory process was demonstrated further by the behavior of inhibited electrolytic iron toward cupric sulfate. It was observed that iron is not passivated in the usual sense when briefly dipped into a pertechnetate solution of inhibiting concentration. In repeated trials, reaction always followed promptly when a specimen was transferred from a pertechnetate solution to dilute cupric sul-

fate. The experiment was then modified as follows. An emeried piece of electrolytic iron 0.4 × 2.0 cm. was inhibited in 5×10^{-4} *f* $KTcO_4$ for 22 hours at 23°. At this time its beta activity corresponded to 1.2×10^{-5} mg. Tc per cm.^{2} Cupric sulfate was next added to the pertechnetate solution to make its concentration 1×10^{-4} *f*. A control specimen was placed in cupric sulfate alone at the same concentration. The control showed definite browning of the surface in 8 minutes and rusting soon followed. After 18 hours in the cupric solution containing technetium, the specimen was completely bright and there was no evidence whatever of precipitation of copper or corrosion of the iron. The beta count was slightly lower than before. The copper concentration was then raised to 2×10^{-4} *f*. After 5.5 hours additional, there was still no evidence of reaction. The specimen was then washed and placed in 1×10^{-4} *f* $CuSO_4$ alone. In a few minutes at 23° it developed brownish splotches similar to those that formed on the uninhibited control, and rusting followed.

The electrode potential measurements showed that in fully aerated pertechnetate solution iron ennobles to 0–100 mv. positive to the saturated calomel electrode. At 0 mv. (S.C.E.), the $Cu(c) \rightleftarrows Cu^{++} + 2e$ half-reaction would be in equilibrium at a cupric ion activity of 5×10^{-4} *f*, whereas at +100 mv. much higher activities would be required. The fact that an inhibited specimen failed to react in the experiments just described but did react when the cupric ion concentration was somewhat higher therefore shows that the difference was due to the effect of the competing sulfate ions. Only after the potential has been debased by the sulfate ion does the reduction of cupric ions become thermodynamically possible, even when their concentration greatly exceeds that used in the tests for passivity.

Discussion

The experimental observations bearing on the degree of reversibility of the process directly concerned in the inhibition are as follows.

a. A rather definite minimum concentration of pertechnetate ions must be maintained in solution to ensure inhibition[14] although there is no continuing consumption of inhibitor.[13]

b. Addition of sulfate ions to an inhibiting pertechnetate solution disturbs the inhibition much more than addition of potassium perrhenate of approximately the same electrical conductivity and at the same normality.

c. In like manner, both sulfate and perrhenate ions debase the potential of iron in a pertechnetate solution, but the sulfate ion is effective at lower concentrations than the perrhenate ion. The changes in potential are rapid and may be reversed by decreasing the concentration of the added ion. The potentials are also promptly responsive to changes in the oxygen concentration.

d. The same kind of lability of inhibited specimens was shown in experiments with addition of cupric sulfate.

All these results point to the conclusion that the inhibited state is labile with respect to the concentrations of the pertechnetate ion and other constituents of the solution. The effects of sulfate ions in debasing the potentials and disturbing the inhibition can hardly be related to any assumption of penetration or dispersal of a protective film. A competing adsorption, which may be partly statistical and partly specific, appears to be the most reasonable interpretation of the results. The fact that 5 p.p.m. of technetium was found[14] to be effective at 250° as well as at 23° is consistent with the view that the reversible process involved in the inhibition has a small energy change. The corrosion process is so complicated, however, that this fact by itself may not be considered as an argument for that view.

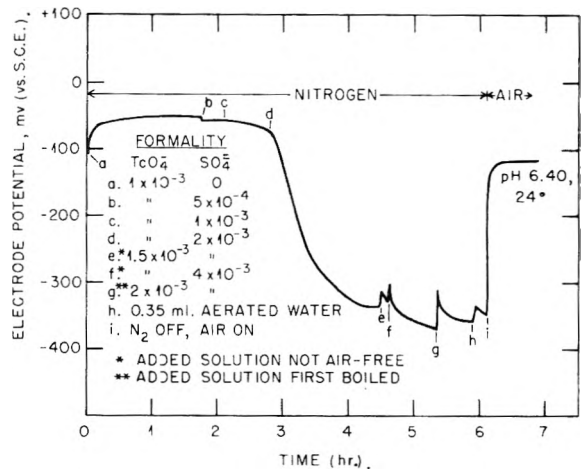

Fig. 4.—Effect of added sulfate and air upon the electrode potential of electrolytic iron in deaerated potassium pertechnetate.

It is important to observe that a weak adsorption is not inconsistent with the relatively large changes in potential observed in the iron–pertechnetate half cells when sulfate ions were present. The base potentials observed in the absence of inhibitor are corrosion potentials not far from the anodic potential, since the cathodic half-reaction is largely polarized. If the inhibitor were perfect, one would then observe the oxidation–reduction potential of the substances active at the interface, such as oxygen and the metal surface compound, or inhibitor in oxidized and reduced states. If inhibition is imperfect, intermediate potentials will be observed on account of the continuing corrosion.[19] The changes in potential here found, therefore, do not measure the energy of adsorption in any way, but indicate, rather, the extent to which the inhibitor has diminished the local-action currents that prevent the full energy of the oxidation–reduction system from being registered by the measured potential.[20]

Previous workers with the chromate ion as inhibitor have variously interpreted their measurements of the activity found after thorough washing of the metal specimen. Brasher and Stove[21] were probably correct in assuming their chromium activity to be Cr_2O_3 (or hydrated oxide), particularly in view of the slowness of the gain in activ-

(19) K. J. Vetter *Z. Elektrochem.*, **55**, 274 (1951).

(20) The argument for the lability of the effective interface is not altered if the effect of electrolytes is ascribed directly to changes in the electrical double layer, since such changes depend, in turn, upon the specific electrical differences among the adsorbed species.

(21) D. M. Brasher and E. R. Stove, *Chemistry and Industry*, **8**, 171 (1952).

ity, which reached its maximum value only after several days. Others have used the ill-defined term "chemisorption" for such binding of the inhibitor, the implication being that the process involves much energy and is irreversible. Hackerman and Powers,[6] and Powers and Hackerman[5] have used this term, though their experiments suggest that the activity is, in part, permanently held on the surface, and, in part, subject to competitive displacement by sulfate or hydroxide ions. It would appear that the permanence of the measured chromium activity even after treatment with 1 *M* sodium sulfate or 1 *M* sodium hydroxide at 100°, as reported by these authors, and the failure of the activity to exchange with inactive Cr(III) or CrO_4^{--} are hardly consistent with the view that the activity counted pertains exclusively to unreduced, competitively adsorbed chromate ions. It appears more in harmony with all the facts to assume both a competing adsorption, by which inhibition, if any, is determined, and also a reaction, wherever conditions are favorable, by which the detectable deposit is produced. The deposit may or may not affect corrosion rates, depending upon its nature. Thus, the permanganate ion might well be an inhibitor for iron or steel at low concentrations if its oxidation–reduction potential were not so high that adsorbed ions rapidly react and form a film which is not protective. If the radioactivity counted in the chromate and technetium experiments really represented adsorbed ions alone, it would be difficult to understand how "saturation" of the surface could arise with so minute a fractional covering as was observed in the technetium experiment in the presence of hydrogen peroxide.[13]

It is interesting to note that the iron electrode was considerably more noble in a pertechnetate solution than it was in a chromate solution of equal concentration and at the same acidity, in spite of the opposite relation of the oxidation–reduction potentials.[22] This result, together with the observation that the iron potential in the chromate system was not sensitive to low concentrations of sulfate ions ($4 \times 10^{-3} f$), indicates that the inhibition may depend upon different processes in the two cases. It would appear legitimate to conclude that the pertechnetate ion produces an essentially perfect inhibition which is, however, very sensitive to competing ions, whereas the chromate ion is less effective with respect to the adsorption process subject to competition but also inhibits by a mechanism involving reduction at active anodes.

(22) Unpublished preliminary measurements that confirm the result of reference 10 so far as $10^{-3} f$ K_2CrO_4 is concerned.

THE MECHANISM OF THE INHIBITION OF CORROSION BY THE PERTECHNETATE ION.[1] III. STUDIES ON THE PERRHENATE ION

BY G. H. CARTLEDGE

Contribution from the Chemistry Division of the Oak Ridge National Laboratory, Oak Ridge, Tennessee

Received June 4, 1955

It has been shown that the perrhenate ion, ReO_4^-, which is very similar to the pertechnetate ion, TcO_4^-, in most respects, differs from it radically in failing to inhibit corrosion under aerated conditions. Radioactive Re^{186} was used, in part, to eliminate the possibility that the radioactivity of technetium is involved in this difference. Measurements of the electrode potential of electrolytic iron in the presence of potassium perrhenate and sodium sulfate demonstrated the weakness of the ennobling effect of the perrhenate ion in aerated solutions and the greater susceptibility of this effect to competition with the sulfate ion, in comparison with the ennobling effect of the pertechnetate ion. In the absence of air, no ennobling by the perrhenate ion was observed. The results are applied to a discussion of the hypothesis that interfacial polarizations arising from the internal charge distribution of the pertechnetate ion are the source of its action.

In a study of the relation of ions and molecules of the general formula XO_4^{n-} to the inhibition of corrosion it was shown[2-5] that the pertechnetate ion, TcO_4^-, is an effective inhibitor for iron and steel over a wide range of temperatures. The elements technetium and rhenium and their corresponding compounds are very similar in their properties because of the lanthanide contraction. Thus, in the 7^+ valence state they form oxides X_2O_7 that are far more stable than M_2O_7; both the acids HXO_4 are strong, and their salts with most heavy metals, so far as known, have high solubilities.[6-9] The XO_4^- ions are approximately tetrahedral in crystals, and the molar volumes of the solid ammonium salts differ by only 1.9%, the perrhenate having the larger value. The oxidation–reduction potentials for the couples $XO_2(c)$–XO_4^- aq. have the values −0.51 v. for rhenium,[10] and −0.738 v. for technetium.[11]

In view of the attempt to relate the action of corrosion inhibitors of the type of the chromate ion to chemisorption with some kind of electronic interaction between the tetrahedral oxygen atoms and the substrate,[12] a comparison of the pertechnetate and perrhenate ions has especial significance. This paper presents the results of experiments which demonstrated that the perrhenate ion differs radi-

(1) This work was done for the U. S. Atomic Energy Commission.
(2) G. H. Cartledge, *J. Am. Chem. Soc.*, **77**, 2658 (1955).
(3) G. H. Cartledge, *Corrosion*, **11**, 335t (1955).
(4) G. H. Cartledge, THIS JOURNAL, **59**, 979 (1955).
(5) G. H. Cartledge, *ibid.* **60**, 28 (1956).
(6) Wm. T. Smith, Jr., and S. H. Long, *J. Am. Chem. Soc.*, **70**, 354 (1948).
(7) Wm. T. Smith, Jr., and G. E. Maxwell, *ibid.*, **71**, 578 (1949).
(8) Wm. T. Smith, Jr., *ibid.*, **73**, 77 (1951).
(9) Wm. T. Smith, Jr., and G. E. Maxwell, *ibid.*, **73**, 658 (1951).
(10) W. M. Latimer, "Oxidation Potentials," Sec. Ed., Prentice–Hall, Inc., New York, N. Y., 1952, p. 244.
(11) G. H. Cartledge and Wm. T. Smith, Jr., THIS JOURNAL, **59**, 1111 (1955).
(12) H. H. Uhlig, "Metal Interfaces," A Symposium, Am. Soc. Metals, Cleveland, Ohio, 1951, pp. 312–335.

cally from the pertechnetate ion in respect to its effect upon the corrosion of iron and steel.

Experimental Materials and Procedures.—Two samples of crystalline potassium perrhenate were used. The first was a commercially available salt obtained from A. D. Mackay, Inc. The second was a salt known to have exceptionally high purity and was obtained through the generosity of the University of Tennessee. Standard solutions of these materials were prepared by dissolution of dried and accurately weighed quantities in distilled water. A 0.01 *f* solution of the Mackay salt when treated with silver nitrate gave a turbidity approximately corresponding to that produced in a potassium chloride solution containing 5 p.p.m. of chloride. (This amount of chloride would have been of no consequence in the inhibition produced by the pertechnetate ion in the low concentrations required.) A similar test on the second sample disclosed the presence of an even lower concentration of chloride. Solutions of the two salts gave absorption spectra in the region of 2200 to 2500 Å. that were entirely similar in detail.

In order to determine the possible influence of radioactivity upon the inhibiting properties of the salt, a 5-ml. portion of 0.01 *f* potassium perrhenate was subjected to neutron irradiation in the Oak Ridge graphite pile, whereby activities due to K^{42}, Re^{186} and Re^{188} were produced.[13]

The test metal was a mild steel containing 0.097% carbon (sample no. 102) and the test procedures were the same as those described in a previous paper.[3] The specimens were abraded with 2/0 emery and degreased in acetone before use.

Results.—Tests for inhibition were made by using potassium perrhenate dissolved in distilled water at the following concentrations: 5×10^{-5}, 1×10^{-4}, 5×10^{-4}, 1×10^{-3}, 3×10^{-3}, 3.5×10^{-2} and 7×10^{-2} *f*, the last solution being saturated at about 30°. The acidity of the solutions initially was approximately *p*H 6. In every case, formation of a black smudge occurred at 100° in a matter of minutes and corrosion proceeded steadily. At the first four concentrations shown above weight losses were measured in tests extending for a week, the temperature being near 100° during the days and 23° at night. The corrosion rate was very similar to that in water alone.

To eliminate the possibility that the Mackay salt used in the preceding experiments was insufficiently pure, a few inhibition tests were made by using the extremely pure potassium perrhenate obtained from the University of Tennessee. When hand-polished specimens of carbon steel were placed in 10^{-3} and 10^{-2} *f* solutions of this salt at 100°, smudge formation and subsequent corrosion occurred exactly as described in the preceding paragraph.

In order to determine whether it is possible to replace a portion of the necessary technetium by rhenium, an experiment was conducted in the customary manner in which the solution contained 3×10^{-5} *f* technetium, which is just insufficient for inhibition, with 1×10^{-4} *f* potassium perrhenate. No inhibition was observed, so that it seems unlikely that even part of the technetium required for inhibition can be replaced by rhenium.

One of the differences between technetium and rhenium is the fact that rhenium has a fairly stable 6^+ valence state. This makes the oxidation–reduction relationships somewhat dissimilar, since the possible reduction of rhenium to the 6^+ state on contact with iron would give a different situation, with respect to potentials, from that existing in the presence of the pertechnetate ion. For this reason a further test for inhibition was made by using a potassium perrhenate solution to which was added a low concentration of hydrogen peroxide to maintain oxidizing conditions. As previously reported,[4] inhibition was maintained by the pertechnetate ion in the presence of hydrogen peroxide. Rapid corrosion ensued in the corresponding perrhenate experiment.

A further difference between technetium and rhenium is the radioactivity of technetium. While it was not considered at all likely that the radioactivity of technetium is responsible for its inhibitory properties, experiments were conducted with potassium perrhenate containing radioactive Re^{186} and Re^{188} produced by neutron bombardment of a solution of inactive potassium perrhenate. In the first experiment, the test solution was 5×10^{-4} *f* and was obtained by adding a small volume of the active material to the inactive solution, the proportions being such that the mixture of potassium and rhenium activities had 8×10^7 counts per min. per ml. on a 2π gas-flow proportional counter. When the steel specimen was placed in the solution at a temperature near 100° a dark smudge appeared in less than 15 minutes and the solution acquired a heavy brown turbidity. In this experiment the total activity was considerably higher than that in a pertechnetate solution of equal concentration. A second experiment was therefore run in a similar manner in which the total activity was reduced to 1.8×10^7 counts per min. per ml. and the total rhenium concentration was raised to 1×10^{-3} *f*. Here again reaction set in immediately. A third experiment was done a week after the preparation of the active material. The total rhenium concentration was again 1×10^{-3} *f*. The K^{42} (12.4 hr. half-life) and Re^{188} (17 hr. half-life) had essentially decayed; the Re^{186} activity in the mixture amounted to 1.07×10^6 counts per min. per ml., which is very close to the counting rate from 50 p.p.m. of technetium. Again corrosion began within 15 minutes, so it must be concluded that the perrhenate ion is incapable of acting as an effective inhibitor at 100° under any of the conditions employed in this study. Characteristically, the corroding specimens quickly became slate colored, reddish-brown iron(III) hydroxide went into suspension in the water, and a spectrographic examination of the thoroughly washed specimen revealed the presence of rhenium in some form.

To supplement the tests for inhibition, the effect of the perrhenate ion upon the electrode potential of electrolytic iron was determined in the manner previously described for the pertechnetate ion.[5] The iron half-cell was stirred by a stream of air and the potential was measured against a saturated calomel half-cell (S.C.E.) of the Beckman type at 24°. When the iron electrode was immersed in 1.0×10^{-3} *f* $KReO_4$ having a *p*H of 6.35 the potential soon became approximately steady at 230 mv. negative to the S.C.E. (European convention). This value was intermediate between the values previously observed in 5×10^{-4} *f* Na_2SO_4 and 1×10^{-3} *f* $KTcO_4$, respectively. Addition of sodium sulfate to the perrhenate solution in amount

(13) The author is indebted to Mr. G. W. Leddicotte of the Analytical Chemistry Division of this Laboratory for the irradiation.

sufficient to make it 1×10^{-3} *f* in sulfate caused a shift to −375 mv. in 9 min., and an increase of the sulfate concentration to 1×10^{-2} *f* gave a further rapid debasing to −460 mv. In the corresponding measurements with potassium pertechnetate, 10^{-3} *f* sulfate had only little effect on the potential, and even 10^{-2} *f* sulfate caused much less debasing than that observed here. These observations are in harmony with the results of the preceding paper[5] in that they indicate a slight, easily reversed adsorption of the perrhenate ion at the interface, but without the production of inhibition against dissolved oxygen.

A similar measurement was then made with a stream of nitrogen, freed from oxygen by hot copper, passing through the solution. The electrolyte was 1×10^{-3} *f* potassium perrhenate, and the potentials of two electrodes were measured. The details of the changes in potential of one of the electrodes are shown in curve I, Fig. 1. The two electrodes behaved in exactly similar manner, and at no point did their potentials differ by more than 35 mv.; at most points they were within 10 mv. of each other. Initially the solution contained air, and the electrode potential was similar to that observed in the preceding experiment. After the nitrogen had been passing for two minutes, the potentials debased rapidly, with an inflection at −425 mv. and a halt at −660 mv. From the normal potential for the ReO_2(c)–ReO_4^- electrode[10] it may be calculated that ReO_2 should begin to form at about −300 mv. (S.C.E.) under the prevailing conditions, and that hydrogen at 1 atm. could form at −570 mv. Experience in attempting to prepare ReO_2 electrodes by electrolyzing potassium perrhenate with platinum cathodes has shown that little ReO_2 is deposited unless hydrogen is being evolved rapidly. It is therefore possible that the halt at −660 mv. indicated the beginning of reduction, since the electrodes appeared unchanged until potentials in the neighborhood of −700 mv. were reached. At point b the electrodes were slate-gray in color, and the solution was clear and colorless.

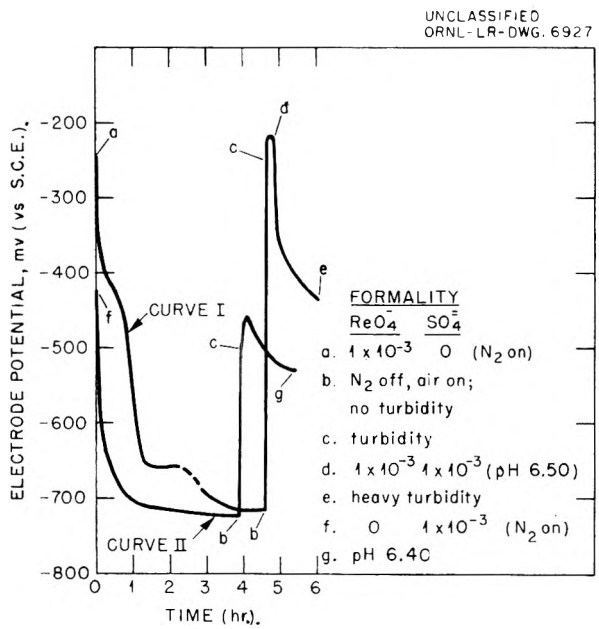

Fig. 1.—Electrode potential of electrolytic iron in potassium perrhenate or sodium sulfate in nitrogen.

At point b the nitrogen was replaced by air. In three minutes the potential rose 470 mv., and in five minutes the electrodes were apparently steady at −215 and −225 mv., respectively. Addition of sufficient sodium sulfate to bring its concentration to 1×10^{-3} *f* again caused an immediate and extensive debasing as shown in Fig. 1. Turbidity in the solution and browning of the electrodes were observed at point c, and the solution was very turbid at the end of the experiment.

In another experiment the potentials of two iron electrodes were measured in 1×10^{-3} *f* sodium sulfate alone, first in nitrogen and then in air (curve II, Fig. 1). It will be seen that the potential fell rapidly to −720 mv. (S.C.E.) and then remained almost constant; the two electrodes were always within 20 mv. of each other. There was no halt such as was observed in the perrhenate experiment. When air was admitted after almost four hours, the potentials rose very rapidly to a maximum of about −450 mv., after which slow debasing and obvious corrosion ensued. From the previous measurements in aerated sodium sulfate[5] it is known that the potential would have continued to fall as corrosion proceeded. Such an abrupt and temporary ennobling which follows admission of air to a corroding system has been observed repeatedly. It is doubtless due to the rapid oxidation of adsorbed or dissolved hydrogen to unstable peroxy products, such as HO_2 or hydrogen peroxide itself.

The results again demonstrated the extreme lability of the electrode interface, as shown in the preceding paper.[5] It is seen, however, that perrhenate ions, in contrast to pertechnetate ions, have no ennobling effect except in the presence of oxygen. In air, the potential is above the thermodynamic potentials for the reduction of either hydrogen ions or perrhenate ions, but the reduction of oxygen is not eliminated, as the corrosion experiments demonstrated. In the absence of air, the potential fell to the same value as was obtained in sodium sulfate.

Discussion.—The negative results obtained with potassium perrhenate convincingly demonstrated that the inhibition is not a property of the XO_4^- ion considered as a whole, but must reside in some intraionic characteristic. By using radioactive Re^{186} and Re^{188}, possible effects due to radiation were eliminated from consideration. By using hydrogen peroxide together with potassium perrhenate any effects due to reduction to Re(VI) were probably eliminated.

If one looks inside the respective ions for possible sources of inhibition, the remaining differences between the pertechnetate and perrhenate ions are (a) their different oxidation-reduction potentials, (b) possibly different activation energies for their reduction, and (c) possibly different degrees of polarity in the X–O bonds. Doubtless these three electrical properties are fundamentally related. The hypothesis may, therefore, be suggested that the type of inhibition exhibited by the pertechnetate ion arises from reversible, dynamic adsorption of the tetrahedral ion in the interface, whereby the sur-

face undergoes an electrostatic polarization under the influence of the intra-ionic polarity of the inhibitor particle. This involves superimposing upon the longer-range image charge a short-range effect in immediate proximity to the adsorbed ion. Whereas the image charge derives from the total charge of the ion as a unit, the short-range effect is specific for each ionic species.

With such a mechanism, the inhibitor would find energy for adsorption in the electrostatic interactions. If the extreme assumption is made that the TcO_4^- ion is polar, the geometry of the ion is such that a simple electrostatic calculation shows that negative charge should concentrate under the Tc^{7+} central atom of the tetrahedral ion having one face adsorbed at an interface as shown in Fig. 2. On a heterogeneous surface the preferred sites energetically would then be those at which the greatest negative charge could be induced that is, the most cathodic spots electrochemically. The polarization would have the effect of binding and shielding the electrons required in the cathodic part of the corrosion process, which is another way of saying that the activation energy for the cathodic reduction of either hydrogen ions or oxygen molecules would be increased. It is possible that the inhibitor ion also displaces adsorbed oxygen, which the experiments show to be involved in the competing process, thereby making its interaction with the substrate more difficult. A further effect should be the interference of the adsorbed ion with the diffusion of ferrous ions away from the interface, because of their electrostatic interaction with the tetrahedral oxygen ions. All these electrostatic interactions would be relatively weak, so that the lability of the inhibited state as reported in the preceding paper[5] would be expected.

The specifications for an inhibitor on such a basis would be as follows: (a) a geometry suitable for adsorption; (b) a high formal central charge (Cr^{6+}, Tc^{7+}) and a high degree of internal polarity ($CrO_4^=$ *vs.* $SO_4^=$); (c) an oxidation–reduction potential low enough, or an activation energy high enough, to prevent rapid reduction of the ion; (d) a solution containing sufficiently low concentrations of competing ions or molecules.

To apply the preceding discussion to the failure of the perrhenate ion to inhibit under any conditions studied, it seems necessary to ascribe this failure tentatively to the assumption that a favorable internal charge distribution is lacking. That the difference between the *adsorption* of the pertechnetate and perrhenate ions is merely one of degree is probably indicated by the measurement of the electrode potentials referred to above. This is also indicated by the behavior of the two ions on anion-exchange resins, in that the pertechnetate ion is the more strongly held.[14] This analogy need not be valid, however, since adsorption on a metal or conducting interfacial film may permit electrical forces to operate that are not available at a resin surface.

If one seeks the origin of the difference between technetium and rhenium with respect to the *inhibitory* property, the following facts are doubtless involved in one way or another. In the Re^{7+} ion the central charge is screened by the development of the 4 *f* electron levels, which are not occupied in technetium. Since the dioxides of technetium and rhenium differ in their free energy of formation by only 2 kcal., the lower oxidation–reduction potential of the perrhenate ion certainly represents a weaker pull on extraneous electrons by the ReO_4^- ion, and hence, conceivably, a weaker polarizing influence. Some evidence that rhenium forms more highly covalent bonds than exist in analogously constituted technetium compounds may be found in the report by Nelson, Boyd and Smith[15] that the hexachlororhenate(IV) ion is distinctly more stable toward hydrolysis than the corresponding technetium compound. The same authors reported also that the lattice constant for the potassium chloro salt is, unexpectedly, smaller in the rhenium compound. The precise effect of the electronic configuration of complexes such as the XO_4 ions upon their oxidation–reduction potentials and activation energies, is, unfortunately, not known, however, so that it does not appear possible to be explicit concerning the internal charge distribution on the basis of present information.

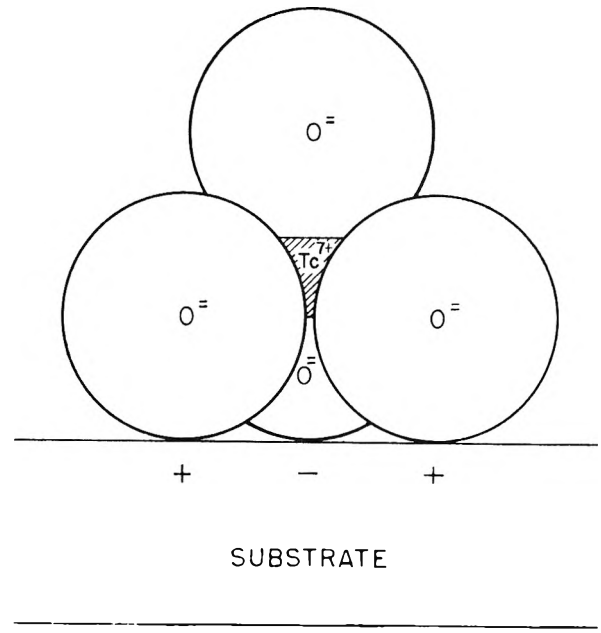

Fig. 2.—Short-range polarization by the pertechnetate ion.

It should be observed, however, that the experiments showed the pertechnetate ion to be effective in aerated water at 100° at somewhat lower concentrations than are required for inhibition by chromate ions. Since the chromate ion is bivalent, whereas the pertechnetate ion is univalent, the effectiveness of the two ions should be in reverse order if it depended in any way upon the gross charge of the ion. Likewise, the order should be reversed if inhibition depended upon the ability of the inhibitor to oxidize ferrous ions. Both of these considerations reinforce the conclusion, necessitated by the perrhenate experiments, that specific interac-

(14) Personal communication from Dr. G. E. Boyd.

(15) C. M. Nelson, G. E. Boyd and Wm. T. Smith, Jr., *J. Am. Chem. Soc.*, **76**, 348 (1954).

tions involving the internal electrical properties of the adsorbed ion are responsible for the action of inhibitors of the type under consideration.

It should be noted also that, if the proposed polarization mechanism has merit, it can account for the well-known stimulating effect of such ions as Cl^- and $S^=$ upon ferrous corrosion without the necessity for *ad hoc* hypotheses. In these cases, polarization under the influence of the net ionic charge would displace negative charge from the site of adsorption, thereby decreasing the activation energy for the cathodic portion of the corrosion process. The negative ions should also facilitate the formation and dissolution of metallic cations by electrostatic action.[16,17]

(16) A possible objection to the assumption of such polarizations may be based upon the recognition that a metal behaves as an infinite reservoir of electrons. This is not pertinent, however, for two reasons. First, actual metals are in no sense homogeneous energetically, so far as corrosion processes are concerned. Second, almost certainly under aerated conditions the "surface" of the substrate is not metallic, but a conducting or semi-conducting oxide film in which electrical discontinuities are or may be prominent.

(17) The author gladly acknowledges the benefit of many conferences with Professor Wm. T. Smith, Jr., of the University of Tennessee, concerning the chemistry of technetium and rhenium, and also his kindness in providing the very pure potassium perrhenate used in certain experiments.

ION EXCHANGE IN CONCENTRATED SOLUTIONS, NaCl–HCl AND LiCl–HCl SYSTEMS

BY HIDETAKE KAKIHANA, NOBUO MARUICHI AND KAZUO YAMASAKI

Contribution from Chemical Institute, Faculty of Science, Nagoya University, Nagoya, Japan

Received June 1, 1955

Ion exchange was studied in the concentrated solutions of NaCl–HCl and LiCl–HCl systems. The amount of water adsorbed in the resin was calculated from the difference of the amount of hydrogen ion before and after the ion-exchange equilibrium. The amount of adsorbed water decreases as the concentration of chloride ion increases both in NaCl–HCl and LiCl–HCl systems. Differences were found between NaCl–HCl and LiCl–HCl systems. The anomaly found in the latter system was explained by assuming the dehydration of Li ion in concentrated solutions. In NaCl–HCl system the Donnan equilibrium was found to exist between the resin and the solution phases. The same equilibrium exists only in 0.1 and 0.3 *N* solutions in the LiCl–HCl system.

Although ion exchange in concentrated solutions has been applied successfully by several investigators to the separation of transuranic elements from rare earths[1] and mutual separation of transition elements,[2] etc., very few investigations have been reported on ion-exchange equilibria in solutions of large ionic strength. The present work is an attempt to study the equilibria of ion exchange in concentrated NaCl–HCl and LiCl–HCl systems.

Experimental

(1) **The Resin.**—The resin used was Amberlite IR-120 (hydrogen form, medium cross-linkage) of mesh size 30–50 obtained by dry screening at 40° and it contained 17% of water. The amount of resin used in one batch experiment was 3.6 g., *i.e.*, about 15 milliequivalents.

(2) **Reagents.**—Sodium chloride was precipitated from its saturated solution by hydrogen chloride. Lithium chloride was prepared by adding hydrochloric acid to lithium carbonate, which has been purified by recrystallization. Hydrochloric acid was distilled twice.

(3) **Procedure.**—A certain amount of resin (exchange capacity E, meq.) was put into a glass-stoppered erlenmeyer flask (capacity 100 ml.) containing a known quantity (V, ml.) of 1–5 *N* NaCl–HCl or 0.1–12 *N* LiCl–HCl mixtures. After shaking for 40 min. in a thermostat at 25.0 ± 0.1°, the resin was quickly separated from the solution by suction on a glass filter. The time required for filtration was 60 sec. An aliquot of the filtered solution was titrated with 0.1 *N* barium hydroxide solution, and the hydrogen ion concentration $(H^+)_S$ was determined. If the volume change of the solution can be neglected before and after the ion exchange, the total amount of hydrogen ion in the solution, $[H^+]_S$, is given by $[H^+]_S = (H^+)_S V$. After the above procedure, the chloride ion concentration $(Cl^-)_S$ was determined by Fajans argentometric titration, using fluorescein as an indicator.[3] If we neglect the volume change as before, the amount of chloride ion in solution, $[Cl^-]_S$, is given by $[Cl^-]_S = (Cl^-)_S V$. The separated resin was then poured into a column (20 cm. × 1 cm. diameter) with water and washed repeatedly with distilled water. The amount of hydrogen and chloride ions in these washings, $[H^+]_Q$ and $[Cl^-]_Q$, were similarly determined by titration. Then 0.1 *N* NaCl solution was passed through the resin column, and the effluent was titrated with 0.1 *N* barium hydroxide. The amount of hydrogen ion which had been retained in the resin, $[H^+]_R$, was thus determined.

Assuming that neither complex species are adsorbed nor volume of the solution changes, relations between the quantities determined above are as

$$\left.\begin{aligned} &[Na^+]_R = E - [H^+]_R \\ &[Cl^-]_R = [Cl^-]_O - [Cl^-]_Q - [Cl^-]_S \\ &[Na^+]_Q = [Cl^-]_Q - [H^+]_Q \\ &[Na^+]_S = [Na^+]_O - [Na^+]_Q - [Na^+]_R = \\ &\qquad\qquad \{(Cl^-)_S - (H^+)_S\}V \\ &[H^+]_S = (H^+)_S V, \\ &[Cl^-]_S = [Cl^-]_O - [Cl^-]_Q \\ &[Cl^-]_O = [H^+]_O - [Na^+]_O \end{aligned}\right\} \quad (1)$$

where parentheses and brackets represent concentration and amounts of ions, respectively. Subscripts O, R, S and Q denote the original solution, the resin phase at equilibrium (the perfect exchange phase), the outer solution phase at equilibrium and the quasi-exchange phase, respectively. The last phase consists of ions which exist in the resin phase or on the surface of the resin at equilibrium, but can be washed out easily with water. That phase includes also the interstitial solution held by the resin bed after the filtration.

Similar relations hold in the LiCl–HCl system too.

Results and Discussion

(1) **Adsorbed Water.**—The study of the water adsorbed by the resin which is in contact with the

(1) K. Street, Jr., and G. T. Seaborg, *J. Am. Chem. Soc.*, **70**, 4268 (1948).

(2) K. A. Kraus, *et al.*, *ibid.*, **71**, 3263, 3855 (1949); **72**, 4293, 5792 (1950); **73**, 9, 13, 2900 (1951); **74**, 843 (1952); **75**, 1460, 3273 (1953); **76**, 984, 5916 (1954); **77**, 1383 (1955).

(3) A 10% Tween-20 (polyoxyethylene sorbitan monolaurate) solution was added to the solution to make the end-point clearer; *cf.* H. Nogami, K. Sekiguchi and F. Nakagawa, *J. Pharm. Soc. Japan*, **74**, 1402 (1954).

outer solution phase, is important in ion exchange and many authors have tried to determine its amount by various methods.[4-7] However, the methods used by previous investigators in dilute solutions cannot be used in the present ion-exchange studies in concentrated solutions. The amount of adsorbed water was therefore estimated indirectly by the following calculation.

The total amount of hydrogen ion in the resin and the solution is equal to

$$(H^+)_S(V - A) + [H^+]_Q + [H^+]_R$$

where A is the volume of water adsorbed in the resin phase at equilibrium, and the first term denotes the amount of hydrogen ion in the outer solution. The total amount of hydrogen ion is also equal to $E + [H^+]_O$. Thus

$$(H^+)_S(V - A) + [H^+]_Q + [H^+]_R = E + [H^+]_O$$

By arranging the equation

$$A = \frac{(H^+)_S V + [H^+]_Q + [H^+]_R - \{E + [H^+]_O\}}{(H^+)_S} = \frac{\Delta[H^+]}{(H^+)_S} \quad (2)$$

As all the terms in (2) are determined experimentally, the amount of adsorbed water A can be calculated. Values of A thus determined for NaCl–HCl and LiCl–HCl systems are shown in Table I. The

TABLE I

NaCl (N)	HCl (N)	Adsorbed water/g. dry resin, ml.	LiCl (N)	HCl (N)	Adsorbed water/g. dry resin, ml.
	0.53	1.00		0.00	1.06
0.5	1.05	0.99		1.18	0.89
	2.06	0.89	0.10	3.53	.87
	0.00	0.92		7.42	.67
	1.05	.87		11.5	.53
1.00	2.01	.77		0.00	0.51
	3.01	.71		0.93	.96
	4.02	.73	1.00	2.78	.96
	0.00	0.89		7.19	.68
	1.01	.79		11.6	.33
2.00	2.02	.69		0.00	0.55
	3.00	.69		0.93	.93
	0.00	0.85	2.00	3.95	.69
3.00	1.01	.73		8.53	.39
	2.01	.65		10.3	.32
				0.00	0.73
				1.97	.56
			4.00	4.31	.45
				7.29	.16
				0.00	0.12
				1.95	.47
			6.00	3.93	.28
				4.86	.05

amount of adsorbed water decreases as the concentration of Cl^- ion increases both in NaCl–HCl and LiCl–HCl systems. However, even in the most concentrated solution the amount of adsorbed water is not negligible, so we had to replace V with $(V - A)$ in formula (1) in the following calculation.

(2) **Adsorption of Complex Species.**—If some complex species were captured by the resin so firmly that they could not be washed out with water, $[Cl^-]_R$, namely, $[Cl^-]_O - [Cl^-]_Q - [Cl^-]_S$ would not be zero. And if some complex species were captured by the resin so loosely that they could be washed out easily with water, there might be some quantitative relations between $[Na^+]_Q$ (or $[Li^+]_Q$), $[Cl^-]_Q$ and $[H^+]_Q$ or at least those values would be rather high compared with normal surface adsorption. However, neither of these cases was observed in our experimental data. We can therefore conclude that, within the experimental error, we are dealing only with $H^+(+H_2O)$–$Na^+(+H_2O)$ or $-Li^+(+H_2O)$ exchange.

(3) **NaCl–HCl System.**—We shall assume that in this NaCl–HCl system Donnan equilibria are established between ions in the resin and the outer solution. Then we have

$$A^R_{Na^+}A^R_{Cl^-} = A^S_{Na^+}A^S_{Cl^-} \quad (3)$$

$$A^R_{H^+}A^R_{Cl^-} = A^S_{H^+}A^S_{Cl^-} \quad (4)$$

where A denotes the activity of an ion. Dividing (3) by (4)

$$A^R_{Na^+}/A^R_{H^+} = A^S_{Na^+}/A^S_{H^+} \quad (5)$$

or

$$A^R_{Na^+}/A^R_{H^+} = \frac{A^R_{Na^+} + A^S_{Na^+}}{A^R_{H^+} + A^S_{H^+}} \quad (6)$$

or

$$A^S_{Na^+}/A^S_{H^+} = \frac{A^R_{Na^+} + A^S_{Na^+}}{A^R_{H^+} + A^S_{H^+}} \quad (7)$$

We can use analytical concentrations in place of activities in equations 6 and 7. Then either of the following relations hold[8]

$$\frac{[Na^+]_R}{[H^+]_R} \fallingdotseq \frac{[Na^+]_S + [Na^+]_Q}{[H^+]_S + [H^+]_Q} = \frac{[Na^+]_R + [Na^+]_S + [Na^+]_Q}{[H^+]_R + [H^+]_S + [H^+]_Q} = \frac{[Na^+]_O}{[H^+]_O + E} \quad (8)$$

$$\frac{[Na^+]_S}{[H^+]_S} \fallingdotseq \frac{[Na^+]_R + [Na^+]_Q}{[H^+]_R + [H^+]_Q} = \frac{[Na^+]_S + [Na^+]_R + [Na^+]_Q}{[H^+]_S + [H^+]_R + [H^+]_Q} = \frac{[Na^+]_O}{[H^+]_O + E} \quad (9)$$

As shown in Fig. 1, our experimental data are expressed by a straight line with the slight deviations in the region of larger values of $[Na^+]_O/\{[H^+]_O + E\}$, if $[Na^+]_R/[H^+]_R$ is plotted against $[Na^+]_O/\{[H^+]_O + E\}$, while the deviations are much more enlarged, if $\{[Na^+]_R + [Na^+]_Q\}/\{[H^+]_R + [H^+]_Q\}$ is plotted against $[Na^+]_O/\{[H^+]_O + E\}$. Again straight lines with gradient 1 are obtained if $[Na^+]_S/[H^+]_S$ and $\{(Na^+]_S + [Na^+]_Q\}/\{[H^+]_S + [H^+]_Q\}$ are plotted against $[Na^+]_O/\{[H^+]_O + E\}$ as in Fig. 2. These facts show that the Donnan equilibria of Na^+ ion and H^+ ion exist between the resin phase and the solution phase and the differences of activity coefficients are not so large even in the resin phase. It is rather difficult to decide which is the better expression, (8) or (9), in our

(4) K. W. Pepper and D. Reichenberg, *Z. Elektrochem.*, **57**, 133 (1953); B. R. Sundheim, M. H. Waxman and H. P. Gregor, THIS JOURNAL, **57**, 974 (1953).

(5) K. W. Pepper., D. Reichenberg and D. K. Hale, *J. Chem. Soc.*, 3129 (1952).

(6) H. P. Gregor, K. M. Held and J. Bellin, *Anal. Chem.*, **23**, 620 (1951).

(7) C. W. Davies and G. D. Yeoman, *Trans. Faraday Soc.*, **49**, 968 975 (1953).

(8) At the present stage the quasi-exchange phase cannot be treated independently, so it is added to either solution phase (8) or resin phase (9) in the following treatment.

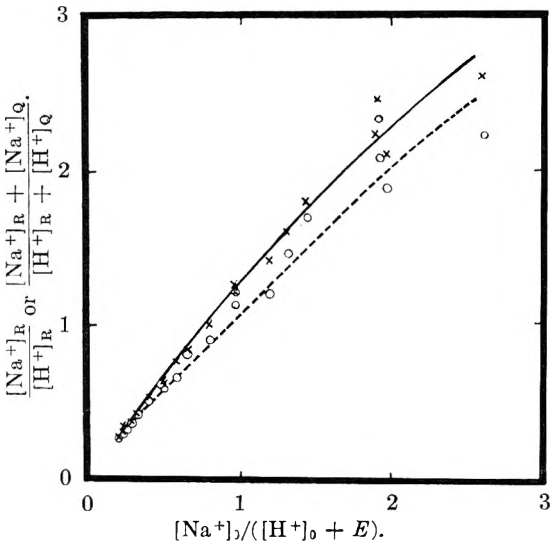

Fig. 1.—Values of $[Na^+]_R/[H^+]_R$ are shown by full line and crosses and those of $\{[Na^+]_R + [Na^+]_Q\}/\{[H^+]_R + [H^+]_Q\}$ by broken line and circles.

present case, though the former seems to be a little better than the latter.

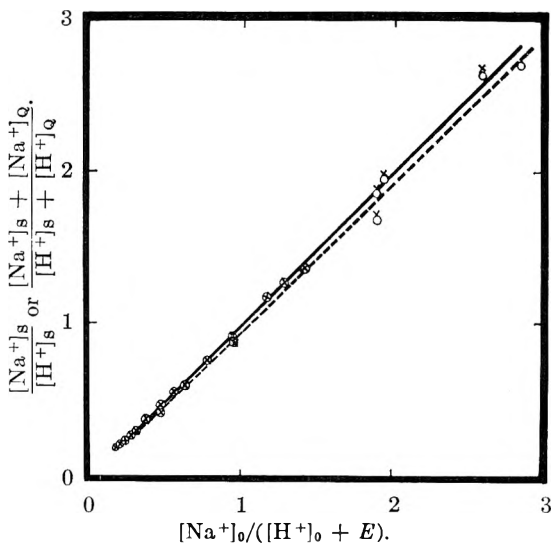

Fig. 2.—Values of $[Na^+]_S/[H^+]_S$ are shown by full line and crosses and those of $\{[Na^+]_S + [Na^+]_Q\}/\{[H^+]_S + [H^+]_Q\}$ by broken line and circles.

It is reported that

$$K_H^{Na}\left(=\frac{(Na^+)_R}{(H^+)_R}\times\frac{(H^+)_S}{(Na^+)_S}\right)$$

is nearly a constant in the case of dilute solutions, but in the case of concentrated solutions its values vary considerably with the molar fraction of Na^+ ion in the resin (β_{Na})[9] (Fig. 3). K_H^{Na} varies very little with increase of HCl in 1 *N* NaCl solution, whereas it varies considerably in 2 and 3 *N* NaCl solutions. These phenomena correspond to the fact that $[Na^+]_R/[H^+]_R$ deviates from a straight line in the region of large values of $[Na^+]_0/\{[H^+]_0 + E\}$.

(4) **LiCl–HCl System.**—The existence of the Donnan equilibrium was found in the LiCl–HCl system too. If we assume the Donnan equilibrium, relations similar to equation 8 and 9 are obtained. Figures 4 and 5 show that relations between

(9) $\beta_{Na} = [Na^+]_R/([Na^+]_R + [H^+]_R$.

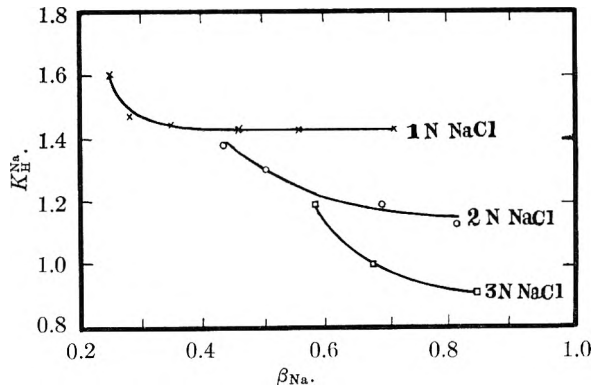

Fig. 3.—Effects of concentrations of NaCl on the relations between K_H^{Na} and molar fraction of Na in the resin, β_{Na}.

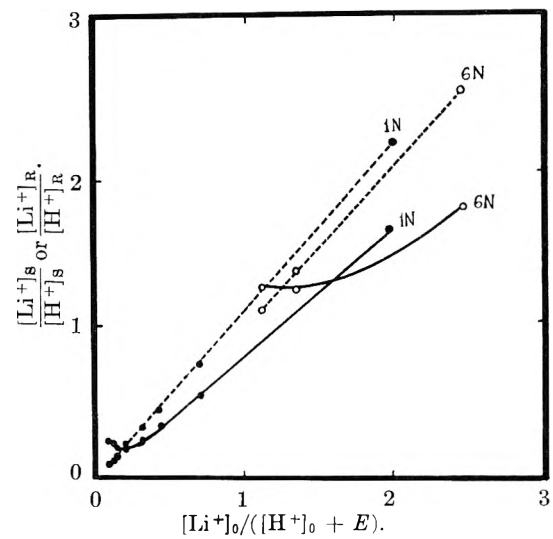

Fig. 4.—Full and broken lines show the ratios of Li and H ions in the resin and the outer solution phases, respectively. Values of 1 and 6 *N* LiCl solutions are shown.

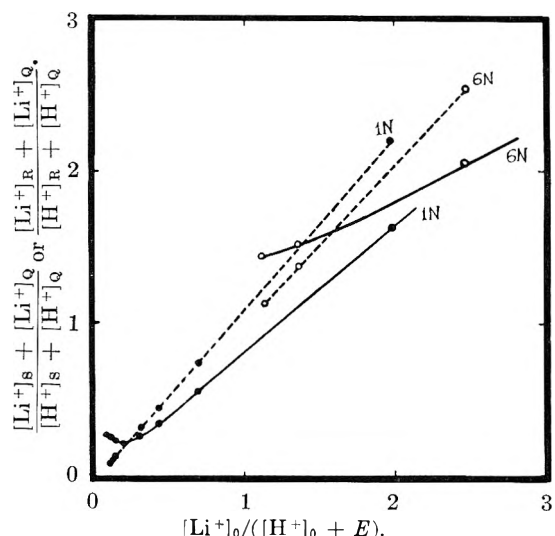

Fig. 5.—Full and broken lines show the values of $([Li^+]_R + [Li^+]_Q)/([H^+]_R + [H^+]_Q)$ and $([Li^+]_S + [Li^+]_Q)/([H^+]_S + [H^+]_Q)$, respectively. The values of 1 and 6 *N* LiCl solutions are shown.

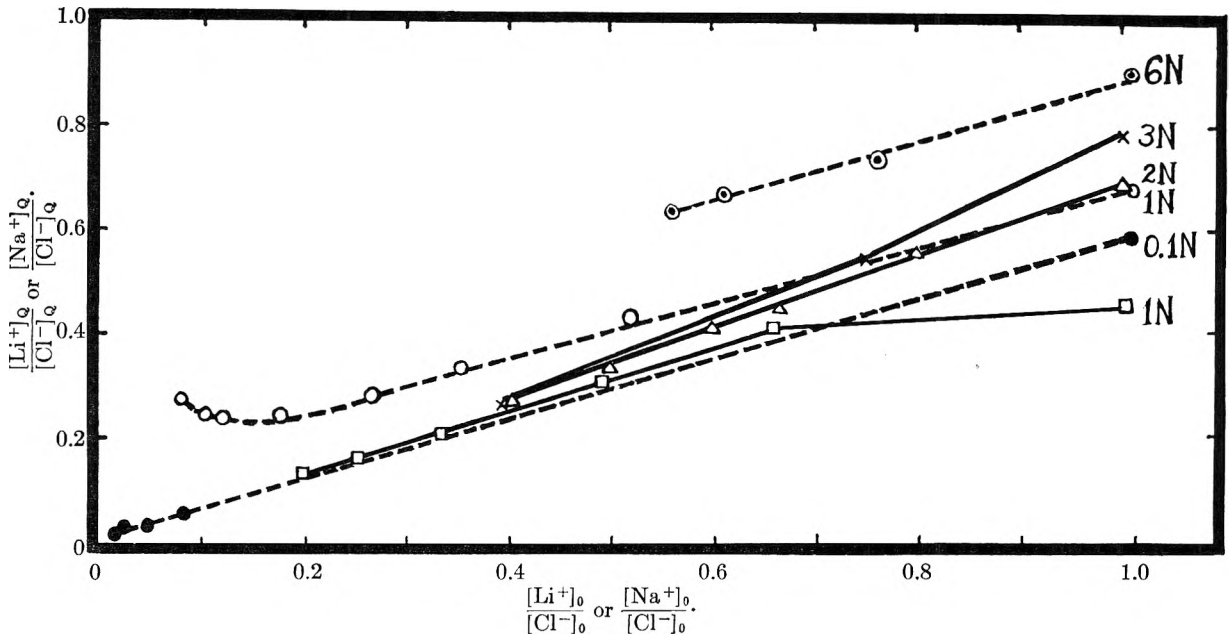

Fig. 6.—Full lines show the values in NaCl and broken lines the values in LiCl system: □, 1 *N*; △, 2 *N*, ×, 3 *N*, of NaCl ●, 0.1 *N*, ○, 1 *N*, ⊙, 6 *N* of LiCl solution.

$[Li^+]_S/[H^+]_S$ or $\{[Li^+]_S + [Li^+]_Q\}/\{[H^+]_S + [H^+]_Q\}$ and $[Li^+]_0/\{[H^+]_0 + E\}$ are expressed by a straight line. These imply the existence of a Donnan equilibrium. There is a minimum in the relation between $[Li^+]_R/[H^+]_R$ or $\{[Li^+]_R + [Li^+]_Q\}/\{[H^+]_R + [H^+]_Q\}$ and $[Li^+]_0/\{[H^+]_0 + E\}$ when the value of $[Li^+]_0/\{[H^+]_0 + E\}$ is small, *i.e.*, the hydrogen ion concentration is large compared with lithium ion concentration.

In order to examine this phenomenon further, the relation between $[Li^+]_0/[Cl^-]_0$ and $[Li^+]_Q/[Cl^-]_Q$ was plotted in Fig. 6. The same relations found for NaCl-HCl system are also shown in the same figure. In Fig. 6, curves for various concentrations of NaCl coincide with each other especially for small values of $[Na^+]_0/[Cl^-]_0$, while curves of the LiCl system do not coincide at all. For the same values of $[Li^+]_0/[Cl^-]_0$, $[Li^+]_Q/[Cl^-]_Q$ is not always constant and the value of $[Li^+]_Q/[Cl^-]_Q$ increases with increase of Li^+ ion concentration. In other words, in the region of higher concentrations of Li^+ ion, more Li^+ ion is captured in the quasi-exchange phase. This may suggest that the hydration of the Li^+ ion decreases in concentrated solution, and its ionic radius decreases and it is, therefore, captured by the resin more easily than in dilute solution.

The same phenomenon may occur if some complex ions such as Li_2Cl^+ are formed. However, as mentioned in (b), we could not confirm the existence of such complex ions from our experimental data. Although at the present stage we cannot tell definitely which is the case, dehydration or complex formation, the hypothesis of dehydration appears to be more probable.

When the hydrogen form of the resin is in contact with LiCl + HCl solution, $[Li^+]_R/[H^+]_R$ (or $\{[Li^+]_R + [Li^+]_Q\}/\{[H^+]_R + [H^+]_Q\}$) decreases to a limiting value as $[Li^+]_0/\{[H^+]_0 + E\}$ decreases as shown in Fig. 4. For example the limiting value is 1.3 when the concentration of Li^+ is 6 *N*.

In the neighborhood of these limiting points the values of K_H^{Li} vary greatly. This can be seen from Figs. 7 and 8 which show the relations between K_H^{Li}

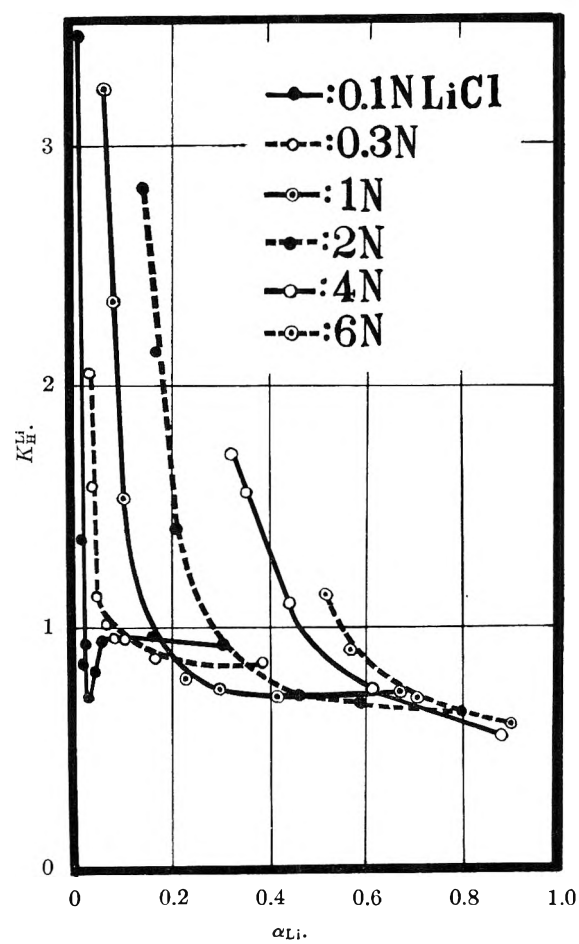

Fig. 7.—Relations between exchange coefficient and molar fraction of Li ion in the outer solution phase.

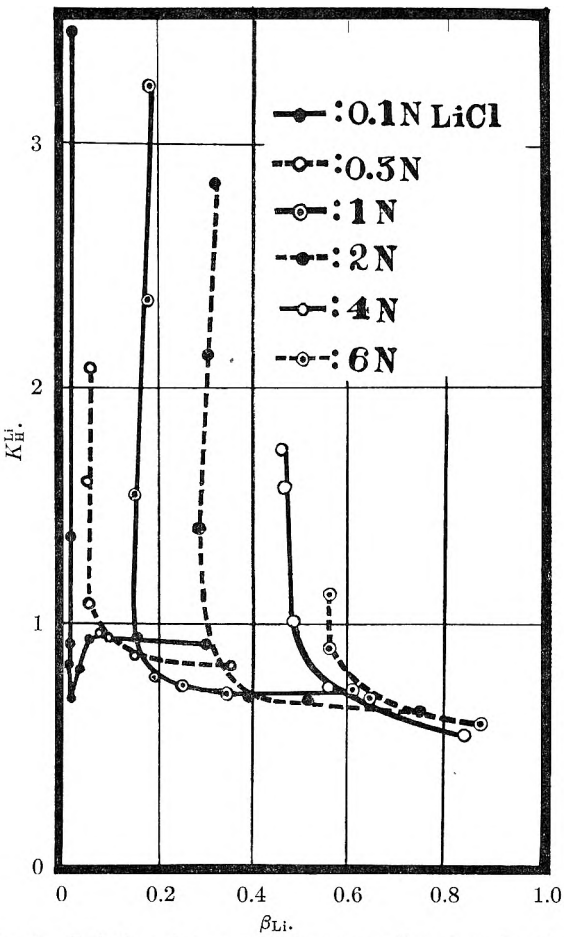

Fig. 8.—Relations between exchange coefficient and molar fraction of Li ion in the resin phase.

and the molar fraction of Li^+ ion in the outer solution phase (α_{Li}) or that in the resin phase (β_{Li}).[10] These figures show that the variation of K_H^{Li} does not depend on the molar fraction of Li^+ in the resin phase (β_{Li}), but on the change of the molar fraction of the outer solution (α_{Li}) (Figs. 7 and 8). In relatively dilute solutions (*e.g.*, 1 or 2 *N* of total concentration) K_H^{Li} is almost constant and independent of the molar fraction of Li^+ in the resin

(10) $\alpha_{Li} = [Li^+]_S/([Li^+]_S + [H^+]_S)$, $\beta_{Li} = [Li^+]_R/([Li^+]_R + [H^+]_R)$.

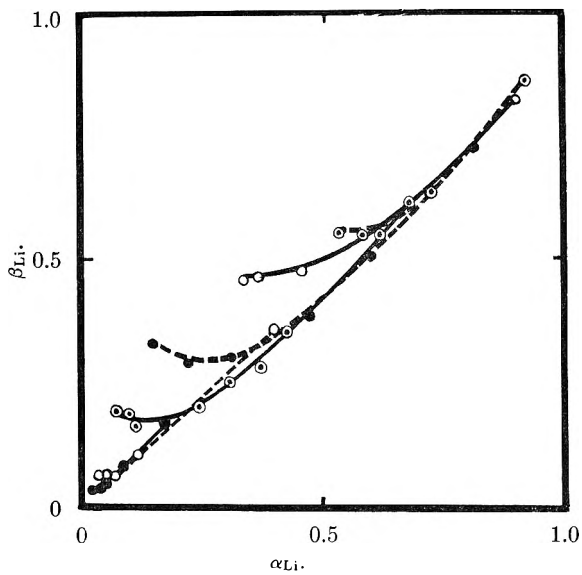

Fig. 9.—Relations between molar fractions of Li ion in the resin and outer solution phases.

phase, but as the concentration increases, K_H^{Li} is no longer a constant. K_H^{Li} is calculated, as follows, taking the Donnan equilibrium into consideration

$$K_H^{Li} = \frac{[Li^+]_R[H^+]_S}{[H^+]_R[Li^+]_S} = \frac{[Li^+]_R}{[Li^+]_S} \times \frac{[H^+]_S}{[H^+]_S} = \frac{[Li^+]_R}{[Li]^+_S} \times \frac{[Li^+]_S + [H^+]_S}{[Li^+]_R + [H^+]_R} = \frac{\beta_{Li}}{\alpha_{Li}}$$

From the gradients of the curves obtained by plotting α_{Li} *versus* β_{Li}, K_H^{Li} was calculated (Fig. 9). Values ranging from 0.84 to 1.19 were obtained. These values are quite different from those calculated from $K_H^{Li} = [Li^+]_R[H^+]_S/[H^+]_R[Li^+]_S$ which were shown in Figs. 7 and 8. Only 0.1 and 0.3 *N* solutions of LiCl gave K_H^{Li} values of 0.84–1.19. More concentrated solutions than 1 *N* gave K_H^{Li} values of 0.6–0.8. These discrepancies between *K* values may be attributed to the change of activities in the concentrated solution.

Acknowledgments.—The expenses of the present study were defrayed by Grant-in-Aid for Fundamental Scientific Research from Ministry of Education.

ISOPIESTIC STUDIES OF AQUEOUS DICARBOXYLIC ACID SOLUTIONS

BY MANSEL DAVIES AND D. K. THOMAS

The Edward Davies Chemical Laboratories, University College of Wales, Aberystwyth, Wales

Received June 2, 1955

A precise and convenient volumetric form of the isopiestic method of studying the vapor pressure lowering of aqueous solutions at various temperatures is described. Using sulfuric acid solutions as standards, the solvent vapor pressure lowering and activities of both solvent and solute for aqueous malonic, methylsuccinic and glutaric acids are determined and the activities of maleic, succinic and malic acid are calculated from previously published data. Over the concentration ranges measured (c 0.5 *m* to 3 *m*) most of the solutes are essentially normal but glutaric acid shows marked departures whose molecular interpretation is considered.

The isopiestic method has been widely used for determination of solvent vapor pressures over solutions of non-volatile solutes, and in the gravimetric form developed by Robinson and Sinclair[1] and by Scatchard, *et al.*,[2] it is capable of yielding activity data of an accuracy comparable with that obtained by e.m.f. and freezing point measurements. It also offers the advantage of being readily operated over a range of temperature. More recently the volumetric form has been described[3] in which attainment of equilibrium is assessed by the constancy in solution volumes, and this is not markedly inferior to the gravimetric procedure. It is a convenient and reasonably rapid arrangement for the volumetric procedure which we wish to describe.

Experimental

Equilibration Procedure.—Our arrangement was based on that of Lassettre and Dickinson[3a] with modifications to allow as rapid equilibration as possible, ease in following small changes in volume, and greater efficiency in the simultaneous control of up to eight pairs of solution whose changes in composition on equilibration at various temperatures could be followed directly.

The Pyrex equilibrators consisted of two hemispherical compartments of diameter *ca.* 4 cm. joined to form a short bent-sausage shape by a 3.5 cm. wide tube (Fig. 1a): the gap between the bulbs was *ca.* 0.5 cm. × 3 cm., and from their centers there extended measuring limbs of total length 10 cm. having end compartments 1.6 cm. diameter, 3.5 cm. long joined to the stem which was of diameter 0.7 cm. (Fig. 1b). About half-way along each stem was a fine etched line from which the meniscus position in the stem could be measured by a cathetometer reading to ±0.001 cm. An open limb (Z, Fig. 1a) allowed an appropriate volume (*ca.* 6 ml.) of each solution being carefully introduced into the separate compartments from a pipet with a long fine stem. In the equilibrating position (Fig. 1a) these formed shallow pools between which free passage of vapor was facilitated by the wide connection and further promoted by gentle rocking and previous evacuation. On turning through 90° the solutions drained into the measuring limbs (Fig. 1b), the narrower stem section ensuring adequate accuracy in measuring volume changes, as 0.001 ml. corresponded to 0.003 cm. in meniscus position. Measurement of the meniscus height for varying weights of mercury in these limbs provided an accurate calibration of the corresponding volumes. For aqueous solutions, the reproducibility of drainage from the compartments into the measuring limbs was one of the limiting factors in our accuracy. To attain the requisite cleanliness of the glass it was found best to allow alcoholic potash to stand in the equilibrator for several hours followed by successive washings with distilled water.

After the two solutions had been introduced without splashing, the equilibrator was turned into the measuring position and the solutions frozen (−20°) before removing the air with a rotary oil pump. A screw-clip on the connection to Z (Fig. 1a) was then closed and the solutions allowed to melt, releasing their dissolved air, refrozen and the evacuation repeated. This time Z was sealed off with a hand-torch. Tests, in which the evacuation was continued for much longer periods than were normally used and the change in weight of the equilibrator and contents determined, showed that negligible concentration changes were produced by the evacuation. The equilibrator was clamped in a stand in which it could be turned precisely, without being touched, from position a to b and the whole placed in the thermostat: all subsequent observations were made on it without moving its stand in the thermostat. This operation was completed before the frozen solutions had warmed up so as to prevent condensation of vapor on any part of the vessel not subsequently reached by the solutions in their transfer from the compartments to the measuring limbs.

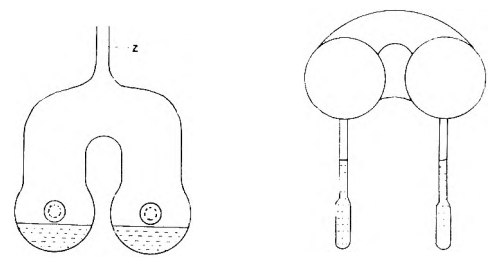

1a 1b

Fig. 1.

Temperature control during equilibration is the most obvious factor limiting the accuracy of the isopiestic method. For dilute aqueous solutions at 25° a temperature difference of 0.002° causes a solvent vapor pressure change of 0.003 mm., whilst an ideal 1 *m* solution has a vapor pressure lowering of only *ca.* 0.4 mm. Our thermostat consisted primarily of a slate tank 20″ × 20″ × 18″ surrounded by 1.5″ of glasswool insulation held in a pressed board box and having a plate-glass window, in which water could be rapidly circulated through inlets in the base connected to a rotary pump. Heating was by four 60-watt units whose positions were chosen to give maximum uniformity of temperature, and control was effected from a long mercury–toluene regulator constructed in a planar serpentine form. The equilibrator stands were mounted in two glass tanks (8″ × 11″ × 14″) placed on a light metal platform pivoted at its center so that the whole could be rocked ±10° by an eccentrically-driven rigid coupling: the whole assembly being immersed in the main thermostat. The rocking served to stir gently the solutions and to promote vapor transfer as well as to stimulate further the water circulation in the thermostat. An essential improvement was found in tapping the main water circulation through the pump to provide controlled streams to the bottom of the immersed glass tanks *via* a long copper spiral in the outer bath. As a result, the temperature within the glass tanks varied neither with position nor with time (up to periods of 100 hours) by more than ±0.002 at 25°: at 45° with a thin oil layer and covers on the thermostat, the variation amounted to ±0.003°. As these were the maximum normal variations read on a Beckmann thermometer, any temperature differences between the closely adjacent compartments of one equilibrator should have been appreciably less. Four equilibrators were maintained (two in each stand) in the two

(1) R. A. Robinson and D. S. Sinclair, *J. Am. Chem. Soc.*, **56**, 1830 (1934).

(2) G. Scatchard, W. J. Hamer and S. E. Wood, *ibid.*, **60**, 3061 (1938).

(3) (a) E. N. Lassettre and R. G. Dickenson, *ibid.*, **61**, 54 (1939); (b) F. T. Wall and P. E. Rouse, *ibid.*, **63**, 3002 (1941); (c) F. T. Wall and F. W. Banes, *ibid.*, **67**, 898 (1945).

glass tanks for final equilibration, whilst four others were simultaneously mounted in the outer bath to come to preliminary equilibrium. After equilibration of all the solutions at one temperature, the latter could be changed and the same set of solutions reëquilibrated.

Aqueous sulfuric acid was used for the standard solution as precise data were available for it at various temperatures. At 25° we accepted the vapor pressure results of Grollman and Frazer[4] which are in excellent agreement with data of Shankman and Gordon,[5] Harned and Hamer,[6] and Stokes[7] up to 2 molal (m) concentration. At 35 and 45° we interpolated the activity results of Harned and Hamer at 20, 25, 40 and 60° to provide the coefficients we required. The concentrations of a number of sulfuric acid solutions were established by gravimetric ($BaSO_4$) methods, the poorest duplicate analyses differing by 0.7%.

All other solutions were made up by weight from pure components so that their molalities (m) were initially known. The precise densities of the solutions allowed of their final concentrations being evaluated *via* the molarities (c) from the volume changes on equilibration. For most of the solutions studied adequate density data were available in the literature but for aqueous glutaric acid we determined values at 25°: it was assumed that these solutions had the same temperature coefficient of expansion as water.

As typical data we reproduce the cathetometer determinations of the heights of menisci relative to the etched lines for solutions of sulfuric acid and malonic acid at 25.01°, initially 1.553 and 3.973 m, respectively.

Time, hr.	Temp. (Beckmann), C.	H_2SO_4 limb, cm.	$CH_2(COOH)_2$ limb, cm.
0	2.824	+1.059	+0.565
12	2.826	0.928	.602
16	2.824	.895	.635
20	2.824	.815	.695
32	2.826	.781	.759
40	2.826	.784	.794
44	2.826	.764	.812
56	2.824	.747	.833
61	2.824	.737	.840
64	2.824	.733	.846
68	2.824	.734	.845

An uncertainty of 0.003 cm. in the final meniscus height corresponds to a volume of 0.001 ml. From the above, the initial 6.089 ml. of H_2SO_4 solution lost 0.105 ml.; the 5.938 ml. of $CH_2(COOH)_2$ solution gained 0.099 ml. These changes are averaged to 0.102 ml. and the isopiestic concentrations are then found to be 1.580 m H_2SO_4 and 3 945 m $CH_2(COOH)_2$. In preliminary experiments some sucrose and sulfuric acid solutions were equilibrated and led to concentrations differing from those of Scatchard, *et al.*, by a maximum of 0.7% at 2 m this corresponded to $\Delta p = 0.007$ mm. or $\Delta T = 0.005°$. It is believed that the later results recorded below are appreciably more accurate than this. The simultaneous handling of eight equilibrators together with the use of direct temperature variation made the method sensibly efficient for routine work.

Thermostat temperatures were observed on a thermometer calibrated at the N.P.L. to ±0.02°.

A prerequisite of the isopiestic method, as of some related techniques, is that the solute should be non-volatile. Owing to the time involved in the equilibration process the method appears to be very sensitive to this criterion. From experience we find that, as a general rule, it is impracticable to employ a solute having a normal b.p. below 210°, even in aqueous solutions at 25°. Solutes whose distillation in the equilibrator we were able to follow include butyric acid (b.p. 164°) and crotonic acid (b.p. 189°): this despite the fact that for 2 m aqueous butyric acid at 25° the partial vapor pressure of the solute must be well below 1×10^{-3} mm.

Materials.—Sulfuric Acid: Analar acid was diluted with distilled water. Densities were taken from I.C.T.

Malonic acid: twice recrystallized from water, eq. wt. = 51.95 (calcd. 52.03).

Methylsuccinic acid: twice recrystallized from water, m.p. 115.0° (lit. 115°), eq. wt. = 65.93 (calcd. 66.05).

Glutaric acid: twice recrystallized from Analar benzene, m.p. 97.5°, (lit. 97.5°) eq. wt. = 66.10 (calcd. 66.05).

Evaluation of Activities

Having determined the equilibrium concentrations, the water vapor pressure over, say, the malonic acid solution (P_1), is given by that of the isopiestic sulfuric acid solution, the solvent activity $a_1 = P_1/P_0$, being the same in both solutions. P_0 is the pure solvent vapor pressure and it is assumed that the departures of its vapor from ideality are negligible.

Lewis and Randall[8] described an appropriate graphical method of evaluating the solute activity (a_2) from the concentration variation of a_1, the two activities being related *via* the form of the Gibbs–Duhem equation $\mathrm{d} \ln a_1 = -N_2/N_1 \, \mathrm{d} \ln a_2$, where N_1 and N_2 are the mole fractions of solvent and solute. A convenient function (h) is defined, $h = 1 + (\ln a_{1/y})$ where $y = N_2/N_1$. Then, for any solution

$$2.303 \log (a_2/m) = -h - \int_0^m (h/m)\mathrm{d}m \qquad (1)$$

Numerically h is $1 + (55.51 \ln a_1)/m$ and determination of the area in the plot of h/m against m allows of a_2 being calculated.

In this calculation the h-function is particularly appropriate for non-electrolytes. Over our measured concentration ranges the degrees of ionization of the dicarboxylic acids are both sufficiently small and constant to provide easily integrable plots but it is quite out of the question to extend the (h/m) curves to zero concentration. In practice this will be very difficult as the second ionization stage of these acids will be incomplete except at extreme dilutions: *e.g.*, half complete at 10^{-5} m. Accordingly, we have used equation 1 only over observed concentration ranges and have accepted the arbitrary value $a_2/m = 1$ at $m = 1.000$ in place of the more usual reference state $a_2/m = 1$ at $m = 0$. In addition to our own isopiestic data, we have also treated the results of Robinson and Smith[9] for aqueous maleic, malic and succinic acids in the same way. Owing to its limited solubility, the succinic acid solutions were referred to $a_2/m = 1$ at $m = 0.500$.

Results

In the following table m is the molality of the aqueous solution, $\Delta P = (P_0 - P_1)$ the vapor pressure lowering in mm., and a_2/m, the activity coefficient on the basis already indicated. The accuracy in the values of a_2/m extends to the third place of decimals as the ΔP values are certainly correct to better than 1%. f is a mean apparent degree of association of the solute evaluated as explained later.

Discussion

It is clear from the activity coefficient values that, except in the case of glutaric acid, no very

(4) A. Grollman and J. C. W. Frazer, *J. Am. Chem. Soc.*, **47**, 712 (1925).

(5) S. Shankman and A. R. Gordon, *ibid.*, **61**, 2370 (1939).

(6) H. S. Harned and W. T. Hamer, *ibid.*, **57**, 27 (1935).

(7) R. H. Stokes, *ibid.*, **67**, 1688 (1945).

(8) G. N. Lewis and M. Randall, "Thermodynamics," McGraw-Hill Book Co., New York, N. Y., 1923, p. 273.

(9) R. A. Robinson, P. K. Smith and E. R. B. Smith, *Trans. Faraday Soc.*, **38**, 63 (1942).

TABLE I

Succinic acid at 25.00°

m	0.399	0.444	0.500	0.511	0.547	0.5555	0.602
ΔP	0.166	0.176	...	0.196	0.206	0.206	0.236
a_2/m	1.005	1.002	(1.000)	0.999	0.998	0.997	1.001
f	1.05	1.09	...	1.12	1.14	1.16	1.095

Maleic acid at 25.00°

m	0.500	1.000	1.500	2.000	2.500	3.000
ΔP	0.236	0.436	0.646	0.826	1.006	1.196
a_2/m	1.140	(1.000)	0.984	0.953	0.926	0.913
f	1.03	1.07	1.06	1.08	1.09	1.09

Malic acid at 25.00°

m	0.500	1.000	1.500	2.000	2.500	3.000
ΔP	0.216	0.436	0.646	0.866	1.086	1.306
a_2/m	1.015	(1.000)	0.997	0.993	0.992	0.989
f	1.01	0.99	0.99	0.97	0.95	0.94

Malonic acid at 24.99°

m	0.461	0.992	1.000	1.729	2.545	2.820	3.436	3.945	4.387	4.838
ΔP	6.208	0.432		0.712	1.000	1.102	1.338	1.531	1.700	1.891
a_2/m	1.070	1.000	(1.000)	0.959	0.910	0.899	0.891	0.885	0.883	0.883
f	1.00	1.01		1.04	1.08	1.08	1.07	1.06	1.05	1.03

Methylsuccinic acid at 24.99°

m	0.300	0.400	0.500	0.564	0.568	0.600	0.700	0.800	0.900	1.000
ΔP	0.125	0.163	0.199	0.219	0.2194	0.233	0.270	0.311	0.350	0.390
a_2/m	1.161	1.125	1.096	1.076	1.069	1.056	1.020	1.021	1.024	(1.000)
f	1.04	1.06	1.08	1.105	1.11	1.10	1.11	1.10	1.09	1.09

Glutaric acid at 25.01°

m	0.493	1.000	1.092	1.416	2.186	2.403	2.880	3.789	4.114
ΔP	0.199	...	0.422	0.480	0.680	0.725	0.806	0.996	1.080
a_2/m	1.142	(1.000)	0.977	0.904	0.755	0.723	0.649	0.567	0.552
f	1.06	...	1.195	1.244	1.343	1.38	1.48	1.566	1.61

Glutaric acid at 35.02°

m	0.325	0.388	0.710	0.945	1.000	1.894	2.637	3.688
ΔP	0.229	0.273	0.480	0.610	...	1.090	1.417	1.777
a_2/m	1.210	1.184	1.080	1.015	(1.000)	0.814	0.676	0.567
f	1.06	1.076	1.12	1.17		1.293	1.396	1.52

Glutaric acid at 45.01°

m	0.325	0.388	0.711	0.943	1.000	1.883	2.613	3.646
ΔP	0.434	0.515	0.877	1.123	...	1.941	2.460	3.094
a_2/m	1.207	1.196	1.064	1.013	(1.000)	0.825	0.714	0.592
f	1.01	1.01	1.04	1.08	...	1.23	1.335	1.464

great departures from ideal behavior occur within our concentration ranges. The variations in (a_2/m) follow the same course and are of much the same magnitudes for maleic, malonic and methylsuccinic acids, whilst for malic acid which, of all the solutes, has the least hydrophobic elements, (a_2/m) varies only by 2.6% between $m = 0.5$ and 3.0.

It is now well-established that simple carboxylic acids associate to the dimeric form not only in the vapor and non-hydroxylic solvents, but that they also do so in water[10]: thus for 1 m aqueous acetic acid at 25° some 15% of the solute is in the form of dimer. Thus, it might have been anticipated that the unsubstituted dicarboxylic acids would show similar behavior to perhaps an even more marked extent. Only for glutaric acid is this anticipation certainly correct.

To assess the molecular state of these solutes from the derived vapor pressure lowerings of their solutions requires assumptions of a non-thermodynamic character. Firstly, it may be pointed out that the ionization in the glutaric acid solutions measured is small: the degree of ionization (β) is, at 25°, 0.021 at 0.2 m, 0.006 at 4.0 m. Accordingly, the influence of ionic factors on the solute behavior will not be large.

Consider now a solution in which the mole fraction of the un-ionized solute, if entirely monomeric, amounts to n, whilst the total effective mole fraction of the un-ionized species is $\bar{n}$ made up of n_1, $n_2 \ldots n_r$ mole fraction values for monomer, dimer, etc. The necessary simplification is made that each of these species behaves, in our concentration range, as a monobasic acid having the same degree of

(10) M. Davies and D. M. L. Griffiths, *Z. physik. Chem., Neue Folge*, **2**, 353 (1954); D. R. Cartwright and C. B. Monk, *ibid.*, in press.

ionization. If the total mole fraction of ions is n_i then $n_0 + \bar{n} + n_i = 1$ where n_0 = mole fraction of solvent. Using m's for molalities

$$n_0 = 55.51/[55.51 + (1 + \beta)\Sigma m_r] = 55.51/s$$
$$\bar{n} = (1 - \beta)\Sigma m_r/s$$
$$n_i = 2\beta\Sigma m_r/s$$

$$\bar{n} + n_i = \frac{(1 + \beta)}{(1 - \beta)} \times n\,(1 + 2\beta)\bar{n}$$

If we now assume that the activities of the individual species are each proportional to their own mole fractions, *i.e.*, obey Raoult's law—then

$$1 - n_0 = \Delta P/P_0 = (1 = 2\beta)\bar{n}$$

It is then possible to evaluate an over-all mean degree of association for the un-ionized species, $f = n/\bar{n}$. This factor has been calculated for each of the solutes. In Figs. 2, 3 and 4 we have plotted f

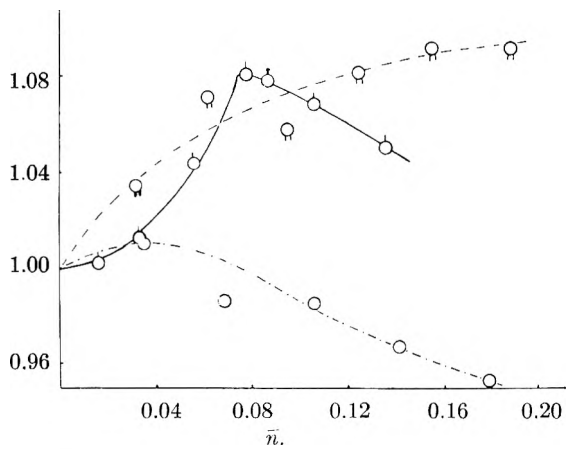

Fig. 2.—Apparent mean degrees of association: ⊙, maleic acid; ⊙, malonic acid ($2n$ plotted); ⊙, malic acid ($4n$ plotted.

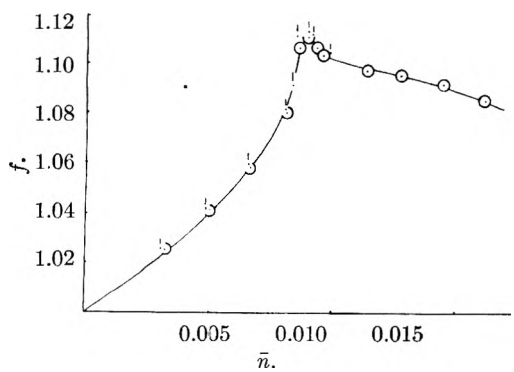

Fig. 3.—Apparent mear degrees of association: ⊙, methylsuccinic acid at 24.99°; !, succinic acid at 25.00°.

against $\bar{n}$, a mode of representation suggested by Kreuzer's analysis of associating systems. Firstly, it can be seen that our data show far less scatter

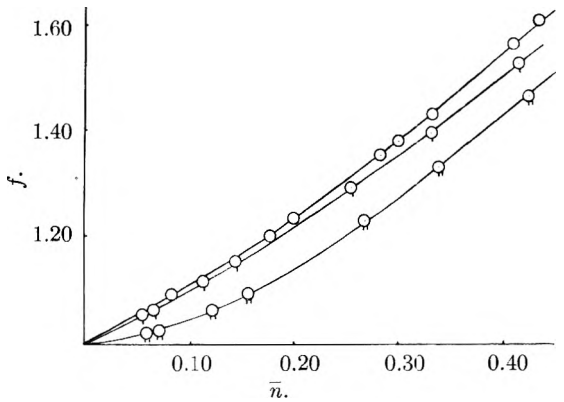

Fig. 4.—Apparent mean degrees of association for glutaric acid in aqueous solutions: ⊙, at 25°; ⊙, at 35°; ⊙, at 45°.

than Smith and Robinson's for maleic (or malic) acid when treated in this way. Secondly, there is a remarkably abrupt turn in the plots for both succinic acid (S and R's data) and for methylsuccinic acid (present work) near $n = 0.009$. We are quite unable to account for this unusual feature.

For glutaric acid Fig. 4 shows the regular increase in apparent molecular complexity of the solute with increasing concentration at each temperature. Whilst the f values in this case can only be reasonably interpreted as meaning actual association of the solute in the water, they do not fit into any simple quantitative scheme although at higher concentrations the approximate linearity of the $f \sim \bar{n}$ plots conforms to the expectations for a sequence of equilibria with increasing r-values. Qualitatively, too, this suggestion is supported both by the large solubility, and its temperature coefficient for glutaric acid in water, features which in a more extreme form are characteristic of micellar aggregation in solution. This difference in the behavior of glutaric acid from that of the other acids studied is perhaps to be correlated with the greater hydrophobic character of the chain between its carboxyl groups. Thus it is noticeable that malic acid gives f-values below 1.0: owing to the assumptions made in their deduction these are quantitatively uncertain, but they may indicate the immobilization of some of the solvent by appreciable solvate formation. Intramolecular interactions *may* play a part in these solutions: all the acids except glutaric could form internal hydrogen bridges involving not more than 7 atoms (counting hydrogen). For glutaric acid, this interaction would require a far less probable 8-membered ring.

Acknowledgment.—We wish to thank the D.S.I.R. for a Maintenance Award to D.K.T. and the Shell Petroleum Company for a grant.

MOLTEN CYANIDE PROCESS OF PURIFYING GERMANIUM FROM COPPER CONTAMINATION

BY PEI WANG

Contribution from Sylvania Electric Products, Inc., Woburn, Mass.

Received June 4, 1955

Copper contamination on the surface and in the bulk of single crystal germanium ingots can be removed by treating the germanium ingots in a molten alkali cyanide-bath at elevated temperatures. The cyanide ions combine with surface copper impurity and any copper ion that diffuses to the germanium surface. As the copper cyanide complex ion is extremely stable, the concentration of free copper ion in the molten cyanide medium is very low such that recontamination of the germanium is practically nil. Germanium thus treated was found to undergo no thermal conversion.

Introduction

The phenomenon of thermal conversion of n-type germanium to p-type by heat treatment is now familiar. It has been pointed out by Theuerer and Schaff[1] that either thermally produced lattice defects or acceptor impurities could be held responsible for the conversion. Later, it became apparent that the generally observed conversion was associated with the presence of impurities, especially copper and nickel, on the germanium surface prior to heating.[2-5] The impurities diffuse into the bulk of germanium upon heating to moderately high temperatures and there is a resultant change of resistivity or a conversion from the n-type to the p-type.

In order to remove the surface impurities such as copper or nickel, Logan[6] rinsed the germanium sample surface with an aqueous solution of potassium cyanide for his study of thermal acceptors. The cyanide ion forms a very stable complex ion with copper. The dissociation constant of $Cu(CN)_4^{-3}$ to Cu^{+1} and four CN^{-1} is 2×10^{-27}, hence the removal of copper is practically almost complete. The removal of copper from the bulk of germanium, as shown by Finn,[7] can be accomplished by heating the germanium sample in high vacuum at elevated temperature, *i.e.*, 500° or higher. Under these conditions when copper diffuses to the germanium surface it is evaporated out of the bulk and condenses on the cold part of the wall of the tube furnace.

From the above reasoning, it was thought that the removal of copper from bulk germanium would be possible by extracting in a molten alkali cyanide medium at elevated temperature. For example, germanium with copper and nickel as principal impurities can be immersed in molten potassium cyanide held at 700°. Copper ions then diffuse through the bulk of germanium, and as soon as they reach the surface, they combine with cyanide ions to form stable complex ions in the liquid phase. Although no data on the dissociation constant of molten alkali cyanides are available, it is not unexpected that a stable complex copper cyanide ion is formed and free copper ion concentration in the liquid phase is extremely low. Consequently the chances of recontaminating the germanium by the copper impurity are very small. The small amounts of impurities in the C.P. grade potassium or sodium cyanide are believed either intrinsically non-harmful or their diffusion constants in germanium are so low that they do not contaminate the germanium appreciably. If the assumptions are correct, such a molten cyanide treatment, allowed enough time, will remove copper or similar rapidly diffusing impurities and yield germanium of higher purity. On being heat treated, germanium material thus prepared will show no thermal conversion and the resistivity will not undergo any drastic changes.

Experimental

For different treatments the following reagents were used: (1) pure potassium cyanide, (2) pure sodium cyanide, (3) mixtures of potassium and sodium cyanide and sodium chloride. The chemicals were of C.P. grade and no special efforts were made to purify them further. An inert atmosphere was generally used and nitrogen was found adequate. Inert gases such as argon and helium were also satisfactory and in some experiments were preferred to nitrogen.

The length of time needed for effective treatments varied with the temperature of the furnace and the thickness of the germanium sample. The minimum time required may be calculated from the equation

$$r^{-2} = 6Dt$$

where r is the average distance traveled by the impurity atom in cm., D the diffusion coefficient, and t the time. The average D value for copper in germanium is given as 2.8×10^{-5} cm.^{2}/sec. in the temperature range 700–900°.[8] Therefore, at 1000°K., for a sample of 1 mm. thickness it would need only about 1 minute for a copper ion, on the average, to travel from one surface through the bulk to the other surface across the thickness. Similarly, a sample of 0.5 cm. thickness would need about half an hour. Therefore, after a sufficiently long time in a molten cyanide medium at a suitable high temperature, most of the copper impurity in the bulk of the germanium would be removed from the surface by combining with cyanide in the liquid phase.

Samples cut from single crystal germanium, pulled either vertically or horizontally, were prepared in various forms: slices about 1 mm. thick; dice of size about 0.05 × 0.4 × 0.8 cm.^{3} and slabs of approximately 0.4 × 0.6 × 2.5 cm.^{3}. The surface of the samples was thoroughly cleaned and dried after the resistivity and Hall constant and the size and weight were measured. The conductivity type was checked with a thermoelectric probe. The samples were then put in a suitable container, usually a clean quartz or porcelain boat. A better practice developed later was to put the samples on a graphite holder placed in the boat. The cyanide reagent was added either as dry powder or applied in the form of a concentrated aqueous solution, then baked dry in an oven. The boat was put in the furnace and nitrogen or argon was passed over the specimens. The furnaces was brought up to the desired temperature, the boat pushed to the hot zone and kept there for a definite time, then cooled down gradually. After the furnace was brought down to room temperature, the boat was pulled

(1) H. C. Theuerer and J. H. Schaff, *J. Metals*, **191**, 59 (1951).

(2) C. S. Fuller and J. D. Struthers *Phys. Rev.*, **87**, 526 (1952).

(3) W. P. Slichter and E. D. Kolb, *ibid.*, **87** 527 (1952).

(4) K. Seiler, *et al.*, *Naturwissenschaften*, **40**, 56 (1953).

(5) F. van der Maeson, *et al.*, *Philips Res. Rep.*, **8**, 241 (1953).

(6) R. A. Logan, *Phys. Rev.*, **91**, 757 (1953).

(7) G. Finn, *ibid.*, **91**, 754 (1953).

(8) C. S. Fuller, *et al.*, *ibid.*, **93**, 1182 (1954).

out and the samples taken out with plastic-coated tweezers. The samples were carefully rinsed in hot water to remove the cyanide and dried in air. Thereafter, they were examined under a microscope, the loss in weight and decrease in thickness determined, and the resistivity and Hall constant again measured. The conductivity type was rechecked with the thermoelectric probe. In some cases, the etching rates of the samples, both before and after molten cyanide treatment, were determined in two different etching solutions.[9]

Results and Discussions

In general, a molten cyanide treatment resulted in a slightly etched surface on the germanium. A treatment at 600° for two to three hours usually gave fine triangular etch pits on (111) surface. For slabs of approximate size of $0.4 \times 0.6 \times 2.5$ cm.^{3}, the loss in weight after the treatment was about 0.1%. Treatments at higher temperatures produced a more severely attacked surface; the etch pits were rounded and irregular. Loss in weight was also higher.

Conductivity Type.—There was no change in type throughout the bulk of the material when various n-type germanium samples were heated in a medium of molten cyanide to around 650° and cooled fairly slowly. Control samples in the same furnace, but not coated with cyanide, changed to p-type. Several other temperatures in the range where thermal conversion was expected were also tested and the same result obtained. These p-type samples, however, were also converted back to n-type of about the original resistivity by a similar cyanide treatment. Further heating of the treated n-type samples in a clean furnace produced no evidence of thermal conversion at temperatures from 500 to 600°, indicating that impurities responsible for the conversion had been removed in the initial treatment.

With p-type germanium, there was observed a thin surface layer with n-type characteristics on the sample after a molten cyanide treatment. The sample retained its p-type conductivity of about the original value after this thin layer was removed either by grinding or etching.

Resistivity and Hall Constant.—In general, when n-type germanium underwent a molten cyanide treatment, the resistivity did not change appreciably. A slight difference was usually observed, possibly due to the creation of thermal acceptors. Some values are given in Table I.

TABLE I

RESISTIVITY CHANGE OF MOLTEN CYANIDE TREATED n-TYPE GERMANIUM

Samples No.	Shape	Treatment in N_2 Temp., °C.	Time, hr.	Resistivity, ohm. cm. Before	After
J 90 II	Slice	700	2	3.9	4.1
		700	2	3.7	3.8
		700	2	3.6	3.7
		700	2	3.2	3.6
		700	2	2.9	3.4
J 71 III	Dice	700	1	2.2	1.9
		700	1	2.1	2.0
J 70 III	Slab	750	2	9.5	9.2
	Dice	700	1	2.5	2.3
		700	1	2.0	1.8

(9) "Hydrofluoric acid–hydrogen peroxide etch," 1 Vol. 48% HF, 1 vol. 30% H_2O_2, 4 vol. water; hydrofluoric acid–nitric acid etch, 1 vol. 48% HF, 1 vol. coned. HNO_3.

In order to illustrate the effectiveness of the process in preventing the introduction of copper acceptors in germanium when the sample was rapidly quenched from a high temperature, the following experiment was performed.[10] An n-type single crystal germanium sample, which had been previously treated in a molten cyanide bath, was coated with a thin layer of potassium cyanide, placed in a closed tube and connected to electrical leads. Argon was introduced and a current passed through the sample bringing it to 800°. The sample was held at this temperature for one minute, then quenched rapidly by turning off the current and giving it a blast of argon. It was cooled to room temperature in less than one minute and the thermal acceptors created were frozen in the germanium ingot.

The molten cyanide treated germanium sample, supposedly "copper free," showed an increase in resistivity of from 3 to 4 ohm cm. to 8 to 10 ohm cm. after the treatment, but remained n-type. It was once more coated with potassium cyanide, brought up to slightly below 700° and annealed. The resistivity of the annealed sample was found later to be back to 3 to 4 ohm cm., approximately the same value as before quenching. The average difference of the number of carriers before and after quenching was about 2.8×10^{14} per cm.^{3}. This figure corresponds, roughly, to the number of thermal acceptors introduced in germanium at that temperature range estimated by Mayburg and Rotandi[11] in their study of vacuum heat treatment of germanium. Several runs under similar conditions gave similar results. The experiments supported the assumption that the formation of thermal acceptors was responsible for the increase in resistivity of the n-type germanium previously treated with molten cyanide. In other words, the process actually removed all or most of the contaminating surface and bulk impurities from the germanium crystal.

The Hall constant of the molten cyanide treated germanium did not change to any appreciable extent.

Effect on Etching Rates of Germanium.—It has been noted that heavy metal ions are catalyzing agents for the activity of etching solutions.[12] In this laboratory, it was observed that a contaminated surface etched at a faster rate than a cleaner surface.[13] Hence experiments were carried out to determine any change in etching rates of germanium before and after a molten cyanide treatment. In these experiments, a slow hydrofluoric acid–hydrogen peroxide etch and a fast hydrofluoric acid–nitric acid etch were used. Typical results on germanium single crystals of resistivity from 2 to 12 ohm cm. showed a decrease in etching rates, as shown in Table II.

The samples were treated in molten potassium cyanide for 2 to 3 hours at 700°.

Effect on the Surface.—It has been established in our laboratory[14] that, under certain conditions

(10) Under the direction of J. Patel of this Laboratory.

(11) S. Mayburg and L. Rotandi, *Phys. Rev.*, **91**, 1015 (1953).

(12) J. P. McKelvey and R. L. Longini, *J. Appl. Phys.*, **25**, 634 (1954).

(13) H. L. Crane, private correspondence.

(14) E. N. Clark, *The Sylvania Technologist*, **7**, 102 (1954).

Table II

Effect of Molten Cyanide Treatment on the Etching Rates of Germanium at 25°

Run no.	Type and orientation	Av. etching rate, g./in.² min. In H_2O_2–HF etch Before	After	In HNO_3–HF etch Before	After
1	n (100)	0.014	0.006	0.50	0.24
2	n (111)	.017	.007	.077	.022
3	p (100)	.0085	.0085	.34	.36
4	p (111)	.009	.014	.30	.020

of controlled oxidation, a stabilized germanium surface can be prepared so that its electrical properties are relatively unaffected by the presence of water vapor and possibly also of other contaminants. Therefore, in addition to the surmised function of the molten cyanide treatment of purification of germanium from copper and similar impurities, the alkali cyanide may serve as a catalyst to convert the surface to a stabilized condition. It is generally known that there is no clean germanium surface. Any germanium surface, after being exposed to air, has a thin germanium oxide layer. Recent work by E. N. Clark[15] on the stabilization of germanium surface indicated that the stabilized oxide surface was very likely of tetragonal structure, whereas the unstabilized oxide surface was probably of the hexagonal form. The latter form is soluble in water and is thermodynamically stable only about 1033°. The former is water insoluble and is the stable form at room temperature. Laubengayer and Morton[16] reported that one way to speed up the conversion of hexagonal germanium oxide to the tetragonal form above 550° was by means of an accelerating flux composed of potassium chloride and lithium chloride (44.6% by weight). Therefore, the potassium or sodium cyanide used in these experiments might also behave in the same way, converting the unstabilized hexagonal germanium oxide to the stable tetragonal form. In fact, in several cases a mixture of sodium chloride and potassium cyanide has been used to bring about stabilization of germanium and good results have been obtained.

(15) E. N. Clark, ACS 1955 Spring Meeting extracts.

(16) A. W. Laubengayer and D. S. Morton, *J. Am. Chem. Soc.*, **54**, 2302 (1932).

Copper-doped Germanium.—Several single crystals of copper-doped n-type germanium were prepared for Dr. J. F. Battey and R. Baum of this Laboratory. Samples were taken from these crystals and treated in a molten potassium cyanide-bath. The resistivity of the treated samples went down considerably as shown in Table III.

Table III

Resistivity Changes in Copper-doped Germanium on Molten Cyanide Treatment

Sample no.	Treatment	n-Type resistivity, ohm. cm. Before	After
JB 1	700°, 2 hr.	4.44	2.10
JB 2	700°, 2 hr.	16.54	1.72

This may be explained on the assumption that the function of copper impurities in germanium was to compensate for donors. After copper acceptors were removed by the cyanide treatment, more donors were released; therefore, the n-type germanium samples showed lower resistivity or higher conductivity as might be expected.

Spectroscopic analysis of the treated and untreated germanium samples showed that the trace amounts of copper were removed in the treated samples. However, this cannot be considered as any absolute evidence because subspectroscopic amounts of copper still can cause thermal conversion of n-type germanium. A more sensitive way to study this would rely on the use of radioactive copper. It is hoped that this may be carried out here in the future.

Acknowledgment.—The author wishes to express his thanks to Dr. C. G. Thornton and Dr. H. I. Crane of this Laboratory for their valuable suggestions and discussions during the course of this work.

THE AMMONIA-AMMONIUM CARBONATE SYSTEM FOR THE CONCENTRATION OF NITROGEN-15

BY G. M. BEGUN, A. A. PALKO AND L. L. BROWN

Contribution from the Materials Chemistry Division, Oak Ridge National Laboratory, Oak Ridge, Tenn.

Received June 6, 1955

The isotopic exchange reaction between gaseous ammonia and ammonium carbonate solution saturated with dissolved ammonia has been studied. Rapid exchange was found between carbamate ion and the other nitrogen species present. The effective separation factor at atmospheric pressure determined from single stage equilibrations was found to be 1.015 at 15.6°, 1.019 at 25.8°, 1.021 at 35.9° and 1.022 at 44.3°. Calculations from the data gave the following values for the separation factor between gaseous ammonia and carbamate ion: 1.023 at 15.6°, 1.021 at 25.8°, 1.021 at 35.9° and 1.019 at 44.3°. In both cases, N^{15} concentrates in the aqueous phase. Column studies were in agreement with this datum and showed the system to be a feasible one for the production of enriched N^{15}.

Introduction

The chemical exchange system for the enrichment of N^{15} employing ammonia gas and aqueous ammonium ion has been studied by a number of investigators. Urey and Aten[1] first proposed the system in 1936 and it has been studied essentially unchanged by other workers.[2-14] Despite the numerous studies of this system very few modifications have been proposed. In most cases, a saturated solution of ammonium nitrate from an infinite reservoir was fed to the top of an exchange column and passed countercurrent to a stream of ammonia gas. Isotopic exchange took place between the ammonia gas and the ammonium nitrate solution with the result that the N^{15} was concentrated at the lower end of the column. In order to establish an isotopic gradient, reflux must take place at the bottom of the column. This was accomplished by adding sodium hydroxide solution to convert ammonium nitrate to ammonia gas which was returned to the exchange column. At the large reflux ratios (of the order of 12,000 to 1) required to produce highly enriched N^{15}, large amounts of chemicals are consumed by this process.

Urey[15] has suggested a modification of this system in which ammonium carbonate would be used in place of ammonium nitrate in the aqueous phase. Such a substitution would make possible a closed reflux cycle in which chemicals from one reflux would be used to accomplish the other reflux. Ammonium carbonate solution from the bottom of the exchange column is neutralized with calcium hydroxide to form calcium carbonate and ammonia. The ammonia formed is passed up the exchange column and the calcium carbonate is calcined to drive off carbon dioxide. The carbon dioxide is recombined with water and ammonia to form ammonium carbonate solution at the top of the exchange column. Calcium hydroxide is reformed by treating the calcium oxide with water. In such a closed cycle system only heat is consumed to accomplish the reflux processes.

The substitution of ammonium carbonate for ammonium nitrate, however, is not a simple substitution of carbonate ion for nitrate ion since aqueous ammonium carbonate solution contains a mixture of bicarbonate, carbonate, and carbamate ions. Formation of carbamate is often slow and it seemed possible that carbamate ion would not exchange nitrogen quickly enough with the other species or gaseous ammonia. If carbamate ion exchanged slowly with the other N-containing species, N^{14} from the waste end of the exchange column would be carried to the product or N^{15} end of the system and the isotopic gradient would be destroyed.

Experimental

Reference to the phase diagram of the CO_2, NH_3, H_2O system[16-18] indicates that solutions approximately 20 *M* in total nitrogen (dissolved ammonia, ammonium ion and carbamate ion) should be possible at 25°. The solutions used were prepared by simultaneously saturating water with gaseous ammonia and commercial ammonium carbonate (a mixture of ammonium bicarbonate and ammonium carbamate). This method was found to produce solutions whose total N and total C content was close to the phase diagram compositions shown by Jänecke[17] although consistently lower in total N content.

In the exchange experiments, a weighed amount of NH_3 gas enriched with N^{15} was equilibrated with a weighed amount of carbonate solution saturated with ammonia. The reaction vessel was a one-liter round bottom flask equipped with a capillary stopcock for gas sampling, a self sealing rubber diaphragm for admitting the liquid phase from a hypodermic needle, and a 10-cm. long nipple which served as a cold trap during the introduction of the ammonia gas. At the beginning of the experiment the flask was evacuated and weighed. Ammonia gas prepared from ammonium nitrate enriched in N^{15} and dried over CaO was admitted and the flask reweighed. Aqueous ammonium carbonate solution aged three weeks to ensure chemical equilibrium was injected through the rubber diaphragm by means of a hypodermic syringe. The weight of solution added was found by weighing the syringe before and after addition of

(1) H. C. Urey and A. H. W. Aten, *Phys. Rev.*, **50**, 575 (1936).
(2) H. C. Urey, M. Fox, J. R. Huffman and H. G. Thode, *J. Am. Chem. Soc.*, **59**, 1407 (1937).
(3) H. C. Urey, J. R. Huffman, H. G. Thode and M. Fox, *J. Chem. Phys.*, **5**, 856 (1937).
(4) H. G. Thode and H. C. Urey, *ibid.*, **7**, 34 (1939).
(5) K. Clusius, E. Becker and H. Lauckner, *Chem. Zentr.*, **113**, **II**, 1089 (1942).
(6) K. Clusius and E. Becker, *Z. physik. Chem.*, **193**, 64 (1943).
(7) E. W. Becker and H. Baumgartel, *Z. Naturforsch.*, **1**, 514 (1946).
(8) I. Kirshenbaum, J. S. Smith, T. Crowell, J. Graff and R. McKee, *J. Chem. Phys.*, **15**, 440 (1947).
(9) E. W. Becker and H. Baumgartel, *Angew. Chem.*, **A59**, 88 (1947).
(10) A. Sugimoto, R. Nakane, R. Shibata, T. Watanabe, S. Motonaga and S. Isomura, *Repts. Sci. Research Inst. (Japan)*, **26**, 1 (1950).
(11) A. Sugimoto, R. Nakane, T. Watanabe, T. Matsuo, S. Isomura and M. Morishita, *ibid.*, **27**, 19 (1951).
(12) A. Sugimoto, R. Nakane and T. Watanabe, *Bull. Chem. Soc. Japan*, **24**, 153 (1951).
(13) R. Nakane, *Repts. Sci. Research Inst. (Japan)*, **28**, 276, 413 (1952).
(14) A. Sugimoto, R. Nakane, T. Watanabe, S. Isomura and K. Morishita, *ibid.*, **29**, 81 (1953).
(15) H. C. Urey, private communication, Dec. 12, 1951.
(16) E. Terres and H. Weiser, *Z. Elektrochem.*, **27**, 177 (1921).
(17) E. Jänecke, *ibid.*, **35**, 716 (1929).
(18) A. Guyer and T. Piechowiez, *Helv. Chim. Acta*, **27**, 858 (1944).

the liquid. The flask was shaken vigorously by hand and samples of the gas phase were taken in evacuated bulbs at intervals. These and other isotopic samples were analyzed on a Consolidated model 21-330 mass spectrometer which was originally designed for water analysis but which was converted to measure mass 28/29 ratios directly. Samples for analysis were neutralized with HCl and converted to N_2 gas using alkaline sodium hypobromite.

Determination of the effective single stage separation factor was made at a number of different temperatures. A one-liter round bottom flask was fitted with a stirrer and outlets for sampling the liquid and gaseous phases. The flask was submerged almost entirely in a constant temperature bath. The liquid phase used was prepared by saturating water with both commercial ammonium carbonate (a mixture of ammonium bicarbonate and ammonium carbamate) and ammonia. This saturated solution was held at constant temperature for a minimum of 5 days before use to ensure chemical equilibrium between all possible molecular species. The gas phase used in these runs was anhydrous tank ammonia.

To make a determination, ammonia was blown through the flask for several minutes to replace all the air. About 60 ml. of ammonium carbonate solution was added, and the stirrer was inserted to seal the system. Stirring was started and continued for 2 to 2.5 hours. After this time, the flask was removed from the bath and the phases quickly separated. A portion of the liquid sample was neutralized with HCl and converted to N_2 for isotopic analysis. The remainder of the liquid was used immediately for chemical analysis. Samples of the gas phase were absorbed in aqueous HCl and prepared for isotopic analysis. Runs were not made at higher temperatures because of the thermal instability of the carbonate solution. Total NH_3, total CO_2 and NH_2COO^- were determined directly. To determine NH_2COO^-, an immediate cold precipitation of carbonate with $Ba(OH)_2$ was made.[19] The precipitate was removed by centrifugation and the solution warmed 1 hour in a steam-bath to convert carbamate to carbonate. The $BaCO_3$ formed was then filtered off and titrated. The NH_4^+ concentration was calculated from the anionic concentration of the solution assuming complete ionization. The dissolved NH_3 was calculated by deducting the NH_4^+ and NH_2COO^- concentrations from the total NH_3 of the solution.

The 2.1 cm. i.d. exchange column used to study the system under countercurrent conditions had a 10.5 foot exchange section packed with 1/8 inch glass helices and was jacketed for temperature control. The reflux column used to take the ammonia from the solution after addition of $Ca(OH)_2$ or NaOH was 2 in. i.d. glass, 15 feet high and had a 14 foot section packed with ceramic saddles. It was wrapped with sections of heating tape so that the temperature of the column could be controlled. In operation, a feed solution of ammonium carbonate, saturated with gaseous ammonia and commercial ammonium carbonate at the desired temperature was pumped to the top of the exchange column. From the bottom of the exchange column the carbonate solution was pumped to a feed point 4 feet from the top of the reflux column. Calcium hydroxide slurry or NaOH solution was preheated and fed into the top of the reflux column. A reboiler at the bottom of the reflux column removed last traces of ammonia from the solution. The ammonia formed passed into the bottom of the exchange column. Although expulsion was accomplished quite efficiently with lime slurry, plugging of the reflux column took place after several hours of operation. This appeared to be due to formation of $CaCO_3$ precipitate in the column. To avoid redesign of the apparatus, NaOH was used in the runs reported. Subsequent operations showed that clogging of the reflux column could be eliminated if the $Ca(OH)_2$ slurry were mixed with the ammonium carbonate solution in a precontact loop before entering the reflux column. The hot solution was circulated by a centrifugal pump and a residence time of 30 minutes was maintained in the loop before passage into the reflux column. A reflux column was operated for several 8-hour intervals in this manner without any signs of plugging. Effluent analysis showed losses of the order of 0.003 mole % of the total N entering the refluxer. No isotopic runs were made using the $Ca(OH)_2$ reflux.

(19) G. H. Burrows and G. N. Lewis, *J. Am. Chem. Soc.*, **34**, 993 (1912).

Since N^{15} concentrates in the aqueous phase at the bottom of the reflux column the conversion of ammonium carbonate to ammonia and separation of the ammonia from the solution must be highly quantitative. Any loss of ammonia in the waste solution would constitute a loss of product N^{15}.

A series of runs were made in order to obtain an estimate of both N, the number of theoretical stages in the column and α, the effective single stage separation factor. The runs were made keeping the feed solution concentration, temperature, pressure and flow rates as constant as possible. In each run a different constant withdrawal rate of NH_3 gas was maintained from the bottom of the exchange column. Samples for isotopic analysis were taken at intervals from the same point.

In order to further investigate the possibility that carbamate ion might exchange slowly with other nitrogen species the isotopic gradient in the column was examined by taking ammonia samples simultaneously from a number of sampling points along the length of the exchange column. These samples were taken after the column had been run at essentially total reflux for 14 and 16 hours.

Experimental Results and Discussion

Isotopic analyses of the gas phase from the ammonia–ammonium carbamate exchange experiment using 3.17 atom % N^{15} in the initial gas phase and normal nitrogen in the solution gave the following values after contacting: 3 min., 0.694 % N^{15}; 20 min., 0.695 % N^{15}; and 45 min., 0.673 % N^{15}. The solution was 19.4 *M* in total N species of which 4.8 *M* was analyzed to be carbamate ion. Exchange with all solution species yields a calculated equilibrium value of 0.770% N^{15} while non-exchange of the carbamate species would give a final value of 0.908% N^{15}. It was concluded that the carbamate ion had completely exchanged under the conditions of the experiment in less than 3 minutes. The discrepancy between the final calculated and determined values could only be explained as due to mass balance difficulties. However, the constancy of the percentage N^{15} with time shows that no further exchange was taking place.

Results of the single stage batch equilibrations are shown in Table I.

TABLE I

VALUES OF SINGLE STAGE SEPARATION FACTORS FOR THE AMMONIA–AMMONIUM CARBONATE SYSTEM

Temp., °C.	15.6	25.8	35.9	44.3
Total N in soln. (mole/l.)	19.35	20.05	20.10	18.10
Total C in soln. (mole/l.)	3.94	6.20	7.50	8.03
NH_2COO^- (mole/l.)	3.71	5.82	6.68	6.81
NH_4^+ (mole/l.)	4.12	6.51	8.02	8.64
NH_3 (dissolved) (mole/l.)	11.52	7.72	5.40	2.65
$(N^{15}/N^{14})_{soln}/(N^{15}/N^{14})_g$	1.015	1.019	1.021	1.022
95% C.I.	±0.003	±0.002	±0.003	±0.004

The three reactions responsible for the isotopic concentrations are

$$N^{14}H_4^+(soln) + N^{15}H_3(g) = N^{15}H_4^+(soln) + N^{14}H_3(g) \quad (1)$$

$$N^{14}H_3(soln) + N^{15}H_3(g) = N^{15}H_3(soln) + N^{14}H_3(g) \quad (2)$$

$$N^{14}H_2COO^-(soln) + N^{15}H_3(g) = N^{15}H_2COO^-(soln) + N^{14}H_3(g) \quad (3)$$

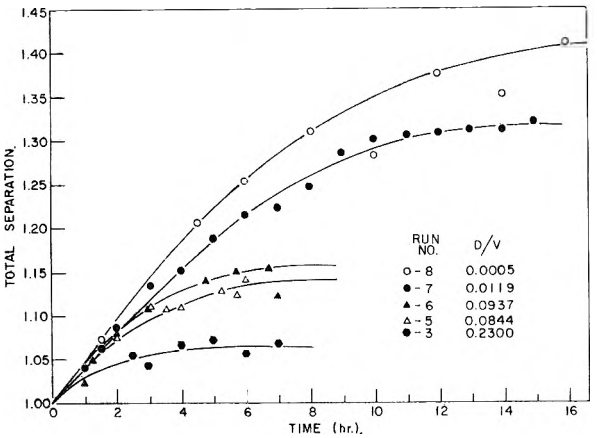

Fig. 1.—Total separation *vs.* time for various D/V ratios in the ammonia–ammonium carbonate system.

If K_1, K_2 and K_3 are the equilibrium constants for the isotopic exchange reactions, it can be shown that at low N^{15} concentrations the effective separation factor α for the system is related to K_1, K_2 and K_3 by the equation

$$(\alpha - 1) = M_1(K_1 - 1) + M_2(K_2 - 1) + M_3(K_3 - 1) \quad (4)$$

where M_1 is the mole fraction of NH_4^+ with respect to the total dissolved N containing species, and M_2 and M_3 are the similar mole fraction of dissolved NH_3 and carbamate ion, respectively. K_1 and K_2 have been determined by Kirshenbaum and coworkers[8] at 25°, and values at various temperatures have been calculated by Nakane.[13] If these values are substituted in equation 4 along with the experimental separation factors and the mole fractions from chemical analysis K_3 can be calculated at the various temperatures. Results of this calculation are given in Table II, along with the values of K_1 and K_2 used.

Table II

Calculated Values for the Separation Factor Between Gaseous Ammonia and Carbamate Ion

T (°C.)	M_1	K_1[a]	M_2	K_2[a]	M_3	K_3
15.6	0.213	1.036	0.595	1.005	0.192	1.023
25.8	.325	1.034	.385	1.005	.290	1.021
35.9	.399	1.032	.269	1.005	.332	1.021
44.3	.477	1.030	.147	1.004	.376	1.019

[a] Values taken from Nakane, ref. 13.

The values for K_3 are seen to decrease with increasing temperature as expected. The increase in over-all separation factor of the system is seen to be due largely to the decreasing mole fraction of dissolved ammonia as the temperature increases. This is somewhat compensated, however, by the decreasing values of K_1, K_2 and K_3 so that the total separation is close to a maximum at 44.3° and would be expected to decrease at higher temperatures.

All the column runs were made at 30° and atmospheric pressure. The feed solution was 18.0–19.0 M in total N species and the feed rate varied from 315 to 360 cc. per hour. Fig. 1 shows the isotopic analyses obtained from samples taken at intervals from the N^{15} end of the column. Total separation is defined as the N^{15}/N^{14} atom ratio of the sample divided by the N^{15}/N^{14} ratio of the feed solution. D/V is the ratio of the rate of product N withdrawal to the rate of flow of total N down the exchange column, and represents the inverse of the reflux ratio. As is expected, with highest D/V ratios the final equilibrium concentration of N^{15} attained is lowest. Using the extrapolated equilibrium N^{15} concentrations from 4 of these runs, values of N the number of stages and α the effective separation factor were calculated. The method of calculation is given by Shacter and Garrett.[20]

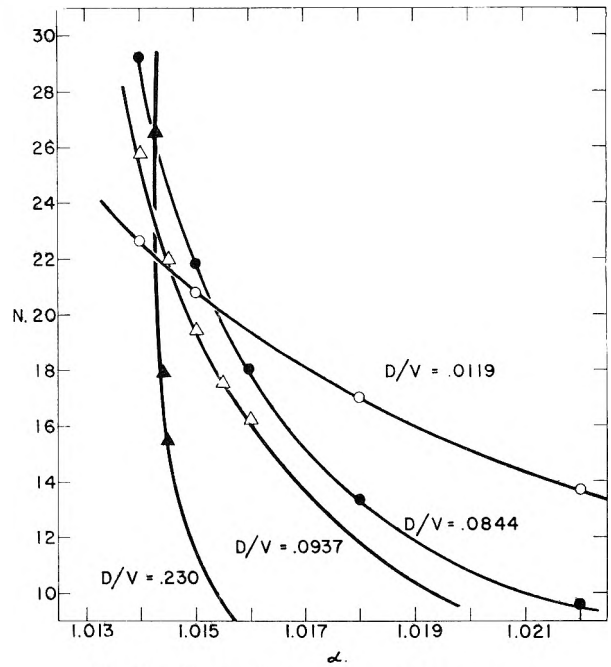

Fig. 2.—N *vs.* α from column exchange runs.

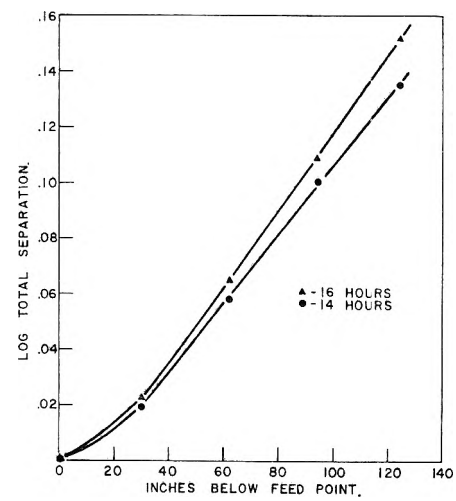

Fig. 3.—Isotopic gradient in the exchange column.

The results of the calculation are shown in Fig. 2. Ideally the curves should intersect at one point giving the actual values of N and α. However, due to experimental variations this usually does not happen and the general area of intersection is taken as a measure of N and α. It was estimated that the number of stages in the column was approximately 23 and the effective separation factor

(20) J. Shacter and G. A. Garrett, AECD-1940, p. 14, May 7, 1948.

about 1.0155. This yields a stage height of 5.5 inches in the exchange column. Considering the many variables in such a determination of thes epa-ration factor, the agreement with the single stage data is satisfactory.

Results of tke isotopic gradient determination are shown in Fig. 3. At equilibrium the plot of log of the total separation *vs.* column length would be expected to give a straight line. The slight bend in the curves at the lower corner shows that the system had not quite reached the equilibrium condition. However, the linearity of the remaining portion of the curves substantiates the exchange data and shows that the N content of the solution must be at isotopic equilibrium. If this were not so, a bowing over of the curve at the upper end would be expected.

Acknowledgments.—The authors wish to thank J. M. Saari of the Y-12 Mass Spectrometer Laboratory for his excellent mass analyses of nitrogen samples, and A. S. Meyer of the Analytical Division for the carbamate analysis.

DIFFUSION IN IDEAL BINARY LIQUID MIXTURES[1,2]

By C. S. Caldwell[3] and A. L. Babb

Department of Chemical Engineering, University of Washington, Seattle, Washington

Received June 6, 1955

Mutual diffusion coefficients of several binary liquid systems that behave nearly ideally have been measured with a Mach-Zehnder Interferometer and a single-channel diffusion cell over a temperature range of 15 to 40°. The diffusion coefficients for these systems vary almost linearly with mole fraction over the entire concentration range. A linear relation between $D\eta/T$ and mole fraction was obtained, so that diffusion coefficients of any non-associated solutions at any composition may be predicted from those at infinite dilution as proposed by Roseveare, Powell and Eyring. In addition, the applicability of the rate-process theory of Eyring to the prediction of diffusion coefficients for these solutions at infinite dilution is discussed.

Introduction

In addition to increasing the understanding of transport processes in liquids, a knowledge of liquid diffusion coefficients is required for the calculation of mass transfer rates across liquid films in distillation, extraction, chemical reaction and mixing. Even though the liquid diffusivities generally do not vary much beyond the range of 1 to 5 $\times$ 10^{-5} cm.^{2}/sec. at room temperature, a large proportion of the transfer resistance resides in these liquid films. Available diffusivity correlations[4,5] are satisfactory for dilute solutions where accuracy is not too important, but the existing methods for estimating diffusivities in concentrated solutions have heretofore not been verified experimentally. Consequently, it was desirable to measure liquid diffusivities and to obtain in particular their temperature and composition dependences for comparison with theory.

As the first step in this direction it was decided to obtain accurate experimental data for the mutual diffusion coefficients of simple liquid mixtures which behaved ideally or nearly so. By establishing basic criteria for the ideal concentration dependence of diffusivity, it was hoped that the abnormal behavior of many other systems of practical importance could then be explained in terms of well-defined deviations from the ideal.

Experimental Method

Previous Experimental Work.—The lack of a reliable technique for obtaining accurate molecular diffusion coefficients in volatile organic liquid systems over a moderate range of temperatures and over the entire range of compositions has been one of the major obstacles in the experimental study of the transport properties of liquid systems. To date, only the work of a few scattered groups has produced experimental data for complete binary liquid systems. Furthermore, most of the earlier work was confined to systems where abnormal effects, such as association or complex formation, were present. Almost all of the other early diffusion work was confined either to dilute solutions of electrolytes or to dilute solutions of organic materials in benzene, the alcohols, or hydrocarbons. Limited measurements of the system tetrachloroethane–tetrabromoethane were made by Cohen and Bruins in 1923,[6] but it was not until the early 1930's that Gerlach,[7] Munter,[8] and Franke[9] began to study concentrated solutions. Unfortunately, for the system carbon tetrachloride–benzene the disagreement between the values of Gerlach and Munter and those of Franke for 20° was as high as 50% for low benzene concentrations as shown in Fig. 1. Franke and Munter both employed the Lamm refractometric technique, while Gerlach used a densitometric method for analysis of the diffusion column.

The first successful attempt to obtain reliable measurements for concentrated solutions was reported in 1938 by Lemonde[10] who used a refractometric technique. Recently, Drickamer and Trevoy[11] have reported a limited amount of diffusion data for systems involving aliphatic hydrocarbons and benzene. Dunning and Washburn,[12] Smith and Storrow,[13] and Stokes,[14] have reported data for aqueous solutions of alcohols but there is considerable disagreement between the reported values particularly at high alcohol concentrations.

Apparatus.—The Mach–Zehnder interferometer employed in this work has been used extensively in engineering research and its typical applications, operational and constructional

(1) This work was supported in part by the Office of Ordnance Research, U. S. Army.

(2) Based in part on a Dissertation submitted by Colin Spencer Caldwell in partial fulfillment of the requirements for the degree of Doctor of Philosophy, University of Washington, Seattle, Washington.

(3) Westinghouse Electric Corp., Pittsburgh, Pa.

(4) J. H. Arnold, *J. Am. Chem. Soc.*, **52**, 3937 (1930).

(5) C. R. Wilke, *Chem. Eng. Progr.*, **45**, 218 (1949).

(6) E. Cohen and H. R. Bruins, *Z. physik. Chem.*, **103**, 404 (1923).

(7) B. Gerlach, *Ann. Physik*, **10**, 437 (1931).

(8) E. Munter, *ibid.*, **11**, 558 (1931).

(9) G. Franke, *ibid.*, **14**, 675 (1932).

(10) H. Lemonde, *ibid.*, **9**, 539 (1938).

(11) D. J. Trevoy and H. G. Drickamer, *J. Chem. Phys.*, **17**, 1117 (1949).

(12) H. N. Dunning and E. R. Washburn, This Journal, **56**, 235 (1952).

(13) E. E. Smith and J. A. Storrow, *J. App. Chem.*, **2**, 225 (1952).

(14) R. H. Stokes, *Trans. Faraday Soc.*, **48**, 887 (1952).

TABLE I

MAXIMUM PERCENTAGE DEVIATIONS FROM MOLAR ADDITIVITY AT ROOM TEMPERATURE

System	Heat of mixing ΔH^m	Molar vol. ΔV^m	Molar surface tension $\Delta E'$	Molar polarization $\Delta P'$	Dielectric constant $\Delta\epsilon$	Molar heat capacity ΔC_p	Raoult's law
C_6H_6–CCl_4	+ 0.5	0	−1.8	0	−0.5	..	+3
C_6H_5Cl–C_6H_5Br	+ 0.3	0	0	0	0	0	0
$C_6H_5CH_3$–C_6H_5Cl	− 0.3	−0.3	−0.5	+7.8	...	..	+3

details, and adjustment, are described in the original thesis.[15] As it was applied to diffusion measurements the interferometer provided a record of the concentration distribution within a single channel diffusion cell, the upper region of which served as a reference section. The high sensitivity of the interferometer fringe-pattern permitted the use of small concentration differences between the original solutions on either side of the boundary, and hence the measured diffusion coefficients could be considered differential coefficients. In order to obtain reproducible starting conditions for each experiment, a double-slit boundary sharpening technique was used. The method differed from existing techniques in that diffusion between solutions of volatile organic solvents could be investigated in the specially designed diffusion cell which required no greased joints or sliding sections.

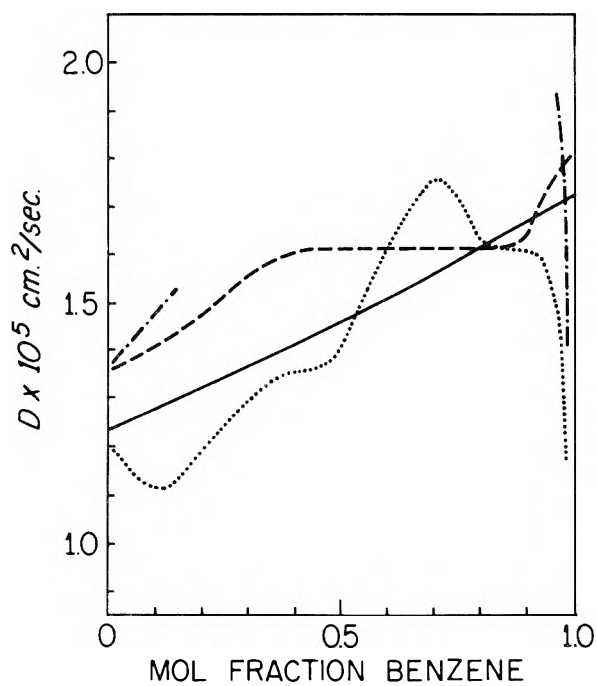

Fig. 1.—Comparison of mutual diffusion coefficients for the system benzene–carbon tetrachloride at 20°: —·— Gerlach; – – –, Munter; ....., Franke; ———, the authors.

It is felt that diffusion coefficients accurate to within 1% can be obtained with this type of interferometer using the double-slit boundary sharpening technique.

Preparation of Solutions.—Binary pairs were selected on the basis of the accepted criteria for solution ideality and also upon the molar additivity of vapor pressure, polarization, dielectric constant and molar surface tension. The maximum deviations from linearity of these parameters are shown in Table I. Since the diffusion measurements were to be made interferometrically using small over-all concentration differences of about 2 mole %, a refractive index difference of 3×10^{-2} was required between the pure components. As a result nearly all of the isomeric pairs which are known to be almost ideal in the liquid state had to be eliminated. In spite of these limitations the following systems were chosen and are listed in order of decreasing expected degree of ideality: chlorobenzene–bromobenzene; toluene–chlorobenzene; and carbon tetrachloride–benzene.

The benzene, carbon tetrachloride and toluene were "Baker Analyzed" Reagent Grade, the bromobenzene was Eastman Kodak Company "White Label" No. 43 Grade, and the chlorobenzene was Matheson, Coleman and Bell, C.P. Grade. The benzene, chlorobenzene and bromobenzene were dried over sodium wire and then distilled to give final values of the refractive index of 1.50072, 1.52433 and 1.55980, respectively. The carbon tetrachloride was dried over phosphorus pentoxide and twice filtered, refractive index = 1.46016. The toluene was sulfur-free, and was used without purification.

The concentration differences between the two solutions used in each diffusion experiment were determined by the cell thickness, L, the total fringe displacement n_1–n_2, and the refractive index-mole fraction relationship, dn_D/dx. For the above solutions, dn_D/dx was constant and equal to n_D between the pure components. Equation 1 gives the relationship between the required mole fraction difference, Δx, and the total fringe displacement, $n_1 - n_2$

$$\Delta x = \frac{(n_1 - n_2)}{\Delta n_D L \lambda'} \qquad (1)$$

where $\lambda' = 5461$ Å.

Procedure.—After the cell had been filled with the desired solutions in accordance with the procedure described previously,[15] the boundary was sharpened in a preliminary fashion before immersing the cell in the thermostat. The temperature of the water-bath was maintained at ±0.001° of the desired temperature. During the period of several hours required for the cell and reservoir contents to attain the bath temperature, slow boundary sharpening was used to flush the upper part of the cell. It was necessary to regulate the flows carefully so that the boundary remained symmetrical and located in line with the slits. Toward the end of the sharpening period, a photograph of the fringe pattern was taken so that the fractional part of the total fringe number difference could be evaluated. For the low molecular weight organic systems, where the diffusion coefficient is approximately 10^{-5} cm.²/sec. the interval between the subsequent exposures was about 300 seconds, and usually ten were taken per experiment.

The resulting interferograms were evaluated by the maximum-ordinate area method developed by Svensson,[16] and details of the calculations for this investigation may be obtained from the original thesis.[15]

Results and Discussion

A summary of the experimental data for the three systems is given in Table II and the diffusivity-mole fraction relationships are given in Figs. 2, 3 and 4. The maximum deviation in D for any of the runs is about 4%, while the average deviation from the curve is somewhat less than 1%.

The general appearance of these curves shows that the diffusion coefficient can be expressed approximately as a linear function of mole fraction across the entire concentration range for an ideal system. The deviations appear to increase with the expected increase in non-ideality and with a decrease in temperature. The fact that the diffusion coefficient changes in a linear manner with a change in mole fraction indicates that the average forces encountered by a given molecule depend only on the mole average of the forces characteristic of the two species. Although the resistance to motion changes with composition, evidently the two

(15) C. S. Caldwell, Ph.D. Thesis, University of Washington, 1955.

(16) H. Svensson, *Acta Chem. Scand.*, **5**, 72 (1951).

TABLE II

SUMMARY OF EXPERIMENTAL AND CALCULATED VALUES

System A	System B	Run no.	Temp., °C.	Av. compn. ($\bar{x}$) of A mole fraction	$D \times 10^5$, cm.²/sec.
C_6H_6	CCl_4	49	10.00	0.02154	1.088
		42	10.00	.02154	1.080
		41	10.00	.02154	1.087
		40	10.00	.2502	1.093
		39	10.00	.5051	1.230
		37	10.00	.7498	1.344
		38	10.00	.9815	1.466
		31	25.20	.02154	1.419
		32	25.26	.2502	1.519
		33	25.26	.5051	1.651
		36	25.34	.7498	1.759
		35	25.26	.9815	1.912
		48	40.0	.02154	1.775
		44	40.0	.2502	1.970
		92	40.0	.5051	2.077
		91	40.0	.7498	2.284
		47	40.0	.9815	2.432
C_6H_5Cl	C_6H_5Br	58	10.01	.0332	1.007
		57	10.01	.2642	1.069
		56	10.01	.5122	1.146
		55	10.01	.7617	1.226
		54	10.01	.9652	1.291
		63	26.78	.0332	1.342
		62	26.78	.2642	1.380
		61	26.78	.5122	1.506
		60	26.78	.7617	1.596
		59	26.78	.9652	1.708
		68	39.97	.0332	1.584
		67	39.97	.2642	1.691
		66	39.97	.5122	1.806
		65	39.97	.7617	1.902
		64	39.97	.9652	1.996
$C_6H_5CH_3$	C_6H_5Cl	73	10.00	.01337	1.346
		72	10.00	.2501	1.404
		71	10.00	.4992	1.556
		70	10.00	.7492	1.652
		69	10.00	.9862	1.759
		78	26.96	.01337	1.756
		77	26.96	.0501	1.852
		76	26.96	.4992	1.985
		75	26.96	.7492	2.128
		74	26.96	.9862	2.264
		84	40.01	.01337	2.113
		82	40.01	.2501	2.277
		81	40.01	.4992	2.435
		80	40.01	.7492	2.586
		79	40.01	.9862	2.714

species involved in the diffusion process do not change their state of aggregation with composition. The system benzene–carbon tetrachloride, however, is a possible exception, since the formation of intermolecular complexes of the 1:1, 1:2 and 1:3 type between benzene and carbon tetrachloride has been reported by Kapustinskii and Drakin[17] and Wyatt[18] from melting point–composition studies. The formation of such complexes in solution is a definite possibility at lower temperatures.

(17) A. F. Kapustinskii and S. I. Drakin, *Bull. acad. sci. USSR, Classe sci. chim.*, 435 (1947).

(18) W. F. Wyatt, *Trans. Faraday Soc.*, **25**, 48 (1929).

TABLE III

EXPERIMENTAL ACTIVATION ENERGIES FOR DIFFUSION AND VISCOSITY

Component	E_{vap}, kcal./mole	E_η, kcal./mole	E_D, kcal./mole	$\frac{E_D}{E_\eta}$	$\frac{n_{vis} = E_{vap}}{E_\eta}$	$\frac{n_{diff} = E_{vap}}{E_D}$
C_6H_5Cl	9.52	1.93	2.63	1.36	4.93	3.61
C_6H_5Br	10.57	1.93	2.63	1.36	5.47	4.02
$C_6H_5CH_3$	8.49	1.98	2.66	1.34	4.28	3.19
C_6H_5Cl	9.52	1.93	2.70	1.40	4.93	3.52
C_6H_6	7.50	2.34	3.00	1.28	3.20	2.50
CCl_4	6.58	2.28	3.23	1.42	2.88	2.04
Av.		2.07	2.80	1.36	4.28	3.15

Comparison with Theory.—The theory of diffusion as a rate process, as proposed by Eyring, may be tested in several different ways to determine whether or not the important functional dependences are predicted correctly for these nearly-ideal systems. By plotting ln D *vs.* $1/T$ for each of the compositions the experimental activation energy for diffusion, E_D, can be calculated, since the temperature dependence of the diffusivity is given by

$$D = Ae^{-E_D/RT} \qquad (2)$$

Eyring[19] has shown on an empirical basis that E_D should be some fraction $1/n$, of the energy of vaporization where n varies between 3 and 4. Furthermore, according to Eyring, the same considerations should apply to the activation energy for viscosity, E_η. As a result, it might be expected that the

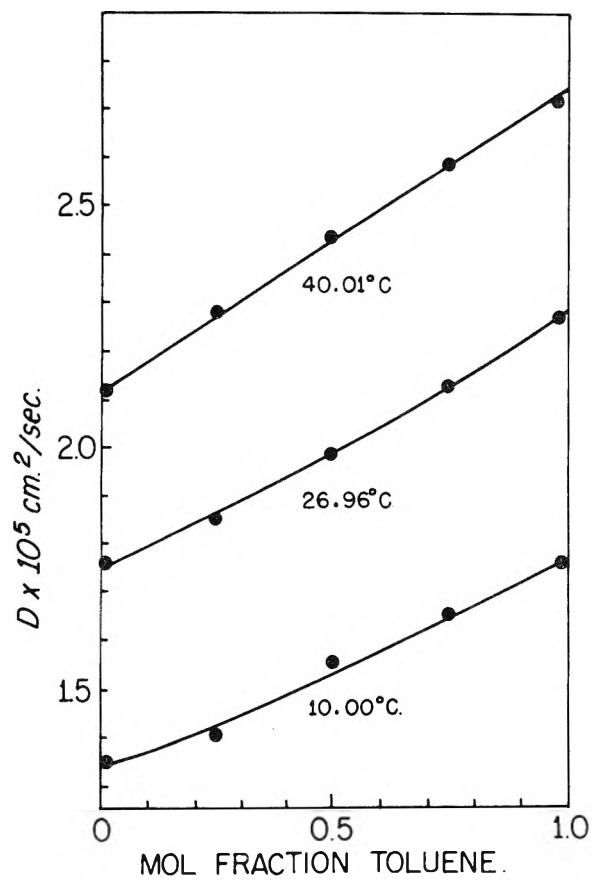

Fig. 2.—Mutual diffusion coefficients for the system toluene–chlorobenzene.

(19) H. Eyring, *J. Chem. Phys.*, **4**, 283 (1936).

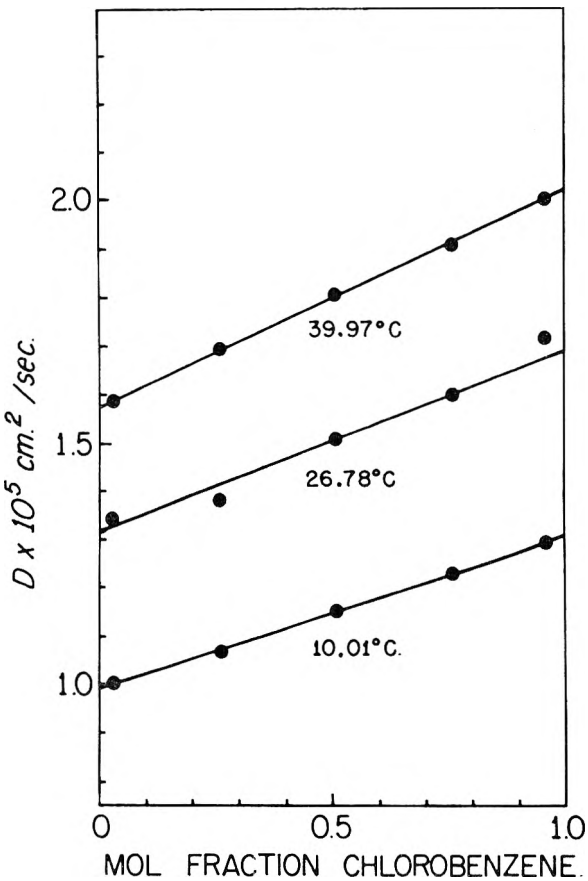

Fig. 3.—Mutual diffusion coefficients for the system chlorobenzene–bromobenzene.

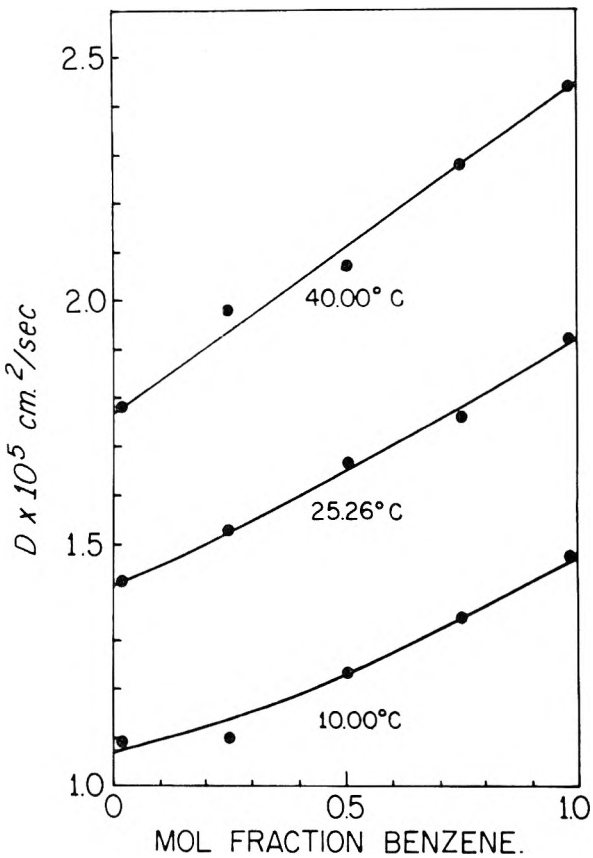

Fig. 4.—Mutual diffusion coefficients for the system benzene–carbon tetrachloride.

systems studied here would demonstrate a rather constant value of n, since the components are of similar constitution. Values of the experimental activation energies for diffusion and viscosity calculated for the pure solvents are listed in Table III. The viscosity data were obtained from Timmermans,[20] while the diffusivity data were extrapolated to mole fractions of 0 and 1 to obtain D^0 for the compositions corresponding to the pure components. From the data given in Table III it is seen that although the energies of vaporization of the components vary over a range of about 4 kcal./mole, E_η and E_D vary only slightly. This variation is reflected in the wide range of values found for n_{vis} and n_{diff}. For these systems, E_D is always higher than E_η by about 0.7 kcal./mole, giving a ratio E_D/E_η which remains nearly constant at 1.36. It appears that for these structurally similar substances, the resultant uncertainty in predicting the activation energy for either viscosity or diffusion by the use of a universal value for n is related to the dissimilarity between the evaporation and hole-formation processes. Furthermore, the relation between viscosity and diffusivity as given by Eyring[19]

$$\frac{D\eta}{kT} = \frac{\lambda_1}{\lambda_2\lambda_3} \qquad (3)$$

is derived on the basis that $E_D = E_\eta$. It is apparent that this equation will not generally be applicable over a large range of temperatures, since $E_D = 1.36E_\eta$.

Table IV gives the experimental values of D for each system at three compositions. The diffusivities at 25° were obtained by interpolation from Figs. 2, 3 and 4. It is seen that the $D\eta$ products do not change markedly with concentration. This is in fair agreement with equation 2, which states that the $D\eta$ product should be inversely proportional to a characteristic dimension, $\lambda = (V/N)^{1/3}$, of the solute molecule. For the case of diffusion of toluene and bromobenzene in chlorobenzene, the ratio of the $D^0\eta^0$ products should be

$$\frac{D^0\eta^0 \text{ (toluene in chlorobenzene)}}{D^0\eta^0 \text{ (bromobenzene in chlorobenzene)}} = \frac{\lambda_{\text{bromobenzene}}}{\lambda_{\text{toluene}}}$$

The ratio of the $D^0\eta^0$ products was 1.276/1.238 = 1.16, whereas the ratio of the λ's was found to be 5.60/5.62 = 1.0. In this case the molar volumes, V, are practically identical and the above relationship is approximately satisfied.

Roseveare, Powell and Eyring[21] have suggested that the quantity $D\eta/T$ should vary linearly with mole fraction for an ideal binary mixture

$$\left[\frac{D\eta}{T}\right]_{x=x} = \left[\frac{D\eta}{T}\right]_{x=0} + x\left\{\left[\frac{D\eta}{T}\right]_{x=1} - \left[\frac{D\eta}{T}\right]_{x=0}\right\} \qquad (4)$$

This relation has been tested at 25° for the three nearly-ideal systems by comparing the experimental value of $D\eta$ at 50 mole % with the value calculated from equation 3. As shown in Table IV

(20) J. Timmermans, "Physico-Chemical Constants of Pure Organic Compounds," Elsevier Publishing Co., New York, N. Y., 1950.

(21) H. Roseveare, R. E. Powell and H. Eyring, *J. App. Phys.*, **12**, 669 (1941).

TABLE IV

DIFFUSIVITY, VISCOSITY AND $D\eta$ PRODUCT AT 25°

System A	System B	Compn. of A, mole fraction	$D \times 10^5$, cm.²/sec.	$\eta \times 10^5$, poises	$D\eta \times 10^7$, dynes	$0.5(D_1^\circ\eta_1^\circ + D_2^\circ\eta_2^\circ)$[a] $\times 10^7$ dynes
C_6H_5Cl	C_6H_5Br	1.0	1.64	755	1.238	
		0.5	1.45	885	1.283	1.287
		0.0	1.26	1060	1.336	
$C_6H_5CH_3$	C_6H_5Cl	1.0	2.21	555	1.227	
		0.5	1.93	652	1.258	1.252
		0.0	1.69	755	1.276	
C_6H_6	CCl_4	1.0	1.92	602	1.156	
		0.5	1.62	740	1.199	1.203
		0.0	1.39	900	1.251	

[a] $D_i^\circ\eta_i^\circ = D_i\eta_i$ at infinite dilution.

TABLE V

EXPERIMENTAL DIFFUSION COEFFICIENTS AT INFINITE DILUTION AND COMPONENT FACTORS COMPARED WITH VALUES CALCULATED FROM EQUATION 5 AT 25°

Solvent	Solute	$A \times 10^3$, cm.²/sec. Eyring[a]	Exp.	% Dev.	$\exp(-E_D/RT)$ Eyring[b]	Exp.	% Dev.	$D^\circ \times 10^5$, cm.²/sec. Eyring[c]	Exp.	% Dev.
C_6H_5Cl	C_6H_5Br	3.22	1.385	+132	0.0046	0.0120	− 62	1.48	1.66	−9
C_6H_5Br	C_6H_5Cl	3.93	1.050	+274	0.0026	0.0120	− 79	1.00	1.26	− 21
$C_6H_5CH_3$	C_6H_6Cl	2.84	1.955	+ 45	0.0081	0.0113	− 28	2.30	2.21	+ 3
C_6H_5Cl	$C_6H_5CK_3$	3.36	1.615	+108	0.0046	0.0104	− 56	1.55	1.68	− 8
C_6H_6	CCl_4	2.30	2.990	− 23	0.0145	0.0064	+127	3.33	1.91	+ 70
CCl_4	C_6H_6	1.93	3.210	− 41	0.0240	0.0043	+458	4.64	1.38	+230

[a] $A_{(Eyring)} = \lambda^2/v_f^{1/3}\{kT/2\pi m_{12}\}^{1/2}$. [b] $E_{D\ (Eyring)} = E_{vap}/3$. [c] $D^\circ = D$ at infinite dilution.

the agreement is excellent for all three systems, which indicates that within the limits of accuracy, the relationship above is exact. It is interesting to note that if D and η were both linear with mole fraction, then the $D\eta$ product would exhibit a maximum. The necessary compensation arises from the fact that for a given system either D or η has a slight negative deviation from linearity.

Finally, the Eyring equation[19]

$$D = \frac{\lambda^2}{v_f^{1/3}}\left\{\frac{kT}{2\pi m_{12}}\right\}^{1/2} \exp\left(-\frac{E_{vap}}{nRT}\right) \qquad (5)$$

was used to calculate D at 25° for both ends of the concentration range for the three systems and the results were compared with the experimental values obtained in this work. In order to make the comparison more meaningful, the frequency factor, A, has been separated from the exponential part and the experimental and calculated factors are compared individually. In the calculations, an average value of n_{diff} was obtained from Table III, m_{12} was taken as the reduced mass of the two molecules, and the free volume was obtained from the expression

$$v_f^{1/3} = \frac{2RT}{E_{vap}}\left\{\frac{V}{N}\right\}^{1/2} \qquad (6)$$

which was derived on the basis of cubical packing.[22] The results of this comparison are shown in Table V, and it would appear that with the exception of carbon tetrachloride, the calculated diffusion coefficients agree quite well with the experimental values. The comparison of the frequency and exponential factors, however, reveals large discrepancies, and it would appear that the model for diffusion represented by equation 5 does not describe the process adequately in simple systems. This is not surprising, since at low concentrations the properties of the solute have virtually no effect on λ or v_f, and since it has been shown that the use of a single constant relating E_D to E_{vap} is not usually justified.

From these comparisons it seems that the Eyring picture is a convenient qualitative representation of the diffusion process, but it does not give quantitative results for the diffusion process in liquids having even relatively simple structures.

Comparison with Semi-empirical Correlations.— The equation of Arnold[23] has been used to predict D values for the three nearly-ideal systems studied

$$D = \frac{B(1/n_1 + 1/n_2)^{1/2}}{A_1A_2\eta^{1/2}S^2} \qquad (7)$$

Since the constant B in equation 7 is available only at 20°, the results tabulated in Table VI are for this temperature. In addition, the general empirical correlations proposed by Othmer and Thakar[24] and Wilke[25] have been tested, and the results are collected in Table VI for infinite dilution. The value of ϕ chosen for use in the Wilke correlation was 0.7.

Both the equation of Arnold and the correlation of Wilke predict values of the diffusivity within 10%, but the Othmer correlation yields values which are consistently low by about 20%. Thus it is seen that the prediction of diffusion coefficients for the entire concentration region of three nearly-ideal systems could be carried out with sufficient accuracy for engineering purposes simply by calculating the two diffusion coefficients at infinite dilution by means of the Arnold or Wilke methods, and

(22) J. F. Kincaid and H. Eyring, *J. Chem. Phys.*, **6**, 620 (1938).

(23) J. H. Arnold *J. Am. Chem. Soc.*, **52**, 3937 (1930).

(24) D. F. Othmer and M. S. Thakar, *Ind. Eng. Chem.*, **45**, 489 (1953).

(25) C. R. Wilke, *Chem. Eng. Progr.*, **45**, 218 (1949).

TABLE VI

EXPERIMENTAL AND CALCULATED DIFFUSION COEFFICIENTS AT INFINITE DILUTION

Components		$D^\circ \times 10^5$, cm.²/sec.			
Solute	Solvent	This work	Arnold	Othmer and Thakar	Wilke $\phi = 0.7$
C_6H_5Br	C_6H_5Cl	1.52	1.43	1.24	1.41
C_6H_5Cl	C_6H_5Br	1.18	1.20	0.86	1.02
C_6H_5Cl	$C_6H_5CH_3$	2.06	2.07	1.60	1.95
$C_6H_5CH_3$	C_6H_5Cl	1.56	1.77	1.25	1.41
C_6H_6	CCl_4	1.25	1.60	1.02	1.18
CCl_4	C_6H_6	1.76	1.96	1.55	1.80
Av. % dev. from exptl. values			10.0	19.4	7.1

then using equation 3. If viscosity data are not available, then as an approximation, D may be assumed to be linear with mole fraction

$$D]_{x=x} = D]_{x=0} + x\{D]_{x=1} - D]_{x=0}\} \qquad (8)$$

Comparison with Previous Work.—Data on the diffusion coefficients for the system benzene–carbon tetrachloride at 20° were reported by Franke,[9] Gerlach,[7] and Munter,[8] in 1931. The data of the three investigators above have been presented in Fig. 1, together with the data obtained in this work. Their data seem to agree within 15–50% of the authors' curve, but it would be difficult to draw any conclusions regarding ideality from their data alone. To the knowledge of the authors, the systems chlorobenzene–bromobenzene and toluene–chlorobenzene have not been studied previously.

Conclusions

By determining the diffusivity–composition–temperature relationships of three nearly-ideal systems using the interferometric technique, it has been established that the diffusion coefficients vary almost linearly with mole fraction. Small negative deviations from linearity appeared as the temperature was lowered. In addition, it was found that the quantity $D\eta/T$ was linear with mole fraction, making it possible to obtain the diffusion coefficients for concentrated solutions from those at infinite dilution. These coefficients at infinite dilution may be estimated within 10% using the correlations of Arnold or Wilke.

The functional dependences of the frequency factor, A, in Eyring's rate-process theory of diffusion are not predicted correctly for the three systems. This is probably due in part to the fact that the calculated frequency factor is insensitive to variations in the properties of the solute. Moreover, it was found that the ratio E_D/E_η remains approximately constant at a value of 1.36 for the nearly-ideal systems.

Acknowledgment.—The authors would also like to acknowledge the financial assistance given by the Engineering Experiment Station of the University of Washington and the Procter and Gamble Company.

NUCLEATION FREQUENCIES FOR THE CRYSTALLIZATION OF SELENIUM GLASS

BY W. B. HILLIG

Contribution from the Metallurgy and Ceramics Research Department, General Electric Research Laboratory, Schenectady, N. Y.

Received June 9, 1955

The crystallization of droplets of high purity selenium, 2 to 15 μ in diameter, has been investigated over the temperature range 60 to 200°. Observed nucleation frequencies were $<10^4$ nuclei cm.$^{-3}$ sec.$^{-1}$. Within the limit of detection (10^3 nuclei cm.$^{-3}$ sec.$^{-1}$), no temperature-dependence of frequency was observed. Application of Turnbull and Fisher's treatment of homogeneous nucleation frequencies indicates that the free surface energy for selenium is >43.8 ergs cm.$^{-2}$. The ratio of the gram atomic free surface energy to the heat of fusion $\sigma_A/\Delta H_f$ is >0.48, whereas for most molecular substances, this ratio is 0.3 ± 0.1. The assumptions and limitations implied in these values are discussed, and the data for S_8, Se, and P_4 compared.

Introduction

The nucleation frequencies previously reported for the crystallization of the glass-like amorphous selenium[1] have been obtained under conditions unfavorable for homogeneous nucleation. On the other hand, the treatment of Turnbull and Fisher[2] permits homogeneous nucleation frequencies to be estimated from available data. Since this treatment previously has been applied mainly to the solidification of liquids having relatively low viscosity, it was the purpose of this investigation to test the relationship for crystallization from a nearly rigid fluid, *viz.*, Se(amorph) → Se(hex).

Experimental

The technique used in this study was similar to that developed by Tammann,[3] by which nuclei are produced at various temperatures and rapidly grown at an elevated temperature. The selenium was dispersed into fine droplets as in the studies of Turnbull and Cech[4] in order to minimize nucleation catalysis on heterogeneous impurities in the sample. The transformed material was readily detectable, since selenium glass is transparent to red light, whereas the hexagonal form is opaque.

Two series of measurements were carried out on droplets sublimed from "high-purity" selenium obtained from the American Selenium Company. The samples were contained in a cell which consisted of a microscope cover glass having a 5 mm. diameter hole, with a second cover-glass cemented

(1) For example, G. Borelius, *et al.*, *Arkiv Fysik*, **1**, 305 (1949–50).

(2) D. Turnbull and J. C. Fisher, *J. Chem. Phys.*, **17**, 71 (1949).

(3) G. Tammann, "The States of Aggregation," translated by R. F. Mehl, D. Van Nostrand Co., New York, N. Y., 1925, pp. 226 ff.

(4) D. Turnbull and R. E. Cech, *J. Applied Phys.*, **21**, 804 (1950).

to the bottom. Powdered selenium was sprinkled into the resulting well, and a freshly blown Pyrex film was cemented onto the top of the cover glass. When the cell was placed for 2 to 10 minutes on a metal block in an oven maintained at 230 ± 10°, the selenium sublimed onto the film as droplets 2 to 5 μ in diameter. The size distribution of the droplets was determined microscopically by measurement of droplets selected at random, using a micrometer eyepiece.

The selenium droplets were heat-treated isothermally every 10 to 20° over the range 50 to 200° by inserting the cells into a hollow between two heavy aluminum blocks maintained to ±1°. The temperature was determined by means of two thermocouples in each block. Holding times at each temperature ranged up to one hour and in some cases reached 48 hours. The cell was then inspected microscopically at room temperature and the number of crystallized droplets counted. The sample cell was then heated for 5 minutes to about 10° below the melting point of selenium in an effort to grow the supercritical nuclei formed at the lower temperature. The number of crystallized droplets was again determined as above. When it was desired to repeat observations, the entire sample was again made amorphous by briefly heating to 10° above the melting point.

Observations were also carried out on several samples of 99.999% selenium obtained from the Canadian Copper Refiners, Ltd., who report the following impurities in parts per million: 0.4 Cu, 0.1 Pb, 0.9 Fe, and 0.1 Fe. These studies were identical with those already described, except that silica glass film was substituted for the Pyrex, and the nuclei were grown at 150° in order to minimize evaporation of the droplets.

The estimated error in counting the crystallized droplets is ±0.1% of the total number of droplets. For the case of 10 μ diameter droplets heat-treated for one hour, the resultant uncertainty in the observed nucleation frequency is $\pm 10^3$ nuclei cm.$^{-3}$ sec.$^{-1}$; for smaller droplets or shorter times, the error is correspondingly larger. (Nucleation frequencies will be given in the above units unless stated otherwise.)

Results

In a preliminary experiment, selenium was condensed on a clean microscope cover glass. After 10 minutes, half of the droplets crystallized at 5 ± 2° supercooling and essentially all crystallized at 10 ± 2° supercooling. This behavior indicates a nucleation frequency of 10^7. However, the droplets in certain clearly defined areas did not crystallize, suggesting that the observed nucleation occurred at singularities on the glass.

When freshly blown Pyrex was used to support the droplets, it was observed in several specimens that condensation of the selenium droplets occurred in chains and clusters in some areas, and that crystallization occurred readily there with only slight undercooling. Further evidence that heterogeneous nucleation occurred is found in the fact that the transformed droplets were multigrained. Substitution of silica glass for the Pyrex film eliminated the clustering.

In regions exclusive of these chains or clusters, nucleation frequencies ranged from 10^3 to 10^6. The larger values were generally observed when the sample was heat-treated for the first time following condensation of the droplets, or when the sample had undergone four or five heat-treatment cycles. However, upon remelting the selenium and repeating the observations, the nucleation frequencies at no temperature exceeded 10^4, *i.e.*, one nucleus per 100 droplets per hour.

No significant difference was observed between the behavior of the pure commercial selenium and that of the 99.999% selenium. No temperature-dependence of the nucleation frequency was observed within the rather large limit of error between 90 and 215°; however, below 80°, no crystallization was detected.

Discussion

Heterogeneities may increase the rate of nucleation, but no way is known for inhibiting homogeneous nucleation in a one-component system. Thus, the smallest rates observed are the significant ones and the maximum rate of nucleation can be taken as $<10^4$.

By application of absolute reaction rate theory, Turnbull and Fisher[2] found the rate of homogeneous nucleation in supercooled liquids to be given by

$$I = C \exp[(\Delta G^* + \Delta G_A)/kT] \qquad (1)$$

where

- I = number of nuclei formed/cm.^{3} of parent phase/sec.
- C = $10^{37 \pm 1}$ cm.$^{-3}$ sec.$^{-1}$, a calculable frequency factor dependent on geometry, concn. and temp.
- ΔG^* = free-energy increase accompanying the formation of a crystalline embryo of critical size from the melt (see below)
- ΔG_A = free energy of activation for the movement of a parent atom across the phase boundary; $\approx \Delta H_A$, the corresponding energy of activation. Neglect of the entropy results in an error in I of only one power of 10 for each 4.6 e.u. of activation
- k = Boltzmann constant
- T = temperature

The energy barrier involved in the advance of the crystal–melt interface may be approximated by that for viscous flow in the melt. The melt viscosity η has been measured only in the ranges above the melting point and near 30°, where η is *ca.* 10^{12} poises.[5] The following values of the "activation energy" ΔH_A have been obtained: 15.1 kcal. above the melting point, 129 kcal. near 30°. The results of Borelius, *et al.*,[1] regarding the velocity of sustained crystal growth in the range of temperatures between the above viscosity measurements, show apparent activation energies which vary smoothly between those observed for viscous flow.

Except for a constant (see eq. 2), ΔG^* can be evaluated from the following data[5]: heat of fusion reported variously as 1.29 and 1.56 kcal./g. atom; temperature of fusion, 221°; and the density of the hexagonal phase, 4.79 g./cm.^{3}.

Following the standard development for crystallization from a melt, ΔG, the free energy difference per cm.^{3} between the melt and a crystalline embryo having a volume V and a surface area A is given by

$$\Delta G = A\sigma + V\Delta G_v$$

where σ is the free surface energy per cm.^{2} and ΔG_v is the volume-free-energy increment per cm.^{3}. When $V = 2A\sigma/3\Delta G_v$, ΔG is a maximum at

$$\Delta G = \Delta G^* = \frac{4}{27}\frac{(A\sigma)^3}{(V\Delta G_v)^2} \qquad (2)$$

and plays the role of a free energy of activation for the formation of crystalline nuclei. If the gram atomic entropy of fusion ΔS_f is assumed to be temperature-independent, then, at temperature T

$$\Delta G_v = \frac{\Delta S_f}{V_A}(T - T_0) \qquad (3)$$

where T_0 is the temperature of fusion and V_A is the gram atomic volume of the crystalline phase.

(5) Gmelins "Handbuch der anorganischen Chemie," 8th ed., Selen, Teil A, Verlag Chemie, G.m.b.h., Weinheim, 1953, pp. 175 ff.

TABLE I

SUMMARY OF PROPERTIES RELATED TO OBSERVED NUCLEATION FREQUENCIES IN SELENIUM, SULFUR, AND PHOSPHORUS

	T_0 = m.p. (°K.)	Max. $I_{obs.}$, cm.$^{-3}$ sec.$^{-1}$	T/T_0 at max. I	ΔS_f, entropy of fusion Per g. atom	Per mole	σ, ergs cm.$^{-2}$	$(\sigma_A/\Delta H_f)$ Per g. atom	Per mole
S_{8rhomb}	388	$<10^5$	>0.4	0.98	7.84	>26.8	>0.90	>0.45
Se_{hex}	493	$<10^4$	>0.4	2.48	...	>43.8	>0.48	...
P_4	317.5	*ca.* 10^5	0.36	0.496	1.984	>13.1	>1.1	>0.7

From nucleation measurements, Turnbull[6] has found that σ_A, the surface free energy of Avogadro's number of surface atoms (or molecules), relates to the gram atomic (or molar) heat of fusion ΔH_f as

$$\sigma_A = B\Delta H_f \qquad (4)$$

where B is an empirical factor which can be expected to vary between about 0.25 and 1.0.

The value of B, calculable by means of eq. 1 to 4 and the observed nucleation frequency, is somewhat dependent on the nucleus geometry assumed. If the critical nucleus is arbitrarily taken to be spherical, B is found to be ≥ 0.5, the value observed for most metals. However, for antimony, bismuth, germanium, water, benzene and other molecular substances, the value[7] is about 0.3, and so it might appear that the linear polymer-like hexagonal selenium should correspond more closely to the latter group of substances. If the nucleation frequency is calculated for $B = 0.3$, a maximum value 10^{18} results at 100° supercooling as compared with the observed frequency $<10^4$.

It is of interest to compare the observed nucleation frequencies of sulfur and phosphorus with those of selenium. Sulfur has been reported[8] to remain non-crystalline at temperatures as low as −45°, whereas liquid phosphorus, even when undercooled 116°, exhibits a relatively small frequency of nucleation to cubic white phosphorus.[9] Table I gives the lower limits for σ for sulfur and selenium as calculated by means of eq. 1, using known physical constants and the upper limit for the observed frequencies. The value for phosphorus also represents a lower limit, since the observed dependence of the frequency upon droplet size indicated that heterogeneous nucleation may have occurred even for the smallest droplets observed (estimated diameter, 50 μ).

Since data regarding elements are frequently tabulated on a gram atom basis, it is noteworthy that B, *i.e.*, $(\sigma_A/\Delta H_f)$, is larger by the factor (atoms/molecule)$^{1/3}$ than the value derived from the corresponding molar quantities. Presumably, since sulfur and phosphorus exist as the molecules S_8 and P_4, the latter is the more appropriate quantity; nevertheless, both are given in Table I. Selenium consists of linear parallel Se chains[10] in the solid, and of polymeric species ranging up to Se_{100} in the amorphous phase.[11] Because the molar quantity corresponding to σ_A is not defined in this case, the gram atom basis must be used.

The B values for the above elements are considerably larger than those observed for other molecular substances. It would, therefore, be of considerable interest to have an independent means for determining either σ or the critical nucleus geometry in order to evaluate the validity of the assumption of sphericity for these materials.[12] For example, assuming selenium embryos to be hexagonal prisms with a height-to-edge ratio equal to the c/a ratio in the unit cell, B is reduced to >0.42; if sulfur embryos are rhombohedra having the proportions observed for macrocrystals, the B value for sulfur becomes >0.32. Thus, embryo geometry may be largely responsible for the large calculated B values.

It is also possible, particularly in highly viscous systems, that the free energy of activation assumed for transport across a crystalline embryo interface is not the same as that for sustained crystal growth. The presence of an interface will influence the ordering of the amorphous phase in its immediate vicinity. If the crystallization is analogous to the growth of one crystalline phase into another, the interface layer is even more disorganized than the bulk amorphous phase, with a resultant increase of mobility across the interface. In the absence of such an interface, the material transport process must be volume self-diffusion. Whether the transport processes involved in viscous flow are identical with those for self-diffusion has not been tested in highly viscous systems.

Finally, since amorphous selenium apparently consists of macromolecules, it may be questioned whether the treatment of Turnbull and Fisher, based on the migration of individual atoms or molecules across the phase boundary, is applicable without modification.

Acknowledgment.—The author is indebted to various members of the Metallurgy Research Department of the General Electric Research Laboratory and especially to David Turnbull for enlightening discussions relative to this work.

(6) D. Turnbull, *J. Applied Phys.*, **21**, 1022 (1950).

(7) J. H. Holloman and D. Turnbull, "Progress in Metal Physics," ed. by B. Chalmers, Vol. 4, Interscience Publishers, Inc., New York, N. Y., 1953, pp. 348ff; D. G. Thomas and L. A. K. Staveley, *J. Chem. Soc.*, 4569 (1952); E. J. de Nordwall and L. A. K. Staveley, *ibid.*, 224 (1954).

(8) G. M. Pound and V. K. LaMer, *J. Am. Chem. Soc.*, **74**, 2323 (1952).

(9) J. H. Hildebrand and G. J. Rotariu, *ibid.*, **73**, 2524 (1951).

(10) "Crystal Structure," ed. by R. W. G. Wyckoff, Vol. I, Interscience Publishers, Inc., New York, N. Y., Chapter II, illus. p. 8.

(11) H. Krebs and W. Morsch, *Z. anorg. allgem. Chem.*, **263**, 305 (1950).

(12) It should be noted that the surface free energy is probably not independent of crystallographic direction. Hence σ, as used in this discussion, represents an average value, weighted according to the area contributions of the bounding crystal planes. According to the Wulff theorem, it is this directionality that leads to a non-spherical geometry.

A KINETIC STUDY OF THE DECOMPOSITION OF HYDROCARBONS BY SILICA–ALUMINA CATALYSTS

BY J. L. FRANKLIN AND D. E. NICHOLSON

Refining Technical and Research Divisions, Humble Oil and Refining Company, Baytown, Texas

Received June 9, 1955

The kinetics of the catalytic decomposition of four *n*-paraffins, three isoparaffins and one cycloparaffin over silica–alumina catalysts have been studied in a static system with product compositions being determined from mass spectrograph analyses. Pressure dependence measurements indicated fractional orders for the rate of disappearance of *n*-butane and *n*-pentane. Rates were also followed as a function of time with constant initial pressures. Activation energies have been estimated for the eight hydrocarbons investigated and the results discussed in terms of ionic reactions on solid surfaces. The rapid decrease in activation energy with increase in molecular weight of the *n*-paraffins parallels the changes in ionization potentials for these compounds; however, 2,2-dimethylpropane, having a lower ionization potential than either 2-methylpropane or 2-methylbutane, is very resistant to catalytic decomposition. Some evidence is presented which suggests that the cracking reaction may have an induction period.

Introduction

From product distributions obtained in catalytic cracking of pure hydrocarbons, it has often been inferred that reaction proceeds through a series of carbonium ion intermediates. There is also the possibility that hydrocarbon molecules may be adsorbed on silica–alumina surfaces and cracking initiated by formation of molecule–ions by transfer of electrons more or less completely to the solid. A number of investigators[1–5] have pointed out that a relationship should exist between reaction rates and the ease of electron transfer from adsorbed molecules to solid catalysts if the rate-controlling step involves partial or complete ionization of the substrate. In catalytic cracking, it can be argued that a correlation of activation energy with ionization potential of a series of compounds should exist, at constant catalyst activity, provided ionization of the hydrocarbon is actually rate determining.

The problem of predicting product composition from both thermal and catalytic decompositions of hydrocarbons is intriguing from theoretical and applied standpoints. A classical approach to interpretation of product distribution from thermal processes has been given by Rice.[6] Modification of the method of Rice by Greensfelder[7] led to a similar treatment employing relative rates of hydride ion removal, rather than relative rates of removal of primary, secondary and tertiary hydrogen atoms. In both methods, it was postulated that the hydrocarbon free radicals or carbonium ions produced by abstraction of hydrogen atoms or hydride ions, respectively, underwent a β-scission, successively yielding lower molecular weight substances. It is conceivable that molecule–ions and carbonium ions here postulated to be active intermediates in catalytic cracking undergo decomposition by mechanisms resembling those by which the same ions split under electron impact in the mass spectrometer.

The present investigation had as its object the determination of rate data for catalytic cracking of propane, *n*-butane, *n*-pentane, *n*-hexane, 2-methylpropane, 2-methylbutane, 2,2-dimethylpropane and cyclohexane to allow estimation of activation energies.

(1) G.-M. Schwab, *Trans. Faraday Soc.*, **42**, 689 (1946).
(2) A. Couper and D. D. Eley, *Nature*, **164**, 578 (1949).
(3) D. A. Dowden, *J. Chem. Soc.*, 242 (1950).
(4) P. W. Reynolds, *ibid.*, 265 (1950).
(5) M. Boudart, *J. Am. Chem. Soc.*, **72**, 1040 (1950); **74**, 1531 (1952).
(6) F. O. and K. K. Rice, "The Aliphatic Free Radicals," Johns Hopkins Press, Baltimore, Md., 1935.
(7) B. S. Greensfelder, H. H. Voge and G. M. Good, *Ind. Eng. Chem.*, **41**, 2573 (1949).

Experimental

Hydrocarbons.—Research Grade hydrocarbons obtained from the Phillips Petroleum Company were used for most kinetic measurements and had the following analyses: C_3H_8, 100 mole %; *n*-C_4H_{10}, 99.85 mole %; *n*-C_5H_{12}, 99.84 mole %; *n*-C_6H_{14}, 99.85 mole %; *i*-C_4H_{10}, 99.90 mole %; *i*-C_5H_{12}, 99.80 mole %; cyclo-C_6H_{12}, 99.95 mole %. 2,2-Dimethylpropane, from the Matheson Company, was found to have approximately 98 mole % purity by mass spectrometric analysis. All samples stored in lecture bottles under pressure were withdrawn from the liquid phase, by inversion of the cylinders, and distilled at least twice in the vacuum line prior to final vaporization into hydrocarbon storage bulbs. *n*-Pentane, *n*-hexane and cyclohexane were freed of air by repeated freezing, evacuation and melting of the solid.

Apparatus.—Kinetic measurements were performed in a static system. The Pyrex reactor of approximately 280 ml. was connected to manifold tubing of 2-mm. capillary, thus maintaining the dead space as a small fraction of the total reactor volume. Gaseous hydrocarbon was admitted to the reactor at a known pressure and cracking carried out under conditions of constant volume, with the pressure change being followed during the course of reaction by a mercury manometer. After a selected time interval, such as 800 sec., the reaction mixture could be rapidly expanded into an evacuated receiver bulb, previously cooled by liquid nitrogen. Reaction products were warmed to room temperature and transferred to mass spectrometer sample bulbs by means of a Töpler pump.

Catalysts and Pretreatment.—The silica–alumina catalyst chosen for this investigation was the commercially available 3A material, having an initial surface area of approximately 600 m.²/g. Chemical analysis gave the following composition of this catalyst: SiO_2, 85.6%; Al_2O_3, 12.9%; H_2O, 1.5%. Two large samples of deactivated catalyst, having surface areas of 81 and 303 m.²/g., were prepared by subjecting the original sample to steam and heat sintering. Cylindrical pellets ($^1/_8$" × $^1/_8$") were prepared using a rotary tablet machine. A standardized tapping technique served to introduce the same weight of catalyst into the reactor. In general, four to ten kinetic experiments were made with one loading of catalyst in the reactor. An extensive series of preliminary experiments indicated that passage of oxygen, saturated with water vapor at 25°, over the catalyst *in situ* at a flow rate of 500–1000 cc./min. for a period of two hours yielded reproducible catalyst activity. Regeneration was accomplished by combustion of coke deposits in a stream of oxygen and water vapor for 30 min. at temperatures of 450–500°.

Reproducibility in catalyst activity was checked by repetition of individual rate measurements with regeneration of the catalyst between these experiments. In general, a typical run could be repeated precisely enough to yield concentrations of uncracked starting material in the product

gas within ±1% of an average value. This agreement is essentially equal to the accuracy of the mass spectrometric analyses. A further check was made to establish the effect of coke deposition on catalyst activity. It was found that repetitive rate measurements *without* regeneration of the catalyst between experiments gave identical conversions of starting materials within ±1%; thus, catalyst deactivation could not be detected as resulting from coke deposition.

All of the measurements reported here were made with 180 g. of catalyst in the 280-ml. Pyrex reactor. In some preliminary studies, smaller quantities of catalyst were employed, and it was found that conversion of starting material decreased in approximately a linear manner as the weight of catalyst in the reactor was decreased. In some related studies in which surface area of the catalyst was varied over a wide range, *i.e.*, from about 60–600 m.²/g., the activity of the catalyst, as measured by conversion of isobutane, was found to vary linearly with surface area. Hence, at least to a first approximation the active centers on the two silica–alumina catalysts chosen for the present investigation are similar in nature.

Temperature Regulation.—Temperature control was effected by a Brown *ElectroniK* recorder-controller in conjunction with an iron–constantan thermocouple. A Hoskins muffle furnace equipped with a stainless steel block contained the Pyrex and Vycor reactors. All thermocouples were calibrated frequently against a 25-ohm platinum resistance thermometer so that absolute temperatures are known to ±0.5° at a fixed point in the reactor. Temperature differences of approximately 2° were observed between the ends of the reactors. Care was taken to maintain the relative geometry of the thermostat and appurtenances fixed.

Results

A pronounced characteristic of the reaction products from the catalytic decomposition studies in the static system was that only small amounts of olefins were present; material balance calculations for the paraffins confirmed that compounds of the type C_nH_{2n} were probably polymerizing on the catalyst and hence not escaping from the reactor. From product distribution data on cracking of cyclohexane, material balances indicated the composition of the coke deposits to be $C_nH_{1.3n}$.

Interference in catalytic cracking from competitive thermal decompositions was measured for seven of the eight hydrocarbons studied. Rates of thermal cracking were essentially nil compared to rates of catalytic cracking for all compounds except pro-

TABLE I

SUMMARY OF RATE DATA FOR THE CATALYTIC DECOMPOSITION OF EIGHT HYDROCARBONS

Compound	Temp., °C.	Surface area of catalyst, sq. m./g.	Initial hydrocarbon pressure, mm.	Range of reaction times, sec.	$k \times 10^4$, sec.$^{-1}$
			Group I		
Propane	525.0 ± 0.5	303	633	300–600 (3)[a]	(11.7 ± 0.4)
	550.0		635	200–400 (3)	(28.0 ± 1.0)
2-Methylpropane	450.0	80	625	600–1200 (3)	(1.25 ± 0.19)
	500.0		625	300–1200 (3)	(66.3 ± 4.9)
2-Methylbutane	400.0	80	365	900–1600 (2)	(3.67 ± 0.08)
	450.0		367	300–1200 (4)	(9.7 ± 0.7)
	476.0		370	300–600 (3)	(16.7 ± 0.6)
2,2-Dimethylpropane	399.0	303	66, 325	1200 (2)	(0.637 ± 0.005)
	454.4		54, 182, 364, 634	300 (4)	(6.3 ± 0.7)
Cyclohexane	400.0	80	62.5	300–1600 (4)	(3.9 ± 0.3)
	450.0		62.0	300–1200 (4)	(10.0 ± 0.7)
			Group II		
					$k \times 10^5$, mm.$^{-1/2}$ sec.$^{-1}$
n-Butane	450.0	303	620	600–1200 (3)	(6.75 ± 0.58)
	500.0		624	150–400 (3)	(2.20 ± 0.14)
n-Pentane	425.0	303	293	300–900 (3)	(12.0 ± 0.8)
	475.0		290	175–400 (4)	(3.25 ± 0.34)
n-Hexane	321.7	303	99	400–1200 (3)	(8.53 ± 1.54)
	346.1		95	300 (2)	(17.7 ± 0.2)
	378.9		82	200–600 (3)	(36.3 ± 3.0)

[a] Numerals in parentheses show the number of experiments upon which rate constants were based.

TABLE II

KINETIC DATA—PRESSURE DEPENDENCE STUDIES

Compound	C_3H_8				*n*-C_4H_{10}				*n*-C_6H_{12}			
Temp., °C.	525.6				451.1				450.0			
Reaction time, sec.	300				600				250			
P_i, mm.	74.1	151.2	455.2	652.1	173.2	361.3	495.7	639.0	43.9	121.3	241.8	315.7
Specific reaction rate constant												
$k \times 10^3$, sec.$^{-1}$ (1.0 order)	0.923	0.1081	0.1060	0.1150	0.384	0.614	0.698	0 814	0.890	1.326	2.41	2.67
$k \times 10^3$, mm.$^{-1/2}$ sec. (1.5 order)	0.1153	0.0955	0.0543	0.0492	0.0714	0.0806	0.0803	0.0839	0.1422	0.1279	0.1817	0.1784
Compound	*i*-C_4H_{10}				*i*-C_5H_{12}							
Temp., °C.	500.0				500.0							
Reaction time, sec.	600		1200		400							
P_i, mm.	626.0	92.6	624	91.5	139.9	197.3	323.0					
Specific reaction rate constant												
$k \times 10^3$, sec.$^{-1}$ (1.0 order)	0.695	0.591	0.705	0.620	2.08	2.10	2.26					
$k \times 10^3$, mm.$^{-1/2}$ sec. (1.5 order)	0.0206	0.0671	0.0351	0.0786	2.18	1.86	1.59					

pane at 550°; blank runs showed that about 20% of the total conversion of propane at 550° was due to thermal cracking.

The rate equations for homogeneous gas reactions apply in heterogeneous catalysis under conditions where the surface is sparsely covered, as is reasonable to expect under the conditions of this investigation. These equations have been used in the present study, and their use is further justified by the constancy of the specific rates. Tables I and II contain summary kinetic data for rates of disappearance *via* catalytic cracking of the eight compounds included in this investigation. The pressure dependence studies were performed some months after completion of the other rate measurements: it will be noted that catalyst activity is slightly different from that in those rate measurements on which activation energies have been based. Within experimental accuracy, the decomposition of propane fits a first-order law: *n*-butane and *n*-pentane follow a 1.5-order law approximately. The low vapor pressure of *n*-hexane at laboratory temperatures prevented varying initial hydrocarbon pressure over a wide range as was done for other compounds. Reference to the data in the tables will show that 2-methylpropane, 2-methylbutane and 2,2-dimethylpropane have rates of catalytic decomposition which are represented by a simple first-order law to a good approximation, *i.e.*, with specific rates which are "constant" within about ±10%. The average deviation of all specific rates determined in this study was found to be ±7%. Straight lines are obtained on plotting log k *vs.* $1/T$ for *n*-hexane and 2-methylbutane, indicating conformity to the Arrhenius equation.

of selected olefins and aromatic compounds is shown in Table IV. Total initial hydrocarbon pressures (625 mm.) and reactor temperatures (450°) were maintained constant in experiments 1–8: reaction time was 210 seconds in every case. The data in column 1 represents an average of four runs performed at intervals between the other experiments. The reproducibility of these runs showed that catalyst activity remained essentially constant throughout the series of studies. Reference to Table IV shows that propene and butene-1 accelerate the rate of disappearance of *n*-butane to an extent which is greater than the average reproducibility of the measurements. Furthermore, it will be noticed that these olefins cause substantially the same increase in rate when present at equal concentrations in the starting material. 2-Methylpropene was found to have little or no influence on cracking of *n*-butane, while benzene and ethylbenzene exhibited a slight inhibiting effect.

TABLE III

ACTIVATION ENERGIES AND IONIZATION POTENTIALS

Compound	$\Delta E\ddagger$, kcal./mole		I_z, kcal./mole	
Propane	41.7		258.5	
		$\Delta = 15.4$		$\Delta = 9.4$
n-Butane	26.3		249.1	
		$\Delta = 5.6$		$\Delta = 6.1$
n-Pentane	20.7		243.0	
		$\Delta = 2.3$		$\Delta = 2.5$
n-Hexane	18.4		240.5	
2-Methylpropane	37.1		247.4	
2-Methylbutane	20.5		243.3	
2,2-Dimethylpropane	40.0		238.7	
Cyclohexane	18.5		238.7	

TABLE IV

INFLUENCE OF ADDED GASES ON CATALYTIC *n*-BUTANE DECOMPOSITION

Expt. No.	1	2	3	4	5	6	7
Added material	None	1-C_4H_8	1-C_4H_8	C_3H_6	*i*-C_4H_8	C_6H_6	$C_6H_5C_2H_5$
Mole % of added material	0	0.4	2.7	2.3	2.3	2.8	1.3
Moles *n*-C_4H_{10} cracked/100 moles *n*-C_4H_{10} charged	19.4 ± 1.0	22.3	27.7	28.0	17.9	15.0	16.6

The specific rate constant for 2-methylpropane at 500° has an average value of 6.7×10^{-4} sec.$^{-1}$, when measured with initial hydrocarbon pressures of approximately 625 mm.: a sevenfold decrease in initial pressure of 2-methylpropane lowered the specific rate to 5.9×10^{-4} sec.$^{-1}$, showing the rate of disappearance of starting material to be comparatively independent of pressure. This difference, amounting to a 12% decrease in specific rate, is not greatly outside the mean reproducibility of the rate constants. Variation of initial pressures of 2-methylbutane from 140 to 323 mm. also revealed a slight increase in rate.

Experimental evidence suggesting existence of an induction period in catalytic cracking was of two types: (1) kinetic measurements in decomposition of 2-methylpropane at short reaction times (*ca.* 100 sec. at 500°) yielded specific rates that were approximately 50% lower than the steady-state rate of 6.3×10^{-4} sec.$^{-1}$; (2) addition of trace quantities of olefins accelerated the rate of decomposition of *n*-butane at low conversions. The influence

It may be noted that rates of catalytic cracking of the *n*-paraffins at 525° are

Compound	Relative rate of decomposition
C_3H_8	1
n-C_4H_{10}	7
n-C_5H_{12}	13
n-C_6H_{14}	20

Now, from Table III it can be seen that the difference in activation energies for cracking of propane and *n*-hexane is of the order of 24 kcal./mole, corresponding to a ratio of relative rates of decomposition at 525° of $e^{24,000\ (2 \times 798)} = 3.3 \times 10^6$. But the experimental ratio of rates is k(*n*-hexane)/k(propane) = 20/1. Obviously, the frequency factors in the Arrhenius equation differ widely for propane and *n*-hexane.

Discussion

The fractional orders observed in cracking *n*-butane and *n*-pentane, at constant reaction times but with varying initial hydrocarbon pressures, may

be attributed (1) to the adsorption–desorption equilibrium between the starting materials and the catalyst, or (2) to the nature of chain initiating and terminating steps in the reaction mechanisms.

Molecular diffusion in the catalyst pores under condition such that the entire surface is not available for reaction could lead to a 1.5-order of reaction for a process that would otherwise be second order; however, calculations based on diffusion theory, applied to constant volume systems, show that the true specific rate constant for cracking of *n*-hexane should not be influenced by mass transfer under the experimental conditions prevailing in the present investigation.[8] Furthermore, the likelihood of diffusion being rate limiting is minimized by virtue of the comparatively high activation energies required for catalytic cracking, *i.e.*, 18–42 kcal./mole. On plotting ionization potential *vs.* activation energy for the *n*-paraffin series a smooth curve obtains. In addition, incremental differences in ionization potentials and activation energies are essentially equal. Since the beginning of the present investigation, evidence has appeared indicating that cracking catalysts function as Lewis acids. Haldeman[9] concluded that the active centers on silica, alumina and silica–alumina were primarily Lewis acids at 500°, and about one-half of the active centers were Brönsted acids at 150°. Mapes and Eischens[10] postulated that if the catalyst be a Brönsted acid, the chemisorbed ammonia will exhibit the characteristic infrared absorption peaks of ammonium ions. If the catalyst is a non-hydrated Lewis acid, only ammonia spectra should be seen. The spectrum of a catalyst on which ammonia was chemisorbed showed a strong band at 3.0 μ due to ammonia: an ammonium band at 6.9 μ was weaker than the 3.0 μ band. In view of a background of supporting data, electron transfer would seem possible as the rate-determining step in cracking of the *n*-paraffins studied in this investigation.

A hydrogen and/or charge transfer mechanism will aid in explaining the gross trends in influence of added olefins upon rate of decomposition of *n*-butane, assuming the important rate step is formation of the molecule-ion $C_4H_{10}^+$ through bimolecular reaction of *n*-butane with the molecule-ion formed from the additive. A few of the possibilities are illustrated.

$$n\text{-}C_4H_{10} + C_3H_6^+ \longrightarrow C_4H_8^+ + C_3H_8$$
$$\Delta H_R = -2 \text{ kcal./mole}$$

$$n\text{-}C_4H_{10} + C_4H_8^+ \text{ (from 1-}C_4H_8) \longrightarrow C_4H_9^+ + C_4H_9\cdot$$
$$\Delta H_R = -24 \text{ kcal./mole}$$

$$n\text{-}C_4H_{10} + C_3H_6^+ \longrightarrow C_4H_9^+ + C_3H_7\cdot$$
$$\Delta H_R = -19 \text{ kcal./mole}$$

$$n\text{-}C_4H_{10} + C_6H_6^+ \longrightarrow C_6H_6 + C_4H_{10}^+$$
$$\Delta H_R = 79 \text{ kcal./mole}$$

In a preponderance of other processes which can be visualized to include ionization of the substance added in small quantities to *n*-butane and reaction of the ion thus produced with *n*-butane, the heats of reaction tend to be less endothermic for the changes involving propene and butene-1 than for those involving isobutylene, benzene and ethylbenzene.

In conclusion, the correlation of ionization potential with activation energy for catalytic decomposition of propane, *n*-butane, *n*-pentane and *n*-hexane is believed to be suggestive that silica–alumina catalysts may function as electron acceptors with respect to adsorbed hydrocarbons. Formation of the alkyl carbonium ions $(C_nH_{2n+1})^+$ is proposed to occur *via* molecule–ion intermediates. Moreover, there are indications that the catalytic cracking process has an induction period; this behavior appears to be similar to that noted by Otvos, *et al.*,[11,12] in the hydrogen exchange reactions of *n*-butane and 2-methylpropane in sulfuric acid where the induction period was shortened by addition of olefins.

(8) A. Wheeler, "Advances in Catalysis," Academic Press, Inc., New York, N. Y., 1951, pp. 300–301.

(9) R. G. Haldeman, *Univ. Pittsburgh Bull.*, **49**, No. 14, 81 (1953).

(10) J. E. Mapes and R. P. Eischens, "The Infrared Spectra of Ammonia Chemisorbed on Cracking Catalysts," 124th Meeting of the Am. Chem. Soc., Chicago, 1953.

(11) O. Beeck, J. W. Otvos, D. P. Stevenson and C. D. Wagner, *J. Chem. Phys.*, **17**, 418 (1949).

(12) J. W. Otvos, O. Beeck, D. P. Stevenson and C. D. Wagner, *J. Am. Chem. Soc.*, **73**, 5741 (1951).

POTENTIOMETRIC DETERMINATION OF THE BASE STRENGTHS OF AMINES IN NON-PROTOLYTIC SOLVENTS

BY H. K. HALL, JR.

Contribution from the Textile Fibers Department, Pioneering Research Division, E. I. du Pont de Nemours & Company, Inc., Wilmington, Delaware

Received June 10, 1955

A reproducible titration method was devised and successful potentiometric titrations were performed on a large number of monoamines and diamines in five solvents of varying nature: ethyl acetate, acetonitrile, nitrobenzene, nitromethane and ethylene dichloride. The titrant acids were perchloric, *p*-toluenesulfonic and perfluorobutyric, all in dioxane solution. Methanesulfonic acid was used as a solution in the given solvent. The mid-point of the titration curve was taken as a measure of the dissociation constant of the amine. The existence of quantitative linear relationships between the midpoint readings ($E_{1/2}$) and the Hammett σ constants in water for *m*- and *p*-substituted anilines was established. For the alkylamines the observed order of base strength was: $NH_3 < RNH_2$, $R_2NH > R_3N$, an order similar to that observed in water or alcohol. As the length of the alkyl chain increased to four or five carbon atoms, the base strength was lowered. Diamines, such as ethylenediamine, hexamethylenediamine and the piperazines behaved in acetonitrile as rather strong bases. Polar substituents in the piperidine ring as in morpholine, monoacylpiperazines, etc., decreased the base strength of the parent amine as expected. The order and even the quantitative strength of the bases were independent of solvent or of acid for the five organic solvents. When data for organic solvents were plotted against those for water, acceptable linear plots were obtained (with one exception—see below). Even this extreme change of solvent does not affect relative base strength. The exception noted above referred to amines containing a strongly polar group near the N atom, such as morpholines and monoacylpiperazines. These bases are much stronger in organic solvents than their pK_a values in water would predict. A discrepancy between the predicted and observed slopes of the plots of $E_{1/2}$ against pK_a is explained in terms of variations in the activity coefficients of the ammonium ions relative to the corresponding amines.

Non-protolytic solvents in which base strengths have been quantitatively studied include benzene,[1-3] chlorobenzene,[4,5] anisole,[5] acetonitrile,[6] nitrobenzene,[7,8] tricresyl phosphate,[9] nitromethane,[10] chloroform[11-13] and carbon tetrachloride.[13] The methods employed have been chiefly indicator ones. Conductimetric determinations, although precise, offer a more complex problem in media of low dielectric constant than in high dielectric solvents. Reaction kinetics methods have been employed, but, according to Grunwald and Berkowitz,[14] often give discordant values of pK_a. Association phenomena which complicate the kinetics methods will be more serious in non-polar media. Infrared methods were used in one investigation.[13] Finally potentiometric methods involving either glass or hydrogen electrodes have been employed on only two occasions[1,15] in non-protolytic media. These difficulties account for the fact that far fewer base strengths in such solvents are known than in protolytic solvents.

Because of the nature of the available experimental methods, investigations in these solvents have been limited to only moderately strong acids. Witschonke and Kraus[8] concluded that any salt less dissociated than pyridine picrate cannot be studied successfully by conductimetric means. Picric and dichloroacetic acids were the strongest which were studied in acetonitrile.[6]

No study has been reported on the interaction of amines with very strong acids except that of Fritz.[15] He performed potentiometric titrations of amines in acetonitrile with perchloric acid in dioxane using glass and calomel electrodes. He made the significant observation that the millivoltage reading at half-neutralization, hereafter called $E_{1/2}$, could be correlated with the base strength of the amine. It appeared, therefore, that base strengths in non-protolytic solvents could be measured by this method. We took this as a starting point for the present study.

Our first experiments using the procedure of Fritz did not give reproducible values of $E_{1/2}$, the millivoltage reading at half-neutralization. It was necessary, as described in the Experimental Section, to standardize the electrodes against an organic buffer solution. When four different sets of electrodes were standardized in this way, their readings upon immersion in various amine solutions agreed to ± 1 mv.

Solvents.—The original paper of Fritz,[15] which served as the starting point of the present study, utilized acetonitrile as the solvent. However, there seemed to be no reason why the study should be confined to this solvent. A recent booklet by Fritz[16] summarizes work on acid-base titrations in a variety of non-aqueous solvents. It appeared that any solvent of even moderate polarity can be used as the solvent. In the present study, five solvents were found to be perfectly satisfactory. Nitromethane, nitrobenzene and acetonitrile are all highly polar. Ethyl acetate is moderately polar and the fact that it gave sharp titration curves occasioned no surprise. Ethylene chloride, however, is quite non-polar, and it was somewhat unexpected to discover that it behaved as well as the other solvents. Other solvents tried,

(1) V. K. Lamer and H. C. Downes, *J. Am. Chem. Soc.*, **55**, 1840 (1933), and references contained therein.
(2) M. M. Davis and H. B. Hetzer, *ibid.*, **76**, 4247 (1954), and references contained therein.
(3) A. A. Maryott, *J. Research Natl. Bur. Standards*, **41**, 7 (1948).
(4) D. C. Griffiths, *J. Chem. Soc.*, 818 (1938).
(5) R. P. Bell and J. W. Bayles, *ibid.*, 1518 (1952).
(6) M. Kilpatrick and M. L. Kilpatrick, *Chem. Revs.*, **13**, 131 (1933).
(7) I. M. Kolthoff, D. Stocesoca and T. S. Lee, *J. Am. Chem. Soc.*, **75**, 1834 (1953).
(8) C. R. Witschonke and C. A. Kraus, *ibid.*, **69**, 2472 (1947).
(9) M. A. Elliott and R. M. Fuoss, *ibid.*, **61**, 294 (1939).
(10) L. C. Smith and L. P. Hammett, *ibid.*, **67**, 23 (1945).
(11) J. A. Moede and C. Curran, *ibid.*, **71**, 852 (1949).
(12) M. M. Davis, *ibid.*, **71**, 3544 (1949).
(13) G. M. Barrow and E. A. Yerger, *ibid.*, **76**, 5211, 5247, 5248 (1954).
(14) E. Grunwald and B. J. Berkowitz, *ibid.*, **73**, 4939 (1951).
(15) J. S. Fritz, *Anal. Chem.*, **25**, 407 (1953).
(16) J. S. Fritz, "Acid-Base Titrations in Non-aqueous Solvents," The G. Frederick Smith Co., Columbus, Ohio, 1952.

which gave drifting millivoltage readings, were benzene, anisole, dioxane, chloroform and methylene chloride.

The question arose as to reaction of the amines with several of the solvents employed. Reaction of amines with nitrobenzene is unlikely, but they might remove a proton from nitromethane or acetonitrile to form the corresponding anions. Amidine formation from the latter is possible. Ethyl acetate might undergo aminolysis, and several modes of decomposition can be visualized for ethylene chloride. There are several reasons for believing that none of these reactions occur: (1) The amine and solvent are in contact for less than five minutes. (2) Precipitation from ethylene chloride solutions should be observable. (3) If reaction were very rapid with ethyl acetate, the ethanol and amide formed would be non-basic, and any decrease in amine concentration would show up as a steady drift in the electrode reading. (4) Establishment of a mobile equilibrium with acetonitrile or nitromethane would not affect the results, since water participates in just such an equilibrium.

Amines.—There was little limitation on the type of amine which could be titrated. Of the aromatic amines, only *p*- and especially *o*-nitroanilines were too weak bases to give sharp titration curves. *m*-Nitroaniline was titrated successfully in several solvents, however, and stronger bases were very easily titrated. At the other extreme, pyrrolidine seemed to be about the strongest base encountered, but there was no reason to believe stronger bases could not be studied.

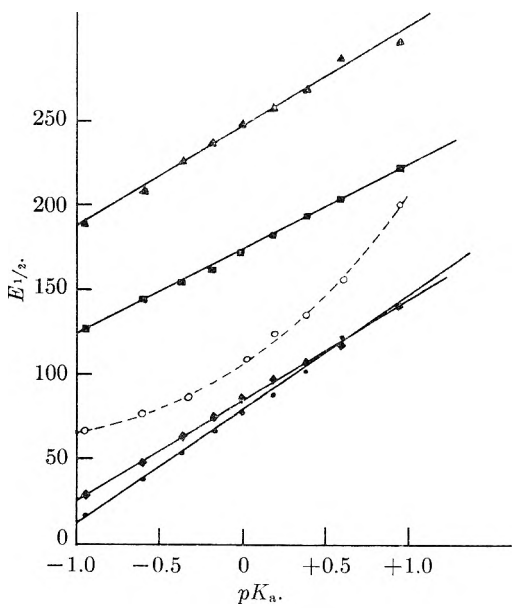

Fig. 1.—Conformity of data to titration equation: ●, diethylamine, nitrobenzene, perchloric acid; ◆, *n*-butylamine, acetonitrile, perchloric acid; ○, piperidine, ethylene dichloride, *p*-toluenesulfonic acid (70 mv. added to observed reading); □, N-ethylmorpholine, acetonitrile, perchloric acid; ▲, N-allylpiperidine, ethyl acetate, perchloric acid.

A serious limitation lay, however, in the insolubility of certain amine salts. With perchloric acid precipitation occurred only in ethylene chloride, only a few other cases being noted. *p*-Toluenesulfonic acid formed precipitates with a variety of amines in each solvent, and this restricted its usefulness.

Acids.—Dilute solutions of 70% perchloric acid in pure dioxane were found to be perfectly stable for many months. *p*-Toluenesulfonic acid, which is readily available in crystalline form, was also chosen as a titrant. Perfluorobutyric acid was strong enough to titrate triethylamine, but not 2,6-dimethylpyridine. It appears, therefore, to be relatively weak.

Conformity to Titration Equation.—It was felt to be necessary to verify that the titration data followed the usual equation. Figure 1 shows plots of log $X/(1 - X)$, where X is the fraction neutralized, against the observed millivoltage value. The plots of all solvents except ethylene dichloride are linear. The simple interpretation of $E_{1/2}$ as a measure of dissociation constant cannot therefore be valid for this very non-polar solvent. The slopes of the lines are not the expected ones of 59 mv. This may be due to lack of constant ionic strength. The titrations are performed at 0.01 *M* concentration.

Results.—The results obtained are given in Tables I–VII. The *relative* base strengths were independent of the titrating acid and, to a first approximation, of the solvent. The observed values can, therefore, be discussed in terms of the structures of the amines. From the data in Tables I–VII, it can be seen that the results are in accord with expectations considering their structures. For example, electron-attracting substituents such as allyl or benzyl cause a marked reduction in base strength.[17] Numerous other examples could be cited. Only the case of the alkylamines will be discussed, since this problem has attracted considerable attention.

For the alkylamines, the complete sequence of base strengths in each solvent (and in water) is $NH_3 < RNH_2$, $R_2NH > R_3N$ (Table I). The exact relative positions of RNH_2 and R_2NH cannot be established because of experimental inaccuracies, but it can be said that they are always very similar. In the past, claims have been made[18] that the true order of base strengths should be $NH_3 < RNH_2 < R_2NH < R_3N$, because of increasing electron supply to the nitrogen atom by the alkyl groups. Deviations from this order in water, methanol,[19] and ethanol[19] are explained in terms of preferential solvation, through H-bonding, of the several ammonium ions. It does not appear to be reasonable to expect that in inert solvents the ideal order should be observed, however, since hydrogen bonding of the ammonium ion will still occur to either another amine molecule,[7] another acid molecule,[7,13,20] or other molecules of salt.[2,8,21] Therefore, it does not appear probable that this order of base strengths toward strong acids can be realized.

(17) The higher the $E_{1/2}$ value, the weaker is the base.

(18) (a) R. G. Pearson and F. V. Williams, *J. Am. Chem. Soc.*, **75**, 258 (1954); (b) A. F. Trotman-Dickenson, *J. Chem. Soc.*, 1293 (1949).

(19) (a) M. Mizutani, *Z. physik. Chem.*, **116**, 350 (1925); (b) **118**, 327 (1925).

(20) H. F. Herbrandson, R. T. Dickerson, Jr., and J. Weinstein, *J. Am. Chem. Soc.*, **76**, 4046 (1954).

(21) A. A. Maryott, *J. Research Natl. Bur. Standards*, **41**, 1 (1948).

TABLE I

MILLIVOLTAGE HALF-NEUTRALIZATION VALUES FOR ALIPHATIC AMINES AND DIAMINES, USING PERCHLORIC ACID

	Amine	pK_a, H_2O	Solvents: Nitromethane	Ethylene dichloride	Ethyl acetate	Nitrobenzene	Acetonitrile
1	Ammonia	9.26	193	..	Ppt.	Ppt.	100
2	Methylamine	10.64	73	Ppt.	98	94	82
						83	
3	Dimethylamine	10.61	101	..	102	59	73
						63	
4	Trimethylamine	10.72	150	..	Ppt.	87	88
						94	
5	Ethylamine	10.75	..	Ppt.	115	100	..
						112	
6	Diethylamine	11.00	..	175	124	78	..
						75	
7	Triethylamine	10.74	60	172	197	87	57
			68	165	198	86	75
8	*n*-Propylamine	10.59	..	..	129	129	..
						121	
9	Di-*n*-propylamine	10.91	..	..	158	108	..
10	Tri-*n*-propylamine	10.70	..	..	228	131	..
11	Isopropylamine	10.63	..	..	127	127	
						110	
12	Diisopropylamine	11.05	..	..	145	..	..
13	*n*-Butylamine	10.61	..	..	130	..	85
14	Di-*n*-butylamine	11.31	..	..	150	..	55
							60
15	Tri-*n*-butylamine	10.89	..	..	210	..	..
16	Isobutylamine	10.42	148	261	162	150	105
			149	259	178		114
					172		
17	Diisobutylamine	10.59	..	..	207	..	..
18	*sec*-Butylamine	10.56	..	..	148	..	..
19	Di-*sec*-butylamine	....	..	..	182	..	..
20	*t*-Butylamine	10.45	..	..	130	..	..
21	Di-*n*-amylamine	11.18	..	..	164	..	..
22	Tri-*n*-amylamine	....	..	..	263	..	..
23	Neopentylamine	10.40	..	..	188	..	..
24	Hexamethylenediamine	11.11	..	..	Ppt.	..	..
25	Ethylenediamine	10.08	..	..	Ppt.	..	62
26	Ethanolamine	9.45	..	..	90	..	119
27	Monoacetylethylenediamine	9.28[a]	..	..	..	..	118
28	Monobenzoylethylenediamine	9.13[a]	..	..	..	..	147

[a] Determined in the present work.

Since the present study has shown that the same order as in water is maintained in such solvents as nitromethane and acetonitrile, it appears more attractive to maintain that the order of base strengths toward H^+ is determined solely by some property of the molecules themselves. The B-strain hypothesis of H. C. Brown[22] is in accord with these results.

Relative Base Strengths of Amines in Water and in Organic Solvents.—The base strengths in water of a great many amines have been determined in the past, but there are very few values available for non-aqueous solvents. It has, therefore, been difficult to assess the importance of the solvent in determining amine base strength. With the large quantity of data collected in the present investigation, it becomes possible for the first time to make an adequate comparison.

***m*- and *p*-Substituted Anilines.**—This class of amine will be dealt with separately since theoretical interpretation of its behavior is particularly simple. If the $E_{1/2}$ values of the present study should be proportional to pK_a, it was expected that a linear relationship should hold between the former and the Hammett σ-value of the substituent. In Fig. 2 the data obtained using perchloric acid have been plotted. In ethylene chloride precipitation of the aromatic amine perchlorates occurred and no data could be obtained. Similar effects hampered the study of *p*-toluenesulfonic acid, where only rudimentary plots were obtained. It is clear that the expected linear relationships hold very well. The lines were determined by the method of least squares and the equations of the lines are given in Table IX. The linear Hammett relationships afford confirmatory evidence that the glass electrode is measuring the activity of H^+ in the solutions, for linearity could not hold otherwise. Although theory predicts that the slopes of the lines should all be +59 mv., it is apparent that this is not the case. The slope depends on the solvent. This must be related to the activity coefficients of the amine and its ion, as will be discussed below.

(22) H. C. Brown, *Rec. Chem. Prog.*, **14**, 83 (1953).

TABLE II

MILLIVOLTAGE HALF-NEUTRALIZATION VALUES FOR NON-AROMATIC CYCLIC BASES, USING PERCHLORIC ACID

	Amine Structure	Name	pK_a, H_2O	Solvents: Nitromethane	Ethylene dichloride	Ethyl acetate	Nitrobenzene	Acetonitrile
29	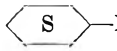	Cyclohexylamine	10.79	..	..	132	..	..
30	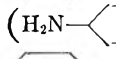	Bis-(*p*-aminocyclohexyl)-methane	...	..	..	..	..	73
31		Pyrrolidine	11.32	..	..	75	..	..
32		Piperidine	11.20	80 77	166 170	130 131 132	78 70	36 47
33		Hexamethyleneimine	11.10[a]	..	..	118	..	..
34		2,2,6,6-Tetramethylpiperidine	11.10[a]	..	..	134	..	..
35		Morpholine	8.36[a]	..	..	191	205	164
36		N-Ethylpiperidine	10.40	63 67	187 190	191 192	..	83 94 76
37		N-Methylmorpholine	7.41[a]	..	..	298	..	..
38	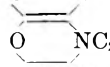	N-Ethylmorpholine	7.70[a]	..	..	290	..	221
39		1-Carbethoxypiperazine	8.28[a]	205 201	Ppt.	260 262	230	207 196 184
40		1-Benzoylpiperazine	7.78[a]	..	..	..	..	210
41		1-Tosylpiperazine	7.44[a]	..	..	285	..	252
42		Anhydrous piperazine	9.81	Ppt.	Ppt.	103 101	..	65 64
43		*trans*-2,5-Dimethylpiperazine	9.69[a]	122	Ppt.	158 148	..	85 101 85
44		*trans*-2,5-Dimethylpiperazine Mono-ion	5.25[a]	425	Ppt.	338 347	..	..
45		N-Allylpiperidine	9.68[a]	..	..	248	.	..
46		N-Allylmorpholine	7.05[a]	..	..	354	292	273

[a] Determined in the present work.

TABLE III

MILLIVOLTAGE HALF-NEUTRALIZATION VALUES FOR ALLYLAMINES, BENZYLAMINES AND GUANIDINES, USING PERCHLORIC ACID

	Amine	pK_a, H_2O	Solvents: Ethyl acetate	Acetonitrile
47	Allylamine	9.53	180	..
48	Benzylamine	9.30	209	..
49	Dibenzylamine	...	288	..
50	Tribenzylamine	...	476	391
51	1,3-Diphenylguanidine	10.00	..	94
52	1,3-Di-*o*-Tolylguanidine	9.67	..	67
53	1,2,3-Triphenylguanidine	9.1	..	180 190

Amines of Varied Structural Type.—The correlation of base strength in water with that in organic solvents cannot be expected to be as exact for amines of varied structural type as it is for the *m*- and *p*-substituted anilines. The reason is that steric effects, solvation effects and entropy changes may enter which are specific for each amine. In illustration of this point, Wooten and Hammett[23] found that only *m*- and *p*-substituted benzoic acids exhibited a quantitatively linear relationship between their strengths in *n*-butyl alcohol and in water. The points for other carboxylic acids deviated to a greater or lesser extent from this line, although the divergencies are not serious. Similar plots are given by Verhoek[24] and Kilpatrick and Kilpatrick,[6] who determined base strengths in formamide and acetonitrile, respectively.

The $E_{1/2}$ values obtained in each solvent with each acid were plotted against the pK_a values of the amines in water solution. Figure 3 shows a representative plot of such data, obtained using acetonitrile and perchloric acid. Ignoring for the moment the points denoted by triangles, it can be seen that fairly good linear relationships hold. The equations of the lines and the average deviations are given in Table IX. The fit is much better for the polar

(23) L. A. Wooten and L. P. Hammett, *J. Am. Chem. Soc.*, **57**, 2289 (1935).

(24) F. H. Verhoek, *ibid.*, **58**, 2577 (1936).

TABLE IV

MILLIVOLTAGE HALF-NEUTRALIZATION VALUES FOR SUBSTITUTED ANILINES USING PERCHLORIC ACID

	Substituted aniline	pK_a, H_2O	Solvents: Nitromethane	Ethyl acetate	Nitrobenzene	Acetonitrile
54	*p*-H	4.60	570	562	560	539
			573	562	577	527
55	*m*-NO_2	2.62	722	700	733	715
			724	700	722	713
				706		
				707		
56	*m*-CN	..	..	688	..	..
				689		
57	*m*-Br	3.51	667	644	..	..
			660	643		
				645		
				638		
58	*p*-Br	3.91	650	628	650	608
			645	629	642	606
59	*m*-Cl	3.52	678	642	..	..
			670	646		
				647		
60	*p*-CH_3	5.30	538	517	547	500
			534	512	552	488
				511		
				520		
61	*p*-OCH_3	5.29	504	488	517	455
			505	478	514	459
				495		
				481		
62	Dimethylaniline	5.06	..	539	..	..
63	Diethylaniline	6.56	..	467	..	425

TABLE V

MILLIVOLTAGE HALF-NEUTRALIZATION VALUES FOR PYRIDINES USING PERCHLORIC ACID

	Substituted pyridine	pK_a, H_2O	Solvents: Nitromethane	Ethylene dichloride	Ethyl acetate	Nitrobenzene	Acetonitrile
64	No substituent	5.22	..	..	Ppt.	..	..
65	2-Methyl-	5.96	..	..	462	..	..
66	3-Methyl-	5.63	..	..	480	..	..
67	2,6-Dimethyl-	6.72	298	430	436	353	331
			307	439	435	347	330

nitro compounds and acetonitrile than for the less polar ethyl acetate. This is in harmony with the conductimetric behavior of electrolytes in these solvents.

The conclusion to be drawn from the existence of such lines is that the base *strength of an amine in water is, broadly speaking, a reliable index of its base strength in organic solvents* Differing degrees of solvation do exist, but they are not important enough to cause major disturbances in the order of base strengths. In the present work, where correlations covering a billion-fold variation in base strength are sought, such minor effects will be neglected. This conclusion is in harmony with those of earlier investigators.

The points denoted by triangles describe amines possessing oxygen or nitrogen atoms in close proximity to the amine nitrogen. They include the piperazines and their monoacyl derivatives, morpholine, ethanolamines and ethylenediamine. These bases are stronger in organic solvents than other amines of comparable strength in water. Figure 3 shows that the former describe a line different from monofunctional amines. They show deviations in the same direction for the other solvents and acids.

TABLE VI

MILLIVOLTAGE HALF-NEUTRALIZATION VALUES, USING *p*-TOLUENESULFONIC ACID

	Amine	pK_a, H_2O	Solvents: Nitromethane	Ethylene dichloride	Ethyl acetate	Nitrobenzene	Acetonitrile
32	Piperidine	11.20	46	33	Ppt.	37	19
							24
36	N-Ethylpiperidine	10.40	Ppt.	91	Ppt.	48	56
							52
7	Triethylamine	10.72	Ppt.	46	135	80	35
16	Isobutylamine	10.42	116	70	103	93	83
67	2,6-Lutidine	7.42	Ppt.	328	..	320	315
61	*p*-Anisidine	5.29	Ppt.	409	..	Ppt.	440
							435
68	*m*-Toluidine	...	Ppt.	460	Ppt.	Ppt.	493
							495
6	Diethylamine	11.00	99	48	75	46	33
					80		
5	Ethylamine	10.75	83	44	Ppt.	Ppt.	35
46	N-Allylmorpholine	7.05[a]	..	..	..	265	256
39	1-Carbethoxypiperazine	8.28[a]	..	..	..	178	186
48	Benzylamine	9.30	..	..	..	..	154

[a] Determined in the present work.

TABLE VII

MILLIVOLTAGE HALF-NEUTRALIZATION VALUES, USING METHANESULFONIC ACID

	Amine	pK_a, H_2O	Solvents: Nitrobenzene	Acetonitrile
67	2,6-Lutidine	7.42	370	308
			370	
7	Triethylamine	10.72	118	31
46	N-Allylmorpholine	7.05[a]	298	254
6	Diethylamine	11.00	80	19
39	N-Carbethoxypiperazine	8.28[a]	185	182
36	N-Ethylpiperidine	10.40	126	92
32	Piperidine	11.20	46	8
			48	
48	Benzylamine	9.30	..	148
16	Isobutylamine	10.42	..	103

[a] Determined in the present work.

A final point relates to the comparative acid strengths of perchloric and *p*-toluenesulfonic acids in organic solvents. In nitromethane and nitrobenzene,[25] it has been shown conductometrically

(25) C. P. Wright, D. M. Murray-Rust and H. Hartley, *J. Chem. Soc.*, 199 (1931); D. M. Murray-Rust, H. J. Hadow and H. Hartley, *ibid.*, 215 (1931).

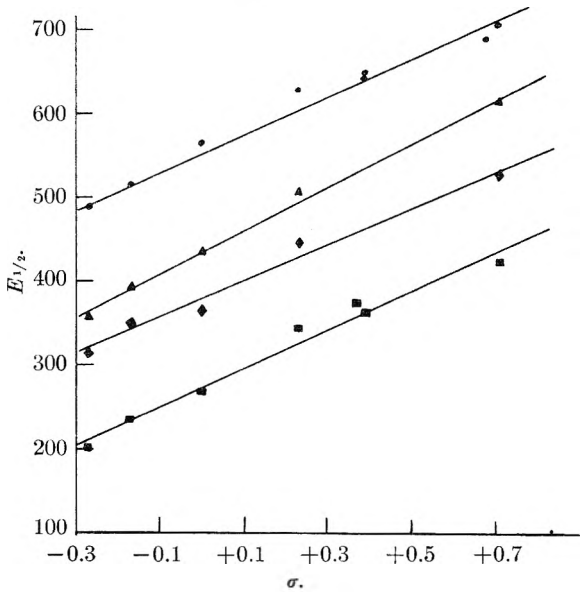

Fig. 2.—Hammett plots obtained using perchloric acid: ●, ethyl acetate; ▲, acetonitrile (100 mv. subtracted from observed reading); ◆, nitrobenzene (200 mv. subtracted); ■, nitromethane (300 mv. subtracted).

that perchloric acid is highly dissociated into free ions, whereas benzenesulfonic acid is not. Nevertheless, the plots of the data obtained here show that both acids are strong in organic solvents by the present criteria.

TABLE VIII

EQUATIONS OF THE LEAST SQUARES LINES IN THE HAMMETT PLOTS USING PERCHLORIC ACID

Solvent	Equation	n	Av. dev. in σ or pK_a
Nitrobenzene	$E_{1/2} = 580.0 + 216.6\sigma$	5	±0.040
	$E_{1/2}$ 580.0 + 78.3 mv. pK_a		± .11
Acetonitrile	$E_{1/2} = 534.7 + 260.7\sigma$	5	± .024
	$E_{1/2} = 534.7 + 94.2$ mv. pK_a		± .07
Nitro-methane	$E_{1/2} = 575.4 + 228.9\sigma$	7	± .033
	$E_{1/2} = 575.4 + 82.7$ mv. pK_a		± .09
Ethyl acetate	$E_{1/2} = 554.2 + 220.3\sigma$	8	± .046
	$E_{1/2} = 554.2 + 79.8$ mv. pK_a		± .13

strength; this appears to be by far the most serious source of error, especially in the solvents of low dielectric constant. This error causes results for different amines not to be strictly comparable. Another error leading to the same conclusion is the variability in the milliequivalents of amine employed, since the amount of amine salt formed will vary. In a medium of high ionic strength this would not be a serious error. However, finding suitable salts to maintain a constant ionic strength was not practicable. First, *p*-toluenesulfonic acid, at least, is not completely ionized in these solvents,[19] although addition of *p*-toluenesulfonate ion probably could not depress the acidity appreciably. Any other anion, being derived from weaker acids, would undoubtedly be protonated. Secondly, solubility considerations would prevent any high ionic strength from being attained. Only lithium or tetraalkylammonium perchlorates could be considered. The coördinating properties of Li^+ made this ion undesirable, while no tetraalkylammonium perchlorate which was appreciably soluble in ethyl acetate could be found. For these reasons, we have neglected to maintain a constant ionic strength, recognizing that it is probably the major source of error.

The precision of the acidity constants compares favorably with that in water. If 59 mv. corresponds to one pK unit, then ±6 mv. will correspond to an uncertainty of ±0.10 pH unit in water. This is about as precise as the values obtained by simple titration.

Nature of the Acid–Base Reaction.—The presence of two equivalents of water in the perchloric acid solutions, and of one in the *p*-toluenesulfonic acid solution, is perhaps unfortunate. In the former case, however, there appears to be no easy way to remove it. The explosion hazard was regarded as too serious to make the attempt. Further, the quantity of water is so small (*ca.* 0.05%) that it is difficult to be sure that the solvent does not already contain comparable amounts. No attempt was made to carry out the titrations under absolutely anhydrous conditions. It is noteworthy that perfluorobutyric and methanesulfonic acids, containing no water, gave reproducible titration curves. It is our opinion that small traces of water have little effect on the $E_{1/2}$ values.

Similarly, the presence of dioxane changes the solvents slightly, but perchloric acid solutions in at least some of the five solvents would probably be unstable (Fritz found this to be true for acetonitrile). The presence of dioxane in ethyl acetate or acetonitrile is probably immaterial since it is of

TABLE IX

EQUATIONS OF THE LEAST SQUARES LINES IN PLOTS OF $E_{1/2}$ VALUES *vs.* pK_a VALUES

Type of amine	Acid	Solvent	Equation	n	Av. dev. (pK_a units)
Monofunctional	Perchloric	Ethyl acetate	$E_{1/2} = 878.8 - 67.6pK_a$	38	±0.39
Contain heteroatoms	Perchloric	Ethyl acetate	$E_{1/2} = 934.4 - 84.9pK_a$	9	± .43
Monofunctional	Perchloric	Acetonitrile	$E_{1/2} = 897.2 - 77.2pK_a$	16	± .21
Contain heteroatoms	Perchloric	Acetonitrile	$E_{1/2} = 758.0 - 69.3pK_a$	10	± .18
Monofunctional	Perchloric	Nitrobenzene	$E_{1/2} = 933.1 - 78.0pK_a$	18	± .27
Monofunctional	Perchloric	Nitromethane	$E_{1/2} = 942.5 - 80.6pK_a$	16	± .21
Monofunctional	*p*-Toluenesulfonic	Acetonitrile	$E_{1/2} = 845.8 - 74.8pK_a$	9	± .22

Errors and Precision.—The errors in the measurement of base strengths are of three types: (1) Temperature; any deviations caused by temperature fluctuations are believed to be minor compared to those from other causes. (2) Irreproducibility of glass electrode readings in organic solvents; it is believed that this effect has been largely eliminated by the careful electrode standardization procedure. (3) Lack of constant ionic

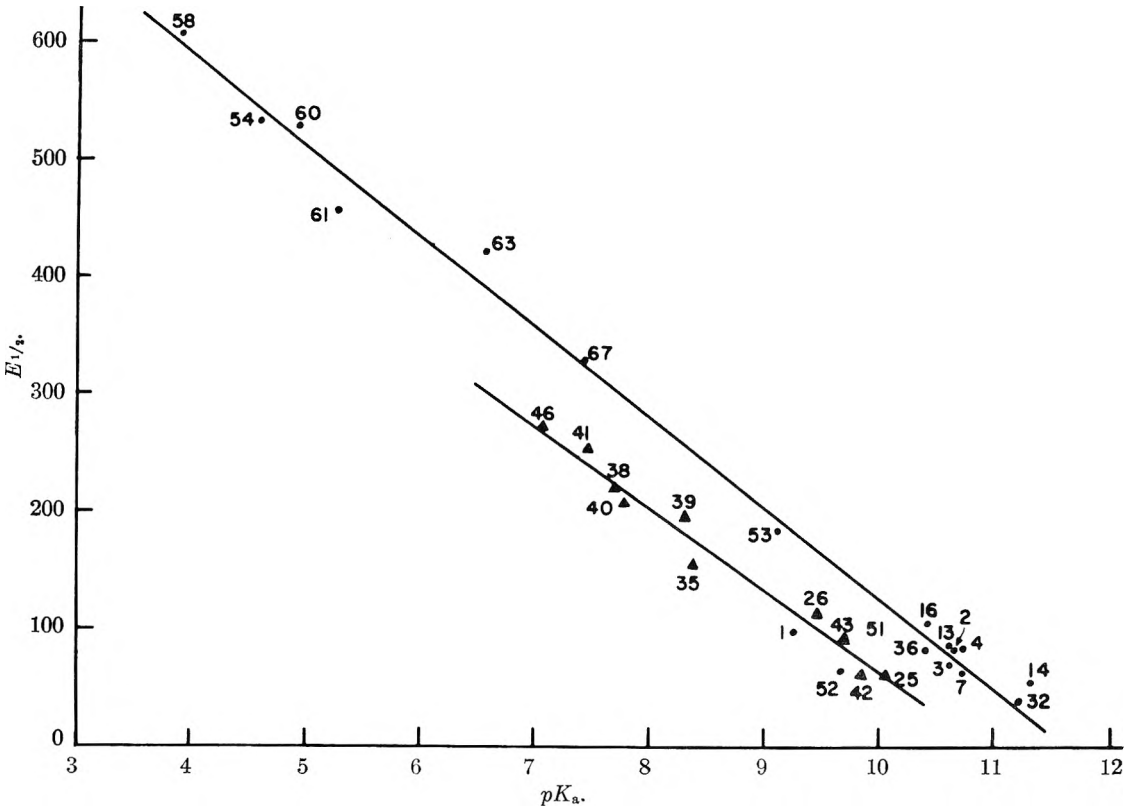

Fig. 3.—Data obtained using perchloric acid and acetonitrile.

comparable basicity toward the solvent. In the other three solvents, it may help to solvate the ammonium ions. That oxygen compounds can apparently do this was shown above in the case of amines, which had oxygen built into the same molecule. Although the oxygen atom is favorably disposed in those cases, 0.25 M dioxane should be able to perform the same function.

The question of what acidic species are actually present arises. In ethyl acetate and acetonitrile probably only the protonated solvent molecules exist. In the other three solvents probably these are of negligible concentration, and oxonium and protonated dioxane molecules are dominant. In light of these considerations the correlations which exist among different solvents appear even more striking since different acidic species are actually involved.

Hydrogen-bonding of the type $R_3NHNR_3^+$ is excluded by the fact that steric hindrance has no effect on base strength. Piperidine and its 2,2,6,6-tetramethyl derivative have identical base strengths

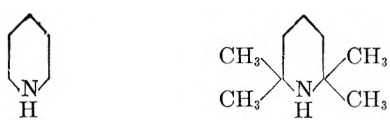

This fact also excludes hydration of the positive ion by the water in the solution so that the latter is probably engaged in solvating the anion.

Abnormal Slopes in Correlation of Base Strengths in Different Solvents.—As noted above, it was established that linear relationships of varying degrees of precision could be obtained by plotting pK_a values against $E_{1/2}$ values of a series of amines using a given solvent and acid. If the ratio of the activity coefficients of the ammonium ions to those of the corresponding amines is a constant, it can readily be shown that the slopes should all be 59 mv. per pK_a unit. The slopes of the various linear plots are given in Table IX. It is clear that a range of values is obtained. Such deviations have been noted previously for solution in benzene,[1] acetonitrile,[6] formamide[24] and n-butyl alcohol.[23,26] As noted by Verhoek,[24] this implies a steady variation on the ratio of the activity coefficient of the ammonium ion to that of the corresponding amine. The ratio of the molar activity coefficients may be constant for various amines in these dilute solutions and the variation is in the ratio of the degenerate activity coefficients.[14]

$$-\ln \frac{f_B}{f_{BH^+}} = \beta p K_a$$

$$E_{1/2} = -59 \text{ mv.} (1 + \beta) p K_a + \alpha$$

The constants α and β are functions of the solvent and possibly of the titrant acid. As noted by previous investigators, β depends on the class of base as well (amine, phenoxide or carboxylate ion). A new feature arising from the present work is that structural modifications within a given class of base can change the value of α and possibly of β. Thus for amines containing no additional heteroatoms, with perchloric acid and ethyl acetate, α equals 878.8 and β equals 0.14. Amines containing additional O or N atoms possess an α value of 934.4 and a β value of 0.44.

(26) A straight line of slope 0.80 can be drawn through the data of ref. 23 for nitrophenols.

An intimation of such subdivisions within structural classes is to be found in the work of Kilpatrick and Kilpatrick.[6] In their Fig. 1 the data can be regarded as describing one line of slope 1.00 for carboxylic acids containing no additional heteroatoms and another of slope 1.4 for carboxylic acids which contain hydroxyl groups.

A final point relates to the possible existence of acidity functions in non-protolytic, highly polar media. Smith and Hammett[9] have already uncovered complex behavior in sulfuric acid solutions in nitromethane. If the variations in activity coefficients described above are real, acidity functions cannot exist in these media. Even in the polar solvent formamide, according to Verhoek's results, such functions will not be found. The existence of two lines describing bases of the same charge type supports this conclusion.

Conclusions.—First, the glass electrode will measure reproducibly the activity of hydrogen ion in a non-hydroxylic organic solvent.

Second, the comparison of base strengths in organic solvents with those in water indicates that the pK_a value in water is a good index of base strength in an organic solvent ($E_{1/2}$), within a particular class, but that monoamines and diamines containing polar groups near the N atom belong to a different class than those without such groups.

Third, the $E_{1/2}$ value of an amine has been shown to be determined by its structure. It can be anticipated, therefore, that such a determination will be useful in identifying small quantities of unknown water-insoluble amines.

Experimental

Solvents.—Ethyl acetate was Mallinckrodt analytical reagent. Ethylene dichloride and nitromethane were distilled through a 3-foot helix-filled column, b.p. 83.5° and 101°, respectively. Acetonitrile was distilled through this column from phosphorus pentoxide, b.p. 82.1°. Nitrobenzene was purified by the method of Kolthoff and coworkers,[7] b.p. 96° (18 mm.).

An indication of the relative basicities of the solvents was obtained by noting the millivoltage readings past the titration end-point. These were in the order: ethylene dichloride > acetonitrile > ethyl acetate.

Amines.—With the exception of the monoacylpiperazines and 2,2,6,6-tetramethylpiperidine, the monoamines were good commercial samples, usually Eastman Kodak Co. White Label. Liquids were tested with potassium hydroxide pellets and if any interaction occurred, were dried and distilled.

The monoacylpiperazines were prepared by the acylation of piperazine in aqueous acetone.[27] 2,2,6,6-Tetramethylpiperidine was prepared by the method of Leonard and Nommensen.[28]

The monoacylethylenediamines were prepared by the method of Hill and Aspinall.[29]

Acids.—Eastman Kodak Co. 72% perchloric acid was dissolved in purified dioxane and standardized against potassium acid phthalate in glacial acetic acid by the Analytical Section. *p*-Toluenesulfonic acid monohydrate was Eastman Kodak Co. White Label. The perfluorobutyric acid was a Minnesota Mining and Manufacturing product. Both were used as received to prepare 1.106 and 0.434 *M* solutions in pure dioxane, respectively. Methanesulfonic acid was Eastman Kodak Co. Practical grade. It was distilled under vacuum, neutral equivalent 100.5. A portion was fractionated in a spinning band column, b.p. 135° (2.5 mm.), neutral equivalent 96.2. Titrations were performed with the latter of these materials, made up just prior to use in the given solvent as approximately an 0.5 *M* solution.

An indication of relative acid strengths was obtained by noting the heights of the potential jumps at the end-point. These were in the order: perchloric > *p*-toluenesulfonic > methanesulfonic > perfluorobutyric. The latter gave reproducible $E_{1/2}$ values toward triethylamine in acetonitrile (24 and 30 mv.) but 2,6-dimethylpyridine gave no detectable break.

Procedure.—The titrations were performed using 50–75 ml. of solvent in a 200-ml. tall form beaker. Magnetic stirring was provided. A Gilmont 1-ml. microburet–pipet was used in the titration. The quantity of amine was such as to require 0.3–1.1 ml. of 0.5 *N* perchloric acid.

The standard buffer solution was prepared by weighing out 1.5000 g. of Sharples diisobutylamine, b.p. 139.7–140.0°, which had been fractionated in a spinning band column,[30] and making it up to 350.0 ml. in volumetric flasks. To this was added by pipet 5.00 ml. of 0.5032 *N* perchloric acid in dioxane. The solution is stable for at least two days.

The electrodes were Beckman #1190-42 and #1170, respectively.[31] They were connected to a Beckman model G *p*H meter by means of a Beckman #8700 six-point manual switching box. Adjustment of the millivoltage reading was made on the latter, the position of the zero adjuster dial on the *p*H meter being immaterial. A small dry cell in the switching box required replacement only at long intervals.

The electrodes were allowed to stand in water when not in use. To standardize, they were wiped with tissue and placed in the buffer solution. The mv. reading (taking care to reset dials I and especially II when changing from *p*H scale) was then adjusted by means of the switching box to +170 mv.

After standardizing, a titration was performed in the usual fashion, using increments of 0.030 ml. until near the end-point (no steady reading may be obtainable until the first increment has been added). A plot was then made of *E vs.* ml. added and $E_{1/2}$ read from the graph in the usual way.

After the titration the electrode was returned to water. A second titration was performed using another pair of electrodes. The first pair was then used again. When checked in the organic buffer, it was always found to read +170 mv.

It was difficult to measure a suitable small amount of the gaseous amines into the solvent. This was overcome by adding 0.030 ml. of acid to the solution and passing in amine until the reading reached a value previously determined as indicating a suitable quantity.

The pK_a values in water marked with an "*a*" were determined in the present work. This was done by potentiometric titration of 100 ml. of *ca.* 0.01 *M* aqueous solution of amine at 25.0° and 0.5 *N* hydrochloric acid, adding the latter from a Gilmont 1-ml. pipet. Other pK_a values are from standard literature references, chiefly references 32–35.

Acknowledgments.—We are deeply indebted to Mr. Donald G. Preis for performing most of the titrations, to Miss Helen Anderson for performing the remainder and to Dr. P. W. Morgan for helpful criticism and encouragement.

(27) (a) T. S. Moore, M. Boyle and V. M. Thorn, *J. Chem. Soc.*, 39 (1929); (b) K. R. Jacobi, *Ber.*, **66**, 113 (1933).

(28) N. J. Leonard and E. W. Nommensen, *J. Am. Chem. Soc.*, **71**, 2808 (1949).

(29) A. J. Hill and S. R. Aspinall, *ibid.*, **61**, 822 (1939).

(30) Careful fractionation was actually unnecessary since Sharples material dried over potassium hydroxide pellets gave identical results to those obtained using purified material.

(31) These electrodes have been shown (B. Gutbezahl and E. Grunwald, *J. Am. Chem. Soc.*, **75**, 559 (1953)) to be the preferred types for non-aqueous media.

(32) N. F. Hall and M. R. Sprinkle, *ibid.*, **54**, 3469 (1932).

(33) J. D. Roberts, R. L. Webb and E. A. McElhill, *ibid.*, **72**, 408 (1950).

(34) R. G. Pearson and F. V. Williams, *ibid.*, **76**, 258 (1954).

(35) R. J. L. Andon, J. D. Cox and E. F. G. Harrington, *Trans. Faraday Soc.*, **50**, 918 (1954).

PARAMAGNETIC RESONANCE IN COPPER CHELATES

BY B. R. MCGARVEY

Department of Chemistry and Chemical Engineering, University of California, Berkeley, California

Received June 11, 1955

Investigation of the paramagnetic resonance of a single crystal of copper(II) acetylacetonate gives $g_{\parallel} = 2.254$ and $g_{\perp} = 2.075$, showing the existence of strong π-bonds and weak σ-bonds. The results are in disagreement with the Pauling covalent theory for copper compounds in that the unpaired electron is not in a $4p_z$ orbital. In addition, the resonances of dilute solutions of copper(II) acetylacetonate in dioxane, pyridine, chloroform and toluene were investigated. The solvents dioxane and pyridine have a marked influence on the gyromagnetic ratio which can be attributed to the formation of weak complexes between the solute and the solvent with the point of attachment being the copper atom. The hyperfine lines in the solution resonances exhibit an unusual assymmetry in that they are of unequal width. Also, their separation is found to be dependent on the nature of the solvent. Solutions of other copper chelates were investigated with similar results.

Introduction

The crystalline field theory as used by Schlapp and Penney,[1] Orgel,[2] and others has been quite successful in explaining the properties, mainly magnetic and optical, of most iron group salts. However, there is a group of salts, the so-called covalent complexes, for which this theory has failed and for these complexes three different theories have been advanced to account for their behavior, namely: the directed valence theory of Pauling,[3] the strong field theory,[4,5] and the molecular orbital theory.[6,7] Van Vleck[8] has shown that all three theories will lead to the same qualitative predictions concerning the behavior of these covalent complexes. The molecular orbital approach to the problem as developed by Stevens[6] and Owen[7] appears, however, to be the best in explaining the detailed behavior.

The purpose of this work was to investigate the nature of the binding in a copper compound which is normally considered to be covalent, the compound chosen being copper(II) acetylacetonate. In the case of the +2 state of copper, the gross magnetic behavior for the compound cannot be used as an indication of how ionic or covalent the bonds are since all theories predict a paramagnetism resulting from one unpaired electron. On the basis of his theory, Pauling[3] has distinguished the covalent from the ionic compounds by their structure, the covalent being square planar and the ionic tetrahedral. This, however, is not a good criterion, as shown by the work of Orgel[2] and Bjerrum,[9] since the crystalline field theory can also give a planar structure in many instances. The only real difference between the ionic and covalent cases lies in the spatial location of the unpaired electron which can be determined by paramagnetic resonance since location of the unpaired electron has a great influence upon the gyromagnetic ratio. For the ionic case, Abragam and Pryce[10] have shown that the values $g_{\parallel} \sim 2.4$ and $g_{\perp} \sim 2.1$ are to be expected and this has been verified by experiments such as those of Bleaney, Penrose, and Plumpton.[11] Pauling's theory of covalency[3] which puts the unpaired electron in a $4p_z$ orbital would predict the values $g_{\parallel} = 2.0$ and $g_{\perp} \sim 2.1$ as shown by Okamura and Date[12] while the molecular orbital theory of Stevens[6] and Owen[7] which does not insist on promotion of the electron to obtain covalent bonds would predict that $g_{\parallel}$ be greater than $g_{\perp}$ as in the ionic case and that both would be smaller than the ionic values, the amount being dependent on the degree of covalency in the bond.

The only work which has been done on covalent complexes of copper is that of Okamura and Date[12] on single crystals of $Cu(NH_3)_4SO_4 \cdot H_2O$ and $Cu(NH_3)_4(NO_3)_2$ and that of Ingram and Bennett[13] on copper phthalocyanine. The data of Okamura and Date[12] is of little value due to lack of knowledge of the structure of the crystals investigated, but that of Ingram and Bennett demonstrates the behavior predicted by the molecular orbital theory and indicates the existence of extensive π- and σ-bonding.

In addition to the work on the single crystal of copper acetylacetonate, some interesting results obtained from solutions of the acetylacetonate and similar compounds in various solvents are discussed in this paper.

Experimental Equipment

The paramagnetic resonance spectrometer used in this work was of conventional design which operates at a wave length of 3.34 cm. and employs a magic tee bridge circuit in which the arm containing the sample cavity is balanced against a dummy load in the opposite arm of the bridge. The cavity itself was a simple full wave length rectangular cavity made from a piece of 3 cm. wave guide. The 723A klystron was stabilized on the sample cavity by use of a conventional pound stabilizing circuit and a directional coupler placed in the sample arm of the bridge to detect the reflected power from the sample cavity. This stabilization system had the advantage over systems in which the stabilization was on a separate cavity in that it allowed the klystron to compensate for any changes in the resonance frequency of the sample cavity due to any evaporation of the liquid samples used in the research. The electromagnet and its power supply were constructed by Varian Associates (Models V-4007 and V-2200 respectively).

An automatic plotting system was used in which the current supplied to the magnet was varied at a constant rate while the derivative of the output of the bridge was plotted by a Brown recorder. The plots were calibrated by use of

(1) R. Schlapp and W. G. Penney, *Phys. Rev.*, **42**, 666 (1932).
(2) L. E. Orgel, *J. Chem. Soc.*, 4756 (1952).
(3) L. Pauling, *J. Am. Chem. Soc.*, **53**, 1367 (1931).
(4) J. B. Howard, *J. Chem. Phys.*, **3**, 813 (1935).
(5) M. Kotani, *J. Phys. Soc., Japan*, **4**, 293 (1949).
(6) K. W. H. Stevens, *Proc. Roy. Soc. (London)*, **A219**, 542 (1953).
(7) J. Owen, *ibid.*, **A227**, 183 (1955); *Trans. Faraday Soc.*, in press, (1955).
(8) J. H. Van Vleck, *J. Chem. Phys.*, **3**, 807 (1935).
(9) J. Bjerrum, C. J. Ballhausen and C. K. Jørgensen, *Acta Chem. Scand.*, **8**, 1275 (1954).
(10) A. Abragam and M. H. L. Pryce, *Proc. Roy. Soc. (London)*, **A206**, 173 (1951).
(11) B. Bleaney, R. P. Penrose and B. I. Plumpton, *ibid.*, **A198**, 406 (1949).
(12) F. Okamura and M. Date, *Phys. Rev.*, **94**, 314 (1954).
(13) D. J. E. Ingram and J. E. Bennett, *J. Chem. Phys.*, **22**, 1136 (1954); *Trans. Faraday Soc*, in press (1955).

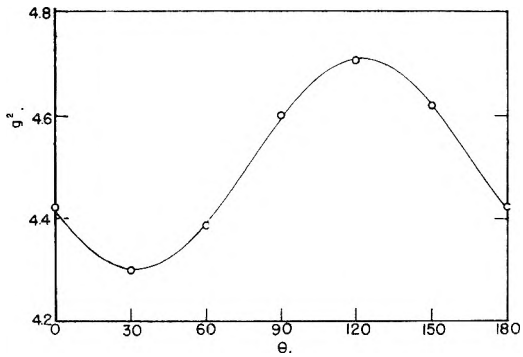

Fig. 1.—Dependence of g^2 on an arbitrary angle θ for a single crystal of copper(II) acetylacetonate when the magnetic field is in the *ac*-plane of the crystal. The circles are from experiment while the solid curve is a plot of equation 3.

a proton resonance spectrometer, an 100 kc. crystal oscillator, and a small crystal of diphenyltrinitrophenylhydrazyl which was placed in the cavity beside the sample being measured. The spectrometer was tuned to the nearest harmonic of the crystal oscillator and when the proton resonance peak crossed the center of the oscilloscope on which it was displayed a marker pip was placed on the recorder plot. The spectrometer was then retuned to the next harmonic and the process repeated resulting in a series of pips on the recorder plot 23.49 gauss apart. The separation of the resonance peaks from that of the reference free radical along with resonance magnetic field of the free radical, which was found by measuring the actual frequency of the proton resonance at this field, was enough to establish the gyromagnetic ratio for any resonance. In making these measurements a gyromagnetic ratio of 2.0038 was taken for the resonance of the free radical.

Results and Discussions

Single Crystal of Copper(II) Acetylacetonate.—The crystal structure of copper acetylacetonate has been determined by Koyama, Saito and Kuroya[14] who found it to be monoclinic with $a = 11.40$, $b = 4.75$, $c = 10.33$, and $\beta = 92.2°$ and to have the symmetry P_{21}/n. The molecules are planar with the normal to the plane making an angle of 53° with the *b*-axis. The single crystals used were prepared by slow evaporation of a chloroform solution and were long needles which frayed easily at the ends. X-Ray analysis showed the copper–copper distance along the long axis of the crystals to be 4.72 ± 0.02 Å.

The analysis of the resonance was similar to that employed by Bleaney, Penrose and Plumpton[11] in their work on the Tutton salts. The *g*-value for the resonance was determined along the *b*-axis and in the *ac*-plane of the crystal which for tetragonal symmetry should be given by the equations

$$g_b^2 = g_{\parallel}^2 \cos^2\alpha + g_{\perp}^2 \sin^2\alpha \quad (1)$$

$$g_{ac}^2 = (g_{\parallel}^2 - g_{\perp}^2) \sin^2\alpha \cos^2(\beta - \phi) + g_{\perp}^2 \quad (2)$$

in which α is the angle between the tetragonal axis and the *b*-axis, β is the angle between the *ac*-projection of the tetragonal axis and the *a*-axis, and ϕ is the angle between the magnetic field in the *ac*-plane and the *a*-axis. To find $g_{\parallel}$, $g_{\perp}$ and α it is sufficient to determine g_b^2 and the maximum and minimum value of g_{ac}^2. Due to the crudeness of the mounting apparatus, it was not possible to determine ϕ with any accuracy so that only the angular difference in settings is known with any accuracy. For this reason the results of measurements in the *ac* plane, which are given in Fig. 1, are given in terms of the arbitrary angle θ. The circles in Fig. 1 are the average of determinations at both the angle θ and $\theta + 180°$ while the solid curve is the $\cos^2$ curve by equation 3.

$$g^2 = 0.409 \cos^2(122° - \theta) + 4.301 \quad (3)$$

The agreement between the points and curve in Fig. 1 shows that equation 2 represents the behavior of g_{ac}^2 in this crystal quite well. The value for g_b^2 was found to be 2.161 ± 0.004 which combined with the maximum and minimum values of g_{ac}^2 of 2.170 ± 0.003 and 2.075 ± 0.001, respectively, gives $g_{\perp} = 2.075 \pm 0.001$, $g_{\parallel} = 2.254 \pm 0.008$, and $\alpha = 47 \pm 1°$.

The value for α is not in agreement with the X-ray value of 53° for the angle between the normal to the molecular plane and the *b*-axis. This may be due to the symmetry being rhombic instead of tetragonal as assumed above. Using the resonance and X-ray data and assuming the rhombic axes to coincide with the symmetry axes of the molecule we obtain $g_z = 2.18$, $g_y = 2.15$ and $g_x = 2.074$ where the *z*-axis is perpendicular to the molecular plane and the *y*-axis lies in the plane and bisects the two 3-position carbon atoms on the rings. Surprisingly the equation for g_{ac}^2 for this case is little different from that of equation 2, the difference being less than experimental error. Whether or not this high degree of rhombic character in the symmetry is actually the case can only be determined by investigations on a dilute single crystal which up to now has not been prepared successfully.

Although the uncertainty in the symmetry leads to some uncertainty concerning the *g*-values, the results do show that both Pauling's theory and the crystalline field theory are incorrect for this compound. $g_{\parallel}$ is not less than $g_{\perp}$ which would be the case for a p_z electron but greater than $g_{\perp}$ and the values of both $g_{\parallel}$ and $g_{\perp}$ are less than would be predicted by the crystalline field theory. The best picture would appear to be the molecular orbital theory as used by Stevens[6] and Owen.[7] In comparing the results with this theory it seems best to assume tetragonal symmetry and use the $g_{\parallel}$ and $g_{\perp}$ values found on this basis. Using the notation of Owen,[7] the ground state orbital for the unpaired electron is the antibonding orbital

$$\sigma^*_{x^2-y^2} = \alpha d_{x^2-y^2} - {}^1/_2(1 - \alpha^2)^{1/2}[-p_1 + p_2 + p_3 - p_4]_{\sigma} \quad (4)$$

while the excited states to which it couples in the calculation of the gyromagnetic ratios are the π antibonding orbitals

$$\pi^*_{xy} = \beta d_{xy} - {}^1/_2(1 - \beta^2)^{1/2}[p_1 + p_2 - p_3 - p_4]_{\pi} \quad (5)$$

$$\pi^*_{xz} = \beta_1 d_{xz} - \frac{1}{\sqrt{2}}(1 - \beta_1^2)^{1/2}[p_1 - p_3]_{\pi} \quad (6)$$

$$\pi^*_{yz} = \beta_1 d_{yz} - \frac{1}{\sqrt{2}}(1 - \beta_1^2)^{1/2}[p_2 - p_4]_{\pi} \quad (7)$$

If we assume that the time spent on each oxygen atom is the same for each π-state, then

$$\beta_1^2 = {}^1/_2(1 + \beta^2) \quad (8)$$

(14) H. Koyama, Y. Saito and H. Kuroya, *J. Inst. Polytech. Osaka City University*, **4**, 43 (1953).

and the equations for $g_{\parallel}$ and $g_{\perp}$ will be

$$g_{\parallel} = 2.0023 - \frac{8\lambda}{\Delta E_{xy}} \alpha^2\beta^2 \qquad (9)$$

$$g_{\perp} = 2.0023 - \frac{\lambda}{\Delta E_{xz}} \alpha^2(1 + \beta^2) \qquad (10)$$

ΔE_{xy} and ΔE_{xz} are the difference in energy between the ground state and the π^*_{xy} and π^*_{xz} states, respectively, and λ is the spin orbit coupling constant for the copper ion. Using the values of $g_{\parallel}$ and $g_{\perp}$ found above and the values of 15,000 and 19,000 cm.$^{-1}$ for ΔE_{xy} and ΔE_{xz} found by Belford,[15] the values of α^2 and β^2 are found to be $\alpha^2 = 1$ and $\beta^2 = 0.5$. For the hydrated copper ion, Owen[7] found $\alpha^2 = 0.84$ assuming $\beta^2 = 1$, but for acetylacetonate it appears that the σ-bonds are as ionic as those in the hydrated ion and the π-bonds are quite covalent. This high covalency in the π-bonds is, of course, due to the π-electron system in the adjoining ion which makes it possible for the electrons in the π-state to be smeared out over the whole molecule and this is apparently the reason for the stability of this chelate. The lower values for $g_{\parallel}$ and $g_{\perp}$ obtained by Ingram and Bennett[13] suggest that for nitrogen bonds the σ-bonds are also appreciably covalent in nature. The values of α^2 and β^2 given for the acetylacetonate should not be taken too literally since the assumptions in this theory are many, but the values are indicative of the general nature of the bonding in this molecule.

The resonance lines observed from the single crystal were slightly asymmetrical at some orientations and had line widths considerably less than those expected from dipolar broadening. The peak to peak separation of the derivative curve varies from a value of 82 gauss at $\theta = 30°$ to 160 gauss at $\theta = 120°$ in the *ac*-plane and has a value of 280 gauss along the *b*-axis. These values are much less than the 500 gauss width in the *ac*-plane and 1000 gauss width along the *b*-axis predicted from Van Vleck's theory[16] for dipolar broadening assuming the curve to be gaussian in shape. This narrowing of the line indicates considerable exchange narrowing as the result of exchange coupling between the equivalent copper atoms along the *b*-axis.

In Solution.—The spectra of solutions of copper acetylacetonate and similar compounds were found to exhibit several interesting phenomena some of which are seen in Fig. 2 which is a plot of the resonance from an 0.01 molar solution of the acetylacetonate in dioxane. The curve consists of four apparently equally spaced absorption lines which are either of different intensity or different widths as the resultant curve is quite asymmetrical in shape. The four peaks must arise from the hyperfine interaction with the copper nucleus of spin $^3/_2$ but normally these hyperfine lines are of equal intensity, since the population of the nuclear levels at room temperature should be equal, and of equal width. That the four lines are of equal intensity and differ only in their widths is demonstrated by the heavy dashed curve in Fig. 2 which has been calculated from the derivative of a curve made up of four equally spaced Lorentzian curves of equal areas but different widths. The Lorentzian curve is given in equation 11

$$B/[1/T_2^2 + (\omega - \omega_0)^2] \qquad (11)$$

in which the width of the line is determined by T_2 and ω_0 is the angular frequency at the center of the line. T_2's chosen for the four lines represented in Fig. 2 are 1.4×10^{-8}, 1.1×10^{-8}, 0.88×10^{-8} and 0.77×10^{-8} sec. The fit between the calculated and experimental curve could be made even better by a slight readjustment of the T_2's but this does not seem worthwhile since the fit is already quite good.

This asymmetry of the resonance lines in solutions has appeared to varying extent in all the copper chelates and solvents thus far studied as may be seen in Fig. 3 which gives some typical plots. In all solutions studied so far the width of the hyperfine lines increases with the gyromagnetic ratio so that the line furthest from the free radical is always the broadest. The variation in the line widths is dependent on both the solvent, with toluene giving the least change in width, and the solute, with copper acetylacetonate having a smaller change in widths than copper 3-ethylacetylacetonate. The shapes of other samples examined were similar to those in Fig. 3 with copper acetylacetonate in mixtures of both toluene plus chloroform and chloroform plus carbon tetrachloride similar to plot 4, copper ethylacetoacetate in dioxane similar to plot 3, and copper salicylaldehyde methylimine in xylene similar to plot 4.

The shapes of these lines were found to be independent of sweep direction, time constants in the circuits, rf intensity, and amplitude of the magnetic field modulation when kept reasonably small. Further, measurements on acetylacetonate solutions in dioxane with concentrations between 0.001 and 0.01 molar showed no effect due to solute concentration and for this reason most of the work was done on 0.01 molar solutions to obtain a better signal to noise ratio.

That the hyperfine structure in these solutions is resolvable at all is of some interest since Bagguley and Griffiths[17] found it impossible to resolve the hyperfine structure in dilute copper Tutton salts at room temperature due to a short spin-lattice relaxation time of about 2×10^{-9} sec. Measurements on the resonance of $Cu(NH_3)_4^{++}$ and $Cu(H_2O)_6^{++}$ ions in water solution have also shown no hyperfine structure, $Cu(NH_3)_4^{++}$ giving a resonance whose peak to peak width was 300 ± 10 gauss and $g = 2.101 \pm 0.005$ and $Cu(H_2O)_6^{++}$ giving a peak to peak width of 115 ± 5 gauss and $g = 2.184 \pm 0.005$. Apparently the spin lattice relaxation times in the chelates is ten times greater than in the ionic Tutton salts. This may be caused by much stronger bonds between the copper and its neighbors with the result that the oscillational frequencies are much higher giving a smaller Fourier component in the region of the resonance frequency.

In addition to the above-mentioned properties for the solution resonances, it was found that both the position and hyperfine splitting for these resonances

(15) R. L. Belford, private communication.

(16) J. H. Van Vleck, *Phys. Rev.*, **74**, 1168 (1948).

(17) D. M. S. Bagguley and J. H. E. Griffiths, *Proc. Phys. Soc. (London)*, **A65**, 594 (1952).

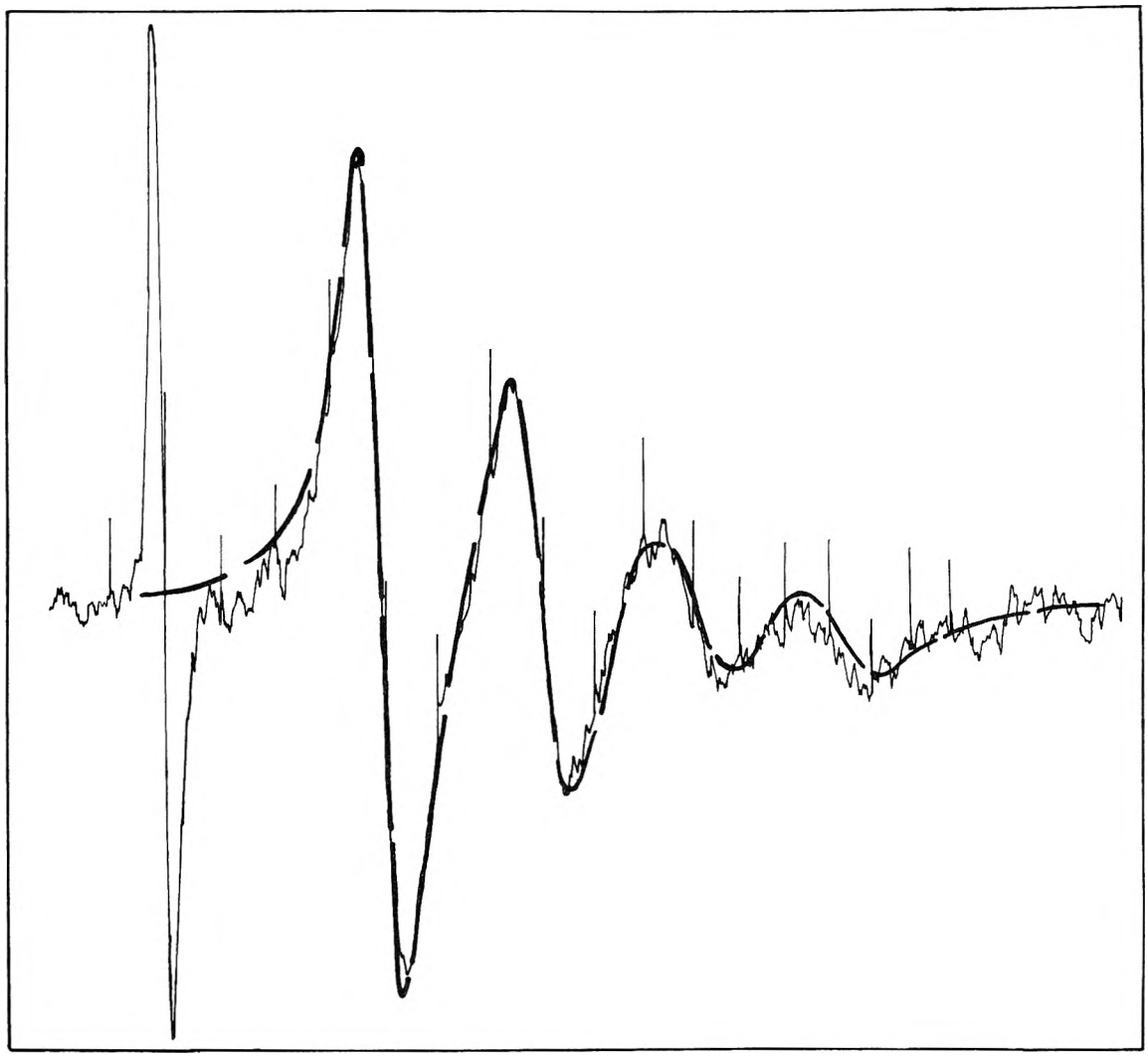

Fig. 2.—Plot of the derivative of the absorption curve for a 0.01 molar solution of copper(II) acetylacetonate in dioxane. The sharp peak on the left is from the reference free radical and the heavy dashed line is a fitted curve constructed from four equally spaced Lorentzian curves of equal area but different widths.

are influenced by some of the solvents employed. The results for all solutions measured are collected in Table I and the effect of solvent upon both the center g and the splitting δH (in gauss) for the resonances of copper acetylacetonate and copper 3-ethylacetylacetonate are given in Fig. 4. The results given in Table I are the average of measurements made on from three to five separate plots of the resonance. For the solvent mixtures, N_s is the mole fraction for the solvents dioxane, chloroform or pyridine. Pyridine and dioxane have a large influence on the resonance while chloroform has very little influence. These three solvents, however, all interact with the solute as evidenced by the increased solubility in these solvents. The larger influence of pyridine and dioxane upon the resonance probably results from the fact that these two solvents interact with the solute by forming weak complexes in which the nitrogen or oxygen is attached to the copper atom while chloroform probably interacts by formation of hydrogen bonds with the oxygens in the solute and will have, therefore, little influence upon the unpaired electron on the copper atom. The stronger interaction of pyridine with the solute over that of dioxane is indicated both by the greater changes in the resonance and in the much greater solubility in pyridine.

In considering these changes from the standpoint of the molecular orbital theory of Stevens[6] and Owen,[7] it is convenient to consider the effect of the solvent molecule as equivalent to that of a small negative charge placed along the z-axis. The change in g is then the result of changes in the energy terms in equations 9 and 10 caused by the presence of the electric field from the negative charge on the z-axis. For the tetragonal field from the molecule itself, there will be four energy levels with the $\sigma^*_{x^2-y^2}$ state the lowest and the $\sigma^*_{3z^2-r^2}$ somewhat above it. The π^*_{xy} and (π^*_{xz}, π^*_{yz}) states will be higher in energy and not too far apart if the tetragonal field is not too far from a cubic field. The doublet (π^*_{xz}, π^*_{yz}) state will have the higher energy of the two. The cylindrically symmetric field from a negative charge on the z-axis will affect the energy of the $\sigma^*_{x^2-y^2}$ and π^*_{xy} levels to the same extent since $d_{x^2-y^2}$ can be converted into d_{xy} by a 45° rotation about the z-axis. Further the (π^*_{xz}, π^*_{yz}) state remains degenerate and will ap-

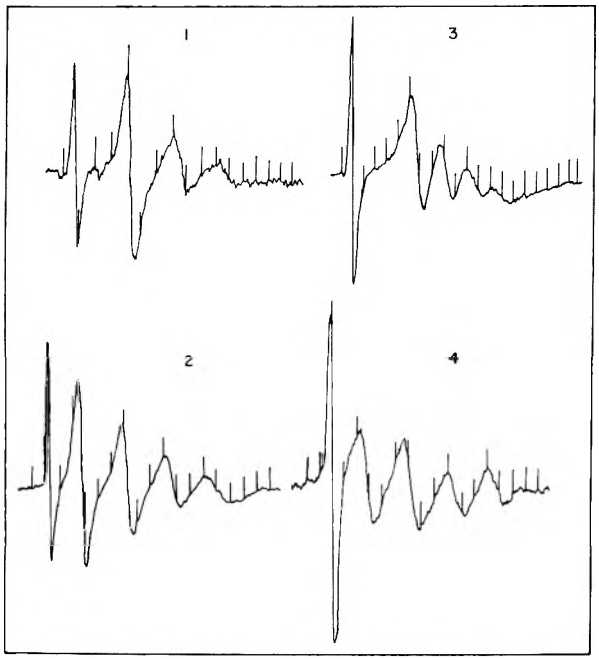

Fig. 3.—Typical recorder plots. The first sharp peak on left is from the reference free radical: 1, copper(II) 3-ethylacetylacetonate in dioxane; 2, copper(II) 3-ethylacetylacetonate in toluene; 3, copper(II) acetylacetonate in pyridine; 4, copper(II) acetylacetonate in toluene.

proach the π^*_{xy} state since the additional negative charge along the z-axis will have the effect of making the tetragonal field surrounding the copper more nearly cubic and in the cubic field both of these lev-

TABLE I

N_3	g_1	g_2	g_3	g_4	g(center)
Cu(II) acetylacetonate in dioxane + toluene					
1.00	2.0638	2.113	2.162	2.214	2.138
0.84	2.0627	2.112	2.165	2.212	2.139
.66	2.0630	2.113	2.162	2.210	2.138
.46	2.0611	2.110	2.164	2.216	2.137
.24	2.0559	2.109	2.159	2.208	2.134
.08	2.0519	2.104	2.155	2.208	2.130
.00	2.0437	2.0981	2.153	2.209	2.125
In chloroform + toluene					
1.00	2.0456	2.100	2.154	2.208	2.127
0.57	2.0450	2.0969	2.157	...	2.127
.36	2.0442	2.0962	2.152	2.209	2.124
.14	2.0429	2.0961	2.152	2.211	2.124
In chloroform + carbon tetrachloride					
0.19	2.0442	2.0986	2.154	2.209	2.126
In pyridine					
	2.0929	2.129	2.169	...	2.149
Cu(II) 3-ethylacetylacetonate in dioxane + toluene					
1.00	2.0575	2.108	2.159	...	2.134
0.67	2.0552	2.106	2.157	...	2.132
.48	2.0532	2.105	2.157	...	2.131
.27	2.0509	2.103	2.154	...	2.129
.00	2.0408	2.0935	2.152	2.208	2.123
Cu(II) ethylacetoacetate in dioxane					
	2.0897	2.129	2.168	...	2.149
Cu(II) salicylaldehyde methylimine in xylene					
	2.0317	2.0848	2.142	2.192	2.113

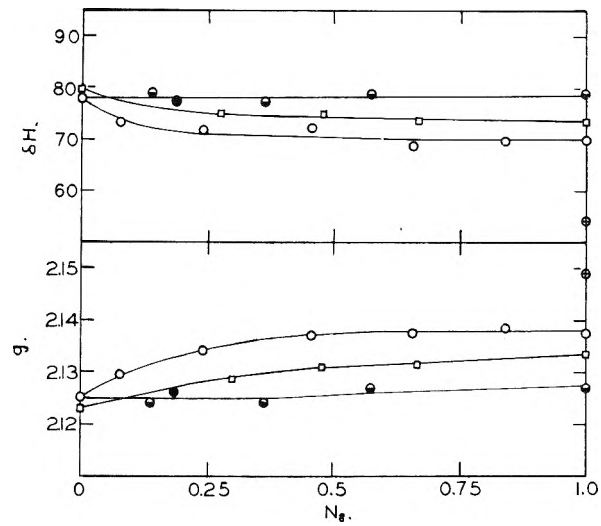

Fig. 4.—Dependence of gyromagnetic ratio g and hyperfine splitting δH (in gauss) upon solvent. The circles are for copper(II) acetylacetonate in various solvent mixtures; the open circles are for mixtures of toluene and dioxane, the half filled circles are for mixtures of toluene and chloroform, the filled circle is for a mixture of carbon tetrachloride and chloroform, and the circle with the cross is for a solution in pyridine. The squares are for copper(II) 3-ethylacetylacetonate in a toluene–dioxane mixture. N_3 is the mole fraction for the solvents dioxane, chloroform and pyridine.

els are degenerate. From the above arguments then it would be expected that ΔE_{xy} would remain constant in different solvents and that ΔE_{xz} would become smaller as the solvating interaction with copper increases and this will in turn cause $g_\parallel$ to remain constant and $g_\perp$ to increase in value. In solution, g is given by

$$g^2 = \frac{1}{3} g_\parallel^2 + \frac{2}{3} g_\perp^2 \qquad (12)$$

so we see that g should increase as the solvating interaction with copper increases which is just what is observed. Further confirmation of this theory has been obtained by R. L. Belford[15] in the absorption spectra of these solutions. He found that for solutions of both copper acetylacetonate and copper 3-ethylacetylacetonate the optical absorption band consisted of two bands one of which was constant at about 15,000 cm.$^{-1}$ while the other band had frequencies of about 19,000, 18,000 and 16,000 cm.$^{-1}$ in toluene, dioxane and pyridine, respectively. The constant band at 15,000 cm.$^{-1}$ can be identified with ΔE_{xy} and the variable top band with ΔE_{xz}.

The hyperfine splitting due to the anisotropic terms are "averaged out" in solution so that the observed splitting is due only to the isotropic term which according to Abragam and Pryce[18] is proportional to the square of the electron's wave function at the nucleus. The variation of the splitting with solvent thus indicates that the stronger the solvated complex the smaller the value of the unpaired electron's wave function at the nucleus. Apparently the bonding solvent pulls the electron away from the copper.

The asymmetrical shape of the resonance curves may be connected with the existence of several spe-

(18) A. Abragam and M. H. L. Pryce, *Proc. Roy. Soc.* (*London*), **206**, 164 (1951).

cies in the solution, but the behavior of the resonance precludes the possibility that it results from the superposition of two resonance curves with different hyperfine splittings and intensities. The existence of one curve for several species must mean that they are exchanging among themselves so rapidly that only one "average resonance" is observed. The frequency of exchange for which this would occur is so rapid, approximately 10^8 cycles/sec., that we cannot expect the actual frequency to be much greater, and this suggests the possibility that the shape may result from the exchange frequency being in the transition range between the case where there are separate resonances for each species and the case where a single "average resonance" is observed for all species. This would give the sort of curve obtained if the species had differing g's and hyperfine splittings. We would need at least three species in the solutions made up with a mixture of solvents in order to explain the observed behavior, otherwise we would expect to see a completely symmetrical line in toluene solutions. If the above explanation is true we should expect the shape of the line to be sensitive to frequency, since the critical frequency for the transition region is proportional to the resonance frequency. To check this, attempts were made to measure the resonance of a copper acetylacetonate solution at 300 megacycles and at 28,000 megacycles. The line is too broad for detection at 300 megacycles but at 28,000 megacycles the resonance was found to be a single broad line with no hyperfine structure but with an asymmetrical tail on the high g side of the line. This would seem to show that the exchange frequency was not much greater than the critical frequency at 3 cm. and would therefore lend support to the above explanation for the different line widths in the hyperfine lines.

Acknowledgments.—I should like to thank Professor M. Calvin who kindly furnished the compounds used in this research and Mr. R. L. Belford who purified the compounds and made up some of the solutions which were used. I would also like to thank Mrs. Dauben who did the X-ray analysis upon the single crystals and Professor A. Kip who made the measurements at 1 cm.

DIFFUSION OF WATER INTO UNCOATED CELLOPHANE. I. FROM RATES OF WATER VAPOR ADSORPTION, AND LIQUID WATER ABSORPTION[1]

BY ALFRED J. STAMM

Forest Products Laboratory,[2] Forest Service, U. S. Department of Agriculture, Madison, Wisconsin

Received June 20, 1955

The rates of liquid water absorption and swelling, and the rates of water vapor adsorption and swelling at 84% relative vapor pressure and different temperatures were measured on uncoated regenerated cellulose films of two thicknesses. All of the data give linear property changes when plotted against the square root of time up to two-thirds of the final change. The square of the property changes per unit of time increase with an increase in temperature as the vapor pressure of water and approximately as the diffusion constant. Diffusion constants calculated by conventional methods and by assuming the moisture gradient across the film to be parabolic are in good agreement. The calculated activation energies are about equal to the heat of swelling plus the heat of condensation. The diffusion of both water vapor and liquid water into regenerated cellulose film can be considered a bound water diffusion under a parabolic moisture gradient. The rate of diffusion at different temperatures is, however, controlled by the rate of molecular impact on the surface (that is, the vapor pressure of the water).

Introduction

Regenerated cellulose films such as Cellophane are used chiefly in the coated form to take advantage of their increased water resistance. It is hence natural that most diffusion studies have been made on coated films. Such measurements, however, give no information on the mechanism of the entrance or passage of water through the cellulose itself. It is hence the object of this research to investigate the takeup and movement of water within uncoated regenerated cellulose film together with the accompanying swelling under both absorption and adsorption conditions with the hope of obtaining information on the mechanism.

(1) Paper presented at the symposium on "Regenerated Cellulose Film" sponsored by the Divisions of Cellulose, Colloid, and Polymer Chemistry, 125th National Meeting of the American Chemical Society, Kansas City, Mo., March 30, 1954.

(2) Maintained at Madison, Wis., in cooperation with the University of Wisconsin.

Previous Findings

Salsburg[3] and Bateman, Hohf and Stamm[4] have investigated the rate of unidirectional drying of wood. They obtained a linear relationship between the amount of water vapor lost and the square root of time that persisted until a significant amount of moisture was lost from the bottom of the mercury-sealed specimens. Long and associates[5–7] have recently shown that the same relationship holds for both adsorption and desorption of benzene and acetone by polyvinyl acetate film and hydrocarbons by polyisobutylene film at 30° and above (above the second-order transition temperature).

(3) H. K. Salsburg, Thesis M.S. degree, Univ. of Wisconsin, 1929.

(4) E. Bateman, J. P. Hohf and A. J. Stamm, *Ind. Eng. Chem.*, **31**, 1150 (1939).

(5) R. J. Kokes and F. A. Long, *J. Am. Chem. Soc.*, **75**, 6142 (1953).

(6) R. J. Kokes, F. A. Long and J. L. Hoard, *J. Chem. Phys.*, **20**, 1711 (1952).

(7) S. Prager and F. A. Long, *J. Am. Chem. Soc.*, **73**, 4072 (1951).

Stamm[8] has shown that the relationship also holds for absorption of liquid water by small blocks of wood in the fiber direction.

Long and associates[5-7] have shown that a linear relationship between weight change and square root of time would be theoretically expected from Boltzmann's solution of Fick's general diffusion equation on the basis of the material being an "infinite solid," the surface of which instantaneously attains the equilibrium conditions. This solution would be expected to hold up to a point where the concentration at the center of the specimen changes significantly.

Long and associates[7] have developed the equation

$$\bar{D} = \frac{\pi a^2}{32}\left(\frac{E_a^2 + E_d^2}{t}\right) \qquad (1)$$

in which $\bar{D}$ is the average integral diffusion constant for adsorption and desorption, a is the thickness of the film, E_a is the fraction of the gainable liquid content under adsorption conditions, and E_d is the fraction of evaporable liquid under desorption conditions at time, t.

Sherwood and Comings[9] have modified the expansion form of Newman's diffusion equation for desorption by dropping all but the first term.

$$D_d = -\frac{a^2}{\pi^2}\frac{\mathrm{d}\ln E_d}{\mathrm{d}t} \qquad (2)$$

in which the symbols have the same significance as in equation 1. They have shown that this equation holds quite well for a number of systems except for the initial periods of time.

Tuttle[10] has calculated the diffusion constant for the drying of wood and Tiselius[11] the diffusion constant for the adsorption of water vapor by zeolites from moisture–distribution data using the equation

$$D = -\frac{(fa/2)^2}{4x^2 t} \qquad (3)$$

in which a is the film thickness, f is the fraction of the distance from the surface to the center of the film at which the differential moisture content, expressed as a fraction of the gainable moisture for adsorption, is E_a and as a fraction of the evaporable moisture for desorption is E_d, and x is a function of both E_a and E_d in the probability integral.

$$E_d = 1 - E_a = \frac{2}{\sqrt{\pi}}\int_0^x e^{-x^2}\,\mathrm{d}x \qquad (4)$$

Tuttle[10] and other investigators at the Forest Products Laboratory have shown that experimental moisture gradients for the drying of wood fall very close to true parabolas.

Materials Used.—Uncoated film material was used exclusively in this research. Most of the measurements were made on a thick grade of regenerated cellulose film (ovendry thickness 4.5 mils) used for sausage casings[12] that contained about 25% of glycerine plasticizer on the basis of the dry weight of the cellulose. The thick material was preferred because of the slower rate of swelling and diffusion, and the greater attainable accuracy in measuring changes in thickness. A limited amount of data was obtained with 600-gage Cellophane (ovendry thickness 1.4 mils) containing about 15% of glycerine on the basis of the dry weight of the cellulose.

Experimental Procedure.—The specific gravity of the films was determined on small strips 0.2 by 1.0 cm. They were oven-dried at 105° for 2 hours. The measurements were made by suspending them in mixtures of toluene and carbon tetrachloride. The concentration at 15° was adjusted so that the strips neither sank or rose. The specific gravity of the equilibrium mixture was determined with calibrated short-range hydrometers. Measurements were made on both unextracted and extracted film. The extraction of glycerine was carried out by soaking the strips in a large volume of distilled water for 18 and 48 hours. No measurable difference in specific gravity between the two soaking times was obtained.

The rate of liquid water absorption measurements were made on squares of the film 9 cm. on a side. The squares were oven-dried for 2 hours at 105°, weighed in a flat wide-mouth weighing bottle, and brought to test temperature by placing the bottle in a tray of distilled water in which the specimens were later immersed (1 cm. deep) for various lengths of time. Upon immersion the specimens were rapidly rubbed with a rubber finger cot to displace adsorbed air. They were then rapidly blotted three times between fresh pieces of absorbent paper and weighed. Madras, McIntosh and Mason[13] have shown that this blotting technique does not remove all surface water when the takeup is above the fiber saturation point. By using exactly the same technique on each square, it is nevertheless felt that the error is small and relative.

The rate of swelling in liquid water in the thickness direction was measured with a dial gage with a circular contact area of approximately 1 cm.^{2}. This was mounted over a crystallizing dish so that it was centered over a flat disk of the same size sealed to the bottom of the dish. The specimens were oven-dried and brought to the measuring temperature in a tray of water in the same way as the water absorption specimens. The dry thickness of the film was measured without water in the gage dish. Water at the correct temperature was quickly poured into the crystallizing dish to immerse the specimen. The gage pressure was instantly released from the specimen and brought down for as brief a time as possible to get the succeeding thickness readings at various intervals of time. This procedure worked well for the thicker films and the lower temperatures. At the higher rates of swelling, the gage pressure was on the specimens enough of the time to slightly retard the swelling. In these cases, new specimens were used for each measurement.

The rate of swelling in liquid water in the sheet directions was obtained by merely measuring the change in length of strips 15 cm. long with a steel scale to 0.02 centimeter while they were immersed 1 cm. deep in a tray of water.

The rate of water vapor adsorption and swelling measurements were made in humidity rooms at 4.5 and 26.7°. Both rooms were controlled at 84.0 ± 0.5% relative humidity as indicated by an electrical resistance hygrometer. Films were suspended in front of an electric fan. They were momentarily removed from the air stream for weighing and measuring the thickness with the dial gage.

Rate of Liquid Water Absorption and Swelling.—Figure 1 gives the rate of weight increase and Fig. 2 gives the rate of swelling in thickness directions under liquid absorption conditions for both the sausage-casing film and the Cellophane plotted against the square root of time. Figure 3 gives the swelling in the sheet direction of sausage-casing film. All three figures give the characteristic linear relationship previously found for both adsorption and absorption over the initial range. The weight increase data, but not the swelling data, are in keeping with data for wood.[8] The swelling of wood initially lags behind the water absorption because the water taken up first by the coarse capillary

(8) A. J. Stamm, *Pulp Paper Mag. Canada*, **54**, [2] 54 (1953).

(9) T. K. Sherwood and E. W. Comings, "Vsessayuznovo Teplotechnishces, Kovo Inst.," H 8, Aug. (1935).

(10) F. J. Tuttle, *J. Franklin Inst.*, **200**, 609 (1925).

(11) A. Tiselius, *Z. physik. Chem.*, **A169**, 425 (1934).

(12) These were kindly furnished by the Visking Corporation, Chicago, Ill.

(13) S. Madras, R. L. McIntosh and G. S. Mason, *Can. J. Research*, **27B**, [9] 764 (1949).

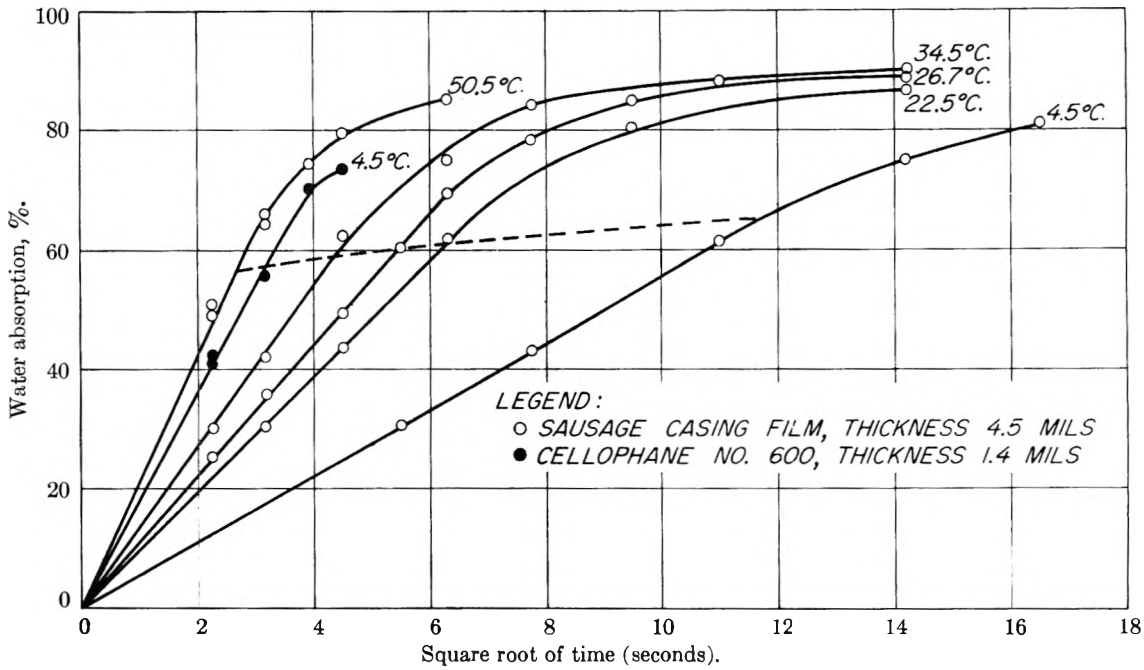

Fig. 1.—Fate of liquid–water absorption by uncoated, glycerine-plasticized, regenerated cellulose films at several different temperatures. Dashed lines are drawn at two-thirds of equilibrium adsorption for the thicker film.

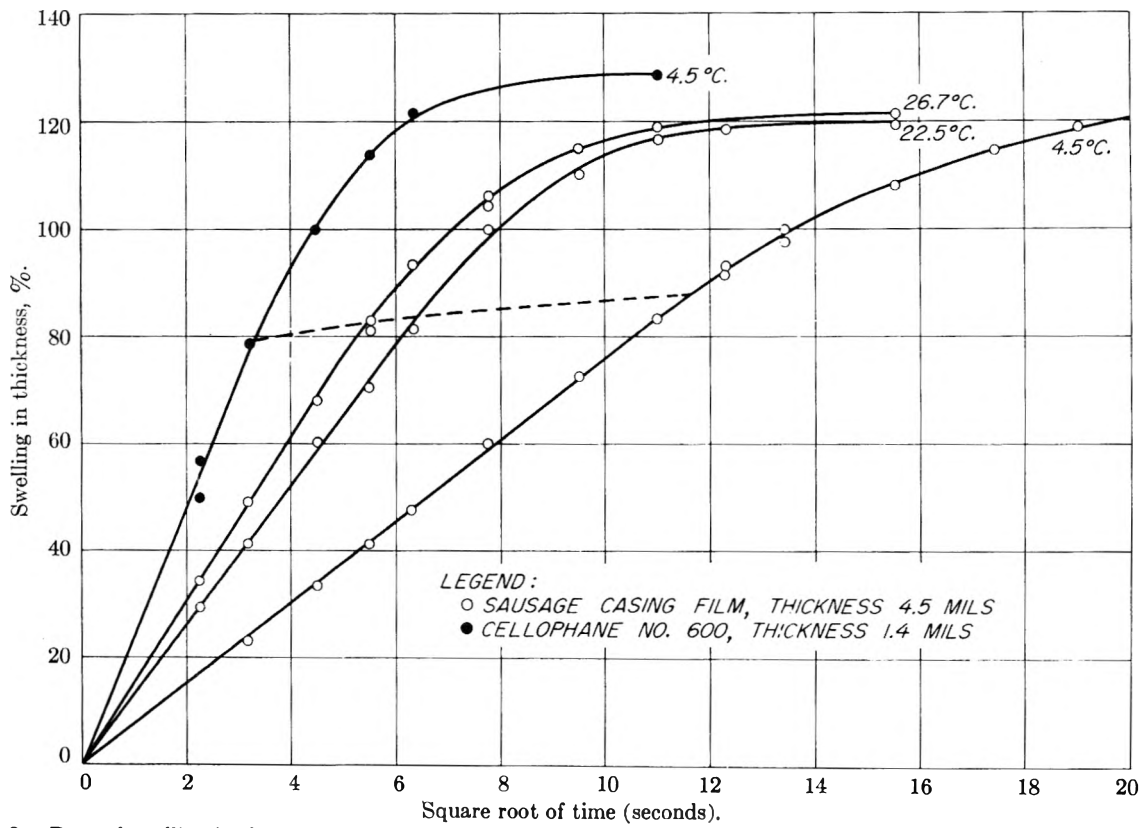

Fig. 2.—Rate of swelling in thickness of uncoated, glycerine-plasticized, regenerated cellulose film in liquid water at several different temperatures. Dashed lines are drawn at two-thirds of equilibrium swelling for the thicker film.

structure has to diffuse into the cell walls before it causes swelling. Because of this, the linear portion of the plot for the rate of swelling of wood does not extrapolate through the origin. The fact that it does for regenerated celloluse film is a further indication that the void volume of regenerated cellulose film must be extremely small.

Dashed lines are drawn in both Figs. 1 and 2 at two-thirds of the equilibrium absorption and swelling for the thicker films. The points of intersection correspond closely to the limit of the linear relationship for the thicker films. This will be referred to again later.

The slopes of the water absorption–square root

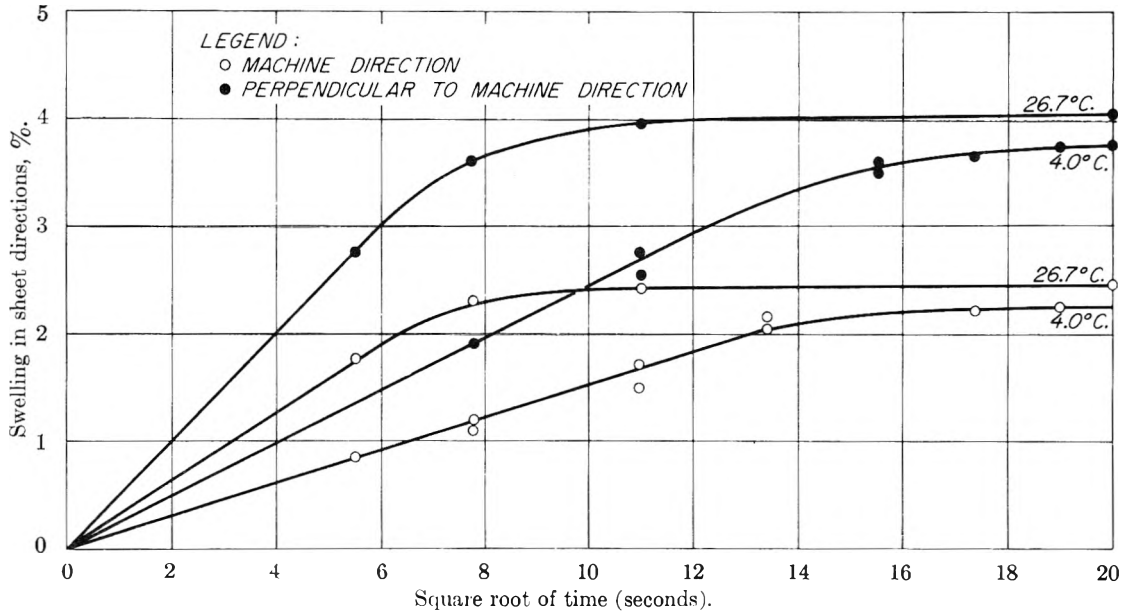

Fig. 3.—Rate of swelling in the sheet direction of glycerine-plasticized, regenerated cellulose sausage-casing film in liquid water at two different temperatures.

of time lines of Fig. 1 and the swelling–square root of time lines of Fig. 2 increase with an increase in temperature and with a decrease in thickness. According to equation 1 the rate of diffusion at constant temperature will vary as E^2/t or as the square of the slopes $(M_c/\sqrt{t})^2$ for moisture absorption and $(S/\sqrt{t})^2$ for swelling where M_c represents moisture content and S represents swelling, and inversely as the square of the thickness. The ratio of the square of slopes for the thin to the thick film for the weight increase data at 4.5° is 10.2 and for the swelling data, 10.3. The reciprocal of the squares of the ratios of the thickness of the thin film to the thickness of the thick film is 10.3. The agreement with theory is thus very good.

Table I gives the slopes of the straight lines of Figs. 1 and 2 and the ratio of the slopes squared for a series of pairs of values at different temperatures. These ratios are virtually the same for both the water absorption and the swelling data and practically the same as the ratio of the vapor pressures and the ratio of the differential diffusion constants. The differential diffusion constants were calculated from the equation

$$dD_a = \frac{\pi a^2}{16} \frac{d[(1 + S)E_a]^2}{dt} \qquad (5)$$

which is the differential form of equation 1 for adsorption conditions taking into account the fractional swelling S. The calculations were made by plotting $[(1 + S)E]^2$ against t and using the slope of the curve at time t when $E_a = 0.333$. If the calculations had been made at constant moisture content rather than constant fractional attainable moisture content, the ratios of the diffusion constants would have been the same as the ratios of the slopes squared (columns 3 and 5 in Table I).

Rate of Water Vapor Adsorption and Swelling.—Figure 4 gives the water vapor adsorption and swelling in the thickness direction at 84.0 ± 0.5% relative humidity and two temperatures for regenerated sausage-casing film plotted against the square root of time. The linear relationship extends to two-thirds of the saturation values, the same as for liquid water absorption. Absorption and desorption data of Long and associates[5–7] also give the linear relationship up to about the same fraction of saturation.

Table II gives the slopes and the ratio of the slopes squared for the linear portions of both the

TABLE I

RELATIVE RATES OF LIQUID WATER ABSORPTION INTO REGENERATED CELLULOSE SAUSAGE-CASING FILMS, 4.5 MILS OVEN-DRY THICKNESS, AT DIFFERENT TEMPERATURES, COMPARED WITH THE RATIOS OF THE RESPECTIVE VAPOR PRESSURES OF WATER AND THE CALCULATED DIFFERENTIAL DIFFUSION CONSTANTS AT $E_a = 0.333$

Temp., °C.	Slopes $(M_c/\sqrt{t})$, [a] sec.$^{-1/2}$	Ratio slopes squared [b]	Slopes $(S/\sqrt{t})$, [c] sec.$^{-1/2}$	Ratio slopes squared [b]	Ratio vapor pressures [b]	Calcd. differential diffusion constant × 10^8, cm.^{2}/sec.	Ratio[2] of diffusion constants
50.5	21.0		..			385.0	
		2.43		..	2.31		2.75
34.5	13.5		..			140.0	
		1.50		..	1.56		1.59
26.7	11.0		15.2			88.0	
		1.28		1.33	1.28		1.33
22.5	9.7		13.2			66.0	
		3.06		3.10	3.24		3.20
4.5	5.55		7.5			20.6	
50.5	21.0		..			385.0	
		14.3		..	15.0		18.7
4.5	5.55		..			20.6	
26.7	11.0		15.2			88.0	
		3.9		4.1	4.2		4.3
4.5	5.55		7.5			20.6	

[a] Moisture content–square root of time relationships. [b] Ratios for preceding to succeeding temperatures. [c] Swelling in the thickness direction–square root of time relationships.

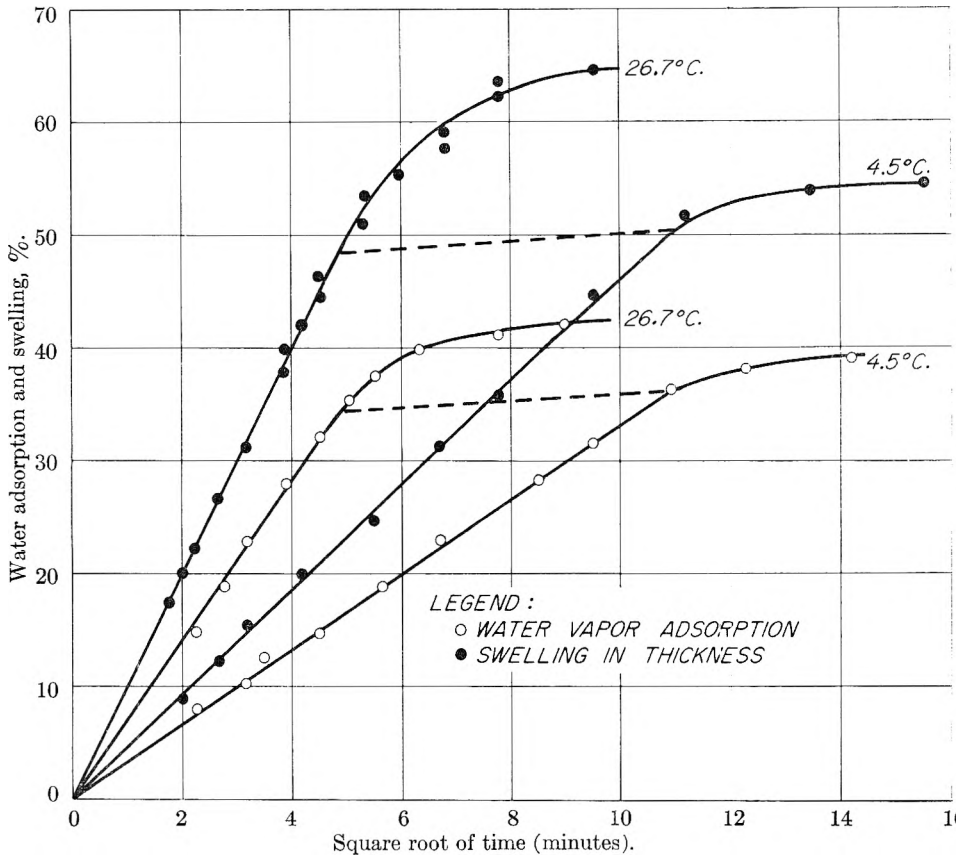

Fig. 4.—Rate of water vapor adsorption and swelling in thickness of glycerine-plasticized, regenerated cellulose sausage-casing film at 84.0% relative humidity and two different temperatures. Dashed lines are drawn at two-thirds of the equilibrium adsorption and swelling.

weight increase and swelling data of Fig. 4. These two ratios are practically the same and nearly equal to the ratios of the vapor pressures and not greatly different from the ratio of the diffusion constants calculated from equation 5 at $E_a = 0.333$.

TABLE II

RELATIVE RATES OF WATER VAPOR ADSORPTION BY REGENERATED CELLULOSE SAUSAGE-CASING FILMS, 4.5 MILS OVEN-DRY THICKNESS, AT 84.0% RELATIVE HUMIDITY AND 2 DIFFERENT TEMPERATURES, COMPARED WITH THE RATIOS OF THE RESPECTIVE VAPOR PRESSURES OF WATER AND THE CALCULATED DIFFERENTIAL DIFFUSION CONSTANTS AT $E_a = 0.333$

Temp., °C.	Slopes $(Mc/\sqrt{t})$,[a] min.$^{-1/2}$	Ratio slopes squared[b]	Slopes $(S/\sqrt{t})$,[c] min.$^{-1/2}$	Ratio slopes squared[b]	Ratio vapor pressures[b]	Calcd. differential diffusion constant × 10^8, cm.^{2}/sec.	Ratio of diffusion constants
26.7	7.00		10.0			1.49	
		4.38		4.33	4.16		4.97
4.5	3.35		4.8			0.30	

[a] Moisture content–square root of time relationship. [b] Ratios for preceding to succeeding temperatures. [c] Swelling in thickness direction–square root of time relationship.

Equation 2 was put into differential form taking into account the variation due to swelling, S

$$dD_a = -\frac{a_0^2}{\pi^2}\frac{d[(1+S)\ln(1-E_a)]}{dt} \qquad (6)$$

where a_0 is the oven-dry thickness of the film. The differential diffusion constant was determined by plotting $(1 + S) \ln (1 - E_a)$ against t and using the slope at $E_a = 0.333$. This gave practically the same values listed in Table II that were obtained with equation 5.

In order to apply equations 3 and 4, it is first necessary to investigate the nature of the moisture gradients set up in the moisture adsorption process.

Effect of Moisture Gradients.—Figure 5 gives a series of parabolic moisture distribution curves that have been shown to conform closely to experimental moisture distribution curves for wood.[10] The moisture content limits are at first fixed, with the distance increasing until moisture is lost from the center of the specimen in desorption. After this the distance becomes fixed and difference between the limits decreases.

The area under the curve XBY represents the amount of water retained under drying conditions when moisture just starts to be lost from the center of the specimen. This area XBYZ is equal to area XACZ, as the area of triangle XAB is equal to the area of BYC. The moisture content for a thin increment of thickness at the point B is thus numerically equal to the integral or average moisture content of the specimen. A similar situation can be shown to exist for adsorption where the area above the curve XBY is equal to the area AWYC. Moisture thus just reaches the center of the specimen under absorption conditions when the average fractional gainable moisture content E_a is 0.333. The equality of the differential and integral moisture

contents occurs at the fractional distance into the wood $f = 0.422$ for all of the distribution curves in which moisture change occurs over the total thickness ($E_a = (1 - f)^2$ for adsorption and $1 - E_d = (1 - f)^2$ for desorption). The author[14] has experimentally shown that the average moisture content of wood occurs at about 0.4 of the distance into the center after a moisture content change has just started to occur at the center in normal drying or adsorbing.

It thus is possible to use equations 3 and 4 to calculate the differential diffusion constant at $E_a = 0.333$ where the average moisture content of the specimen is equal to the increment moisture content at 0.422 of the distance from the surface to the center of the specimen. This gave a value of 1.40×10^{-8} cm.²/sec. at 26.7° for the differential diffusion constant in contrast to 1.49×10^{-8} cm.²/sec. from equation 5 and 1.50×10^{-8} cm.²/sec. from equation 6. At 4.5° the corresponding values are 0.287×10^{-8}, 0.304×10^{-8} and 0.303×10^{-8} cm.²/sec. The slightly lower values calculated from equations 3 and 4 on the assumption that the moisture distribution follows a true parabola may be due to the moisture distributions differing slightly from true parabolas under the extreme swelling conditions. The agreement is sufficiently good, however, to indicate that the moisture distributions attained under adsorbing conditions are close to true parabolas.

Heat of Activation.—Heats of activation for the absorption of liquid water and for the adsorption of water vapor at 84% relative humidity were calculated from the diffusion constants. The former gave a value of 11,250 cal./mole, and the latter of 12,000 cal./mole. The values are not a great deal higher than the heat of condensation of water, 10,550 cal./mole. The heat of swelling of viscose in water is about 25 cal./g. of viscose,[15] or 1,280 cal./mole of water. This is approximately the amount by which the activation energies for diffusion into the films exceed the heat of condensation.

The heat of activation for the adsorption of water vapor by uncoated Cellophane calculated from the data of Church and Scroggie[16] is 10,400 cal./mole. This is only slightly less than the value for regenerated cellulose sausage-casing film calculated from the data of this research. It is of interest that the energies of activation for the adsorption of water vapor by Pliofilm (rubber hydrochloride), 13,000 cal./mole,[17] and by polyvinyl acetate, 15,000 cal./mole,[5] are of the same order of magnitude.

Supplementary Findings

Void Volume.—The specific gravity of both extracted sausage-casing film and 600-gage Cellophane were found to be the same within the range of experimental error, namely, 1.524 to 1.526. The unextracted sausage-casing film gave values of 1.478 to 1.482. The unextracted 600-gage Cellophane gave a value of 1.492.

(14) A. J. Stamm, *Ind. Eng. Chem., Anal. Ed.*, **2**, 240 (1930).

(15) W. H. Rees, *J. Text. Inst.*, **39**, T3 1 (1948).

(16) W. H. Church and A. G. Scroggie, *Paper Trade J.*, **101**, [14] 13 (1935).

(17) P. M. Doty, W. H. Aiken and H. M. Mark, *Ind. Eng. Chem., Anal. Ed.*, **16**, 686 (1944).

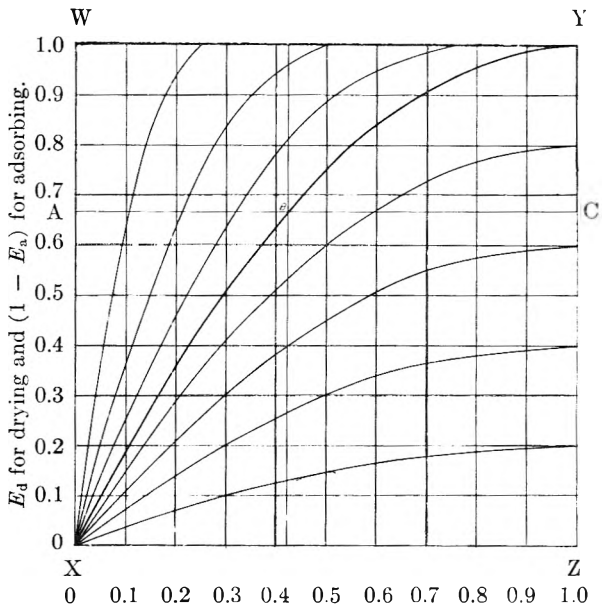

Fig. 5.—Theoretical parabolic moisture-distribution curves in which the moisture content is expressed in terms of the fraction of the original uniformly distributed evaporable water, E_d, for desorption and the fraction of the final uniform gainable water, E_a, for adsorption.

Hermans[18] has calculated from crystal structure data for cellulose II that crystalline regenerated cellulose should have a specific volume of 0.628. The experimental specific volume is 0.656, or 4.3% greater. According to this, over-dry plasticizer-free, regenerated cellulose has only the small void volume of 4.3% in the amorphous regions. The lower specific gravity of glycerine-plasticized film results from the fact that glycerine, with the lower specific gravity of 1.264 at 15°, has roughly added its volume to the volume of the film. The calculated specific volume, on the basis of the mixture law, for the 600-gage Cellophane containing 15% of glycerine is 0.674, and for the sausage-casing film containing 25% of glycerine is 0.683. The experimental values are somewhat lower, namely, 0.670 and 0.676, respectively. This is due to the fact that part of the glycerine enters the void volume without adding its volume to that of the film, and also because of compressive adsorption.[19]

The small void volume of dry regenerated cellulose film, combined with the fact that the permeability to non-swelling gases is extremely small,[20] indicates that these voids are not continuous and probably of molecular dimensions. Because of this, only an insignificant part of the passage of water through regenerated cellulose film can be through existing void structure. The movement of water through the film must thus be almost entirely through created structure as bound water and not as capillary condensed water.

Anisotropy of Films.—Liquid water is rapidly absorbed by uncoated cellulose film, causing an appreciable swelling. The equilibrium swelling of the plasticized sausage-casing film with an oven-dry

(18) P. H. Hermans, "Contributions to the Physics of Cellulose Fibers," Elsevier Publishing Co., New York, N. Y., 1946.

(19) A. J. Stamm, *Text. Research J.*, **20**, [9] 631 (1950).

(20) D. W. Davis, *Paper Trade J.*, **123**, [9] 33 (1946).

thickness of 4.5 mils (thousandths of an inch) was 127% (120% in 2 minutes) at 26.7° in the thickness direction. The swelling in the sheet directions was far less, being only 2.5% in the machine direction and 4% at right angles to the machine direction. Plasticized 600-gage Cellophane, with an oven-dry thickness of 1.4 mils, swelled 119% in thickness, 1.6% in the machine direction, and 12.1% at right angles to the machine direction. The far greater swelling in the thickness direction than in the sheet directions in both cases indicates a highly preferred orientation of the cellulose chains in the plane of the sheets. Although the swellings in the sheet directions of the two forms of regenerated cellulose films are quite different, the volumetric swelling, as approximated by the sum of the swelling in the three structural directions, is practically identical. In the case of the 600-gage Cellophane, there must be a considerable further preferred orientation in the machine direction. The large difference in swelling in the two sheet directions in the case of 600-gage Cellophane is due to the fact that the sheet is subjected to a tensile stress in forming and drying in the machine direction, but not at right angles to the machine direction. In the case of sausage-casing film, the material is cast and dried under circumferential well as longitudinal restraint.

Conclusions

Several important conclusions can be drawn from the findings of this research.

(1) The void volume of oven-dry regenerated cellulose film (both plasticized and unplasticized) is extremely small. This rules out the possibility of the passage of water through the film being a capillary movement.

(2) Both the rate of liquid water absorption and water vapor adsorption by regenerated cellulose films (at constant moisture content but different temperatures) vary as the vapor pressures of water.

(3) The corresponding rates of swelling vary in the same way. Unlike porous wood, the swelling does not lag behind the water absorption. This would be expected in the absence of capillary condensation.

(4) The takeup of water in the surface lamina of the film materials by vapor adsorption must be controlled by the frequency of impact of the surface by water molecules, as the frequency of impact is a function of the vapor pressure. This must also be true for absorption of water from the liquid phase. It appears that even at an air-free water–cellulose film interface, the penetration of the film must be by the more energetic water molecules leaving the liquid one at a time as in vaporization. This is not surprising for a material such as the regenerated cellulose film in which the only void capillaries are of molecular size. These cannot be penetrated by bulk water. Evidently the same increasing energy of the water with increasing temperature that leads to vaporization also leads to increased film penetration. It is thus possible for molecular penetration to be from the liquid phase and proportional to an energy factor, which in turn is proportional to vapor pressure.

(5) On the basis of a parabolic moisture distribution through the thickness of a film, as is the case for wood, the differential moisture content under specific conditions can be related to the average moisture content. When moisture just begins to be lost or gained at the center of the film, the differential moisture content at 0.422 of the distance from the surface to the center of the film corresponds to an average moisture content of two-thirds of the evaporable or one-third of the gainable moisture.

(6) Differential diffusion constants calculated on the basis of the findings under (5) are in quite good agreement with values calculated by methods that do not involve the moisture distribution, thus indicating that the moisture distribution must be close to parabolic.

(7) The energies of activation calculated from the differential diffusion constants are greater than the heat of condensation of water by an amount expected from the heat of swelling.

(8) Although the diffusion of water into regenerated cellulose film is activated at different temperatures by an energy factor practically proportional to the vapor pressure of water, the diffusion can be considered a bound water diffusion under a parabolic moisture content gradient.

DIFFUSION OF WATER INTO UNCOATED CELLOPHANE. II. FROM STEADY-STATE DIFFUSION MEASUREMENTS[1]

BY ALFRED J. STAMM

Forest Products Laboratory,[2] Forest Service, U. S. Department of Agriculture, Madison, Wisconsin

Received June 20, 1955

Measurements were made of the diffusion of water through uncoated regenerated cellulose sausage casing films at two different temperatures by the steady-state cup method with various relative humidity boundary conditions and with internal stirring. The need for internal stirring with permeable films is shown. Diffusion constants were calculated on the basis of linear vapor pressure gradients and parabolic bound-water gradients, the latter being experimentally justified. The diffusion constants on both bases increase exponentially with an increase in the fractional water volume. The data indicate that the diffusion is controlled by vapor pressure.

Introduction

The preceding article[3] gave experimental information on the diffusion of both liquid water and water vapor into uncoated regenerated cellulose film from rate of absorption and adsorption data. This paper gives data on the same system obtained by steady-state diffusion measurements in order to further elucidate the mechanism of the movement of water in these films.

Previous Findings

Steady-state diffusion measurements have usually been made by the cup method and modifications thereof.[4-12] The membrane is sealed over the top of a crystallizing dish containing water, a saturated salt solution, or desiccant. It is exposed to constant temperature and relative humidity conditions in an oven, humidity cabinet, or humidity room. The cups are weighed at suitable intervals to determine the loss or gain in weight per unit of time after equilibrium is attained.

In general, the test has been performed under adequate external circulation. Burr and the author[13] have shown the need for internal stirring when the permeability is high. They devised a simple internal magnetic stirrer that increased the rate of moisture passage through Cellophane by as much as 50%.

Steady-state diffusion is the simplest type of diffusion from the mathematical standpoint, as the boundary conditions are held constant throughout the measurement. After equilibrium is established, the rate of passage of the diffusing substance through the film becomes constant.

Most of the previous investigators have expressed their results in terms of permeabilities in grams of vapor passing through the films per 24 hours for arbitrarily chosen areas, thicknesses and relative humidity differences. The results are thus relative only for a fixed set of conditions.

The measurements may, however, be definitely expressed by the equation

$$D_{vp} = \frac{a}{A} \times \frac{m}{t} \times \frac{1}{(p_1 - p_2)} \qquad (1)$$

in which D_{vp} is the vapor pressure diffusion constant in grams per centimeter per second, m is the mass of liquid or vapor diffusing through the film in time, t, and p_1 and p_2 are the relative vapor pressures in equilibrium with the two surfaces of the film. Equation 1 may be modified to give a vapor diffusion constant D_{vc} in the conventional units of cm.^{2}/sec. by dividing by w the weight of water vapor per cubic centimeter of air, thus

$$D_{vc} = \frac{a}{A} \times \frac{m}{t} \times \frac{1}{(p_1 - p_2)w} \qquad (2)$$

This puts the equation on a vapor concentration rather than a vapor pressure basis.

Experimental Procedure.—The films used are the same as those described in the previous paper.[3] The steady-state diffusion measurements were made by the cup method using three crystallizing dishes (diameter, 8 cm.) with light aluminum flanges sealed to the upper rim. Films were sealed over the openings by bolting them between the flange and an aluminum ring with a rubber gasket on the flange side. The exposed effective area of the films was 50.2 cm.^{2}.

The internal stirrers were similar in principle to those previously described by Burr and the author.[13] They consisted of 1/2 inch lengths of 1-inch diameter thin-walled electrical conduit pipe sealed into two polyethylene bottle caps so as to form small sealed hollow drum floats. A small polyethylene vane was sealed upright on the top face of each to stir the air. These were floated on the liquid in the evaporating dish cups. The cups were placed on three turntables rotated at about 100 revolutions per minute. Permanent magnets placed near the periphery of the cups held the stirrer floats against the sides of the cups. The rotation of the cups caused the floats to rotate in place. Both the air and the liquid were thus stirred quite adequately. Air was also circulated over the outer face with an electric fan.

Measurements were made with one of the following liquids in the cups: concentrated sulfuric acid, giving a relative vapor pressure of practically zero; a saturated sodium nitrite solution, giving a relative vapor pressure of 0.635; a saturated sodium chloride solution, giving a relative vapor pressure of 0.758; or a saturated barium chloride solution, giving a relative vapor pressure of 0.895 at 28°, as checked with an electrical resistance hygrometer. In each case an excess of salt was present to maintain saturation. When water was used in the cups, it was found that condensation occurred on the membrane due to temperature fluctuations of about 0.2°. Hence, no data using water in the cups are recorded.

(1) Paper presented at the symposium on "Regenerated Cellulose Films" sponsored by the Divisions of Cellulose, Colloid, and Polymer Chemistry, 125th National Meeting of the American Chemical Society, Kansas City, Mo., March 30, 1954.

(2) Maintained at Madison, Wis., in cooperation with the University of Wisconsin.

(3) A. J. Stamm, THIS JOURNAL, **60**, 76 (1956).

(4) A. Abrams and J. G. Brabender, *Paper Trade J.*, **102**, TS204 (1936).

( ) A. Abrams and W. A. Chilson *ibid.*, **91**, [18] 175 (1930).

(6) Amer. Soc. Testing Materials, Tentative Method of Test, D895-47T (1947).

(7) Army-Navy Aeronautical Specification, AN-C-67, Dec. 11, 1942.

(8) (a) J. D. Babbitt, *Can. J. Research*, **20A**, 143 (1943). (b) R. M. Barrer, "Diffusion in and Through Solids," Cambridge Univ. Press, England, 1941.

(9) F. T. Carson, Bur. Standards Misc. Pub., M127 (1937).

(10) C. G. Weber, *Modern Packaging*, **16**, [3] 78, 82, 100 (1942).

(11) C. G. Weber, *Paper Trade J.*, **111**, T61 (1940); **118**, T37 (1944).

(12) Tech. Assoc. Pulp and Paper Ind., Standard T448m (1944).

(13) H. K. Burr and A. J. Stamm, *Ind. Eng. Chem., Anal. Ed.*, **13**, 655 (1941).

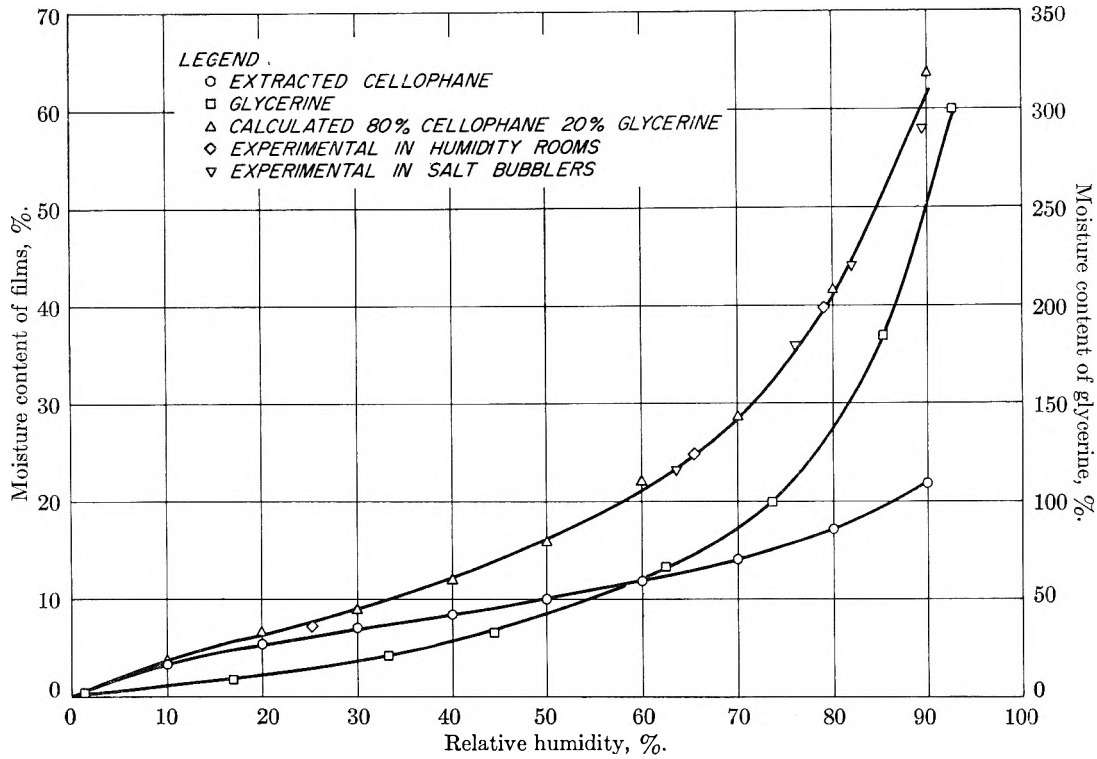

Fig. 1.—Adsorption isotherms for extracted Cellophane and glycerine at 25° and the calculated value for plastiticized film containing 25% of glycerine on the basis of the dry weight of the film, together with experimental values for the plasticized film determined in humidity rooms and in salt bubblers at 28°.

The steady-state condition was usually attained in 2 to 4 hours. However, with sulfuric acid in the cups and an outside relative vapor pressure of 0.255, it took between 8 and 10 hours to attain the steady-state condition. This is in keeping with Hermans'[14] finding with model viscose fibers that the rate of attainment of moisture equilibrium is quite slow at low moisture contents, as compared to higher moisture contents.

Runs were made over a 24- to 48-hour period. A few were made without a stirrer in one of the cups. The weight change per unit of time in each of these cases ranged from 10 to 50% lower than for the cups in which stirring was maintained. The error increased with an increase in the weight change per unit of time.

At the conclusion of a run, the membranes were cut from the surface of the cups with a razor blade, the equilibrium thickness was measured rapidly, and the specimens weighed and oven-dried to determine the equilibrium moisture content.

Moisture Content–Relative Vapor Pressure Relationships.—In order to check the calculations of the diffusion constants from the steady-state data on a moisture-content gradient basis, it was necessary to know the average equilibrium moisture content values at various relative vapor pressures. Figure 1 gives the data for glycerine-free Cellophane obtained by Urquhart, Bostock and Eckersoll[15] and data for glycerine taken from the International Critical Tables. The figure also gives data for sausage-casing film containing 25% of glycerine plasticizer per unit of dry weight of the cellulose, calculated from a combination of the data for the Cellophane and that for glycerine on the basis of the mixture law. A few experimental values are also given that were obtained by exposure in the humidity rooms and by conditioning over salt solutions. The relative humidities in each case were checked with an electrical resistance hygrometer. These experimental values agree quite well with the calculated values.

Steady-state Diffusion.—Table I gives the data for the steady-state measurements. The differential moisture contents at the surfaces of the film (on the cup and room sides) are those in equilibrium with the prevailing relative humidities. They were obtained from Fig. 1. The calculated average moisture contents were obtained by considering the moisture gradients through the films to be parabolic, as was found to be the case in the rate studies of the previous paper.[16] They are $^2/_3$ of the difference between the differential moisture contents at the two surfaces of the film plus the lower moisture content. This follows from the previous finding that the differential moisture content at $^2/_3$ of the evaporable moisture content, E_d, or $^1/_3$ of the gainable moisture content, E_a, is equal to the average moisture content.[16] The agreement of the calculated values with the experimental values is further confirmation that the moisture gradients are parabolic.

Because of the large variation in equilibrium film thickness with relative humidity, equation 2 should be put in a differential form

$$dD_{vc} = \frac{1}{Aw} \times \frac{m}{t} \times \frac{da}{dp} \qquad (3)$$

The symbols have the same significance as in equation 2. If the vapor pressure gradient through the thickness of the film is considered to be linear, as is

(14) P. H. Hermans, "Contributions to the Physics of Cellulose Fibers," Elsevier Publishing Co., New York, N. Y., 1946.

(15) A. R. Urquhart, W. Bostock and N. Eckersoll, *J. Text. Inst.*, **23** T135 (1932).

(16) A. J. Stamm, *Ind. Eng. Chem., Anal. Ed.*, **1**, 94 (1929).

TABLE I

STEADY-STATE DIFFUSION DATA FOR WATER VAPOR THROUGH UNCOATED REGENERATED CELLULOSE FILM AT 28° (OVEN-DRY THICKNESS 4.5 MILS)

Relative vapor pressure, %		Moisture content, %				Fractional			
Cup	Room	Cup side	Room side	Av. expt.	Av. calcd.	water vol.	m/t, g./hr.	$dD_w \times 10^8$, cm.²/sec.	$dD_{vc} \times 10^4$, cm.²/sec.
0	25.5	0	7.5	5.1	5.0	0.070	0.015	0.12	0.77
63.5	26.0	23.5	7.7	18.6	18.2	.216	.095	1.45	1.30
75.8	25.5	36.0	7.5	24.0	26.5	.262	.173	3.18	2.83
75.8	57.0	36.0	19.0	30.0	30.3	.305	.182	3.50	4.30
89.5	61.0	58.0	22.0	42.8	45.3	.386	.315	7.35	12.05
0	87.0	0	54.0	36.1	36.0	.348	.396	7.88	5.26
0	86.0	0	52.0	34.7	34.5	.338	.358	6.80	4.75
0	84.7	0	53.0	36.3	35.4	.350	.083[a]	1.59[a]	1.10[a]

[a] 4.5° instead of 28°.

usually the case, then dD_{vc} can be determined by using the slope of a plot of a against p at the average value of p in the calculations.

Values of dD_{vc} calculated in this way are plotted against the fractional moisture content in Fig. 2. The diffusion constant is shown to increase exponentially with an increase in the fractional water volume. This will be considered again later.

It is also possible to consider the movement of water through the films being activated by a moisture content gradient through the films as well as considering it due to a water vapor concentration in the air at the two faces of the film as in equation 2. Under these conditions, the diffusion constant in cm.²/sec.

$$D_w = \frac{a}{A} \times \frac{m}{t} \times \frac{1}{(c_1 - c_2)g} \qquad (4)$$

where c_1 and c_2 are the differential moisture content of the film at the two surfaces in grams of moisture per gram of dry film, g is the equilibrium density of the film in terms of dry weight and swollen volume, and the other symbols have the same significance as in equations 1 and 2. This equation will give average diffusion constants only when a and g are constant and when the moisture gradient is linear. Neither of these are true for the regenerated cellulose film–water system. The equation may, however, be put in a usable differential form

$$dD_w = \frac{1}{A} \times \frac{m}{t} \times \frac{d(a/g)}{dM_c} \qquad (5)$$

in which dM_c is the differential moisture content of the film at $^2/_3$ of the difference between the surface moisture contents (equal to the average moisture content).[3] The other symbols have the same significance as in the preceding equations. The differential bound-water diffusion constants were obtained by plotting a/g against the moisture content and using the slope at dM_c.

Figure 3 gives the differential bound-water diffusion constants for the data of Table I plotted against the fractional water volume. Values calculated from the rate of adsorption measurements of the previous paper[3] are also plotted for comparison. The agreement between the values obtained by the two different types of measurements is quite good. The figure shows that the differential bound-water diffusion constant increases exponentially with an increase in the fractional water volume. Similar exponential increases in integral diffusion constants have been found by Long and associates.[17,18]

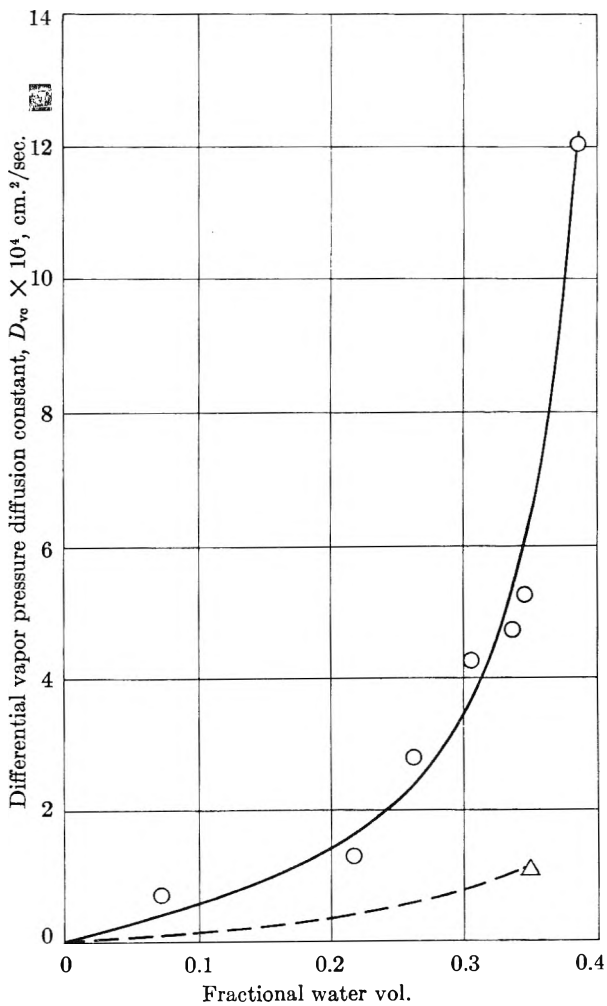

Fig. 2.—Differential water vapor diffusion constants *versus* the fractional water volume: circles 28°; triangles, 4.5°.

Discussion

The rapid increase in diffusion constant with increasing moisture content or fractional volume of water is not surprising. All cellulosic materials hold water by polymolecular adsorption up to about

(17) A. J. Kokes and F. A. Long, *J. Am. Chem. Soc.*, **75**, 6142 (1953).
(18) S. Prager and F. A. Long, *ibid.*, **73**, 4072 (1951).

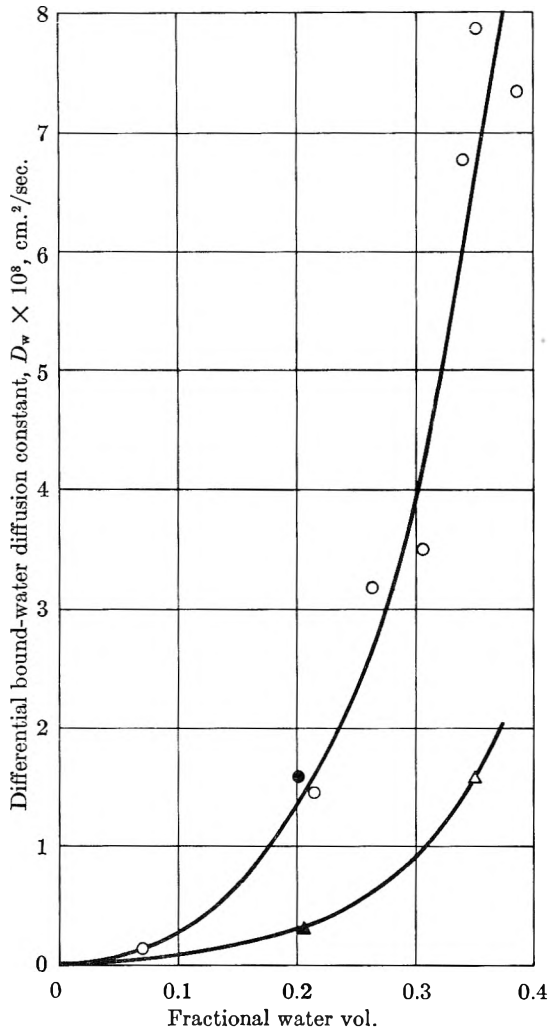

Fig. 3.—Differential bound-water diffusion constants *versus* the fractional water volume: circles 28°; triangles, 4.5°; open symbols from steady-state measurements, shaded symbols from rate of adsorption measurements.[16]

seven molecular layers, presumably by hydrogen bonding.[8] The force of attraction of one layer for the next drops off very rapidly with distance (probably exponentially). Water in moving a molecule at a time through such a system at first has to break a cellulose–cellulose bond and wedge its way into the structure. It becomes temporarily immobilized because of its great attractive force for the cellulose. It will move on into the structure only in response to finding a more favorable nearby position where it is attracted by a greater force. Additional molecules will move in more readily at points where there is already some water, as less structural resistance has to be overcome. Molecules will readily move from polymolecular positions at the surface to unimolecular positions further into the structure. Eventually when the fiber saturation point of the film is almost attained, water to form the seventh molecular layer will move into and through the film almost as readily as free water, because of the small attraction to the sixth layer. The ease of movement of water into the film should thus vary exponentially with the distance of the molecule from the expanded internal cellulose surface.

The author[16] has previously shown that the logarithm of the electrical conductivity of wood increases directly with the moisture constant over a broad range. The diffusion of electrons through wood is thus quite analogous to the diffusion of water.

Conclusions

The differential diffusion constants for the diffusion of water into regenerated cellulose film both on a vapor pressure gradient and a bound-water gradient basis calculated from steady-state diffusion data increase exponentially with the fractional water volume. The former were calculated on the basis of a straight-line vapor pressure gradient existing across the membrane. The latter were calculated on the basis of a parabolic moisture gradient. The existence of the parabolic gradient was confirmed by the agreement between the experimental average moisture contents and the calculated average moisture contents based on the assumption of a parabolic distribution. This is in agreement with the findings of the previous paper[3] that the moisture gradients in rate of adsorption measurements are also parabolic.

The fact that the gradients on a vapor pressure basis are linear makes it appear that the diffusion must be controlled by vapor pressure. This is in keeping with the temperature effect findings of the previous paper and the following: the ratio of the dD_w value in Table I at a fractional water volume of 0.348 and 28° to that at 4.5° is 4.95. The ratio of the corresponding dD_{vc} values is 4.78. The ratio of the vapor pressures at the two temperatures is 4.50. These values are in quite good agreement with those given in the previous paper[3] and are further confirmation of the vapor pressure control of the rate.

STUDIES ON THE COÖRDINATE BOND. IV. THE MECHANISM OF FORMATION AND OF DISSOCIATION OF THE TRIS-(2,2′-DIPYRIDYL)-IRON(II) COMPLEX[1]

BY P. KRUMHOLZ

Contribution from the Research Laboratory of Orquima S. A., São Paulo, Brazil

Received June 21, 1955

The rate of formation of the tris-(2,2′-dipyridyl)-iron(II) complex was determined in solutions up to 2.2 *M* in hydrochloric acid and compared with the rate of dissociation of that complex determined under similar conditions. The rates of those two reactions both show the same dependence on the hydrogen ion concentration. The experimental rate laws are mathematically equivalent to expressions derived by means of the steady state approximation applied to a reaction scheme involving intermediates in whch 2,2′-dipyridyl behaves as a monodentate group. It was found that 2,2′-dipyridyl behaves in strongly acid solutions as a biacid base and the value of the corresponding dissociation constant is reported.

The rate of dissociation of the complex tris-(2,2′-dipyridyl)-iron(II) ion (= FeD_3^{+2}) shows, contrary to the behavior of the analogous complex of 1,10-phenanthroline[2] a particular dependence on the hydrogen ion concentration.[3] The kinetics of that reaction in acid solutions follows closely the rate expression[3]

$$\frac{d(FeD_3^{+2})}{dt} = F_{(H)^-}(FeD_3^{+2}) \qquad (1a)$$

with $$F_{(H)^-} = \{k_a^- k_c + k_b^-(H^+)\}/\{(H^+) + k_c\} \qquad (1b)$$

We interpreted[3c] this expression as representing the simultaneous dissociation of FeD_3^{+2} (rate constant k_a^-) and that of an intermediate FeD_3H^{+3} (rate constant k_b^-), the latter supposed to be in equilibrium with FeD_3^{+2} and H^+ (instability constant k_c).[4] According to the value of k_c ($\doteq 0.5$), FeD_3H^{+3} should exist in strongly acid solutions in amounts commensurable with that of FeD_3^{+2}.

Basolo, Hayes and Neumann[5] proposed recently a different mechanism for the dissociation of FeD_3^{+2}, suggesting as primary reaction step the rupture of a single bond between the iron atom and one of the nitrogen atoms of 2,2′-dipyridyl. One pyridine moiety of that molecule is now free to turn its nitrogen atom away from the iron atom and to add a proton. The "half-bonded" intermediate FeD_3H^{+3} represents here, contrary to our assumption, a stationary intermediate existing only in a very low concentration. Applying the steady-state approximation to their reaction scheme, Basolo, *et al.*,[5] deduced a rate expression, mathematically equivalent to that given by equations 1. Thus existing kinetic evidence does not permit a clear decision, which of both mechanisms is the correct one.[6]

We thought that a study of the equilibrium between FeD_3^{+2} and its components in strongly acid solutions could answer the question, whether or not FeD_3H^{+3} exists under such conditions in concentrations commensurable with that of FeD_3^{+2}. The experimental results, reported in the following answer that question in the negative. Those results induced us to study the kinetics of formation of FeD_3^{+2}, previously[3] investigated only at low acidities, in strongly acid solutions. If Basolo's mechanism is the correct one it should be equally valid for the formation as for the dissociation of FeD_3^{+2}. It will be shown in the following that the results of the kinetic measurements are in full agreement with the new mechanism, proposed by Basolo, *et al.*[5]

Remarks on Equilibrium and Rate Measurements at High Acidities.—The correct interpretation of equilibrium and rate measurements at high acidities is made difficult by the circumstance that activity coefficients depend not only on the total ionic strength but also on the qualitative composition of the solutions. The latter effect, due to specific ionic interactions, increases strongly with increasing molarity of the solutes. In our experiments the concentration of the strong (hydrochloric) acid was varied between about 0.01 and 2.2 *M*. Even at constant ionic strength the activity coefficients of all solutes will in general vary in a rather unpredictable way if the concentration of the acid and thus the composition of the solution is varied within such wide limits. In the rather unique system hydrochloric acid–lithium chloride, however, the activity coefficient of the acid is nearly independent of the relative proportions of both electrolytes, provided that the total molarity is maintained constant.[7] This behavior justifies the supposition that the activity coefficients of other solutes, present in small amounts in mixed solutions of hydrochloric acid and lithium chloride of constant total molarity will not depend strongly on the relative proportions of the latter.[8] Equilibria and reaction rates studied in such solutions should thus be little disturbed by specific ionic interactions even if the concentration of the acid is varied within wide limits. Earlier measurements[3d] of the rate of dissociation of FeD_3^{+2} as well as the equilibrium

(1) Paper III, *J. Am. Chem. Soc.*, **77**, 777 (1955).

(2) T. S. Lee, I. M. Kolthoff and D. L. Leussing, *ibid.*, **70**, 2596 (1948).

(3) (a) J. H. Baxendale and P. George, *Nature*, **162**, 777 (1948); (b) *Trans. Faraday Soc.*, **46**, 736 (1950); (c) P. Krumholz, *Nature*, **163**, 724 (1949); (d) *Anais Acad. brasil. cienc.*, **22**, 263 (1950).

(4) This interpretation implies the supposition that (FeD_3^{+2}) in (1a) represents actually the sum of the concentrations of FeD_3^{+2} and of FeD_3H^{+3}. Since (FeD_3^{+2}) was determined by a photometric method it means furthermore that this method cannot distinguish between FeD_3^{+2} and the protonated complex.

(5) F. Basolo, J. C. Hayes and H. M. Neumann, *J. Am. Chem. Soc.*, **76**, 3807 (1954).

(6) The observation,[5] that the spectrum of FeD_3^{+2} is the same in neutral as in strongly acid solutions (see also ref. 4) is not necessarily at variance with our reaction scheme (see ref. 3b).

(7) See H. S. Harned and B. B. Owen, "The Physical Chemistry of Electrolytic Solutions," Second edition, Reinhold Publ. Corp., New York, N. Y., 1950, p. 444 *ff.*

(8) The activity coefficients of the minor solutes will depend very little on their own concentration as long as that concentration is much smaller than the total molarity of HCl and LiCl (see ref. 7).

and rate measurements to be reported in the following seem to confirm this supposition. All those measurements have been performed at 25° in solutions containing hydrochloric acid and lithium chloride at a constant total molarity of 2.2.

Equilibrium Studies.—The concentration formation constant of FeD_3^{+2}

$$K_{FeD_3} = (FeD_3^{+2})(Fe^{+2})^{-1}(D)^{-3} \qquad (2)$$

was determined by measuring the equilibrium concentration (FeD_3^{+2}) in solutions of known initial composition.[9] Potentiometric measurements[10] seemed to indicate, that 2,2′-dipyridyl (= D) can only behave as a monoacid base. Accordingly its concentration in acid solution was expressed by means of

$$(D) = K_{HD}(D)_t/\{K_{HD} + (H^+)\} \qquad (3)$$

where K_{HD} is the concentration dissociation constant of the 2,2′-dipyridylium ion HD^+ and $(D)_t$ the total concentration of 2,2′-dipyridyl, free or combined with H^+. At acidities up to about 0.06 *M*, expression (3) leads to self-consistent values of K_{FeD_3}.[9] This is no longer true at higher acidities. Table I lists (under column *a*) the values of $K_{HD}{}^3K_{FeD_3}$[11] as computed[12] by means of equations 2 and 3 from measurements in solutions about 0.01 to 2 *M* in hydrochloric acid. Those values, nearly constant at acidities below 0.05 *M* decrease strongly at higher acidities. This decrease cannot be attributed to the formation of the intermediate FeD_3H^{+3}, which on the contrary should result in too high a value of (FeD_3^{+2})(see ref. 4) and thus in a too high apparent value of K_{FeD_3}. It points rather toward a different explanation, namely, that HD^+ may add in strongly acid solutions a second proton. In that case the concentration of free 2,2′-dipyridyl (in acid solutions) must be expressed according to

$$(D) = \frac{K_{HD}(D)_t}{(H^+) + K_{HD}K_{H_2D}/\{(H^+) + K_{H_2D}\}} \frac{K_{H_2D}}{(H^+) + K_{H_2D}} \qquad (4)$$

where K_{H_2D} is the concentration dissociation constant of H_2D^{+2}. The values of $K_{HD}{}^3K_{FeD_3}$ computed by means of equations 2 and 4 and using the value $K_{H_2D} = 1.67$ (obtained by trial and error) are now (see column *b*, in Table I) perfectly consistent, at least for acidities up to about 1.2 *M*. The increase of those values at still higher acidities is most probably due to a not quite perfect elimination of the influence of specific ionic interactions.

In order to confirm the correctness of this explanation, based on the supposed formation of H_2D^{+2}, we tried to obtain a direct evidence of the existence of this ion. We found indeed, that the ultraviolet absorption spectrum of HD^+[13] is shifted in strongly acid solutions as a whole toward shorter wave lengths. Spectral measurements performed in solutions of different acidities permitted the approximate evaluation of the dissociation constant of H_2D^{+2}. The value so obtained, $K_{H_2D} = 1.4 \pm 0.3$ (in 2.2 *M* HCl or LiCl) is in fair agreement with the more exact value calculated from the equilibrium measurements of FeD_3^{+2}. It is interesting to note that the value of this constant is considerably higher than the values of the corresponding constants of other isomeric 2,X′-dipyridyls.[14] The addition of a second proton to HD^+ requires, in the case of the 2,2′-isomer (and only in that case), the breaking of a hydrogen bond and a rotation around the central C–C bond, away from the *cis*-position of the two nitrogen atoms. Otherwise, repulsive actions, both of steric and electrostatic origin, will prevent the addition of the second proton.[15]

The results of the equilibrium measurements just discussed seem to exclude definitively the possibility that FeD_3H^{+3} might exist in acid solutions of FeD_3^{+2} in concentrations as high as requested by our original interpretation of the rate equations 1.

Rate Studies.—It was found previously[3] that the rate of formation of FeD_3^{+2} follows, at acidities up to 0.06 *M*, approximately the expression

$$\frac{d(FeD_3)}{dt} = F_{(H)}{}^+(Fe^{+2})(D)^3 = \{k_a{}'^+ + k_b{}'^+(H^+)/K_{HD}\}(Fe^{+2})(D)^3 \qquad (5)$$

if (D) is computed by means of equation 3. We interpreted[3c] this expression as representing the simultaneous reactions between the rapidly formed intermediate FeD_3^{+2} and (D) on one side (rate constant $k_a{}'^+$) and HD^+ on the other (rate constant $k_b{}'^+$). It follows from the results of the equilibrium measurements in strongly acid solutions that (D) in equation 5 must be expressed in that case by means of equation 4. We actually used those equations for the calculation[12] of the values of $K_{HD}{}^3F_{(H)}{}^+$[11] from rate measurements in solutions, about 0.01 to 2*M* in hydrochloric acid. At acidities greater than 1.2 *M*, those values were multiplied with the quo-

TABLE I

DEPENDENCE OF $K_{HD}{}^3K_{FeD_3}$ ON THE INITIAL CONCENTRATION OF HYDROCHLORIC ACID, $(HCl)_0$

$(HCl)_0$	$K_{HD}{}^3K_{FeD_3} \times 10^{-3}$ a	b
7.40×10^{-3}	3.65	3.70
1.47×10^{-2}	3.70	3.80
1.48×10^{-2}	3.60	3.70
2.94×10^{-2}	3.73	3.90
7.35×10^{-2}	3.45	3.90
1.47×10^{-1}	3.00	3.82
2.20×10^{-1}	2.65	3.80
2.93×10^{-1}	2.35	3.75
4.40×10^{-1}	1.90	3.73
5.85×10^{-1}	1.62	3.82
7.30×10^{-1}	1.32	3.75
8.80×10^{-1}	1.12	3.80
1.17	0.81	3.75
1.47	0.67	4.05
1.47	0.69	4.13
1.76	0.52	4.15
2.20	0.42	4.70

[a] As calculated by means of equations 2 and 3. [b] As calculated by means of equations 2 and 4. $T = 25°$, ionic strength of 2.2 (LiCl + HCl).

(9) See J. H. Baxendale and P. George, *Trans. Faraday Soc.*, **46**, 55 (1950); P. Krumholz, ref. 3d.

(10) P. Krumholz, *J. Am. Chem. Soc.*, **71**, 3654 (1949); J. H. Baxendale and P. George, ref. 9.

(11) We use that expression instead of K_{FeD_3} itself in order to avoid the uncertainty introduced otherwise by the somewhat doubtful (see Experimental part) value of K_{HD}.

(12) The method of calculation actually followed will be given in the Experimental part.

(13) See J. Baxendale and P. George, ref. 9.

(14) See P. Krumholz, *J. Am. Chem. Soc.*, **73**, 3487 (1951).

(15) Kolthoff, *et al.*,[2] explained in this way the mono-basicity of the rigid 1,10-phenanthroline molecule.

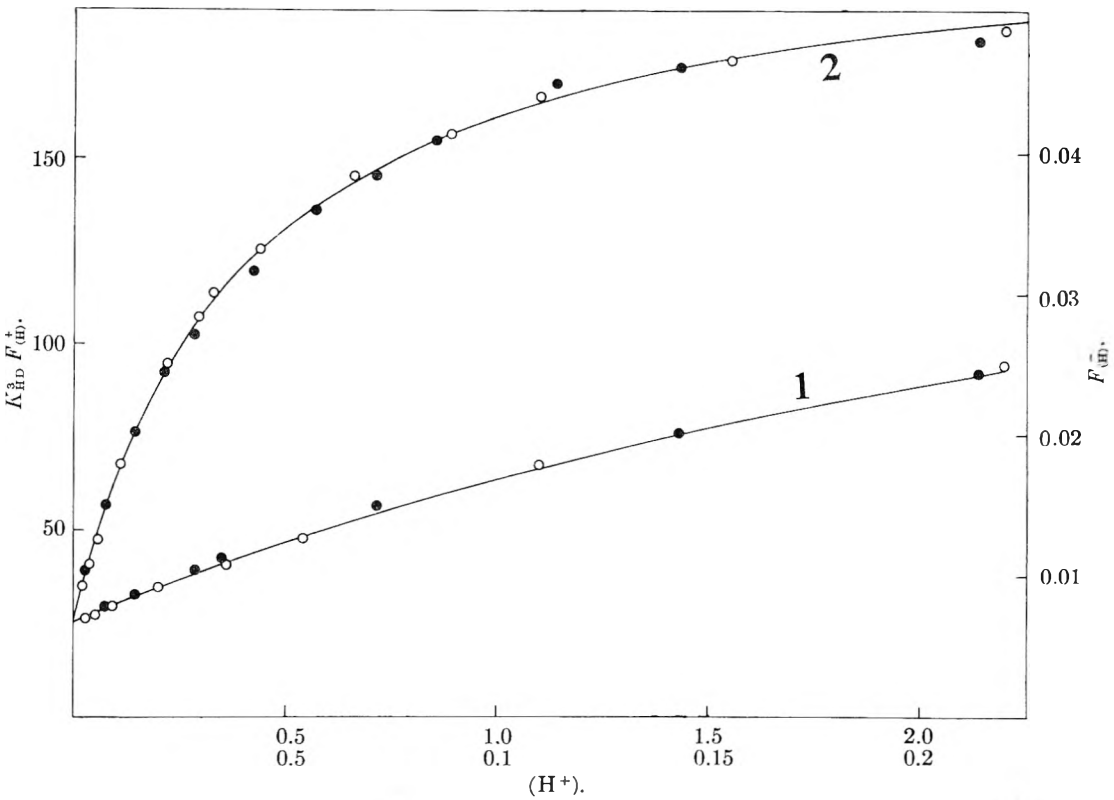

Fig. 1.—Dependence of the rate factors $F_{(\bar{H})}$ (open circles and ordinate scale on the right) and $K_{HD}^{3}\,F_{(\bar{H})}^{+}$ (filled circles and ordinate scale on the left) on the hydrogen ion concentration, (H^+); upper abscissa scale, curve 2; lower abscissa scale, curve 1; $T = 25°$; ionic strength of 2.2 (HCl + LiCl).

tient between the constant value of $K_{HD}{}^{3}K_{FeD_3}$ at acidities lower than 1.2 M and its value at the given higher acidity. This correction should eliminate to a great extent the influence of the ionic composition on $K_{HD}{}^{3}F_{(H)}{}^{+}$.[16] The values of $K_{HD}{}^{3}F_{(H)}{}^{+}$ obtained in this way are plotted in Fig. 1 as functions of the concentration of hydrochloric acid. This figure contains furthermore the values of $F_{(H)}{}^{-}$ (see equation 1b) as determined previously[3d] under identical experimental conditions, multiplied with a constant K, such as to make $KF_{(H)}{}^{-}$ coincide with $K_{HD}{}^{3}F_{(H)}{}^{+}$ at some arbitrary acidity. Inspection of Fig. 1 shows that this coincidence extends over the whole range of acidities, experimentally investigated. The value of the constant K actually used, is $K = 3.80 \times 10^{3}$ in excellent agreement with the average of the values of $K_{HD}{}^{3}K_{FeD_3}$ determined at acidities lower than 1.2 M (see Table I). Thus, quite independently of the acidity, $F_{(H)}{}^{+}/F_{(H)}{}^{-} = K_{FeD_3}$. This means again that the expression for $F_{(H)}{}^{+}$ must be mathematically equivalent to the expression for $F_{(H)}{}^{-}$ (see equation 1b), or that

$$F_{(H)}{}^{+} = \{k_a{}^{+}k_c + k_b{}^{+}(H^+)\}/\{(H^+) + k_c\} \quad (6)$$

k_c being equal in equations 6 and 1b. The expression given in equation 5 for $F_{(H)}{}^{+}$ is obviously only a limiting form of (6), approximately valid at $(H^+) \ll k_c$.

In order to show that equations 1b and 6 fit quantitatively to the experimental data, we computed by means of equation 1b, $F_{(H)}{}^{-}$ as function of (H^+), using the following values of the individual constants[3d] $k_a{}^{-} = 6.7 \times 10^{-3}$ min.$^{-1}$; $k_b{}^{-} = 5.7 \times 10^{-2}$ min.$^{-1}$ and $k_c = 0.40$. The agreement between the so computed curve (in Fig. 1) and the points representing the experimental values of $F_{(H)}{}^{-}$ is actually as good as possibly can be expected.

It will be shown in the following that the experimental rate laws are fully consistent with an extended Basolo mechanism.[5]

Theoretical Considerations.—We shall admit that the two first steps in the reaction between Fe^{+2} and 2,2′-dipyridyl are the formations of the intermediates FeD^{+2} and $FeD_2{}^{+2}$, remaining during the course of the reaction in equilibrium with its components.[17] We shall admit, furthermore, that all reactions involving only D and H^+ can be similarly treated as preceding equilibria. We can then represent the reaction between Fe^{+2} and D (and the reverse reaction) by the following reaction scheme[18]

$$\begin{array}{l} Fe^{+2} + D \underset{}{\overset{K_1}{\rightleftharpoons}} FeD^{+2} + D \overset{K_2}{\rightleftharpoons} \\ \overset{K_2}{\rightleftharpoons} FeD_2{}^{+2} + D \underset{k_3}{\overset{k_4}{\rightleftharpoons}} \overline{FeD_3}{}^{+2} \underset{k_1}{\overset{k_2}{\rightleftharpoons}} FeD_3{}^{+2} \quad (7) \\ \qquad\qquad + \qquad\qquad + \\ \qquad HD^{+} \underset{k_7}{\overset{k_8}{\rightleftharpoons}} \overline{FeD_3}H^{+3} \underset{k_5}{\overset{k_6}{\rightleftharpoons}} H^{+} \end{array}$$

(16) This follows most simply from the relation $F_{(H)}{}^{+} = K_{FeD_3} \cdot F_{(H)}{}^{-}$ (see later) and from the negligible dependence of $F_{(H)}{}^{-}$ on the ionic composition (in the special case of HCl–LiCl mixtures).

(17) See ref. 3. The preceding equilibrium hypothesis seems to be justified by the agreement between experiment and theory under the prevailing experimental conditions.

(18) This scheme neglects in the first steps, treated as equilibria, the probable but purely speculative participation of HD^{+}, as well as that of half-bonded structures.

where $\overline{FeD_3}^{+2}$ and $\overline{FeD_3}H^{+3}$ are "half-bonded" stationary intermediates in the sense of Basolo, *et al.*[5] Representing according to

$$K_{FeD_3} = K_1K_2k_4/k_1k_3 = K_1K_2k_6k_8/k_1k_5k_7K_{HD} \quad (8)$$

the over-all equilibrium constant of FeD_3^{+2} as product of the equilibrium constants of the elementary reaction steps and applying the steady-state approximation to the reaction scheme (7) one obtains easily the expressions

$$F_{(H)}^- = k_1G_{(H)} \qquad F_{(H)}^+ = \{K_1K_2k_2k_4/k_3\}\,G_{(H)} \quad (9)$$

with

$$G_{(H)} \equiv \{k_3(k_6 + k_7) + k_5k_7(H^+)\}/\{(k_2 + k_3)(k_6 + k_7) + k_5k_7(H^+)\} \quad (10)$$

Those expressions are mathematically equivalent to the expressions for $F_{(H)}^-$ and $F_{(H)}^+$ as given in equations 1b and 6. It follows furthermore from equations 8 and 9 that $F_{(H)}^+/F_{(H)}^- = K_{FeD_3}$ for any value of (H^+). Basolo's mechanism[5] is thus fully consistent with our experimental results.

We find in accordance with Basolo's simplified treatment[18a] of the dissociation reaction that

$$k_1 = k_b^- = k_\infty^- \text{ and } k_1k_3/(k_2 + k_3) = k_a = k_0^- \quad (11)$$

where k_0 and k_∞ represent the rate constants for $(H^+) = 0$ and $(H^+) = \infty$, respectively. We deduce in addition the following relations

$$K_1K_2k_2k_4/k_3 = k_b^+ = k_\infty^+ = k_b^-K_{FeD_3}$$
$$(k_2 + k_3)(k_6 + k_7)/k_5k_7 = k_c$$
$$k_3k_6k_8/k_4k_5k_7 = K_{HD} \quad (12)$$

No more information on the individual constants can be expected from the experimental measurements.

Introducing the experimentally determined values we find that (at 25° in 2.2 *M* HCl or LiCl) $k_1 = 5.7 \times 10^{-2}$ min.$^{-1}$ and $k_2/k_3 = 7.7$. We can furthermore compute a lower limit for $k_5/k_2 \geq 2.8$ (the equality sign being valid for $k_6 \ll k_7$). The numerical calculation of k_4 requires the values of K_1 $(= K_{FeD})$, of K_2 and of K_{HD} (the latter for the calculation of K_{FeD_3} or of k_b^+) to be known. The first constant has been determined experimentally as $K_{FeD} = 5 \times 10^4$. K_2 cannot be much greater than K_{FeD} (see ref. 9) and is probably smaller by a factor of ten.[19] The value of K_{HD} is 1.15×10^{-5}. We find thus for k_4 the value $k_4 \doteq 10^8$, which at least should give the correct order of magnitude of that constant. Using this value we can finally deduce that $k_6k_8/k_7 \geq 2.5 \times 10^4$ min.$^{-1}$.

The information obtained on the reaction steps involving the intermediate FeD_3H^{+3} is rather scarce and limited to relations between rate constants. It is however the very existence of those reaction steps which permits the numerical calculation of at least two individual rate constants and that of k_1, and of k_4. There is little prospect that the other rate constants will individually be accessible by experiment.

(18a) The expression given by Basolo, *et al.*,[5] for $F_{(H)}^-$ results from the complete expression (9) and (10) by admitting that $k_6 < k_7$.

(19) As pointed out previously,[3d] FeD^{+2} and $FeEn^{+2}$ have nearly the same stability. FeD_2^{+2} is most probably of the same bond type like FeD^{+2}, and not like FeD_3^{+3}.[3d] It is thus very probable that the relation between the stability constants of the mono- and the bis-2,2'-dipyridyl-iron(II) complex will be near to that of the analogous complexes of ethylenediamine (actually about 1:10).

Experimental Part

Materials.—2,2'-Dipyridyl was purified by several recrystallizations from hexane and from ethanol–water mixtures. All other chemicals were of reagent grade.

Dissociation Constants of HD^+ and of H_2D^{+2}.—It is rather difficult to determine the value of K_{HD} at the high ionic strength of 2.2 with a reasonable precision. We tried to use for that purpose the cell combination

glass electrode $\left|\begin{matrix}D,DHCl\ (10^{-z}M)\\ LiCl\ (2.2\ M)\end{matrix}\right|$ $KCl_{sat.}$, HgCl–Hg (I)

glass electrode $\left|\begin{matrix}HCl\ (10^{-3} - 10^{-2}M)\\ LiCl\ (2.2\ M)\end{matrix}\right|$ $KCl_{sat.}$ HgCl–Hg (II)

similar to one proposed by Harned and Robinson and by Güntelberg and Schiodt.[20] The value $K_{HD} = (1.15 \pm 0.05) \times 10^{-5}$ computed from the corresponding measurements[21] at 25° seems rather low if compared with the values of that constant obtained previously[21] at lower ionic strengths. This may be due to the fact that the concentration of HCl in cell II could not be lowered below 10^{-3} *M*,[22] whereas in cell I (H^+) was about 10^{-5} *M*. The corresponding extrapolation may introduce a considerable error.

The value of the dissociation constant of H_2D^{+2} was computed by trial and error from the equilibrium measurements of FeD_3^{+2}. A less accurate but reasonably agreeing value, was obtained by direct spectrophotometric measurements. The absorption spectra of 5×10^{-6} *M* solutions of 2,2'-dipyridyl, containing HCl and LiCl at a constant total molarity of 2.2 were measured at acidities varying between 0.01 and 2.2 *M*. The measurements were performed at 25 ± 1° with a Beckman D.U. spectrophotometer. It was observed that LiCl itself shifts the spectrum of HD^+ slightly to longer wave lengths (by about 10 Å. in 2.2 *M* solutions). We consider thus for the calculation of K_{H_2D} only measurements near to the absorption maximum of HD^+, where the influence of LiCl on the absorbancy is smallest. The spectrum measured in weakly (about 0.01 *M*) acid solutions, 2.2 *M* in LiCl was considered as the reference spectrum of pure HD^+. We computed from those measurements for the value of the dissociation constant of H_2D the value $K_{H_2D} = 1.4 \pm 0.3$. The absorption spectrum of H_2D^{+2} as obtained from an extrapolation of our measurements to $(H^+) = \infty$ is rather similar to the spectrum of HD^{+}[13]. The principal absorption maximum of HD^+ at 3010 Å. is shifted in the spectrum of H_2D^{+2} to about 2900 Å. The corresponding absorbancy indexes of both ions are nearly equal ($\epsilon = (15.5 \pm 0.5) \times 10^3$).

Equilibrium Constant of FeD_3^{+2}.—The equilibrium measurements were performed in solutions, 2 to 5×10^{-4} *M* in $FeSO_4$ and about 0.01 to 2 *M* in HCl. The concentration of 2,2'-dipyridyl was maintained in constant relation to the concentration of HCl, $(D)_t = 0.025$ (HCl). Enough LiCl was added to maintain a constant ionic strength of 2.2. The reaction mixture was thermostated during 24 hr. at 25 ± 0.1° and thereupon transferred to a rectangular absorption cell of 40 mm. light path. The temperature of the cell was maintained constant (±0.1°) by circulating water through the cell holder, provided with suitable channels. The absorbancy was measured at the absorption maximum of FeD_3^{+2} (5230 Å.) by means of a spectrophotometer, previously[23] described. The precision of the absorbancy measurements was ±1%.

The formation constant K_{FeD_3} was computed from the measured equilibrium concentration of FeD_3^{+2} by means of equations 2 and 3, respectively. The equilibrium concentrations appearing in those equations were expressed as functions of the initial concentrations $()_0$, the measured concentration of FeD_3^{+2} and that of FeD^{+2} (see ref. 3d) as

$$(D)_t = (D) + (HD^+) + (H_2D^{+2}) \quad (a)$$

$$(D)_0 = (D)_t + (FeD^{+2}) + 3(FeD_3^{+2}) \quad (b)$$

$$(Fe^{+2})_0 = (Fe^{+2}) + (FeD^{+2}) + (FeD_3^{+2}) \quad (c)$$

(20) H. S. Harned and R. A. Robinson, *J. Am. Chem. Soc.*, **50**, 3157 (1928); E. Güntelberg and E. Schiodt, *Z. physik. Chem.*, **135**, 393 (1928).

(21) See P. Krumholz, *ibid.*, **71**, 3654 (1949), for the experimental arrangement.

(22) See Harned and Owen, ref. 7, p. 321.

(23) P. Krumholz, *Rev. Sci. Inst.*, **22**, 362 (1951).

$$(HCl)_0 = (H^+) + (D)_0 + (H_2D^{+2}) - (FeD^{+2}) - 3(FeD_3^{+2}) \quad (d)$$

with

$$(FeD^{+2}) \doteq K_{FeD}K_{HD}K_{H_2D}(Fe^{+2})(D)_t/\{(H^+)[(H^+) + K_{H_2D}]\} \quad (e)$$

$$(H_2D^{+2}) \doteq (H^+)(D)_t/\{(H^+) + K_{H_2D}\} \quad (f)$$

The formation constant of FeD^{+2} necessary for the numerical calculations was determined by means of the photometric method, previously[10] described as $K_{FeD} = (5 \pm 1) \times 10^4$ (in 2.2 M LiCl). Expressions (a) to (f) were solved by successive approximations. As under the prevailing experimental conditions (FeD^{+2}) and (H_2D^{+2}) were only small corrective factors calculations were actually not too cumbersome.

Rate of Formation of FeD_3^{+2}.—The rate of formation of FeD_3^{+2} was determined by the method used by Lee, Kolthoff and Leussing[2] in the analogous case of the reaction between Fe^{+2} and 1,10-phenanthroline. Using concentrations of the reactants large relative to the amount of FeD_3^{+2} formed, the kinetics may be treated[2] as a pseudo-zero-order formation, followed by a first-order dissociation. In our measurements this condition was always fulfilled, at least until (FeD_3^{+2}) reached 10 to 20% of its equilibrium value. The rate constant of the dissociation reaction, necessary for the calculations was taken from earlier measurements[3d] performed under identical experimental conditions. The solutions used in the rate measurements had the same composition as those used in the equilibrium measurements. The solution containing all components, but Fe^{+2}, was put into the absorption cell, placed in the constant temperature cell compartment of the spectrophotometer and maintained at 25 ± 0.1°. Hereupon the solution of $FeSO_4$ (1 to 2 ml.), brought previously to 25° was blown rapidly into the main solution and the absorbancy measured at suitable time intervals.

The concentrations of the reactants entering the rate equations were computed by means of a set of equations identical with (a) to (f) but suppressing the term (FeD_3^{+2}). The rate factors $F_{(H)^+}$ could be evaluated with a precision of about ±3%.

FERRIC CHLORIDE DECAHYDRATE; THE SYSTEMS $FeCl_3$–H_2O AND $FeCl_3$–HCl–H_2O BELOW 0°

BY WILLIAM F. LINKE

Contribution from the Wm. H. Nichols Laboratory of New York University, New York, N. Y.

Received June 23, 1955

A decahydrate of ferric chloride which melts incongruently at 0° is reported. Reinvestigation of the system $FeCl_3$–H_2O shows the stable eutectic to occur at −35.0° with ice and $FeCl_3 \cdot 10H_2O$ saturating a solution containing 28.7% $FeCl_3$. The −20° isotherm of the system $FeCl_3$–HCl–H_2O was studied in order to establish the composition of the decahydrate. On the basis of solubilities, heating curves and visual data, the phase relationships of the decahydrate in the polythermal system $FeCl_3$–HCl–H_2O have been determined.

During an investigation of the double salts formed by ferric chloride and the alkali chlorides, it was observed that a highly hydrated ferric chloride phase existed below 0°. According to the classical work of Roozeboom,[1,2] the hexahydrate, $FeCl_3 \cdot 6H_2O$, is the stable saturating phase from its melting point (37°), to the eutectic (−55°). Since the phase encountered here seemed to contain nearly twice as many moles of water per mole of salt as the hexahydrate, the systems $FeCl_3$–H_2O and $FeCl_3$–HCl–H_2O were reinvestigated in order to establish its identity and stability.

Materials and Methods

Reagents.—C.P. $FeCl_3 \cdot 6H_2O$ was found to contain 20.52% Fe and 39.23% Cl, indicating the presence of about 0.15% HCl (a flame test showed no significant color) and a slight excess of water. The analytical composition of the salt was used in the various calculations. Whenever stock solutions of ferric chloride were prepared they were stabilized by the addition of a small amount of HCl. This excess acid was also considered in the calculations.

$FeCl_3 \cdot 10H_2O$ was prepared by stirring a concentrated solution of ferric chloride at −20° for several hours. Scratching and seeding speeded the precipitation, but it was always very slow. Very little solid formed before 4 to 6 hours of stirring, and most samples had to be stirred overnight. The presence of HCl greatly retarded the precipitation, especially when the degree of supersaturation was small. In one solution which contained about 7% HCl only about 5% of the total precipitation had occurred after two days at −20°. The solid obtained in this way was bright yellow, microcrystalline, and settled very slowly. A coarsely crystalline product which adhered to the walls of the glass container was obtained by allowing the decahydrate to form without stirring, but long periods of time (1–2 months) were required. This compact yellow-brown solid was composed of grains about 1 mm. in diameter which were quite hard When uncrushed, these crystals settled rapidly and were useful in eliminating sampling difficulties.

Anhydrous $FeCl_3$, needed to prepare a few mixtures used for thermal analysis, was a sublimed product that was used without purification or analysis.

Temperatures were read from calibrated mercury or hexane thermometers. The work at −20° was done in a mechanically cooled thermostat in which the temperature variation did not exceed ±0.1°. Three solubility determinations at −31.6° were done in a bath of melting bromobenzene.

Sampling of the solutions for analysis was done with precooled pipets which were fitted with filter paper tips. Since the microcrystalline decahydrate clogged the filter, gentle suction was applied for long periods (up to 1 hour) in order to obtain clear samples.

Analysis for chloride was done by the Volhard method, and for iron by titration with ceric sulfate after passing the solution through a Jones reductor.

Results and Discussion

The data for the system $FeCl_3$–H_2O are listed in Table I and plotted in Fig. 1. The values at −20 and −31.6° were determined by stirring the decahydrate with water for periods of from one hour to 8 days. At −20° equilibrium was approached from both under- and supersaturation, and the average deviation of 7 determinations on 4 different solutions was 0.13%. All other data on the decahydrate saturation curve were obtained from the heating curves of mixtures of known composition. These mixtures were prepared by weighing together analyzed $FeCl_3 \cdot 6H_2O$ and water, and stirring to dissolve the solid. They were then cooled to −20°, seeded with decahydrate and allowed to

(1) H. W. B. Roozeboom, *Z. physik. Chem.*, **10**, 477 (1892).

(2) H. W. B. Roozeboom and F. A. H. Schreinemakers, *ibid.*, **15**, 588 (1894).

TABLE I

THE SYSTEM $FeCl_3$–H_2O

T, °C.	Satd. soln., wt. % $FeCl_3$	Solid	T, °C.	Satd. soln., wt. % $FeCl_3$	Solid
25.0	49.38	6[a]	−35.0[c]	28.7[c]	10 + ice
0.0	42.40	6			
−20.0[b]	38.35	6	−38.3[b]	29.8	ice
0.0[c]	42.4[c]	6 + 10[d]	−32.1	27.9	ice
− 0.4	42.0	10	−27.7	26.0	ice
− 3.2	39.6	10	−24.8	24.7	ice
− 6 4	37 3_4	10	−23.9	24.5	ice
− 9.8	35.7_4	10	−20.5	22.7	ice
−20.0	32.0_0	10			
−31.6	29.2_8	10			

[a] 6 = $FeCl_3 \cdot 6H_2O$. [b] Metastable. [c] Extrapolated. [d] 10 = $FeCl_3 \cdot 10H_2O$.

stand (sometimes with stirring) overnight. Enough decahydrate had then precipitated to permit the determination of the heating curve. The mixtures were placed in a small Dewar flask, stirred at constant rate and the time–temperature curves plotted. Duplicate determinations on the same mixture (after reprecipitating the decahydrate) agreed within ±0.2°. At the end of the experiment, several of the solutions were analyzed for iron in order to confirm their compositions. Errors which might have been introduced by seeding or by evaporation were thereby eliminated.

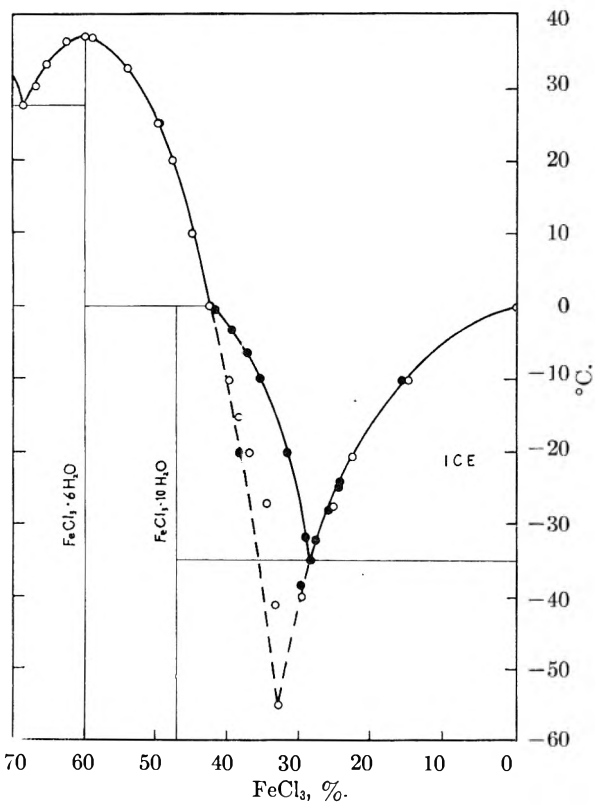

Fig. 1.—The system $FeCl_3$–H_2O: ●, this research; ○, Roozeboom.

Attempts were made to extend the heating curve method to mixtures containing less than 35% $FeCl_3$, but were unsuccessful. In a sample containing 33.9% $FeCl_3$ for example, no break in the heating curve was obtained although the disappearance of the solid at about −15° was easily observed. A second attempt, using only a 2° temperature gradient between the sample and the surrounding jacket, was also fruitless.

Several attempts were made to obtain the eutectic temperature directly. Mixtures of $FeCl_3 \cdot 10H_2O$, ice and a solution of approximately the eutectic composition were stirred together in a Dewar flask, but no constancy of temperature was observed, and the temperature never fell below the initial temperature of mixing. In other trials, $FeCl_3 \cdot 10H_2O$, ice and solution were cooled to −45°. Upon slow heating (1° per minute), no break in the curve was found.

In order to fix the eutectic more exactly, the ice curve of the system was redetermined. The data (from cooling curves) agree well with those reported by Roozeboom.[1] From the extrapolated intersection of the curves the eutectic is found to occur at −35.0 ± 0.5° with 28.7 ± 0.3% $FeCl_3$ in solution. The transition $FeCl_3 \cdot 10H_2O \rightleftarrows FeCl_3 \cdot 6H_2O$ + solution occurs at 0.0 ± 0.2° in contact with a solution containing 42.4 ± 0.1% $FeCl_3$. $FeCl_3 \cdot 10H_2O$ is thus the only hydrate of ferric chloride which does not melt congruently.

Roozeboom's data for the solubility of the hexahydrate were checked at 25, 0 and −20° by stirring the solid with water for an hour or more. At −20° the value reported here is significantly greater than that of Roozeboom. It may be seen from Fig. 1 that below 0° the older data become increasingly divergent from a smooth curve to the (metastable) eutectic. Since these deviations are in the direction of lower solubility, they can now be interpreted as indicating a transition from hexahydrate to decahydrate, which progressed furthest under conditions of greatest supersaturation (lower temperatures).

The identity of the decahydrate was established through a study of the system $FeCl_3$–HCl–H_2O at −20°. Complexes of predetermined composition were prepared from $FeCl_3 \cdot 6H_2O$ (or a $FeCl_3$ solution of known composition), concd. HCl and water. All liquids were kept at or below 0° during the transfer operations in order to minimize the loss of HCl. After seeding, the complexes were brought to equilibrium (from supersaturation) by stirring or by waiting for precipitation to occur spontaneously. In a few cases water was added to a complex in which the decahydrate had already formed, and equilibrium was approached from undersaturation.

TABLE II

EQUILIBRIUM IN THE SYSTEM $FeCl_3$–HCl–H_2O

Satd. soln., $FeCl_3$	Wt. % HCl	Original complex $FeCl_3$	Original complex HCl	Wet residue (R) or turbid soln. (S)		% $FeCl_3$ in solid (extrapd.)
		Results at −20°				
32.00	0	...	...	...	...	...
27.77	3.61	...	...	...	...	...
25.45	5.80	...	...	...	...	...
19.17	11.86	...	...	...	...	...
19.65	12.21	27.53	8.80	...	...	47.90
...	...	31.89	7.43	22.93	11.50(S)	47.58
				35.18	5.72(R)	
19.35	14.22	30.53	8.67	24.45	11.59(S)	47.57
				36.43	5.55(R)	
19.43	14.56	...	...	...	...	...
18.37	15.39	27.33	10.62	...	...	47.44
22.70	13.51	28.95	10.14	36.72	5.75(R)	47.21
22.69	14.15	...	...	35.60	6.69(R)	47.21
24.59[a]	13.09	27.47	11.52	39.76	4.62(R)	48.10
					Av.	47.57
38.35	0	...	...			
27.11	10.08	33.51	8.29			
25.04	12.01	33.63	9.15			
23.03	14.79	...	...	Solid phase		
22.15	15.30	32.89	11.22	$FeCl_3 \cdot 6H_2O$		
19.39	19.20	28.99	14.65			
20.25	21.01	29.81	15.94			
24.35	21.91	34.79	15.44			
		Results at −31.6°				
13.14	23.1	17.85	20.82	Solid phase		
16.14	27.2	...	...	$FeCl_3 \cdot 6H_2O$		

[a] I, Probably saturated with both $FeCl_3 \cdot 10H_2O$ and $FeCl_3 \cdot 6H_2O$.

Samples of the saturated solutions and wet residues were taken after periods ranging from a few hours to 2 months, depending on the method of approaching equilibrium. In some cases turbid samples of the solution were obtained and analyzed. Although these did not fix the solubility of the decahydrate, they were useful in determining the directions of the tie-lines. Several tie-lines were fixed by three, and in one case by four independent analyses (saturated solution, turbid solution, original complex, wet residue).

Whenever the tie-line was established by more than two analyses, the deviation of the individual analytical compositions from linearity was negligibly small (less than 0.1% HCl). This indicated first that the procedure for the preparation of the original complexes introduced no appreciable error due to loss of HCl or water, and second that the analytical methods were sufficiently accurate to establish the positions of the tie-lines.

The data are given in Table II and shown in Fig. 2. The tie-lines may be seen to converge sharply at the composition of the decahydrate. Since many points were used to fix the lines, it was convenient to determine the water content of the solid phase by graphical rather than the usually more reliable algebraic extrapolation. The values in the last column of Table II were read from a graph whose scale was comparable to the accuracy of the procedural techniques. The average value for seven determinations is 47.57 ± 0.24% $FeCl_3$ in the solid, compared to the theoretical 47.38% $FeCl_3$ in $FeCl_3 \cdot 10H_2O$. Complex I has been included in the extrapolations although it is probably saturated with both deca- and hexahydrates. Its saturated solution lies at the intersection of the two solubility curves, and its extrapolation is the highest of all values. If it is omitted from the average, the remaining data average 47.49 ± 0.20% $FeCl_3$.

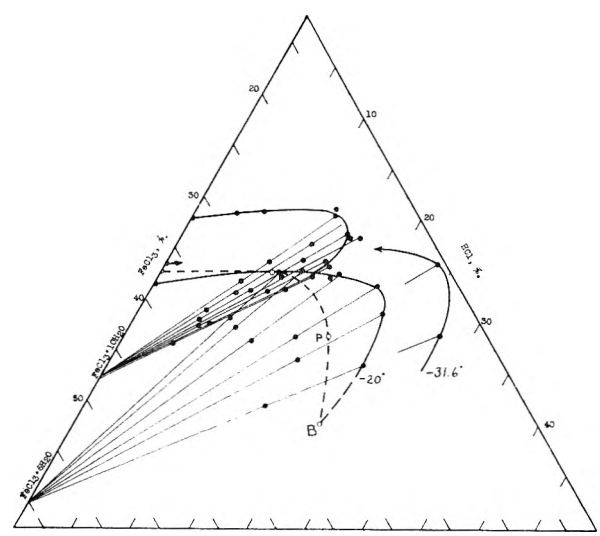

Fig. 2.—−20 and −31.6° isotherms in the system $FeCl_3$–HCl–H_2O: ●, this research; ○, Roozeboom and Schreinemakers.

It may be noticed that although the convergence of the tie-lines is excellent, the compositions of the saturated solutions do not describe a very smooth curve. This may have been caused by the inad-

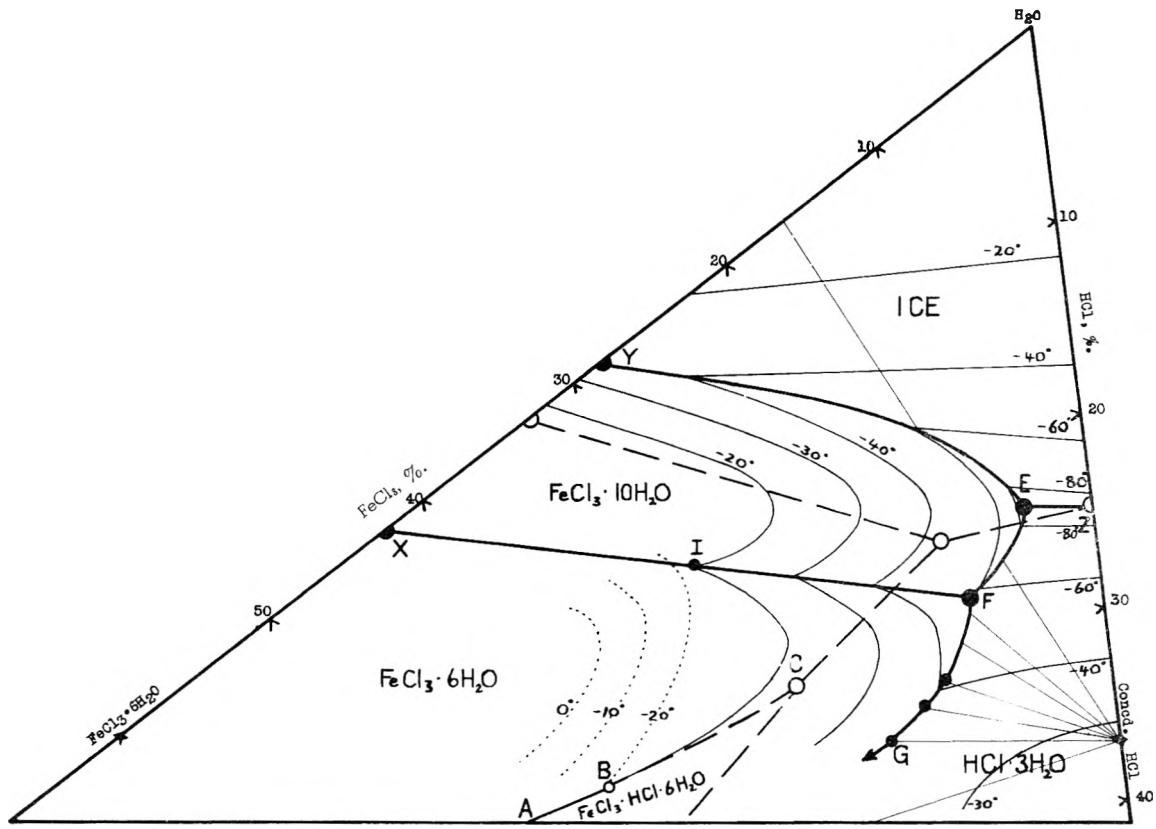

Fig. 3.—The system $FeCl_3 \cdot 6H_2O$-concd.–HCl–H_2O below 0°: ●, this research; ○, Roozeboom and Schreinemakers.

vertent inclusion of small amounts of solid during sampling, or by small temperature differences. Neither of these effects would alter the course of the tie-lines.

In order to determine the limits of stability of the decahydrate in the polytherm of the system $FeCl_3$–HCl–H_2O, the solubility of the hexahydrate in HCl solutions was also determined. Known complexes containing this phase were stirred from either under or supersaturation for from 1 to 20 hours. The results are included in Table II and Fig. 2.

In solutions containing up to about 13% HCl (the portion of the curve metastable with respect to the decahydrate), the data agree with those of Roozeboom and Schreinemakers[2] (broken line in Fig. 2), but at higher concentrations of HCl, $FeCl_3 \cdot 6H_2O$ is now found to considerably less soluble than previously reported. The curve is distinctly retrograde; the minimum solubility (19% $FeCl_3$) occurs when the solution contains 20.5% HCl. (The minimum solubility of the decahydrate at −20° is also about 19%, but in a solution containing 14% HCl.)

It should be noted that the isothermal curve drawn by Roozeboom and Schreinemakers was fixed by only four experimental points. Only one of these points (P) is in disagreement with the present determinations, but the shape of the isotherm has been changed significantly. Furthermore, a study of the older data shows that this one point was the only determination which defined this segment of the contours below 0°. The importance of this lies in the fact that although both Roozeboom's and the present curve terminate at point B, their directions of approach to B are considerably different. It was this direction of approach which led Roozeboom and Schreinemakers to erroneous speculations on the portion of the system (rich in HCl) which they did not investigate.

According to Roozeboom and Schreinemakers, point B lies on a curve of two phase saturation (AB) along which $FeCl_3 \cdot 6H_2O$ is in equilibrium with the double salt $FeCl_3 \cdot HCl \cdot 6H_2O$ (see Fig. 3). The direction of this polythermal curve was fixed by four points, but point B, on the −20° isotherm, is the limit of their experimental data. Roozeboom and Schreinemakers drew a reasonable extension of curve AB to C, the invariant solution saturated with $FeCl_3 \cdot 6H_2O$, $FeCl_3 \cdot HCl \cdot 6H_2O$ and $HCl \cdot 3H_2O$, which they estimated to lie at −60° and to contain 18.9% $FeCl_3$. The newly defined isotherm at −20° shows that these speculations are grossly in error. Roozeboom and Schreinemakers thought that curve ABC intersected the hexahydrate surface contours at a relatively large angle (see dotted curves in Fig. 3). However, the true curvature of the $FeCl_3 \cdot 6H_2O$ saturation surface is such that the direction of curve ABC is nearly parallel to the contours! Thus a solution at composition C is saturated at −23° rather than the previously estimated −60°, a discrepancy of nearly 40°.

In order to establish limits of stability of the decahydrate, the polythermal diagram of the system within the limits $FeCl_3 \cdot 6H_2O$–concd. HCl–H_2O was established by investigation of a number of cross-sections. The shapes of the saturation surfaces were determined from cooling or heating

TABLE III

INTERPOLATED POLYTHERMAL DATA IN THE SYSTEM $FeCl_3$–HCl–H_2O

Temp., °C.	Satd. soln., wt. % $FeCl_3$	HCl	Solid
	Cross-section 1		
−28.7	0	37.15	3[a]
−30	6.2	34.0	3
−35	20	30	3[c]
	Cross-section 2		
−30	5.4	33.8	3
−35	14.5	28.2	3 + 6[b]
−30	18.6	25.7	6
	Cross-section 3		
−30	2.8	34.9	3
−35	9.1	30.0	3
−37	11.2	28.4	3 + 6
−35	12.8	26.7	6
−30	16.1	24.6	6
	Cross-section 4		
−30	2.2	35.1	3
−35	6.3	32.2	3
−40	9.2	28.4	3
−42	10.2	27.6	3 + 6
−40	10.6	27.2	6
−30	12.7	25.3	6
−30	1.2	35.7	3
−40	6.1	29.5	3
−50	9.1	25.8	3[c]
−60	11.5	22.9	3[c]
	Cross-section 6		
−30	0.8	35.9	3
−40	4.7	30.2	3
−50	7.0	26.7	3
−60	8.8	23.9	3[c]
	Cross-section 7		
−50	3.5	28.6	3
−60	4.9	26.0	3
−70	6.0	23.7	3[c]
−80	7.0	21.5	3[c]
−89	7.5	20.0	3 + ice[c]
−80	8.2	18.5	ice[c]
−70	7.9	16.8	ice[c]
−60	9.8	14.7	ice
−50	10.7	12.7	ice
−40	11.8	10.4	ice
−30	12.9	7.7	ice
−20	14.3	4.3	ice
−10	16.3	0	ice

[a] 3 = $HCl·3H_2O$. [b] 6 = $FeCl_3·6H_2O$. [c] Metastable.

curves, or from observation of the temperature at which the saturating solid disappeared. Cooling curves were of limited usefulness because the phases readily formed supersaturated solutions. Most of the mixtures were cooled with acetone–Dry Ice or liquid nitrogen until precipitation occurred (after seeding and scratching) and then used for the heating determinations.

The polythermal determinations were made in seven series. In each series varying amounts of concd. HCl were mixed with a $FeCl_3$ solution of known composition, solid $FeCl_3·6H_2O$, or solid $FeCl_3$. The resultant data were thus linear cross sections of the polythermal system.

Cooling and heating curves were reproducible to ±0.2°, and the visual method to ±0.5°, although the accuracy of the latter method is probably not better than ±1°. In addition, it has been the author's experience that observations involving the disappearance of salt phases are often low by 2–3°, when compared with solubility determinations. This was found to be true in the case of the temperatures observed with $FeCl_3·6H_2O$ as solid phase. In addition to the data at −20°, two solubility determinations at −31.6° (Table II) were used to help correct this error. Uncorrected, the location of the univariant curve FG (Fig. 3) would have been error by about 1% $FeCl_3$ and 1°. The determinations at −31.6° confirmed the curvature of the hexahydrate solubility curve that had been found at −20° (Fig. 2).

In Fig. 4 the original data for the cross-sections are projected orthogonally on a plane parallel to the $FeCl_2$–H_2O face of the polythermal diagram. These projections were used to determine the curve of intersection of the $FeCl_3·6H_2O$ and $HCl·3H_2O$ saturation surfaces, and to establish the temperature contours listed in Table III and drawn in Fig. 3. The cross-sections are indicated in Fig. 3 by lines radiating from the composition of concd. HCl.

The portion of the ternary system covered in this

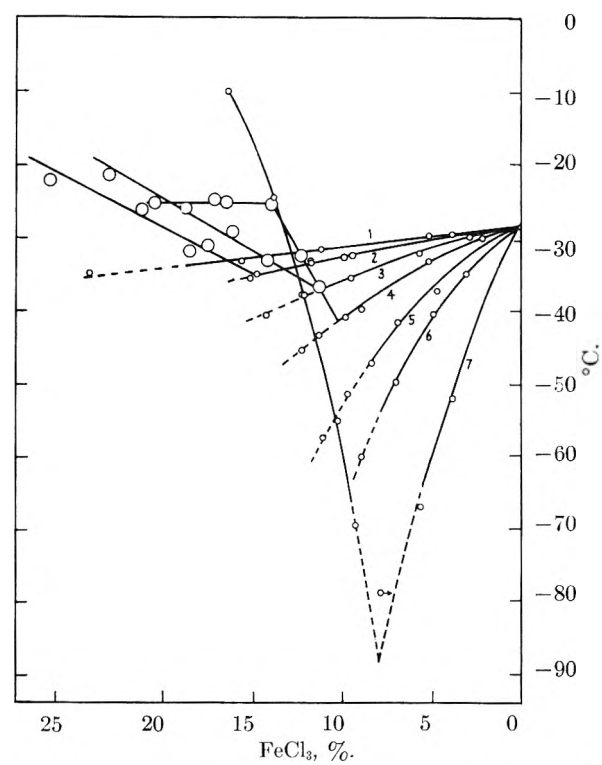

Fig. 4.—Cross sections of the system $FeCl_3$–HCl–H_2O. Size of circles indicates the approximate accuracy of the determinations.

research consists of four bivariant saturation surfaces which intersect along five univariant curves. Three curves intersect at transition point F and at eutectic E (Fig. 3). Only curves XF and GF were determined experimentally. Transition point F, lying at 7.8% $FeCl_3$, 24.7% HCl, −58°, is the point at which $FeCl_3 \cdot 6H_2O$, $FeCl_3 \cdot 10H_2O$ and $HCl \cdot 3H_2O$ are in equilibrium. It was located by extending curve XI (on which points X and I are experimental values) linearly until it intersected curve GF. Curve GF, the boundary between the $FeCl_3 \cdot 6H_2O$ and $HCl \cdot 3H_2O$ surfaces, was drawn through the points determined by thermal methods along cross sections 2, 3 and 4 (Fig. 4), corrected for possible observational errors. As might be expected, curve GF follows the curvature (contours) of the hexahydrate surface. Indeed, since ferric chloride did not precipitate along sections 5 and 6, it may curve even more than shown in Fig. 3, and point F may occur in a solution somewhat richer in $FeCl_3$.

The shape of the $HCl \cdot 3H_2O$ surface was fixed by the data along all six cross-sections, and from the binary system HCl–H_2O.[3] It should be pointed out that these data were much more reproducible than those involving $FeCl_3 \cdot 6H_2O$. Heating curves checked the visual data within ±0.2° when $HCl \cdot 3H_2O$ was the solid phase.

The ice field was plotted from the data of cross-section 7 and the two binary systems. The linearity of these isotherms confirms the work of Kurnakov and Nikitina.[4] It can be seen that the contours of the ice and $HCl \cdot 3H_2O$ surfaces are nearly parallel at the intersection of the two fields, and hence the direction of curve ZE is fixed. Furthermore, the temperature of the ternary eutectic E cannot be much lower than that of the HCl–H_2O binary eutectic Z.

Because of the slowness of precipitation of the decahydrate, no experimental data were determined along curve XF. The isotherms on the decahydrate surface were drawn to parallel that found at −20°, using the known contours of the other surfaces and the binary system as a guide. From their shape, it is fairly certain that curve XF must describe an arc convex to the water axis of the diagram. Addition of HCl to the binary $FeCl_3$–H_2O eutectic Y causes a sharp decrease in the concentration of $FeCl_3$ in the solution. By extending the decahydrate isotherms below −35° (using the metastable extension of the binary solubility curve as a guide), it can be seen that curve YE begins its course by paralleling curve XIF. As it approaches the eutectic E, it curves more sharply, following in general the shape of the decahydrate surface as it intersects the nearly planar ice field. Thus located, the eutectic should lie at about 4.0% $FeCl_3$, 22.5% HCl, at −88°. Ice, $FeCl_3 \cdot 10H_2O$ and $HCl \cdot 3H_2O$ saturate the solution.

Curve EF must similarly follow the surface intersections. Since the decahydrate did not form during the cross-section experiments, no direct data defining its course were obtained.

It may seem from Fig. 3 that the decahydrate is the stable saturating phase over a fairly wide range of temperatures and solution compositions, and that it (not the hexahydrate) saturates the eutectic solution. The results of this investigation may be compared with the speculations of Roozeboom and Schreinemakers (broken lines) for the system.[5] The presence of the decahydrate, of course, introduces fundamental changes in the diagram but, aside from this, both the locations and temperatures of the univariant curves were incorrectly estimated.

It may be pointed out that curve FG must eventually meet Roozeboom and Schreinemakers' curve AB, but the nature of this junction is beyond the scope of this research. Because of the positions and directions of these curves it is not clear where this junction occurs. AB may curve toward FG, or point B may have been incorrectly located. Another possibility is that a portion of the presently defined $FeCl_3 \cdot 6H_2O$ surface is metastable with respect to $FeCl_3 \cdot HCl \cdot 6H_2O$, and that the extension of curve AB intersects curve FG between F and G. In any case the role of the decahydrate would not be affected.

Acknowledgment.—The author is grateful to Dr. A. Langley Searles for his help in maintaining the solid phases at low temperatures.

(3) A. Seidell, "Solubilities of Inorganic and Metal Organic Compounds," 3rd Ed., Vol. 1, D. Van Nostrand Co., New York, N. Y., 1953, p. 571.

(4) N. S. Kurnakov and E. A. Nikitina, *Bull. acad. sci. U.R.S.S., Classe sci. math. nat., Ser. chim.*, 433 (1938).

(5) The original data of Roozeboom and Schreinemakers, plotted in moles per 100 moles H_2O are also reproduced in A. Findlay and A. N. Campbell, "The Phase Rule and Its Applications," Longmans, Green and Co., New York, N. Y., 1938, p. 264. A diagram plotted on triangular coördinates which indicates the various speculative as well as experimental curves appears in H. W. B. Roozeboom, "Der Heterogenen Gleichgewichte," Vol. 3, Vieweg und Sohn, Braunschweig, Germany, 1911, p. 176.

THE QUENCHING OF FLAMES OF PROPANE–OXYGEN–ARGON AND PROPANE–OXYGEN–HELIUM MIXTURES

BY A. E. POTTER, JR., AND A. L. BERLAD

Contribution from the Lewis Flight Propulsion Laboratory of the National Advisory Committee for Aeronautics, Cleveland, Ohio

Received June 27, 1955

An experimental study was made of the quenching of helium– and argon–oxygen–propane flames. Lower flammability limits also were measured for these flames. The effect on quenching distance of the replacement of helium by argon as predicted by thermal and diffusional quenching equations was compared with the observed effect. The results of this comparison favor the thermal quenching equation.

The replacement of one inert gas by another in an inflammable mixture produces interesting and useful changes in the combustion properties of the mixture. For example, if argon is replaced by helium, while combustible and oxygen concentrations are held constant, only diffusion coefficients and thermal conductivities are affected; equilibrium flame temperatures and compositions remain unchanged. Since the thermal conductivity is affected to a different extent than the diffusion coefficient, the effect on any flame property can be used in an attempt to distinguish between thermal and diffusional mechanisms. In this paper, the influence of inert diluents on the process of flame quenching will be considered.

The study of flame quenching depends on a simple experiment. A flame is introduced into one end of a tube filled with a combustible mixture. The flame will either burn through the length of the tube or will be extinguished (quenched) by the tube. Experiments show that the ability of a flame to get through the tube depends on several factors: (1) pressure, (2) temperature, (3) kind of fuel, oxidant and inert diluent, (4) relative concentrations of fuel, oxidant and inert diluent and (5) the cross-sectional shape and size of the tube. Usually, a tube of simple shape such as a cylinder is used for the experiment, and the tube size which will just quench a flame found as a function of one variable, holding the other constant.

There appear in the literature three sets of data for the effect on quenching distance of the replacement of helium by argon; two for hydrogen–oxygen–inert flames,[1,2] and one for methane–oxygen–inert flames.[3] Quenching distance was measured as a function of fuel concentration in these studies. Mellish and Linnett[4] have discussed the data for the methane system in terms of the thermal treatments of quenching available at that time. They found fair agreement between experiment and the theory of Friedman.[1]

Recently, a diffusional quenching equation[5] has been proposed. This equation correlates the effect on quenching of such diverse factors as fuel type,[5] tube geometry,[6] fuel and oxygen concentrations,[5,7] and temperature.[8] A thermal analog of this equation has been developed,[9] and shown to correlate the same quenching data satisfactorily.

The two equations predict effects of different extent when helium is replaced by argon in an inflammable mixture. Thus, comparisons with experiment should indicate which of the two approaches is the more useful. Consequently, a study was made of the effect produced by replacement of helium by argon on the quenching of propane–oxygen–inert flames. The quenching distance was measured as a function of both fuel concentration and pressure. In addition, lower flammability limits were measured, since values of this quantity are necessary for calculation of the effects predicted by the diffusional equation.

Experimental

Materials.—The inflammable mixtures for the quenching work were prepared from propane (manufacturer's stated purity, 99+%) and inert–oxygen mixtures for which the manufacturer's stated percentage of oxygen was 20.8 ± 0.2%. Inert–oxygen mixtures for lower flammability limit determinations were prepared and found by analysis to have 20.8 ± 0.1% oxygen.

Quenching Distance.—The quenching measurements were were made by determination of the lowest pressure at which a flame burning atop a rectangular slot burner would flash back through the rectangular burner channel when flow to the burner was interrupted. The burner channel width (identified as the rectangular quenching distance, d_r) and the equivalence ratio were varied so as to obtain limiting pressure as a function of equivalence ratio for various rectangular quenching distances. The quenching distance burner, the sonic orifice gas metering system and the arrangements for maintaining any desired pressure around the burner have been described previously.[7] The walls of the burner were held at 40°. The data obtained for the helium- and argon-containing flames are presented in Table I.

Lean Flammability Limit.—Essentially, the procedure recommended by Coward and Jones[10] and Burgoyne and Williams-Leir[11] was used to determine the lean flammability limit. A 5.3 cm. i.d. tube, 115 cm. long was filled with the test mixture at atmospheric pressure. The mixture was ignited at the lower end by introduction of an alcohol flame.

(1) R. Friedman, "Third Symposium on Combustion and Flame and Explosion Phenomena," The Williams and Wilkins Co., Baltimore, Md., 1949, pp. 110–120.

(2) B. Lewis and G. von Elbe, "Combustion, Flames and Explosions of Gases," Academic Press, Inc., New York, N. Y., 1951, p. 414.

(3) M. V. Blanc, P. G. Guest, B. Lewis and G. von Elbe, *J. Chem. Phys.*, **15**, 798 (1948); see also B. Lewis and G. von Elbe, "Combustion, Flames and Explosions of Gases," Academic Press, Inc., New York, N. Y., 1951, p. 406.

(4) C. E. Mellish and J. W. Linnett, "Fourth Symposium (International) on Combustion," The Williams and Wilkins Co., Baltimore, Md., 1953, pp. 407–420.

(5) D. M. Simon, F. E. Belles and A. E. Spakowski, "Fourth Symposium (International) on Combustion," The Williams and Wilkins Co., Baltimore, Md., 1953, pp. 126–138.

(6) A. L. Berlad and A. E. Potter, Jr., "Fifth Symposium (International) on Combustion," Reinhold Publishing Corp., New York N. Y., 1955, pp. 728–735.

(7) A. L. Berlad, THIS JOURNAL, **58**, 1023 (1954).

(8) F. E. Belles and A. L. Berlad, "Chain Breaking and Branching in the Active-Particle Diffusion Concept of Quenching," NACA TN 3409.

(9) A. E. Potter, Jr., and A. L. Berlad, "A Thermal Equation for Flame Quenching," NACA TN 3398.

(10) H. F. Coward and G. W. Jones, U. S. Bureau Mines, Bull. No. 503, 1952.

(11) J. H. Burgoyne and G. Williams-Leir, *Fuel*, **27**, 113 (1948).

TABLE I

QUENCHING CONDITIONS FOR ARGON- AND HELIUM-OXYGEN-PROPANE FLAMES. LIMITING PRESSURE AS A FUNCTION OF EQUIVALENCE RATIO FOR VARIOUS QUENCHING DISTANCES[a]

(a) Propane with 20.8% oxygen–79.2% argon mixtures

φ	P, atm.	φ	P, atm.	φ	P, atm.
d_r, 0.244; d_p, 0.242		0.929	0.289	1.618	0.320
		.997	.278	1.812	.463
0.585	0.897	1.116	.273	1.961	.635
.663	.692	1.308	.297	2.067	.837
.750	.571	1.477	.383		
.867	.493	1.566	.490	d_r, 0.762; d_p, 0.748	
.883	.462	1.800	.649		
1.011	.420	1.939	.822	0.462	0.729
1.100	.408			.470	.457
1.222	.422	d_r, 0.508; d_p, 0.502		.535	.296
1.388	.491			.628	.208
1.491	.561	0.467	0.845	.629	.208
1.618	.693	.497	.634	.732	.169
1.760	.896	.545	.454	.851	.144
		.643	.315	.920	.138
d_r, 0.355; d_p, 0.352		.730	.264	.998	.131
		.775	.242	1.129	.129
0.517	0.851	.833	.220	1.298	.139
.552	.657	.915	.208	1.556	.183
.606	.520	.977	.202	1.808	.296
.712	.394	1.047	.195	2.003	.460
.819	.324	1.338	.218	2.124	.801
.872	.309	1.572	.301	2.133	.623

(b) Propane with 20.8% oxygen–79.2% helium mixtures

d_r, 0.508; d_p, 0.502		0.995	.323	1.410	.247
		.997	.326	1.445	.272
0.741	0.861	1.084	.293	1.547	.333
.821	.687	1.086	.309	1.692	.442
.904	.545	1.198	.291	1.759	.574
1.018	.462	1.202	.308	0.653	.410
1.129	.430	1.302	.303	.714	.334
1.221	.426	1.304	.327	.764	.281
1.296	.435	1.492	.407	.870	.234
1.400	.471	1.630	.540	.873	.235
1.437	.546	1.723	.691	.964	.212
1.557	.683			.966	.209
1.648	.852	d_r, 1.016; d_p, 0.991		1.095	.196
				1.097	.193
d_r, 0.610; d_p, 0.601		1.230	0.195		
		1.436	.215	d_r, 1.270; d_p, 1.231	
0.676	0.797	1.523	257		
.728	.660	1.526	.253	0.672	0.341
.800	.539	1.628	.324	.732	.303
.936	.423	1.633	.317	.863	.222
1.024	.398	1.738	.457	.950	.199
1.133	.378	1.748	.426	1.100	.183
1.222	.380	1.805	.507	1.230	.183
1.401	.439	1.805	.526	1.303	.191
1.304	.390			1.426	.222
1.460	.527	d_r, 1.118; d_p, 1.088		1.463	.198
1.690	.660			1.552	.231
1.748	.834	0.687	0.396	1.677	.390
		.759	.316	1.692	.307
d_r, 0.762; d_p, 0.748		.892	.247	1.794	.420
		1.006	.221	1.874	.526
0.661	0.683	1.097	.214		
.704	.507	1.217	.215		
.831	.394	1.320	.229		

[a] d_r and d_p are in cm.

The upper end of the tube was closed. The data obtained with this apparatus are shown in Table II.

TABLE II

LOWER FLAMMABILITY LIMITS

Inert–oxygen mixture	Lower limit, % propane
20.8% O_2–79.2% He	1.92
20.8% O_2–79.2% A	1.79
21.0% O_2–79.0% N_2 (air)[a]	2.38
21.0% O_2–79.0% N_2 (air)[b]	2.37

[a] This research. [b] Reference 11.

The last helium-containing mixture which could be ignited (1.93% propane) acoustically excited the tube, producing a sound judged to be the fundamental mode of the half-open tube. Richer mixtures did not excite the tube.

Theoretical

List of Symbols

- A constant which appears in the diffusional equation; defined as the fraction of the total no. of molecules present which must react in the reaction zone in order for the flame to propagate
- b_r rectangular slot length
- C_p heat capacity, cal./(°K.)(mole)
- c concentration, molecules/cc.
- D diffusion coefficient at T_0 and 1 atm., cm.²/sec.
- d_c cylindrical quenching distance
- d_p plane parallel plate quenching distance
- d_r rectangular slot quenching distance
- F constant which appears in the thermal quenching equation; defined as the fraction of reaction events normally occurring upon passage of a flame which must take place in the reaction zone for flame propagation, or the fraction of the total heat produced by combustion which must be contained in the reaction zone for flame propagation.
- G constant associated with quenching geometry (12 for plane parallel plates, 32 for cylinders, $12\left[1 - 0.3\left(\frac{d_r}{b_r}\right) - 0.047\left(\frac{d_r}{b_r}\right)^2\right]^{-2}$ for rectangular slots)
- k rate constant for reaction of active particles and fuel molecules, cc./(molecules)(sec.)
- N Avogadro's number
- n exponent describing the pressure dependence of quenching distance, $d\alpha P^{-n}$
- P pressure, atm.
- T temperature, °K.
- U burning velocity, cm./sec.
- w reaction rate, molecules/(cc.)(sec.)
- X mole fraction
- λ thermal conductivity, cal./(cm.)(sec.)(°K.)
- φ equivalence ratio

Subscripts:

- A argon-containing mixture
- F flame
- f fuel
- He helium-containing mixture
- i active particle species
- L lean flammability limit
- o initial
- r reaction zone

Simon, Belles and Spakowski[5] have proposed a diffusional quenching equation based on the hypothesis that the number of reaction events per unit volume in the gas ahead of the burning zone must not fall below some critical value in order for the flame to propagate. They define this critical value to be a constant fraction, A, of the total number of molecules present per unit volume. From this criterion for flame propagation, it is shown that the quenching distance for any channel geometry is given by

$$d = \left[\left(\frac{AG}{k}\right)\left(\frac{T_f^2}{T_0^2 c_f}\right)\left(\frac{1}{\sum_i P_i/P_i}\right)\right]^{1/2} \qquad (1)$$

This equation has been used to correlate a wide variety of quenching data.[5–8] One disadvantage of this equation is that it does not seem to be suitable for rich mixtures, possibly because the reaction mechanism implicit in the equation (the active particle-fuel reaction) is unsuitable. In an attempt to overcome this difficulty and extend the quenching concepts expressed in reference 5 to rich mixtures, a thermal analog to this equation was derived.[9] The thermal equation was derived using the same initial hypothesis as the diffusional equation. A difference between the two derivations is in definition of the number of reactions per unit volume which must occur in the reaction zone for flame propagation. For the thermal equation, this number is assumed to be a constant fraction, F, of the total number of reactions occurring when a flame passes through a unit volume. This assumption results in a criterion for flame propagation which states that the reaction zone must contain a critical fraction, F, of the total heat produced by combustion in order for the flame to exist. The final form of the thermal quenching equation is

$$d = \left(\frac{FGN\lambda_r X_f}{C_{p,r}w}\right)^{1/2} \qquad (2)$$

Equation 2 differs from other thermal quenching equations in that burning velocity or ignition energy does not appear. Also the geometric constant, G, is known or can be calculated for any shape of quenching tube. In this equation, the rate-controlling reaction is not specified. Consequently, any suitable reaction may be chosen as rate-determining. Choice of either the oxygen-fuel or active-particle-fuel reaction resulted in an equation which successfully correlated the effects of tube geometry, oxygen concentration, temperature and pressure on quenching distance for propane–oxygen–nitrogen flames.[9] Used with the oxygen–fuel reaction, the equation correlated the effect of propane concentration on quenching distance for both rich and lean mixtures. If the equation was used with the active-particle–fuel reaction, only data for lean and slightly rich ($\varphi = 1.2$) mixtures were correlated.

Replacement of helium by argon in an inflammable mixture should affect only diffusion coefficients and thermal conductivities. Thus, terms involving equilibrium flame temperature, composition and reaction rates in the quenching equations will cancel one another if the ratio of quenching distances for the two systems is found at constant fuel and oxygen concentration and total pressure. The predicted ratios are then quite simple, and can be written

(a) diffusional quenching equation

$$\left(\frac{d_A}{d_{He}}\right)_{diff} = \left[\frac{A_A}{A_{He}} \frac{\left(\sum_i \frac{P_i}{D_i}\right)_{He}}{\left(\sum_i \frac{P_i}{D_i}\right)_A}\right]^{1/2} \qquad (3)$$

(b) thermal quenching equation

$$\left(\frac{d_A}{d_{He}}\right)_{thermal} = \left(\frac{F_A}{F_{He}} \frac{\lambda_{r,A}}{\lambda_{r,He}}\right)^{1/2} \qquad (4)$$

It is now necessary to examine the constants A and F which appear in the ratios. Because of the approximations made in derivation of the quenching equations, the exact nature of these constants is not clear. The constant A which appears in the diffusion equation has been found[5] to be proportional to X_L the fuel mole fraction at the lean flammability limit by calculation of A values from data for several different hydrocarbons. The best way to define F is to apply to the thermal quenching equation the procedures used in reference 5 to find A. This was done in the following way. First, as in reference 5, the rate-determining reaction step was assumed to be the active-particle–fuel reaction. Equation 2 can then be written as

$$d = F^{1/2}\left[\frac{GN\lambda_r X_f}{C_{p,r}kc_f \sum_i c_i}\right]^{1/2} \qquad (5)$$

Then, values of the bracketed quantity in equation 5 were calculated for the quenching data reported in reference 5 for propane, 2,2,4-trimethylpentane and ethylene flames with air. When quenching distance was plotted against the quantity in brackets, it was found that the data for all three hydrocarbons could be fairly represented by a single line. This indicates that F is independent of fuel type to a good approximation.

The average deviation of data points from this line is 7.7%. The diffusional equation of reference 5 correlates the same data with an average deviation of 4.1%. The values of k used for this calculation were obtained by Simon[12] from burning velocity measurements. Active particle concentrations were taken to be 0.7 of the equilibrium flame concentrations and the reaction zone temperature was assumed to be 0.7 of the adiabatic flame temperature. The calculated adiabatic equilibrium flame temperatures and compositions were taken from reference 5.

It seems, therefore, that for air–hydrocarbon mixtures, A is proportional to X_L lean limit fuel mole fraction, and F is a constant, independent of fuel type. It seems reasonable to extend these findings to the helium– and argon–oxygen–propane systems. Equations 3 and 4 can then be rewritten as

$$\left(\frac{d_A}{d_{He}}\right)_{diff} = \left(\frac{X_{L,A}}{X_{L,He}} \frac{\sum_i [P_i/D_i]_{He}}{\sum_i [P_i/D_i]_A}\right)^{1/2} \qquad (6)$$

$$\left(\frac{d_A}{d_{He}}\right)_{thermal} = \left(\frac{\lambda_{r,A}}{\lambda_{r,He}}\right)^{1/2} \qquad (7)$$

In order to use equation 6, values of the lean flammability limit are necessary. Since no values are reported in the literature for helium– and argon–oxygen–propane flames, experimental measurements were made of these quantities.

Conclusions drawn from a comparison of experiment and the predictions of equations 6 and 7 are subject to two uncertainties. First, while the assumptions made concerning A and F seem quite reasonable, it is possible that these empirical constants may contain factors unaccounted for in changing from one inert gas to another. Second, considerable uncertainty exists concerning the calculation of transport properties of mixtures at high temperatures. In an effort to reduce this second possibility of error as much as possible, methods which were believed to be among the best available

(12) D. M. Simon, *J. Am. Chem. Soc.*, **73**, 422 (1951).

were used for transport coefficient calculations. These methods are described in the appendix.

Results and Discussion

The quenching distances observed were for long rectangular slots of various length to width ratios. In order to reduce all the data to a common basis, the observed quenching data were converted to infinite plane parallel plate data by means of the equation[6]

$$\frac{d_p}{d_r} = 1 - 0.300\left(\frac{d_r}{b_r}\right) - 0.047\left(\frac{d_r}{b_r}\right)^2 \qquad (10)$$

Here, d_p is the separation of plane parallel plates of infinite extent which quenches exactly as does a rectangular slot of width d_r, and length b_r. (The burner slot length, b_r, was 12.7 cm. in these experiments.) The calculated d_p values are given in Table I along with the observed d_r values.

Next, the limiting pressure was plotted against equivalence ratio using the data in Table I. A different curve is obtained for each plane parallel plate quenching distance, d_p. These curves were then cross-plotted so as to determine quenching distance as a function of limiting pressure at constant equivalence ratio. Data of this kind fit an equation of the form $(d/d^\circ) = (P/P^\circ)^{-n}$. The pressure exponent n was obtained by the method of least squares from a log plot of d against P. The values obtained are given in Table III.

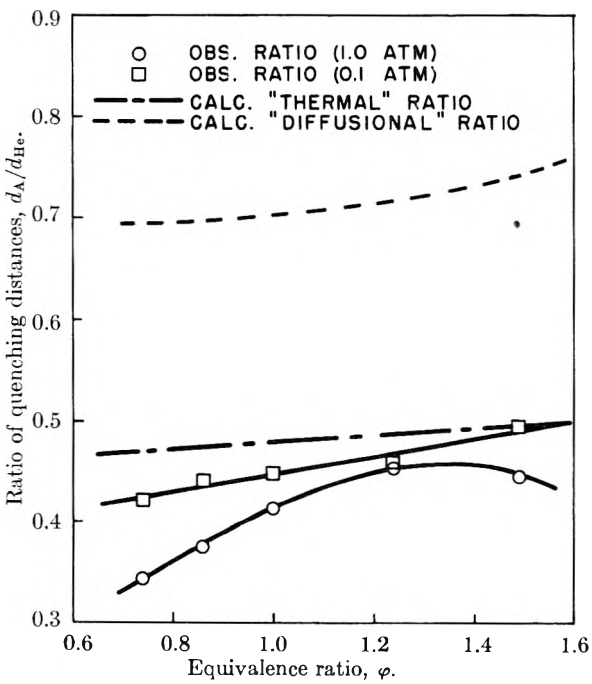

Fig. 1.—Comparison of observed and predicted ratios of quenching distance for argon– and helium–oxygen–propane flames.

It is interesting to compare the pressure dependence of quenching distance for the two systems. From Table III, it can be seen that the pressure exponents (n) at a given equivalence ratio differ from one another with a regular trend to larger differences as φ differs from 1.0. This is surprising, since no such difference is expected on the basis of either theory. Replacement of argon by helium should not affect the chemical processes which give rise to the pressure dependence of d. The differences are not much larger than the expected experimental error, but the regularity of the difference argues for its reality. This side effect may be related to other anomalies observed in flames containing helium. Morgan and Kane[13] have observed a considerable effect of burner size on the burning velocity for helium-containing flames.

Table III

Quenching Distance as a Function of Pressure at Constant Equivalence Ratio; Constants[a] in the Equation $\frac{d_p}{d_p^\circ} = \left(\frac{P}{P^\circ}\right)^{-n}$

Equiv. ratio, φ	d_p°, c.m. Helium "air"	d_p°, c.m. Argon "air"	n Helium "air"	n Argon "air"	Av. dev. of limiting pressure, % Helium "air"	Av. dev. of limiting pressure, % Argon "air"
0.593	...	0.214	..	0.86	..	0.8
.738	0.427	.147	0.81	.90	4.1	1.3
.864	.316	.119	.87	.94	2.2	1.2
1.00	.253	.104	.93	.97	2.8	1.0
1.24	.229	.104	.98	.98	3.4	1.0
1.49	.312	.139	.90	.95	4.1	1.6

[a] P° is taken as one atmosphere; then d_p° is the quenching distance at one atmosphere.

As the next step in treatment of the data, ratios of d_A to d_{He} at constant propane and oxygen concentrations and pressure were calculated over a range of equivalence ratios. Smoothed values of the quenching distance, found from the equations in Table III, were used for this calculation. Since the pressure dependence of quenching distance differs slightly for the two systems, the ratio of quenching distances displays a small pressure dependence. Consequently, ratios were calculated at both 0.1 and 1.0 atmosphere. These ratios are plotted against equivalence ratio in Fig. 1. In this figure, there are also plotted the ratios calculated from equations 6 and 7. The "thermal" ratios (calculated from eq. 7) agree quite well with the observed ratios. The "diffusional" ratios (calculated from eq. 6) are all about twice the observed ratios. Had the constant A been assumed to be unaffected by replacement of argon by helium, the "diffusional" ratios would have been increased about 3.5%.

Data for the quenching of propane–air flames are available from the literature.[5,7,14] Consequently, it is possible to compare observed and predicted effects when argon or helium is replaced by nitrogen. A useful interpretation of such a comparison is difficult, since replacement of a rare gas by nitrogen affects not only the transport coefficients, but also temperature and therefore reaction rates in the flame. This is because the heat capacity of the mixture is altered by the substitution. As a result, when the ratio of d_{N_2} to d_A or d_{He} is written according to equations 1 and 2, terms which involve flame temperature and reaction rate do not cancel. This greatly complicates the situation. Before, when dealing with argon and helium "airs," only the transport process had to be

(13) G. H. Morgan and W. R. Kane, "Fourth Symposium (International) on Combustion," The Williams and Wilkins Co., Baltimore Md., 1953, pp. 313–320.

(14) R. Friedman and W. C. Johnston, *J. Appl. Phys.*, **21**, 791 (1950).

considered. Now, not only the transport process, but also the rate-controlling reaction must be specified. In the case of the diffusional quenching equation, the rate controlling reaction is assumed to be between active particles and fuel molecules. For the thermal equation, two reactions have been used with success: the active-particle–fuel reaction and the oxygen–fuel reaction. Thus, one ratio may be calculated from the diffusional quenching equation and two from the thermal quenching equation. These three types of ratios were calculated and are shown in Table IV with the observed values (found from data given in ref. 7). Here, it is seen that the combination which best agrees with experiment for both the helium and argon systems is the thermal equation used with the active-particle–fuel reaction.

TABLE IV

Equiv. ratio, φ	Obsd. d_{N_2}/d_A	Calcd., d_{N_2}/d_A		
		Diffusional eq.	Thermal equation: Active-particle–fuel reaction	Thermal equation: Oxygen fuel reaction
(a) d_{N_2}/d_A at one atmosphere				
0.738	2.27	2.26	2.25	3.01
1.00	1.91	1.90	1.96	2.80
1.49	2.56	3.48	3.11	3.05
(b) d_{N_2}/d_{He} at one atmosphere				
0.738	0.78	1.58	1.07	1.43
1.00	.79	1.34	0.94	1.35
1.49	1.14	2.60	1.55	1.52

The calculated ratios were found using the assumptions concerning the rate-controlling reactions presented in references 5 and 9. Equilibrium flame temperatures and compositions necessary for the propane-air flames were taken from reference 7.

Concluding Remarks

It was found that a thermal quenching equation satisfactorily predicted the effect on quenching distance of replacement of argon by helium. A similar quenching equation, based on diffusional effects, did not. The success of the thermal equation should not be interpreted as conclusive evidence that flame quenching is entirely a thermal process, because both thermal and diffusional equations are, in reality, quite approximate. The true relative importance of thermal and diffusional effects can only be evaluated when a complete theory of quenching, including both heat and mass transfer, becomes available.

Appendix—Calculations

Equilibrium adiabatic flame temperature and product compositions were calculated by the matrix method,[15] using tables of thermodynamic constants[16] and heat of formation values of propane.[16]

Thermal conductivities for the Lennard-Jones (6–12) potential at 0.7 equilibrium adiabatic flame temperature were calculated for individual components of the unburned gas, using the procedures and data given in reference 17, chapter 8. Mixture conductivities were calculated by the methods described in reference 18. The viscosity equation given by Hirschfelder[17] was used in the Lindsay–Bromley mixing rule rather than the Sutherland equation. For propane–oxygen–nitrogen mixtures, a simple linear mixing rule was used because of the similar conductivities of oxygen and nitrogen.

The procedure used for calculation of the diffusion coefficients for the various active particles is described in reference 7.

Acknowledgment.—The authors wish to thank Dr. R. S. Brokaw of this Laboratory for helpful discussions concerning calculation of the transport coefficients.

(15) V. N. Huff, S. Gordon and V. E. Morrell, NACA Rep. 1037, 1951 (Supersedes NACA TN's 2113 and 2161.)

(16) F. D. Rossini, *et al.*, Nat. Bur. Standards, Circular C461 (1947).

(17) J. O. Hirschfelder, C. F. Curtiss and R. B. Bird, "Molecular Theory of Gases and Liquids," John Wiley and Sons, Inc., New York, N. Y., 1954.

(18) A. L. Lindsay and L. H. Bromley, *Ind. Eng. Chem.*, **42**, 1508 (1950).

ADSORPTION ISOTHERMS, ISOBARS AND ISOSTERES OF DIBORANE ON BORON NITRIDE AND PALLADIUM ON CHARCOAL

BY HAROLD C. BEACHELL AND HAROLD S. VELORIC[1]

Department of Chemistry, University of Delaware, Newark, Delaware

Received June 29, 1955

Adsorption isotherms, isobars and isosteres of diborane on boron nitride and palladium on charcoal were obtained in the pressure range of 200 to 750 mm. and temperature range of 180 to 300°K. The sorption isotherms were found to be Langmuir, Type I, with negligible hysteresis even at the lowest temperatures. Fit of the Langmuir low pressure adsorption isotherm to the data was found in the case of palladium on charcoal. Calculations of the isosteric heat of adsorption as a function of the quantity of gas adsorbed were made. It was concluded that the adsorption process represents pure Van der Waals adsorption which fits the Langmuir hypothesis for low pressure adsorption. No evidence was found for chemisorption.

Introduction

In view of the numerous gas phase reactions of diborane a systematic investigation of the sorption properties of the compound was initiated. A complete study of the adsorption phenomena includes isotherms, isobars and isosteres.

The Langmuir[2] adsorption isotherm is frequently employed to express the variation of adsorbent, at constant temperature, with pressure.

$$\frac{X}{m} = \frac{abp}{1 + ap}$$

At low pressure the isotherm simplifies to

$$\frac{X}{m} = K_0 P$$

A great deal of additional work[3] has shown that in many cases when the surface is clean and the pressure is low curious relationships frequently are found[4] between the total amount of gas adsorbed and the temperature; at very low temperature the amount decreases with increasing temperature and then rises as the temperature increases. At the lower temperatures the adsorption is entirely van der Waals type, at higher temperatures the rate of chemisorption increases giving an increase in the total amount of adsorption. By this criterion the adsorption isobar is a good indication of the physical or chemical nature of adsorption.

Brunauer[5] has developed by thermodynamic means an indirect method of calculating the isosteric heat of adsorption.

$$\ln \frac{p^1}{p^2}\Big|_{\frac{x}{m}} = \frac{Q_{iso}}{RT} + K$$

The heats of van der Waals adsorption are of the same order of magnitude as the heats of liquefaction of gases. Ordinarily the heats of adsorption vary considerably with the amounts of gas adsorbed.

Experimental

Materials.—Boron nitride was of the highest available commercial purity. The palladium on charcoal was a commercially available surface active agent purchased from Baker and Adamson. Diborane was prepared by the method described by Shapiro and Smith.[6] The vapor pressure of the B_2H_6 at 185°K. was 22.5 mm. The purity of the gas was checked by infrared analysis.

Apparatus and Procedure.—The high vacuum system used was similar to the adsorption apparatus developed by Pease.[7] It consists of a high vacuum side, McLeod gage, closed end manometer with a leveling bulb attachment, a series of catalysts bulbs and a water cooled precision gas buret.

The dead space was measured by introducing "Matheson" helium from the gas buret at known temperature and pressure. The samples of boron nitride and palladium on carbon were prepared according to the method of Bischoff and Adkins.[8]

The temperature of the water-cooled gas buret was maintained to ±1°. The pressure was read on the closed end manometer to ±1 mm. The temperatures of the sample tube were obtained by placing about the tubes Dewar flasks containing ice-water, liquid nitrogen–carbon tetrachloride mixtures, liquid nitrogen–chloroform, liquid nitrogen–acetone, and liquid nitrogen–methanol mixtures. The temperatures were measured with a calibrated copper–constantan thermocouple. Diborane was passed from the gas buret into a catalyst bulb after the catalyst sample had been exposed to prolonged evacuation at 10^{-6} mm. The pressure of the system was varied at constant volume and temperature. The purity of the diborane was monitored with infrared analysis to make certain no chemical changes had taken place.

Results and Discussion

For the palladium on charcoal the adsorption was studied at pressures of 30 to 70 cm. and at temperatures varying from 200 to 300°K. In the case of the adsorption of diborane on boron nitride the temperature range was 180 to 315°K. and pressures varying from 18 to 75 cm. Each recorded point is the average of two measurements. Hysteresis effects even at the lowest temperatures were small enough to be neglected.

In this range of temperature and pressure all of the palladium on charcoal isotherms showed a linear variation with pressure. K_0 did not vary with temperature and was equal to 0.24 cc./g. cm. The diborane on charcoal isobar also showed a linear variation, the slope of each line being equal to −1.3 cc./g. K°. Lower temperatures could not be conveniently utilized since the gas liquefies at 181°K., higher temperatures were not investigated because the rate of decomposition becomes too large.[9,10]

The isotherms for diborane on boron nitride approximated the Langmuir type isotherm as the temperature was lowered. No break in the adsorption isobar was observed for either adsorbent. The adsorption isotherms are shown in Figs. 1 and 2. The

(1) H. S. Veloric, Ph.D. Dissertation, University of Delaware, Newark, Delaware, June 1955.

(2) I. Langmuir, *J. Am. Chem. Soc.*, **38**, 2267 (1916).

(3) J. W. McBain and Britton, *ibid.*, **52**, 2198 (1930).

(4) A. W. Gauger and H. S. Taylor, *ibid.*, **45**, 1920 (1923).

(5) S. Brunauer, "The Adsorption of Gases and Vapors," Princeton, New Jersey, 1943, p. 222.

(6) I. Shapiro and G. B. Smith, *J. Am. Chem. Soc.*, **74**, 901 (1952).

(7) R. N. Pease, *ibid.*, **45**, 1196 (1923).

(8) J. Bischoff and H. Adkins, *ibid.*, **47**, 823 (1925).

(9) R. P. Clarke and R. N. Pease, *ibid.*, **73**, 2132 (1951).

(10) J. K. Bragg and L. V. McCarty, *ibid.*, **73**, 2134 (1951).

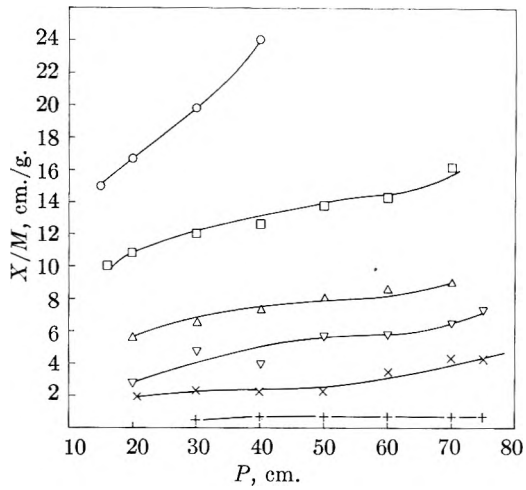

Fig. 1.—Adsorption isotherms B_2H_6 on BN: ○, T = 178°K.; □, 210; △, 251; ▽, 273· X, 296; +, 314.

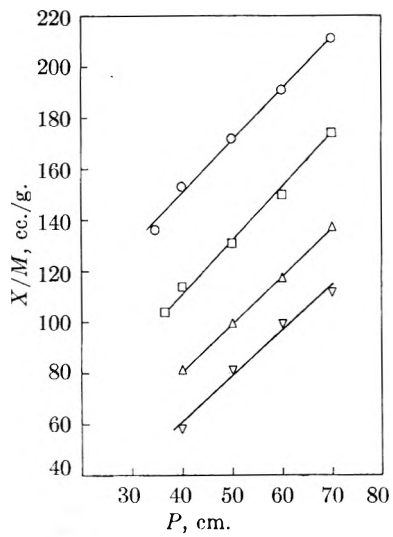

Fig. 2.—Adsorption isotherms diborane on Pd on charcoal: ○, T = 203°K.; □, 246; △, 273; ▽, 297.

diborane on charcoal isoster showed a good fit to a straight line when ln P was plotted *versus* $1/T$. The expected decrease of Q_{iso} with increased adsorption was observed. The calculated isosteric heats of adsorption corresponding to various values of X/m are given in Table I.

TABLE I

ISOSTERIC HEATS OF ADSORPTION CALCULATED FROM GRAPH 3

Adsorbent palladium on charcoal

X/m (cc./g.)	50	80	100	120	140	170
Q (kcal.)—net energy of adsorption	0.63	0.47	0.41	0.37	0.31	0.27

The diborane on boron nitride isoster showed a good fit to a straight line over a wide range of pressure. In this case Q_{iso} was independent of the value of X/m, which varied from 2 to 10, and was equal to 10 kcal./mole. The ratio of the heat of adsorption to the heat of liquefaction for this adsorbent is $(10 \times 10^3)/(3.8 \times 10^3) \simeq 2.6$.[11] This value is in good agreement, with the value of 2.5 obtained for other gases in this boiling range with various absorbents.[5]

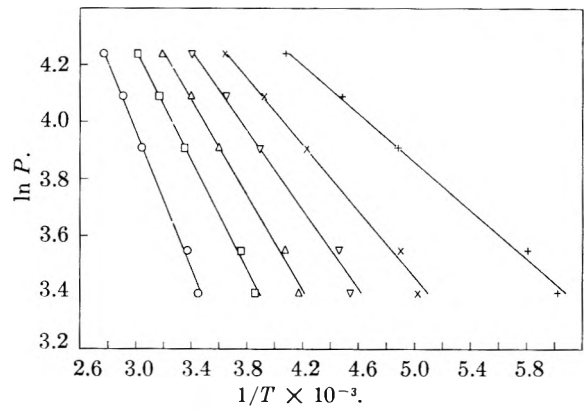

Fig. 3.—Isosteres B_2H_6 on Pd on charcoal: ○, X/M = 50; □, 80; △, 100; ▽, 120; × 140; +, 170.

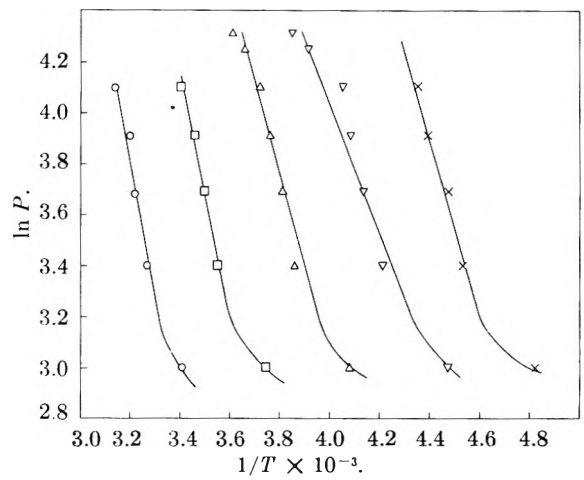

Fig. 4.—Adsorption isosteres of B_2H_6 on BN: ○, X/M = 2; □, 4; △, 6; ▽, 8; ×, 10.

The data indicate that the surface area of the charcoal catalyst is much larger than that of the boron nitride. Although the values of X/m are large for the palladium on charcoal no leveling off of the heat of adsorption is observed.

Conclusions

From the complete reversibility of adsorption the low isosteric heat of adsorption, and the continual decrease of adsorption with increasing temperature it is concluded that physical adsorption is taking place. The expected decrease of the isosteric heat of adsorption with increasing values of X/m was observed for the palladium on charcoal adsorbent. No evidence of decomposition was found.

(11) This value E_1 was calculated with the Trouton approximation.

MELTING POINT MEASUREMENTS OF THE SYSTEM HNO_3–N_2O_4–H_2O[1]

BY GERARD W. ELVERUM, JR., AND DAVID M. MASON[2]

Jet Propulsion Laboratory, Pasadena, California

Received July 5, 1955

The solid–liquid equilibrium phase behavior of the HNO_3–N_2O_4 system was determined from melting point measurements near atmospheric pressure over the range of composition 0 to 100 weight % N_2O_4. The existence of a solid compound is indicated which consists of 2 moles of HNO_3 and 1 mole of N_2O_4. The solid–liquid phase behavior for the HNO_3–N_2O_4–H_2O system was similarly measured over the range of composition of 0 to 25 weight % N_2O_4 and of 0 to 18 weight % H_2O. The minimum melting points in the composition range studied for the HNO_3–N_2O_4 system were −65° at the eutectic mixture of 25.6 weight % N_2O_4 and for HNO_3–N_2O_4–H_2O system about −78° at the eutectic mixture of 18 weight % N_2O_4 and 4 weight % H_2O. The interpretation of these data in the light of chemical equilibria which occur in nitric acid solutions is discussed.

I. Introduction

In connection with a program at the Jet Propulsion Laboratory for the study of several of the physical and chemical properties of fuming nitric acid,[3] the equilibrium melting points of the system HNO_3–N_2O_4–H_2O have been measured.

Data on the solid–liquid and liquid–liquid phase relations of the binary system HNO_3–N_2O_4 were published by Pascal and Garnier[4] in 1919. Based on their interpretation of cooling curve thermal data, these data indicated that a eutectic mixture containing 18 weight % N_2O_4 froze at a temperature of −73°, and that a solid compound corresponding to the formula $N_2O_4 \cdot N_2O_5 \cdot H_2O$ should exist at 42.2 weight % N_2O_4.

Measurements of the liquid–solid phase equilibria in the system HNO_3–H_2O were made by Kuster and Kremann.[5] These data have been used for the HNO_3–H_2O boundary of the ternary diagram given in this paper. The freezing point of pure HNO_3 has been found by Dunning and Nutt[6] to be −41.62 ± 0.05° based on the maximum freezing point obtained at 50 mole % N_2O_5 for the binary system N_2O_5–H_2O. Forsythe and Giauque[7] report a value of −41.59°. The value found in the present study is −41.7°.

The work of Pascal and Garnier[4] indicates that a two-liquid phase region exists in the binary system HNO_3–N_2O_4 above 48 weight % N_2O_4. This region was studied in detail by Klemenc and Spiess[8a] and by Corcoran, *et al.*,[8b] and both sets of data are reproduced in the present paper to show the complete two-phase data for the HNO_3–N_2O_4 system.

The freezing point of pure N_2O_4 has been reported by Whittaker, *et al.*,[9] as −11.23°. Giauque and Kemp[10] give −11.20° as the equilibrium melting point, and the value of −11.2° from the present investigation agrees with these values.

II. Description of Apparatus and Procedures

The apparatus used in the determination of the melting points consisted of a vacuum jacketed glass tube. Temperatures were measured by means of a calibrated copper–constantan thermocouple, one end of which was located in the tip of a thin glass well entering the bottom of the glass tube. Equilibrium in the solutions was facilitated with agitation by means of a coiled-glass stirrer which moved up and down. Its displacement was such that the stirrer agitated the contents of the tube including the region adjacent to the thermocouple well at the bottom of its stroke. The stirrer was connected to a glass-enclosed steel rod, the upper end of which was attached to a stainless-steel spring. The rod was actuated by a solenoid the current of which was controlled by a motor-driven rheostat. The apparatus was flushed with dry nitrogen, and solutions were added through a small opening in the top of the tube by means of a hypodermic syringe to which a long stainless-steel capillary tube was attached. Several series of measurements were made by successively adding liquid N_2O_4 to a weighed amount of HNO_3 in the melting point apparatus by means of a calibrated syringe assembly. H_2O from an ice-bath was circulated through the syringe jacket to maintain the N_2O_4 near 0°. The density of N_2O_4 at this temperature was determined at this Laboratory to be 1.489 g./cc. This syringe was similarly used to add water to HNO_3 solutions containing known amounts of N_2O_4. Another series of measurements was obtained by making up individual solutions by weight. Because of the extensive tendency of HNO_3 solutions to supercool, the method of measuring temperature *vs.* time for the melting process instead of the freezing process was used to establish the phase equilibria. In some measurements in which there was only a small change in solubility of the solid phase in the liquid phase over a relatively large temperature interval, the melting point was determined by observing under magnification the disappearance of the last few crystals and the reappearance of the first few crystals while the temperature of the outer bath was allowed to change very slowly.

III. Materials

The HNO_3 was prepared by vacuum distillation at room temperature of a mixture of reagent-grade concentrated sulfuric acid and potassium nitrate. The colorless product was collected in a container at about −70° and stored at about −20°. H_2O used was distilled in the laboratory. Commercial N_2O_4 was purified by bubbling oxygen through it and passing the vapors through a furnace at 300° to oxidize any NO present and decompose any N_2O_5. The remainder of the purification train was essentially that described in reference 11. The N_2O_4 obtained froze to a colorless solid at −11.2°.

(1) This paper presents the results of one phase of research carried out at the Jet Propulsion Laboratory, California Institute of Technology, under Contract No. DA-04-495-Ord 18, sponsored by the Department of the Army, Ordnance Corps.

(2) Department of Chemistry and Chemical Engineering, Stanford University, Stanford, California.

(3) The term fuming nitric acid refers to the ternary system HNO_3–N_2O_4–H_2O in the range of composition rich in HNO_3. Compositions in general are expressed on a formal basis unless otherwise stated, *i.e.*, in terms of the formula of a compound disregarding the molecular species that may result in its solution.

(4) P. Pascal and Garnier, *Bull. soc. chim. France*, **25**, 309 (1919).

(5) F. W. Kuster and R. Kremann, *Z. anorg. allgem. Chem.*, **41**, 1 (1904).

(6) W. J. Dunning and C. W. Nutt, *Trans. Faraday Soc.*, **47**, 15 (1951).

(7) W. R. Forsythe and W. F. Giauque, *J. Am. Chem. Soc.*, **64**, 48 (1942).

(8) (a) A. Klemenc and Th. Spiess, *Monatsh.*, **77**, 216 (1947); (b) W. H. Corcoran, H. H. Reamer and B. H. Sage, *Ind. Eng. Chem.*, **46**, 2541 (1954).

(9) A. G. Whittaker, P. W. Sprague, A. Skolnik and G. B. L. Smith, *J. Am. Chem. Soc.*, **74**, 4794 (1952).

(10) W. F. Giauque and J. D. Kemp, *J. Chem. Phys.*, **6**, 40 (1938).

(11) A. Klemen, "Die Behandlung und Reindarstellung von Gasen," Edwards Brothers Inc., Ann Arbor, Michigan, 1943.

IV. Results

The complete phase diagram showing the solid–liquid phase behavior at 1 atmosphere pressure and liquid–liquid phase behavior near bubble point for the binary system HNO_3–N_2O_4 is presented in Fig. 1. The experimental data used to construct the

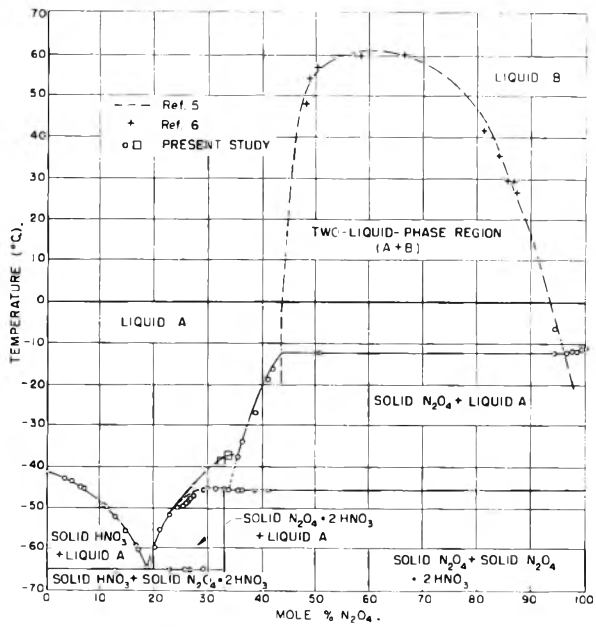

Fig. 1.

solid–liquid phase portion of the diagram are given in Table I. This binary system exhibits two eutectic points, one at 25.6 weight % N_2O_4 and −65°,

TABLE I

MELTING POINTS OF HNO_3–N_2O_4 SYSTEM

N_2O_4, mole %	M.p., °C.	N_2O_4, mole %	M.p., °C.
0	−41.7	27.46	−47.1
3.27	−43.1	29.21	−45.7
4.55	−43.8	29.83	−45.5
6.31	−45.2	31.55	−45.4
6.66	−45.4	32.24	−39.0
10.61	−49.5	33.19	−45.3
10.91	−49.9	33.53	−37.1
12.77	−52.4	33.93	−45.6
14.78	−55.6	35.48	−37.6
16.67	−59.3	35.72	−37.6
17.20	−60.2	36.33	−34.0
18.73	−64.5	38.89	−26.9
20.21	−59.8	41.21	−18.6
21.10	−55.4	42.10	−16.4
22.93	−51.9	50.67	−12.6
24.40	−50.0	94.18	−12.7
25.22	−49.5	96.56	−12.5
25.35	−49.2	97.53	−12.2
26.02	−48.8	98.45	−12.0
26.46	−48.4	99.19	−11.7
26.68	−47.7	100.00	−11.2

and the other at 43 weight % N_2O_4 and −45.7°. In Fig. 2, which gives in detail the phase diagram for the region between 93 and 100 mole % N_2O_4, it can be seen that an invariant point at 1 atmosphere exists at a temperature of −12.7° and a concentration of 95.0 mole % N_2O_4. At this point two liquid

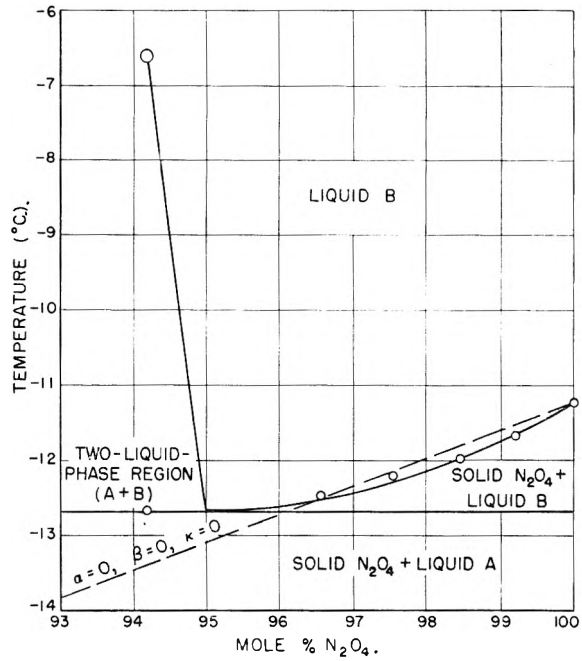

Fig. 2.

phases are in equilibrium with solid N_2O_4. The addition of HNO_3 above 5.0 mole % at the temperature −12.7° decreases the amount of solid N_2O_4 until at approximately 44.2 mole % N_2O_4 the concentration of the second liquid phase of the invariant system is reached (Fig. 1), and further addition of HNO_3 results in a single liquid system. The letters A and B are used in Figs. 1 and 2 to designate the homogeneous liquids on the HNO_3-rich and N_2O_4-rich sides, respectively, of the critical solution point near 62 mole % N_2O_4 and 61°.

The existence of a solid compound consisting of 2 moles of HNO_3 and 1 mole of N_2O_4 as was indicated by the original data of Pascal and Garnier[3] is definitely established (Fig. 1). A slight break in the curve at 26.3 mole % N_2O_4 and −48.7° seems to indicate the possibility of two crystalline forms for this 2:1 compound which are designated by α and β. The possibility that this break is indicative of a compound having a 3:1 mole ratio of HNO_3 to N_2O_4 is precluded by the fact that −65° eutectic points were measured at concentrations as high as 29.21 mole % N_2O_4 (Fig. 1). The two points shown by squares in Fig. 1 are included since a check of the data showed no detectable error in either their compositions or their melting points. These points suggest the possibility of the existence of a metastable condition for the compound $N_2O_4 \cdot 2HNO_3$.

A portion of the HNO_3–N_2O_4–H_2O system showing curves of constant melting point is presented in Fig. 3. A ternary eutectic point is indicated in the region around 18 weight % N_2O_4 and 4 weight % H_2O and at a temperature near −78°. The original data from which Fig. 3 was constructed are given in Table II.

V. Evaluation

The initial portions of the phase diagrams for the systems HNO_3–KNO_3 and HNO_3–NH_4NO_3[6] and the

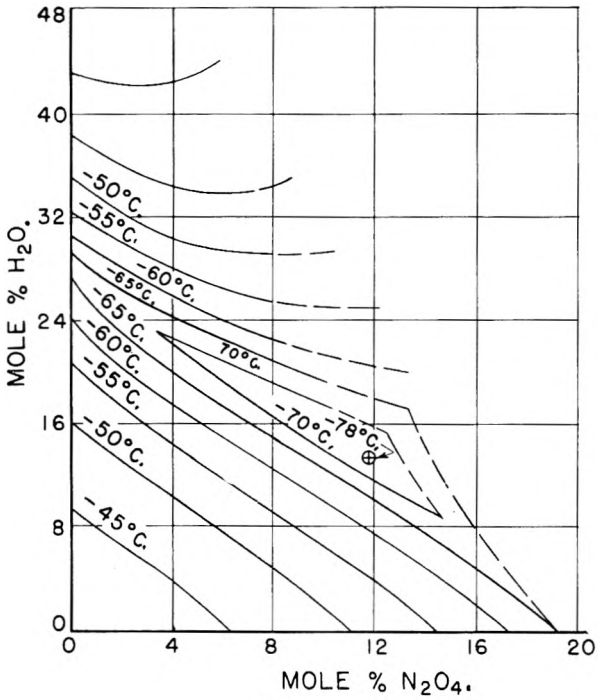

Fig. 3.

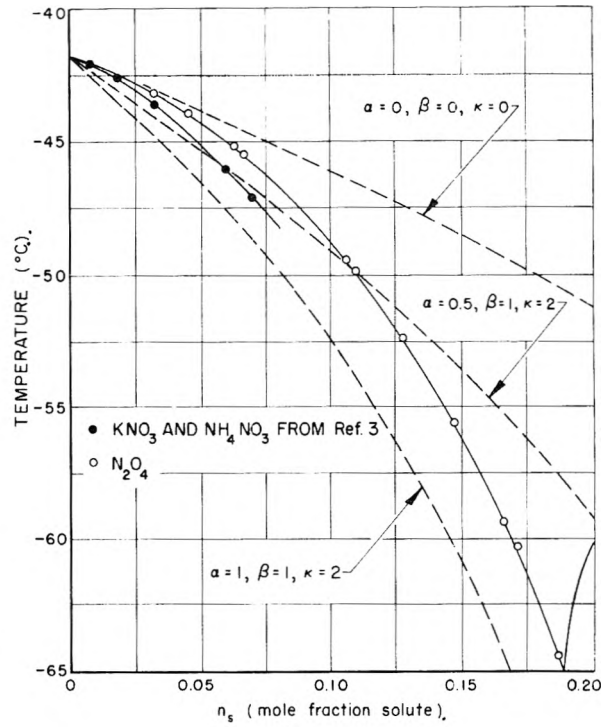

Fig. 4.

region of the phase diagram for HNO_3–N_2O_4 in which the solid phase is pure HNO_3 are shown in Fig. 4. Also shown are three curves based on the thermodynamic equation[12]

$$\frac{d \ln a}{dT} = \frac{\Delta H_{fu}}{RT^2} \qquad (1)$$

where ΔH_{fu} is the molar heat of fusion of the pure solvent (HNO_3) at the temperature T, and a is the activity of the solvent. For very low concentrations of solute, the heat of fusion may be taken

TABLE II

MELTING POINTS OF HNO_3–N_2O_4–H_2O SYSTEM

N_2O_4, mole %	H_2O, mole %	M.p., °C.
4.55	0	−43.8
4.15	8.49	−48.2
3.82	16.05	−57.6
3.52	22.50	−68.7
3.23	28.93	−54.0
2.94	35.37	−44.8
2.50	44.87	−39.2
10.61	0	−49.5
9.51	10.31	−60.4
8.63	18.66	−69.4
7.62	28.23	−50.5
6.42	39.48	−41.3

as a constant, but at higher concentrations one must take into account the change in the molar heat of fusion of the pure solvent due to the change in melting temperature and also to the partial molar heat of solution of the solvent in the solution at the concentration of interest; *e.g.*

$$\Delta H_{fu} = \Delta H^0_{fu} + \Delta C_p (T - T_0) + \Delta H_s \qquad (2)$$

where ΔH^0_{fu} is the heat of fusion of pure solvent at its melting point T_0; ΔC_p is the difference in molar isobaric heat capacity between the liquid and the solid solvent; and ΔH_s is the partial molar heat of solution of the solvent in the solution at the melting point T. Over temperature intervals of the order of 30°, ΔC_p may be taken as constant. Values for ΔH_s were calculated from data reported in reference 13 which gives the heats of solution of N_2O_4 in HNO_3 at 0°. Since the values of the heat capacities of the solutions[13] were nearly equal to the heat capacity of pure HNO_3 the heats of solution at the melting point were taken to be equal to those reported at 0° for making the correction in equation 2. Values of ΔH_s could be compared with values of the melting point T obtained from the phase diagram of HNO_3–N_2O_4 at the corresponding concentrations. This comparison showed that up to about 15 mole % N_2O_4 the heat of solution could be represented fairly well by

$$\Delta H_s \simeq -K(T - T_0)^2 \qquad (3)$$

where $K = 1$ cal./deg.^{2} mole. Therefore, if $-T' = T - T_0$, Equation 1 may be expressed as

$$-\frac{d \ln a}{dT'} = \frac{\Delta H^0_{fu} + \Delta C_p (-T') - (T')^2}{R(T_0 - T')^2} \qquad (4)$$

Integrating, expanding, and letting $y = T'/T_0$

$$-R \ln a = \frac{\Delta H^0_{fu}}{T_0} y + \left(\frac{\Delta H^0_{fu}}{T_0} - \frac{\Delta C_p}{2}\right) y^2 + \left(\frac{\Delta H^0_{fu}}{T_0} - \frac{2\Delta C_p}{3} - \frac{T_0}{3}\right) y^3 + \left(\frac{\Delta H^0_{fu}}{T_0} - \frac{3\Delta C_p}{4} - \frac{T_0}{2}\right) y^4 + \ldots \qquad (5)$$

(12) S. Glasstone, "Thermodynamics for Chemists," D. Van Nostrand Co., New York, N. Y., 1947.

(13) D. M. Mason, K. Booman and G. W. Elverum, Jr., "Heats of Solution of Nitrogen Dioxide in the Nitric Acid–Nitrogen Dioxide System at 0°" (Progress Report No. 20-216, Jet Propulsion Laboratory, Pasadena, 1954).

If one now makes the assumption that the activity of the HNO_3 species is equal to the actual mole fraction of the HNO_3 species existing in the solution (*i.e.*, the solution behaves in accordance with Raoult's law), then one may replace a by the mole fraction of the species HNO_3 (*i.e.*, $1 - X_s$), where X_s is the effective mole fraction of solute due to total number of solute species resulting from solution. In Fig. 4, n_s represents the formal mole fraction of solute as N_2O_4, KNO_3 or NH_4NO_3. A series of values of X_s for these nitric acid systems may now be found from the equation

$$X_s = \frac{[(1 - \alpha) + \alpha j]\, n_s}{[(1 - n_s) - \beta k \alpha n_s] + [(1 - \alpha) + \alpha j] n_s} \quad (6)$$

where α may be defined as the fraction of total solute molecules ionized, j as the number of ions formed per solute molecule ionized, k as the number of solvent molecules associated with one of the solute ions, and β as the fraction of one of the ionic species actually associated with solvent molecules. For the solutes KNO_3, NH_4NO_3 and N_2O_4, the value of j is 2, and equation 6 reduces to

$$X_s = \frac{(1 + \alpha) n_s}{1 + \alpha n_s (1 - \beta k)} \quad (7)$$

From equations 5 and 7 a series of curves may be obtained of T *vs.* n_s for various values of α, β and k. Three of these curves are presented in Fig. 4. The value of $\Delta H°_{fu}$ for nitric acid was taken to be 2503 cal./mole, and the values used for the heat capacities of solid and liquid nitric acid were 15.82 and 26.70 cal./mole, respectively.[7]

It can be seen that both KNO_3 and NH_4NO_3 give the same curve for the freezing point depression. Inasmuch as both KNO_3 and NH_4NO_3 may be expected to be completely ionized at low concentrations in HNO_3, one would expect (assuming no association) that these data would lie along the curve for $\alpha = 1$, $\beta = 0$, $k = 0$. This curve is not shown in Fig. 4, but at low concentrations it would lie very close to the $\alpha = 1$, $\beta = 1$, $k = 2$ curve shown. However, it can be seen that the actual freezing point depression approaches tangentially the curve $\alpha = 0$, $\beta = 0$, $k = 0$ for small concentrations of solute. The explanation for this behavior is to be found in the measurements of the Raman spectra of HNO_3,[14] which indicate that liquid HNO_3 undergoes self-ionization to the extent of about 3 to 5 mole % according to the expression

$$2HNO_3 \rightleftarrows NO_2^+ + NO_3^- + H_2O \quad (8)$$

Measurements of the specific conductance also support the existence of this ionization.[15] It can be seen that initially the addition of NO_3^- would shift this equilibrium to the HNO_3 side of equation 8 so that the net number of particles of the group NO_2^+, NO_3^- and H_2O would increase very slowly at first. The initial freezing point depression would thus essentially be due to the ions K^+ or NH_4^+ and would therefore lie along the line $\alpha = 0$, $\beta = 0$, $k = 0$, as shown. Assuming a self-ionization of HNO_3 of 4 mole %, an apparent value of α to be expected at 1 mole % of added NO_3^- would be about 0.1. At higher concentrations of solute, the freezing point curve becomes parallel with the line $\alpha = 1$, $\beta = 1$, $k = 2$, indicating that the self-ionization has been suppressed, that 2 molecules of HNO_3 are associated with one of the ions of KNO_3 or NH_4NO_3, and that this association is nearly complete. Raman spectral studies have also shown that the following equilibrium association exists[16]

$$2HNO_3 + NO_3^- \rightleftarrows NO_3^- \cdot (HNO_3)_2 \quad (9)$$

and the spectral data indicate that this equilibrium lies quite far to the right, a fact which is consistent with $\beta = 1$ and $k = 2$ in Equation (7).

The initial phase behavior of the system N_2O_4–HNO_3 can be seen to lie along the curve $\alpha = 0$, $\beta = 0$, $k = 0$ out to about 0.025 mole fraction solute. The phase diagram shows that beyond a few mole per cent. the curve rapidly bends down to parallel the curve $\alpha = 1$, $\beta = 1$, $k = 2$, supporting the known fact that N_2O_4 becomes ionized in solution according to the equilibrium

$$N_2O_4 \rightleftarrows NO^+ + NO_3^- \quad (10)$$

The existence of this equilibrium has been shown by Raman spectral studies of the N_2O_4–HNO_3 system[17] and is supported by electrical conductance measurements.[15] The existence of the solid compound $N_2O_4 \cdot 2HNO_3$ also gives evidence that association takes place in solution according to equation 9. The fact that the N_2O_4 curve initially follows the curve $\alpha = 0$, $\beta = 0$, $k = 0$ may thus be explained by the suppression of the self-ionization of HNO_3 by NO_3^- ions. It may be noted that approximately twice as many moles of N_2O_4 as KNO_3 or NH_4NO_3 are required to suppress the self-ionization of HNO_3. This result would indicate that N_2O_4 was only about 50% ionized in solution. It can be seen, however, that the curve at higher concentrations does not follow parallel to the curve $\alpha = 0.5$, $\beta = 1$, $k = 2$ (as it should for 50% ionization) but that it becomes parallel to the curve $\alpha = 1$, $\beta = 1$, $k = 2$, indicating nearly 100% ionization. This situation suggests that the ionization of N_2O_4 decreases as the solution becomes more dilute, a result which would not normally be expected. If however it is assumed that the ionization of N_2O_4 according to equation 10 is not complete compared with KNO_3 ,which may be assumed to be completely ionized, then it follows that the NO_3^- ions from the self-ionization of nitric acid[10] shift the equilibrium of equation 10 to the N_2O_4 side at very low concentrations of N_2O_4. An ionization of the order of 90% at a mole fraction of N_2O_4 of 0.1 would be reduced to an ionization of about 50% at a mole fraction of N_2O_4 of 0.01. Thus, although the N_2O_4 curve nearly follows the $\alpha = 1$, $\beta = 1$, $k = 2$ slope at high concentrations to the eutectic point, it requires a larger amount of N_2O_4 than of KNO_3, to suppress the self-ionization of HNO_3. The initial slope of $\alpha = 0$, $\beta = 0$, $k = 0$ also precludes the equilibria

$$N_2O_4 \rightleftarrows 2NO_2 \quad (11)$$

(14) E. D. Hughes, C. K. Ingold and R. I. Reed, *J. Chem. Soc.*, 2400 (1950).

(15) G. D. Robertson, D. M. Mason and B. H. Sage, "Electrolytic Conductance of the Ternary System of Nitric Acid–Nitrogen Dioxide–Water at 32°F. and Atmospheric Pressure" (Progress Report No. 20-155, Jet Propulsion Laboratory, Pasadena, 1951).

(16) J. Chédin and S. Fénéant, *Compt. rend.*, **228**, 242 (1949).

(17) J. D. S. Goulden and D. J. Millen, *J. Chem. Soc.*, 2620 (1950).

from lying more than a few per cent. to the right except in extremely dilute solutions.

A dashed curve based on equations 5 and 7 is shown in Fig. 2. The value used[10] for the heat of fusion of N_2O_4 was 3502 cal./mole (as N_2O_4). It can be seen that the depression of the melting point of N_2O_4 by HNO_3 initially follows fairly close to the curve for $\alpha = 0$, $\beta = 0$, $k = 0$. The behavior of the experimental curve, however, shows a positive deviation from Raoult's law at higher concentrations of HNO_3. The association of the polar HNO_3 molecules at higher concentrations which finally result in the separation of a second liquid phase accounts for this behavior.

THE THERMODYNAMICS OF THE LIQUID SOLUTIONS IN THE TRIAD Cu–Ag–Au. I. THE Cu–Ag SYSTEM[1]

BY RUSSELL K. EDWARDS AND JAMES H. DOWNING

Contribution from the Department of Chemistry, Illinois Institute of Technology, Chicago, Ill.

Received July 7, 1955

The thermodynamics of the liquid Cu–Ag system have been investigated as part of a general study in the Cu–Ag–Au triad to consider the energetic relationships and chemical bonding among these elements. The study was conducted by the method of determination of the partial pressures over the liquid solutions as a function of composition and temperature. Partial pressures were measured by the molecular effusion technique and were related to the vapor pressures of the pure liquids similarly measured, and activities were calculated. The related thermodynamic properties for the mean temperature 1428°K. are reported, based on the temperature and composition dependencies of the activity data. The activities of both components demonstrate marked positive deviation from ideal solution behavior in the system, as might have been expected in view of the fact that a wide miscibility gap exists in the solid state for this system. Large positive values for partial and integral enthalpies of mixing were found. The partial and integral excess entropies of mixing are positive.

Introduction

The investigation in the liquid Cu–Ag system was chosen to institute a general thermodynamic study in the triad, Cu–Ag–Au, to consider the energetic relationships and chemical bonding among these elements. The atomic radius for Cu is about 12% less than that of Ag, and the atomic radius for the latter is practically identical to that of Au. On the other hand, the cohesive energy of Cu is about 17% greater than that of Ag whereas the value for Au is about 27% greater than that of Ag. An investigation of the binary permutations among the three elements offers an opportunity of observing the effects of the major variables—cohesive energy and atomic radius—while other variables, in particular valence, can reasonably be expected to remain relatively constant.

The study was conducted by the method of determination of the partial pressures over the liquid solutions as a function of composition and temperature. Partial pressures were measured by the molecular effusion technique and were related to the vapor pressures of the pure liquids similarly measured, to obtain self-consistent data from which activities were then calculated. It was imperative that activities be determined only from self-consistent data obtained by relative measurements under identical conditions since reported[2] absolute vapor pressure data by various different investigators have varied by as much as 100%.

The thermodynamic properties for the liquid solutions were calculated from the temperature and composition dependencies of the activity data. Inasmuch as the vapor pressure of Cu in the temperature range studied (1300 to 1700°K.) is approximately a factor of ten lower than that of Ag, Cu was a minor but not negligible constituent in most of the effusates. Consequently the activities of Ag were subject to more accurate direct determination than were the activities of Cu, and the best values of the activities of Cu were taken from Gibbs-Duhem integration of the Ag activity data. However, in addition, directly obtained Cu activity data were evaluated in order to check the validity of the Gibbs–Duhem integration.

Experimental

Apparatus.—The vacuum apparatus used for the effusion measurements is shown in Fig. 1. The essential features of the apparatus are (a) an evacuated porcelain tube section heated by, (b) a furnace, shown schematically, having Globar elements, (c) a graphite crucible with a small effusion orifice, (d) a thermocouple, enclosed in a silica glass protection tube, for measuring the temperature in the region of the crucible and (e) a water-cooled cold finger which served to collect samples of the Cu–Ag gas mixture which effused from the crucible as a molecular beam. The crucible was detachable through a polished sliding fit from the graphite support rod shown in the figure. The support rod itself was capable of being moved as desired while under vacuum by means of an external electromagnetic coil acting on an iron section affixed to the end of the rod. Vacuum pumping from both ends of the apparatus was used to ensure a high speed system. The mercury diffusion pumps used were isolated from the system by liquid nitrogen traps and so operated as to prohibit exposure of the system to any mercury vapor. Vacuum pressures were measured by means of a Pirani gage mounted just outside the main vacuum chamber along one of the 20 mm. tubing sections and also by means of an ionization gage similarly mounted along the other 20 mm. tubing section. Dynamic vacuum pressures of less than 10^{-4} mm. were maintained during the vapor pressure measurements.

Furnace Temperature Control.—The furnace temperature was controlled by means of a Micromax automatic potentiometer with recorder and controller, operating on the signal from a Pt, Pt-Rh (10%) thermocouple located in the vicinity of the furnace heater elements. In general this arrangement could hold the temperature of the heater element environment to ± 5°, and the temperature of the

(1) (a) Presented at the 126th Meeting of the American Chemical Society, New York, September, 1954. (b) Based on part of a thesis by J. H. Downing, submitted to the Illinois Institute of Technology in partial fulfillment of the requirements for the Ph.D. degree, May, 1954. (c) This work was supported by the U. S. Office of Naval Research, U. S. Navy, through Contract N7-onr-329, Task Order II, and Contract NONR 1406, Task Order II.

(2) H. N. Hersh, *J. Am. Chem. Soc.*, **75**, 1529 (1953).

effusion crucible to a much better tolerance. However, to compensate for the tendency of the temperature to drift within the above tolerance, due to thermal lags in the system, a manual resetting of the Micromax controller was performed from time to time.

Rate of Effusion.—The rate of effusion was determined from measurement of the time of effusion and weight loss of the crucible plus contents. Weight losses were determined by use of an Ainsworth semi-micro balance. The sensitivity and zero point were determined at the time of each weighing. Careful, systematic procedures were adopted to eliminate errors due to adsorption of gases or moisture by the cell while outside the vacuum line. The cell was never touched except with a rubber test-tube holder or a dry cloth. One hour was allowed after removal of the crucible from the vacuum line so that it would attain a steady-state relationship with the weighing environment, both with respect to gas adsorption and to temperature. Check measurements showed that the weight uptake during this period was of the order of a few hundredths of a mg. and contributed no significant error to the results since the same systematic procedure was always followed. Errors due to buoyancy factors were less than 1%. Blank effusion runs with the empty crucibles showed that the crucibles themselves suffered no measurable weight loss under the normal experimental conditions.

Effusion Crucibles.—Three different effusion crucibles, with significantly different effusion orifice sizes, were used; thus crucibles could be used which had orifices appropriate, in terms of true effusion conditions, to the various pressure ranges. Calibration of the effective effusion orifice areas by measurement of the rate of vaporization of mercury from these crucibles has been discussed elsewhere.[3]

As was anticipated at the outset of this study, some diffusion of the metals through the graphite crucible walls was encountered. It had been expected that the diffusion mechanism would be that of capillary flow through the graphite pores. Since such a mechanism is equivalent to effusive flow out of an orifice, it was supposed that the extraneous weight loss contribution would be accountable through the "effective" orifice area obtained by the calibration procedure. In any case, error in the effective orifice area would cancel out in the calculation of activities. Edwards and Downing[3] found that silver does diffuse through graphite by the capillary flow mechanism, but that copper diffuses through by activated diffusion. Even so, activities are relative and therefore still calculable; however, this surprising circumstance complicates the calculation of gas phase compositions as is noted below.

Composition of the Gas Phase.—Samples of the effusates were collected on the cold finger, the face of which was located three inches from the crucible effusion orifice. The stainless steel surface was highly polished to facilitate removal of condensate samples. Samples could either be brushed off or scraped off with a steel knife. Care was taken to avoid marring the polished surface. The cold finger was afterward cleaned with fine steel wool and washed with carbon tetrachloride.

Micro-analytical techniques were required for chemical analysis of the effusate materials because of the very small amounts, ranging from 2 to 10 mg. In the effusates copper was always the minor constituent; therefore analysis for copper was requisite but silver could be obtained by difference. Spectrographic analyses showed that no other components were present in the effusates to any significant amount. The concentration of the colored cupric ammonia complex can be spectrophotometrically determined in the presence of silver without interference. The wave length of the absorption peak for this complex is 620 mμ; however, the height of the peak is a function of the ammonia concentration.[4] In order to avoid difficulties arising from this concentration dependence, a peak of 580 mμ[5] was used in the present investigation since at this wave length the absorption is independent of the ammonia concentration. Beer's law has been reported[4] to hold under these conditions, a fact that was amply verified in the present work.

Had all the weight loss been by the effusive and capillary flow mechanisms, it would have been simple to obtain the weight loss of each species from knowledge of the total weight loss and the composition of the collected effusate sample on the cold finger. Since, however, extraneous loss of copper took place by activated diffusion, it was necessary to apply a correction to the composition nominally obtained from the analysis of the collected material. Therefore we experimentally measured the collection probabilities for both orifice loss and for the extraneous loss by the diffusion processes. The latter measurement was carried out by using one of the crucibles with a cap having no orifice. From this information, and that available from the study of the rates of the diffusion processes,[3] the correction could be made. The correction produced only a small alteration of the calculated partial pressures of silver but considerably altered the calculated partial pressures of copper, as would be expected since the latter was the minor constituent in the effusates. As anticipated, the size of the correction required was significantly larger for the crucible of the smallest orifice.

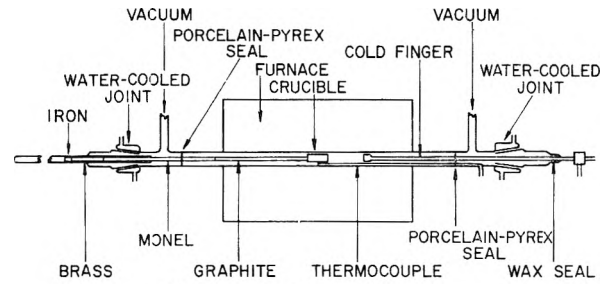

Fig. 1.—Effusion apparatus.

Agreement of partial pressures obtained using the crucibles of three different orifice sizes, shown in Fig. 2, attests to the validity of the correction treatment. There the data points on the curve representing the partial pressure of silver in equilibrium with a liquid solution of composition 49 atom % silver belong about equally to the three different crucibles with different orifice sizes. A similar plot (not shown) for the partial pressure of copper over this solution was equally consistent.

Composition of the Liquid Phase.—Homogeneous two-phase Cu–Ag alloys were prepared by melting under vacuum the appropriate mixtures in a long graphite tube of about 1/4 inch dameter. The preparations were stirred and then quenched by rapid cooling so that segregation of phases could be avoided. The solid rod obtained was then machined until free from any adhering graphite particles. The reductive action of the graphite was expected to remove any oxide contamination.

Portions of the rods used were analyzed iodimetrically for copper before introduction into the effusion crucibles; residues in the crucibles after a series of runs on a liquid of a given composition were again analyzed for copper to ascertain the change in composition that took place during the effusion runs. The change was always less than one atom %, and the mean value was used.

Emptying and Cleaning the Crucibles.—An auxiliary apparatus consisting of a graphite holder with a long graphite handle permitted shaking out the liquid metal solutions from the inverted crucibles (with caps removed) while in an argon atmosphere. Thereafter the crucible was baked out at high temperature under vacuum until it came to a constant weight. This procedure was carried out whenever a change in the liquid composition was made.

Freedom from Errors Due to Impurities.—High purity silver and copper of better than 99.98 and 99.99%, respectively, were used. However, in such a study as this it is more important to establish that no impurities of high volatility contribute to effusion loss. In the present work effusates from first runs on the pure materials were analyzed by semi-quantitative spectrographic examination. Less than 0.1% impurity was found in the effusates for either of the two materials and thus the maximum error due to impurities was established.

Sequence of Determinations.—Some re-evaporization of the material which had condensed along the cooler portion of the porcelain tube was inevitable, and the following sequence of operation was adopted in order to minimize error in effusate compositions arising from condensation of some of this revaporized material. Before a series of runs with a

(3) R. K. Edwards and J. H. Downing, THIS JOURNAL, **59**, 1079 (1955).

(4) F. Snell and C. Snell, "Colorimetric Methods of Analysis," Third Edition, D. Van Nostrand, Inc., New York, N. Y., 1949.

(5) C. Milner, *Ind. Eng. Chem., Anal. Ed.*, **18**, 94 (1946).

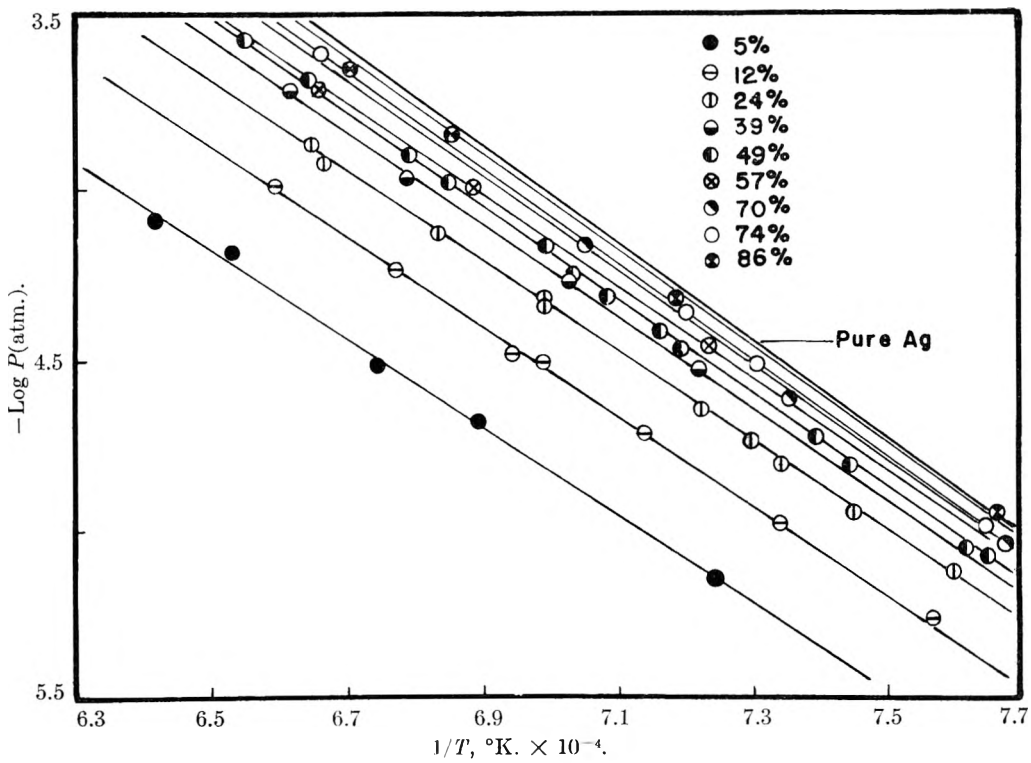

Fig. 2.—Silver partial pressures over Cu–Ag liquid solutions (compositions given in atom % Ag).

new alloy composition was begun, the apparatus was held under vacuum at a temperature appreciably higher than that at which any of the subsequent experimental runs were to be carried out. In this way condensates would be moved down along the porcelain walls to a cooler region. When the series of runs with the new alloy were begun, the highest temperature run was made first and so on toward decreasing temperatures. Thus the condensing zone would gradually advance toward the center of the furnace and re-evaporization of the condensate would likely be of negligible importance.

Temperature Measurement and Calibration.—Two Pt, Pt–Rh (10%) thermocouples, made from the same original wires, were used in this work. One, which we shall call the "proximate" thermocouple, is shown in Fig. 1. It served as the working thermocouple. The cold junction of this thermocouple was held at the ice point in an ice–water–air mixture, external to the vacuum, under which it was joined to copper–lead wires. These were connected to a Brown Electronik recording potentiometer, in series with a Rubicon portable precision potentiometer. The latter was used to buck out excess millivoltage. A continuous temperature record for any run was thus obtained. At periodic intervals the recorded millivoltage on the Brown instrument was checked by a direct reading on the Rubicon potentiometer. The other thermocouple we shall term the laboratory "reference" thermocouple. It was calibrated at the melting points of National Bureau of Standards tin and zinc and also at the melting point of the high purity silver used here in the vapor pressure work. Its millivoltage–temperature curve was found to be in good accord in this temperature interval with National Bureau of Standards tabulations for high quality thermocouples of this kind.

Calibration of the proximate thermocouple in terms of the actual temperature existing within the graphite effusion crucible was accomplished as follows. A replica was made of the graphite effusion crucibles used, except that the hole normally in the base for the support rod was bored completely through to the interior of the effusion chamber. The reference thermocouple, with its junction in the center of the effusion chamber and its porcelain two-hole protection tube, now served to support the crucible. In this calibration work and in all effusion runs, the crucible position at the center of the uniform temperature zone of the furnace was carefully reproduced by referring to index markers along the apparatus. Comparison under normal vacuum conditions showed the two thermocouples to agree precisely over the complete temperature range when under steady-state temperature conditions. This calibration procedure was periodically repeated throughout the entire study in order to apprehend any possible deterioration of the proximate working thermocouple; this could readily have occurred if any cracks developed in the silica glass protection tube, permitting alloying with the effusate material. No deterioration was found; the proximate thermocouple remained completely equivalent to the laboratory reference thermocouple throughout the work.

Since the fundamental temperature scale in the range pertinent to these vapor pressure measurements is based on the radiation laws, an additional calibration of the proximate thermocouple in terms of a Leeds and Northrup optical pyrometer was performed to ascertain whether the thermocouple millivoltage–temperature relationship remained compatible with the National Bureau of Standards tabulated values at these higher temperatures. A long thin-walled porcelain support tube was fitted into the base of the replica crucible so that it served also as a sighting tube, giving a view of the "black body" interior of the effusion chamber. An optical window was affixed in the appropriate position and the comparison between the optical pyrometer and the proximate thermocouple was made from the silver melting point temperature on up, under normal vacuum conditions. The silver point having been previously established, the optical pyrometer constant, C, containing the window absorption corrections, was obtained for the relationship

$$1/T_t = 1/T_0 + C$$

where T_t refers to the true temperature and T_0 refers to the observed optical pyrometer temperature, both on the absolute scale. Thereafter the equation was used to obtain the true temperature in the higher temperature range from the observed pyrometer temperature. The correlation between the two scales was good to within the reproducibility of the optical pyrometer readings. These deviations were random, with an average deviation of ±3°.

The optical pyrometer used was itself calibrated against a similar optical pyrometer which had been calibrated by the National Bureau of Standards.

Effective Average Temperature of a Run.—The procedure used in starting a run was to first bring the furnace temperature to a value about 50° higher than desired and to permit

TABLE I

THERMODYNAMIC FUNCTIONS FOR MIXING AT 1428°K. FOR Cu–Ag LIQUID SOLUTIONS

Compn. (atom % Ag)	Silver, partial molar quantities			Copper, partial molar quantities			Integral molar quantities		
	$-\Delta\overline{F}°$, cal./mole	$\Delta\overline{H}°$, cal./mole	$\Delta\overline{S}°$, cal./mole-deg.	$-\Delta\overline{F}°$, cal./mole	$\Delta\overline{H}°$, cal./mole	$\Delta\overline{S}°$, cal./mole-deg.	$-\Delta F°$, cal./mole	$\Delta H°$, cal./mole	$\Delta S°$, cal./mole-deg.
10	3,610	5,700	6.6	260	200	0.3	590	800	0.9
20	2,330	4,800	5.0	490	600	0.7	860	1,300	1.6
30	1,730	3,800	3.9	690	900	1.1	1,000	1,700	1.9
40	1,310	3,000	3.0	890	1,100	1.4	1,050	1,900	2.0
50	990	2,500	2.3	1,140	1,500	1.9	1,070	2,000	2.1
60	740	1,900	1.8	1,440	2,200	2.5	1,020	1,900	2.1
70	510	1,500	1.4	1,820	2,600	3.1	910	1,800	1.9
80	330	1,000	0.9	2,280	4,300	4.7	720	1,600	1.7
90	160	600	0.6	3,060	6,700	7.0	450	1,200	1.2

time for final degassing. Just before the crucible was rapidly introduced into the hot zone by use of the external electromagnet, the furnace power was reduced to meet the anticipated new lower temperature produced by the heat loss to the crucible. Rapid withdrawal of the crucible at the end of a run was also simply accomplished. The usual method[2] of obtaining the effective average temperature was employed; this corrects the finite heating up and cooling off time as well as for temperature fluctuations during a run. In only a few of the shortest runs was this temperature significantly different from our arithmetically averaged temperature.

Results and Discussion

Silver partial pressure curves for the several liquid solutions investigated are shown in Fig. 2. A similar family of curves was obtained for copper partial pressures. Activities with reference to the pure components were derived from three different temperatures, and the curves for the mean temperature of 1428°K. are shown in Fig. 3. The data for the silver activities are shown, with carefully estimated maximum uncertainties indicated. These data were then treated by the Gibbs–Duhem integration to obtain the curve shown for copper activities. The directly evaluated copper activities, as we have pointed out, are subject to considerably greater uncertainties than are the silver activities, and the best values are without doubt those obtained through the Gibbs–Duhem integration. The agreement of the values directly obtained with the latter is substantial, and the deviations therefrom are random.

The free energy data listed in Table I have been taken from the smoothed activity curves at 1428°K. The other thermodynamic quantities listed in Table I have been derived through the appropriate temperature dependences shown by similar smoothed activity curves for three different temperatures. An error analysis of our work leads to probable errors of ±600 cal. per mole in the enthalpy data, ±0.45 cal. mole^{-1} deg.$^{-1}$ in the entropy data, and ±40 cal. per mole in the free energy data.

In support of the enthalpy data, it is of note that Edwards, Downing and Cubicciotti[6] obtained for copper a partial molar enthalpy of mixing of 1610 cal. for the composition 54 atom % silver, and this value falls nicely in line with the present work. Their result was from a somewhat limited study by the galvanic cell method. The integral enthalpies of mixing obtained calorimetrically by Kawakami[7] are approximately 50% lower than the values obtained in the present work. With regard to the discrepancy, it is of note that Kawakami[6] obtained essentially zero enthalpy of mixing in the copper–gold liquid system whereas both Edwards and Brodsky,[8] and Oriani,[9] by the vapor pressure method and galvanic cell respectively, have obtained large negative values.

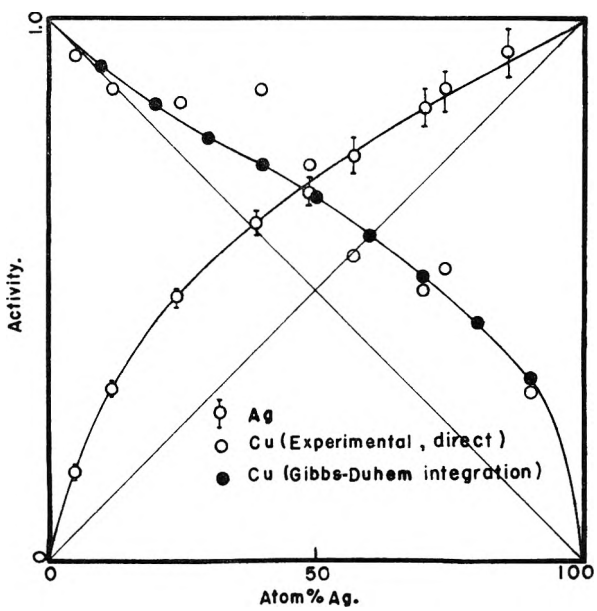

Fig. 3.—Activities of Cu–Ag liquid solutions at 7.0 × 10^{-4}/°K. (1428°K.) ("Experimental" data for Cu are from direct evaluation of data; "Gibbs-Duhem" data for Cu are from a Gibbs-Duhem treatment of the Ag data).

The marked positive deviation of the activities of the liquid Cu–Ag solutions is well in accord with the fact that the Cu–Ag system shows a large miscibility gap in the solid state. Moreover, the extent of the positive deviation decreases with temperature, also as would be expected and leads to rather large positive enthalpies of mixing. The excess entropies of mixing relative to values expected for an ideal solution appear to be positive beyond the experimental error. When the results of the related studies in the Cu–Au and Ag–Au liquid systems are available for comparison, we will discuss the fundamental significance of this study more thoroughly.

(6) R. K. Edwards, J. H. Downing and D. Cubicciotti, to be published.

(7) M. Kawakami, *Sci. Rep., Tohoku Imp. Univ.*, **19**, 521 (1930).

(8) R. K. Edwards and M. B. Brodsky, to be published.

(9) R. A. Oriani, private communication, July 27, 1954.

THE STOICHIOMETRY OF THE HYDRATION OF TRICALCIUM SILICATE AT ROOM TEMPERATURE. I. HYDRATION IN A BALL MILL

BY STEPHEN BRUNAUER, L. E. COPELAND AND R. H. BRAGG

Portland Cement Association Research and Development Laboratories, Chicago, Illinois

Received July 11, 1955

When tricalcium silicate, Ca_3SiO_5, is hydrated in a ball mill, the stoichiometry of the reaction at 23° in a saturated calcium hydroxide solution is represented by the equation $2Ca_3SiO_5 + 6H_2O = Ca_3(SiO_3OH)_2 \cdot 2H_2O + 3Ca(OH)_2$. An H_2O/Ca_3SiO_5 weight ratio of 9 was used in the ball mill, and complete hydration was attained in six days. The calcium silicate hydrate produced was afwillite. The afwillite was colloidal in dimensions; most of the particles were roughly spherical, and their diameter was of the order of 300 Å. The density was 2.647 ± 0.01 g./cc.; the mean index of refraction was 1.62 ± 0.01. No difference, except in the dimensions of the particles, was found between the natural mineral and artificial afwillite.

Introduction

Primarily because tricalcium silicate, Ca_3SiO_5, is one of the important constituents of portland cement, its hydration has been extensively investigated. These, as well as other investigations of the $CaO–SiO_2–H_2O$ system, were critically reviewed by Steinour.[1] Although valuable information has been gathered by several investigators, the stoichiometry of the hydration of Ca_3SiO_5 has not been settled.

When Ca_3SiO_5 is treated with solutions of lime in water, the reaction products are $Ca(OH)_2$ and calcium silicate hydrates of various compositions. At a concentration of 2 mmoles of CaO per liter, the molar ratio of CaO to SiO_2 is around 1.0 (or possibly as low as 0.8); at or near the saturation concentration the ratio is about 1.5. Taylor,[2] who made the most complete investigation of this system, designated the hydrates as calcium silicate hydrate (I) or CSH (I). Because of their similarity to the natural mineral tobermorite,[3] we shall call them tobermorites.

If in a mixture of water and Ca_3SiO_5 the weight ratio of water to Ca_3SiO_5 is less than about 300, the water becomes saturated with $Ca(OH)_2$. It follows from this that unless a very large excess of water is used, the hydration takes place—or at least ends—in a saturated lime solution. Of especial importance is the hydration in saturated calcium hydroxide solution because in the hydration of portland cement lime saturation is quickly established, and thereafter the Ca_3SiO_5 component of portland cement hydrates in a saturated solution. To determine by chemical means the composition of the calcium silicate hydrate produced, the calcium hydroxide must be removed from the system, but methods so far proposed usually remove also some of the lime from the calcium silicate hydrate. Because of this, the stoichiometry of the hydration can be reliably solved only if the chemical composition and nature of the reaction products can be determined *in situ*, without disturbing the reaction system.

An *in situ* technique was used recently by Graham, Spinks and Thorvaldson,[4] who investigated the hydration of Ca_3SiO_5 and β-Ca_2SiO_4 (β-dicalcium silicate) by employing a radioactive tracer, Ca^{45}. They concluded that the calcium silicate hydrate obtained from both silicates in saturated lime solution had a molar CaO/SiO_2 ratio of 1.5. Taylor[2] and Bessey[5] found that the CaO/SiO_2 ratio of the calcium silicate hydrate *close to* lime saturation was 1.5, but both investigators believed that *at lime saturation* the CaO/SiO_2 ratio of the stable hydrate was 2.0. Our results confirm the result of Graham, Spinks and Thorvaldson for Ca_3SiO_5, and give additional information on the stoichiometry of the hydration of Ca_3SiO_5 at room temperature in saturated lime solution. We employed a number of experimental approaches, among them *in situ* techniques; the main tool for identification and quantitative determination was an X-ray diffractometer.

We investigated the hydration reaction at 23° under two conditions: (a) Ca_3SiO_5 was hydrated in a small steel ball mill; and (b) it was hydrated in the form of "paste"—imitating its presumed mode of hydration in portland cement. The former is discussed in the present paper; the latter in the second paper.

Experimental

Preparation and Hydration of Ca_3SiO_5.—We used two lots of Ca_3SiO_5, designated as Ca_3SiO_5(I) and Ca_3SiO_5(II). The first lot was identical with that described by Brunauer, Hayes and Hass[6]; the second was prepared in the same manner, but it had a slightly different composition. The approximate composition of both lots was 96% Ca_3SiO_5, 3% Ca_2SiO_4 and 1% of other impurities.

Hydration was carried out in two small steel ball mills, designed by Grunwald.[7] Each mill had a capacity of about 400 cc. and was used with approximately 400 g. of steel balls of assorted sizes (3/8 to 3/4" diameter, Rockwell hardness No. 60–62). The internal dimensions of the mills were approximately 6" diameter and 1" width. The interior surfaces were hardened to a depth of 1/32" (Rockwell hardness No. 60–62); the exterior surfaces were plated with chromium. The mills were rotated at approximately 50 r.p.m. for 15 minutes of each hour.

The mills were operated in a room kept at 23 ± 0.5°. The water-to-solid weight ratio was 9. We investigated two ball-mill-hydrated batches of Ca_3SiO_5, prepared from Ca_3SiO_5 (I) and (II).

Removal of Uncombined Water.—The ball-mill slurries, at the end of the grinding period, were spooned or pipetted out of the mill and transferred to erlenmeyer flasks for freezing. The practice of freezing the slurries was adopted

(1) H. H. Steinour, *Chem. Revs.*, **40**, 391 (1947); "Proceedings of the Third International Symposium on the Chemistry of Cement," London, 1952, p. 261.

(2) H. F. W. Taylor, *J. Chem. Soc.*, 3682 (1950).

(3) G. F. Claringbull and M. H. Hey, *Mineral. Mag.*, **29**, 960 (1952).

(4) W. A. G. Graham, J. W. T. Spinks and T. Thorvaldson, *Can. J. Chem.*, **32**, 129 (1954).

(5) G. E. Bessey, "Proceedings of the Symposium on the Chemistry of Cements," Stockholm, 1938, p. 178.

(6) S. Brunauer, J. C. Hayes and W. E. Hass, THIS JOURNAL, **58**, 279 (1954).

(7) Ernest M. Grunwald, unpublished Portland Cement Association reports; Chem. Dept., Florida State University, Tallahassee, Florida.

by Copeland and Hayes[8] to avoid sample losses owing to frothing and "boiling," which occur when the slurry is placed on the vacuum line directly. After most of the water had been removed, the samples were homogenized by thorough mixing to eliminate stratification; the rest of the adsorbed water was then removed by the procedure described by Brunauer, Hayes and Hass.[6] Drying was considered complete when the loss of water was less than 1 mg./g. of sample in two days.

All operations, to the extent possible, were conducted in a controlled atmosphere manipulation cabinet equipped with Ascarite filters, to minimize contamination of samples by CO_2.

Extraction of Calcium Hydroxide.—This was done by a modification of the method of Franke[9] for the quantitative determination of lime. A solvent mixture, made up of 60 cc. of isobutyl alcohol, 9 cc. of acetoacetic ester (ethyl acetoacetate) and 15 cc. of ethyl ether, was added to 1 g. of sample; the mixture was refluxed at 70 to 80° for three hours, filtered, and the lime in the filtrate was determined gravimetrically or volumetrically. The extraction process was then repeated on the residue; and if the filtrate obtained in the second extraction contained a sizable quantity of lime, a third extraction was performed. On some samples cold extractions were performed. Instead of refluxing the mixture, it was shaken on a rotating table for 24 hours.

Preparation of Calcium Hydroxide.—Two preparations of calcium hydroxide were used.

(a) $Ca(OH)_2$(I).—CaO was prepared by the ignition of whiting ($CaCO_3$) at 950 to 1000° for 24 hours. The CaO was then hydrated by exposure to an atmosphere of saturated water vapor at 23° for two months. The containers were lined with ceresin. The specific surface area of the calcium hydroxide was determined by the B.E.T. method,[10] using nitrogen adsorption; it was found to be 36.8 m.²/g.

(b) $Ca(OH)_2$(II).—The same CaO was used, but it was hydrated in boiling water. The surface area of this sample was 5.8 m.²/g.

Ignition loss and carbon dioxide determinations indicated complete hydration and very slight carbonation for both preparations.

Other Operations.—The ignition loss and carbon dioxide content were determined, the chemical analyses were performed, and the compositions of the substances were calculated according to the methods described by Brunauer, Hayes and Hass.[6]

Density determinations were made at 27° by the liquid-displacement method. The liquid used was a saturated solution of calcium hydroxide in water.

Dr. Greenberg of the Johns-Manville Research Center examined several of our samples by the methods[11] of differential thermal analysis and Chevenard thermobalance measurements.

X-Ray Investigations.—Cu Kα radiation was used in all cases. X-Ray diffraction patterns were obtained with a 114.6 mm. diameter Debye–Sherrer camera, a Norelco Wide Range Geiger Counter Diffractometer, or with a Norelco Counting Rate Computer used in conjunction with the diffractometer. This combination performs "fixed count" scanning automatically.

Specimens were protected from carbon dioxide and water vapor during use of the diffractometer by a simple modification of the scatter shield of the instrument. A thin sheet of polyethylene was sealed over the X-ray beam opening of the scatter shield, thereby providing a sealed chamber for the specimen during normal operation, with negligible loss of intensity. A test in which a sample of $Ca(OH)_2$(I) was held for 24 hours in the sealed enclosure showed no measurable change in carbon dioxide content, and a barely perceptible increase in ignition loss.

Except for the materials which were already sufficiently fine-grained, all samples were ground to pass a 200-mesh sieve and then further ground by hand for about 30 minutes in a mullite mortar. This procedure ensures good mixing of the constituents of the prepared mixtures, and it produces the fine-grained material necessary for reproducible intensity measurements.[12] The grinding was carried out in the controlled-atmosphere cabinet.

The most troublesome aspect of X-ray quantitative analysis, particularly of mixtures containing platy or fibrous materials, is preferred orientation. A modification of the technique described by Swanson and Tatge[13] enabled us to produce specimens for the diffractometer remarkably free from preferred orientation. Details of the specimen-preparation technique will be published later by Copeland and Bragg.

All quantitative analyses were performed with the diffractometer. Intensity data were obtained either by means of rate-meter recording, with the goniometer scanning at $1/8°$ 2θ/minute, or by means of automatic "fixed count" scanning with the computer set for angular increments of $0.05°2\theta$. Corrections for Geiger counter lost counts were found to be unnecessary. The number of counts was such that the instrumental error in intensity measurements was usually less than 1%.

Results and Discussion

The stoichiometry of the hydration of Ca_3SiO_5 at 23° in a saturated calcium hydroxide solution can be represented by the equation

$$2Ca_3SiO_5 + 6H_2O = Ca_3Si_2O_7{\cdot}3H_2O + 3Ca(OH)_2 \quad (1)$$

The formula, $Ca_3Si_2O_7{\cdot}3H_2O$, is not intended to imply here anything about the structure of the calcium silicate hydrate. The water may be present in the hydroxylic form or as molecular water in the compound. Both ball-mill hydration and paste hydration can be *formally* represented by the same equation, but the calcium silicate hydrates are different. In ball-mill hydration the hydrate produced *is* afwillite; in paste hydration the product obtained *is similar to* tobermorite. To distinguish between the two calcium silicate hydrates, we shall adopt the notation $Ca_3Si_2O_7{\cdot}3H_2O$ (A) for afwillite and $Ca_3Si_2O_7{\cdot}3H_2O$ (T) for the tobermorite-like hydrate.

The Water of Hydration.—Jacquemin[14] hydrated Ca_3SiO_5 in a ball mill, and he concluded that the water of hydration was 3 molecules per molecule. Grunwald,[7] who investigated ball-mill hydration at our laboratory a few years ago, arrived at the same conclusion.

We hydrated several batches of Ca_3SiO_5 in the ball mill and obtained complete hydration in about 6 days, as will be shown later. The water of hydration corresponded almost exactly to 3 molecules of water per molecule of Ca_3SiO_5. We may mention two examples of this. The total water of hydration of one batch of hydrated Ca_3SiO_5(I), calculated on the assumption that Ca_3SiO_5 takes up 3 and Ca_2SiO_4 2 molecules of water, was 23.21% on ignited-weight basis. The experimental value was 23.11%. The total calculated water of hydration of another batch of hydrated Ca_3SiO_5(I) was 23.25%; the experimental value was 23.16%.

It is somewhat surprising to obtain such close agreement between theoretical and experimental values in a colloidal system. Afwillite, the calcium silicate hydrate produced in the ball-mill hydration of Ca_3SiO_5, is obtained in the form of particles hav-

(8) L. E. Copeland and J. C. Hayes, ASTM Bulletin, No. 194, December, 1953.

(9) B. Franke, *Z. anorg. allgem. Chem.*, **247**, 180 (1941).

(10) S. Brunauer, P. H. Emmett and E. Teller, *J. Am. Chem. Soc.*, **60**, 309 (1938).

(11) S. A. Greenberg, THIS JOURNAL, **58**, 362 (1954).

(12) L. Alexander, H. P. King and E. Kummer, *J. Appl. Phys.*, **19**, 742 (1948).

(13) H. E. Swanson and E. Tatge, *J. Research Natl. Bur. Standards* **46**, 318 (1951).

(14) R. Jacquemin, "Recherches sur l'hydration des liants hydrauliques," Dissertation, University of Liege, Desoer, Liege, 1944.

ing an average dimension of less than 300 Å. Nevertheless, afwillite even in this size range is stable at a water vapor pressure of 5×10^{-4} mm., indicating that its dissociation pressure at 23° has a lower value than that.

The Reaction Products.—There was no evidence of unhydrated Ca_3SiO_5 on any of our X-ray diffractometer charts after 6 days of ball-mill hydration. All lines on the charts were attributable to calcium hydroxide and the calcium silicate hydrate.

The amount of $Ca(OH)_2$ in the products was first determined by the modified Franke method, described earlier. The result corresponded almost exactly to 1.5 molecules of $Ca(OH)_2$ per molecule of Ca_3SiO_5. Three examples are given below.

1. Batch I of hydrated Ca_3SiO_5(I) contained a total calculated value of 35.79% uncombined CaO. We assumed that the hydration of Ca_3SiO_5 produced 1.5 molecules of $Ca(OH)_2$ per molecule, and the hydration of Ca_2SiO_4 0.5 molecule of $Ca(OH)_2$ per molecule. The experimental result was 35.76% uncombined CaO.

2. Batch II of hydrated Ca_3SiO_5(I) had a calculated uncombined CaO content of 35.30%. The experimental value was 35.42%.

3. The above analyses were performed by hot extractions. Cold extraction of batch II of hydrated Ca_3SiO_5(I) gave an experimental value of 35.33%.

In spite of the extraordinary agreement between the calculated and experimental values, chemical analysis did not settle the stoichiometry of the hydration of Ca_3SiO_5. It did not seem impossible, or even unlikely, that the extraction process had altered the hydration products. For example, it seemed possible, especially on the basis of prior information,[2] that the hydration proceeded according to the reaction

$$Ca_3SiO_5 + 3H_2O = Ca_2SiO_4 \cdot 2H_2O + Ca(OH)_2 \quad (2)$$

and that during extraction the higher-lime hydrate decomposed

$$2(Ca_2SiO_4 \cdot 2H_2O) = Ca_3Si_2O_7 \cdot 3H_2O + Ca(OH)_2 \quad (3)$$

X-Ray investigation of the hydration products before and after extraction settled the question definitely. Diffractometer charts of the hydration products established the fact that in both cases the calcium silicate hydrate was afwillite, $Ca_3Si_2O_7 \cdot 3H_2O$ (A). Other than the calcium hydroxide lines only the lines of afwillite were present, with one possible exception. On some charts there was a vague indication of the strongest line of the tobermorite-like hydrate, $Ca_3Si_2O_7 \cdot 3H_2O$ (T), the one at 3.03 Å. Although a quantitative estimation could not be made, probably less than 5% of the calcium silicate hydrate was tobermorite.

The material from which the calcium hydroxide had been extracted showed complete absence of the calcium hydroxide lines on the charts; only afwillite lines were present. This was true of both the hot-extracted [Afwillite (H)] and the cold-extracted [Afwillite (C)] material. We mixed Afwillite (C) with $Ca(OH)_2$ in the proportion of three moles of $Ca(OH)_2$ to one mole of afwillite. Two mixtures were prepared: mixture A [Afwillite (C) plus $Ca(OH)_2$I] and mixture B [Afwillite (C) plus $Ca(OH)_2$-II].

X-Ray diffractometer charts of the two mixtures were prepared, and they were compared with charts of completely hydrated, unextracted Ca_3SiO_5 (Hydrated Ca_3SiO_5). The comparisons were based on the intensities of the four strongest lines of afwillite and the two strongest lines of calcium hydroxide. The line intensities obtained on seven charts are given in Table I.

TABLE I

LINE INTENSITY MEASUREMENTS

	$Ca(OH)_2$ lines		Afwillite lines			
	4.90 Å.	2.63 Å.	6.61 Å.	3.18 Å.	2.83 Å.	2.73 Å.
Alfwillite (H)			269	457	680	423
Afwillite (C)			246	424	604	391
Hydrated		981		311	473	293
Ca_3SiO_5	718	914	168	291	435	267
Mixture A	547	986	137	260	377	243
Mixture B		885			488	288
Mixture B	501	823	157	264	392	248

The intensities are given in arbitrary units (actually the number of squares on our charts). To ascertain whether the relative amounts of calcium hydroxide and afwillite were the same in hydrated Ca_3SiO_5 and in the two mixtures, we calculated the ratios of the intensities of each of the afwillite lines to each of the calcium hydroxide lines for each chart and compared the ratios obtained for hydrated Ca_3SiO_5 with the ratios obtained for the mixtures. The intensities shown in Table I enabled us to make 26 such comparisons. The result was that the afwillite content of hydrated Ca_3SiO_5 was 98.7% of the afwillite content of mixture A or B (or, what is the same thing, the calcium hydroxide content of hydrated Ca_3SiO_5 was 101.3% of the calcium hydroxide content of mixture A or B). The standard error of the mean was 3.4%. It will be noted that in the comparison we used *relative* intensities, the calcium hydroxide serving as an internal standard for the afwillite and *vice versa*.[15]

We can definitely conclude from these data that the stoichiometry of the hydration of Ca_3SiO_5 in the ball mill at 23° in saturated calcium hydroxide solution is represented by the equation

$$2Ca_3SiO_5 + 6H_2O = Ca_2Si_2O_7 \cdot 3H_2O(A) + 3Ca(OH)_2 \quad (4)$$

Calcium Hydroxide.—The calcium hydroxide produced in the hydration of Ca_3SiO_5 appeared in the form of crystals having larger than colloidal dimensions. The calcium hydroxide in mixture A had a surface area of 36.8 m.²/g.; that in mixture B a surface area of 5.8 m.²/g. Comparison of the half-intensity widths of the calcium hydroxide lines obtained for these mixtures with those of the calcium hydroxide lines obtained for hydrated Ca_3SiO_5 indicated that the dimensions of the calcium hydroxide crystallites in the latter were intermediate between the dimensions of the crystallites in the two mixtures and closer to the dimensions of the low-surface calcium hydroxide. The line widths also clearly indicated that the crystallites of calcium hydroxide were stubby. Surface-area determinations by water-vapor adsorption indicated about

(15) L. Alexander and H. P. Klug, *Anal. Chem.*, **20**, 886 (1948).

the same average particle dimension as X-ray line broadening did.

Afwillite.—The d spacings of the X-ray diffraction lines of the afwillite produced in the ball-mill hydration of Ca_3SiO_5 showed a very close correspondence to the d spacings published by various investigators for the natural mineral afwillite, especially to those published by Switzer and Bailey.[16] Interestingly, however, the relative intensities of our lines did not show such a close correspondence to published values. A comparison between our results and those of others for the four strongest lines of afwillite is given in Table II.

TABLE II

RELATIVE INTENSITIES OF AFWILLITE LINES

	Afwillite lines 6.61 Å.	3.18 Å.	2.83 Å.	2.73 Å.
A. Our Values				
Afwillite (H)	40	67	100	62
Afwillite (C)	41	70	100	65
Hydrated Ca_3SiO_5	..	66	100	62
Hydrated Ca_3SiO_5	39	67	100	61
Mixture A	36	69	100	64
Mixture B	..	..	100	59
Mixture B	40	67	100	63
Av.	40	67	100	62
B. Values of Others				
Switzer and Bailey[16]	90	90	100	90
Imperial Chemical Industries, Ltd.[17]	70	90	100	90
McMurdie and Flint[18]	80	100	100	80
Av. of others' values	80	93	100	87

The discrepancy between our results and those of others is explainable on the basis of preferred orientation in the samples of other investigators. Our artificial afwillite was obtained in colloidal dimensions, after six days of grinding; we believe, therefore, that the particles had random orientation. This is evidenced also by the close agreement between the relative intensities obtained on seven charts, shown in Table II.

We received from the U. S. National Museum a sample of natural afwillite, which came from the Dutoitspan mine, Kimberly, South Africa. Debye–Sherrer patterns made on parts of the sample showed that (a) the 2.83 Å. line was the strongest line; (b) the 3.18 and 2.73 Å. lines had about the same intensities, and their intensities were about two-thirds of the intensity of the 2.83 Å. line; and (c) the intensity of the line at 6.61 Å. had about one-half the intensity of the 2.83 Å. line. The Debye–Sherrer patterns of our artificial afwillite were indistinguishable from those of natural afwillite.

We prepared six X-ray diffractometer charts of natural afwillite and calculated the relative intensities. The results are shown in Table III.

A comparison of Table III with Table II shows that the relative intensities of the four strongest lines of natural and artificial afwillite are in very good agreement. On the basis of these results we conclude that there is no difference, detectable by the X-ray techniques employed by us, between the natural mineral afwillite and the artificial afwillite obtained in the ball-mill hydration of Ca_3SiO_5.

TABLE III

RELATIVE INTENSITIES OF NATURAL AFWILLITE LINES

Chart no.	Afwillite lines 6.61 Å.	3.18 Å.	2.83 Å.	2.73 Å.
1	48.2	59.9	100	69.0
2	57.3	61.7	100	78.7
3	41.1	60.3	100	79.1
4	46.1	67.9	100	56.5
5	47.0	77.4	100	79.3
6	41.3	63.5	100	51.6
Av.	46.8	65.1	100	69.0
Standard error of mean, %	2.4	2.7	..	5.0

Megaw[19] recently determined the crystal structure of afwillite and showed that the formula $Ca_3(SiO_3OH)_2 \cdot 2H_2O$ best represented its structure. From the structure data she calculated the density of afwillite to be 2.643 ± 0.005 g./cc. She used natural afwillite from the Dutoitspan mine for the structure determination. We determined the density of our afwillite, obtained from ball-mill-hydrated Ca_3SiO_5 by hot-extraction of calcium hydroxide. The experimental density was 2.642 ±0.01 g./cc., the density corrected for impurities (on additive basis) was 2.647 ± 0.01 g./cc.

For the indices of refraction of afwillite from Crestmore, California, Switzer and Bailey[16] reported the values $\alpha = 1.616$, $\beta = 1.619$, $\gamma = 1.631$. The average index of refraction of our sample of Dutoitspan afwillite was 1.62 ± 0.01. The average index of refraction of our artificial colloidal afwillite was also 1.62 ± 0.01.

The specific surface area of afwillite obtained from the ball-mill hydration of Ca_3SiO_5 was found to be 84 ± 4 m.²/g. by the B.E.T. method.[10] It was determined both by nitrogen adsorption at the boiling point of nitrogen and by water vapor adsorption at 25°. Using the customary value of 16.2 Å.² for the molecular area of nitrogen, we obtain identical surface area with water vapor, if we assume that the latter had a molecular area of 11.8 Å.²; a reasonable molecular area.

If the afwillite particles were spherical and all the same size, the surface area would indicate a particle diameter of about 285 Å. Electron micrographs, obtained by Swerdlow, McMurdie and Heckman[20] from our artificial afwillite showed that the particles were roughly spherical and had dimensions of the order of 250 Å.

Differential thermal analysis results were reported by Moody[21] for natural afwillite from Kimberly. She stated that the chart "shows an endothermic reaction proceeding in several steps in the temperature range 250–450°, the most marked re-

(16) G. Switzer and E. H. Bailey, *Am. Mineralogist*, **38**, 629 (1953).

(17) Imperial Chemical Industries, Norwich.

(18) H. F. McMurdie and E. P. Flint, *J. Research Natl. Bur. Standards*, **31**, 227 (1943).

(19) H. D. Megaw, *Acta Cryst.*, **5**, 477 (1952).

(20) M. Swerdlow, H. F. McMurdie and F. A. Heckman, "Proc. of the International Conference on Electron Microscopy," London, 1954; *J. Roy. Micr. Soc.* (in press).

(21) K. M. Moody, *Mineral. Mag.*, **29**, 838 (1952).

action occurring at approximately 370°, and an exothermic reaction which takes place at about 820°. It seems clear that these correspond to the dehydration process and to the formation of rankinite, respectively."

The main features of the differential thermal analysis curve of our artificial afwillite were the same as those of natural afwillite. There were endothermic minima at 240, 320 and 470°, which, doubtless, correspond to the steps reported by Moody for the temperature range 250–450°. The slight shifts in temperature are not significant; they may be caused by differences in techniques. The minima at 240 and 320° probably correspond to the loss of the two types of water in afwillite, $Ca_3(SiO_3OH)_2 \cdot 2H_2O$. The most marked reaction occurs at 320°. There is a strong exothermic peak at 820°, which may possibly be due to the formation of wollastonite, β-$CaSiO_3$, rather than rankinite, $Ca_3Si_2O_7$. In addition to the peaks reported by Moody, Greenberg obtained an endothermic peak at 125°, which may be due to the loss of adsorbed water. The absence of the peak in natural afwillite may be explained on the basis of difference in surface area; our artificial afwillite had colloidal dimensions, whereas the specific surface area of natural afwillite was negligible compared with that of our artificial afwillite.

Acknowledgments.—We wish to express our great indebtedness to Dr. S. A. Greenberg for the thermobalance and D.T.A. measurements; to Dr. D. L. Kantro for preparing most of the materials used by us, for the density determinations and for a part of the surface-area measurements; to Mr. E. E. Pressler for all chemical analyses and extractions; to Dr. L. S. Brown for the index of refraction determinations; to Miss Edith Turtle for a part of the surface area measurements; and to Mr. T. C. Powers and Dr. H. H. Steinour for many helpful discussions and suggestions.

We also wish to express our sincere appreciation to Dr. A. B. Cummins, for permitting and encouraging the cooperation between the Johns-Manville Research Center and the Portland Cement Association Research and Development Laboratories, and to Drs. Remington Kellogg, W. F. Foshag, and George Switzer for the donation of a sample of the natural mineral afwillite by the Smithsonian Institution to the Portland Cement Association.

THE STOICHIOMETRY OF THE HYDRATION OF TRICALCIUM SILICATE AT ROOM TEMPERATURE. II. HYDRATION IN PASTE FORM

BY STEPHEN BRUNAUER, L. E. COPELAND AND R. H. BRAGG

Portland Cement Association Research and Development Laboratories, Chicago, Illinois

Received July 11, 1955

Evidence is presented that the stoichiometry of the hydration of tricalcium silicate, Ca_3SiO_5, in the form of hardened paste in a saturated calcium hydroxide solution at 23° may be represented by the equation $2Ca_3SiO_5 + 6H_2O = Ca_3Si_2O_7 \cdot 3H_2O + 3Ca(OH)_2$. An initial H_2O/Ca_3SiO_5 weight ratio of 0.7 was used, and the pastes were hydrated for 2 to 2.5 years. X-Ray and microscopic examinations indicated almost complete hydration. The calcium silicate hydrate produced was similar to the natural mineral tobermorite; its density was 2.44 ± 0.01 g./cc., and its average index of refraction was 1.56 ± 0.015. Bernal proposed the structural formula $Ca_2[SiO_2(OH)_2]_2[Ca(OH)_2]$ for the hydrate. The artificial tobermorite was colloidal in dimensions; nitrogen adsorption, X-ray line broadening and electron micrographs indicated on average dimension of about 100 Å. About 15% of the calcium hydroxide was adsorbed on the tobermorite surface; the rest of the calcium hydroxide appeared in the form of relatively large crystals, visible under the microscope.

Introduction

The stoichiometry of the hydration of tricalcium silicate, Ca_3SiO_5, in a steel ball mill in a saturated calcium hydroxide solution at 23° was discussed in the previous paper.[1] The present paper discusses the stoichiometry of the hydration of Ca_3SiO_5 in the form of "paste." The term "paste" as used by cement chemists, and as used here, means a plastic or semi-fluid mixture of a hydraulic material, such as portland cement, Ca_3SiO_5 or Ca_2SiO_4, with water. After a few hours the paste "sets" and then hardens; the present investigations were carried out on hardened pastes.

Experimental

The experimental techniques employed were in most respects identical with those described before.[1] Only a few additional remarks are needed here.

Pastes of Ca_3SiO_5 were prepared by the method described by Brunauer, Hayes and Hass,[2] except that the pastes were cast as solid cylinders, without a hole in the center. The water-to-Ca_3SiO_5 weight ratio was 0.7. The pastes prepared from Ca_3SiO_5(I) were hydrated for 21 months; those prepared from Ca_3SiO_5(II) were hydrated for 30 months. The hydration was conducted in a room kept at 23 ± 0.5°.

The uncombined water was removed by the method described by Brunauer, Hayes and Hass.[2]

The calcium hydroxide, $Ca(OH)_2$(III), used in the present experiments was different from those described before.[1] Calcium oxide was prepared from "Baker analyzed" reagent grade $CaCO_3$, low in alkalies, by ignition at 900 to 950° for 16 hours. The hydration was carried out in a polyethylene bottle, by letting the CaO stand in water at 25° for three months and shaking the bottle once or twice a day.

Results and Discussion

X-Ray diffractometer charts of the hydrated Ca_3SiO_5 pastes showed the presence of calcium hydroxide and tobermorite lines only. The calcium silicate hydrates designated as tobermorites, vary in molar CaO/SiO_2 ratio from 1.0 (or 0.8) to 1.5. In a saturated calcium hydroxide solution the compound with the highest lime-to-silica ratio is obtained.[1] This compound has the formula $Ca_3Si_2O_7 \cdot 3H_2O$ according to Bernal,[3] and the formula

(1) S. Brunauer, L. E. Copeland and R. H. Bragg, THIS JOURNAL, **60**, 112 (1956).

(2) S. Brunauer, J. C. Hayes and W. E. Hass, *ibid.*, **58**, 279 (1954).

(3) J. D. Bernal, "Proceedings of the Third International Symposium on the Chemistry of Cement," London, 1952, p. 216.

$Ca_3Si_2O_7 \cdot 2H_2O$ according to Taylor.[4] The formulas, as written here, are not intended to imply anything about the structures of the molecules; water may be present in the structure either in the molecular or in the hydroxylic form, or in both forms.

The stoichiometry of the hydration of Ca_3SiO_5 may be represented by the equation

$$2Ca_3SiO_5 + 6H_2O = Ca_3Si_2O_7 \cdot 3H_2O(T) + 3Ca(OH)_2 \quad (1)$$

if Bernal's formula is correct, or by the equation

$$2Ca_3SiO_5 + 5H_2O = Ca_3Si_2O_7 \cdot 2H_2O + 3Ca(OH)_2 \quad (2)$$

if Taylor's formula is right. (The (T) after $Ca_3Si_2O_7 \cdot 3H_2O$ is added to distinguish this compound from afwillite.[1]) It will be shown that the weight of evidence favors eq. 1. Other reactions than those represented by eq. 1 and 2 will be considered in the last section of the paper.

The Water of Hydration.—The water of hydration was determined by the same method that was employed for the ball-mill hydration products.[1] If we call the stoichiometric water of hydration, according to eq. 1, 100%, then two pastes prepared from Ca_3SiO_5(I) contained 86.0 and 83.7, and one paste prepared from Ca_3SiO_5(II) contained 84.5% of the stoichiometric quantity of water. These numbers represent *minimum* values. Both Ca_3SiO_5 preparations contained approximately 96% Ca_3SiO_5, 3% β-Ca_2SiO_4 and 1% of other impurities. The values for the water of hydration were calculated on the assumptions that (1) the hydratable impurities (tricalcium aluminate, calcium oxide and magnesium oxide) were fully hydrated; and (2) the fraction of β-Ca_2SiO_4 hydrated was the same as the fraction of Ca_3SiO_5 hydrated.

Pure β-Ca_2SiO_4 hydrates at a much slower rate than Ca_3SiO_5. A hardened paste of β-Ca_2SiO_4, which had hydrated for about the same period as the three Ca_3SiO_5 pastes, contained only 37.5% of the stoichiometric amount of water of hydration (2 molecules of water per molecule of Ca_2SiO_4).[2] If we assume that the Ca_2SiO_4 in the Ca_3SiO_5 paste hydrated at the same rate as in its own paste, then the Ca_3SiO_5 in the three pastes contained 87.3, 85.0 and 85.3% of the stoichiometric quantity of water according to eq. 1. These are not necessarily *maximum* values, since in this calculation we have assumed again that all hydratable impurities, with the exception of Ca_2SiO_4, were fully hydrated. The water of hydration of Ca_3SiO_5 in the three pastes was probably between the two sets of values given above.

Equation 2 implies that the water of hydration is only $^5/_6$ of that indicated by eq. 1, or 83.3%. Our values were between 83.7 and 87.3%. Two arguments may be advanced against eq. 2.

1. The first may be adduced from consideration of the sizes of the tobermorite particles. We shall show later that the average particle dimension is of the order of 100 Å. which approaches the lower size range even in colloidal systems. The dissociation pressure of the calcium silicate hydrate in this size range should be greater than that of normal crystals; the water content of the hydrate at a vapor pressure of 5×10^{-4} mm. should, therefore, be *at most* equal to and probably smaller than the stoichiometric water content in a saturated calcium hydroxide solution. This could explain why the water contents of the pastes were smaller than the quantities indicated by eq. 1, but all our water values were greater than that corresponding to eq. 2.

2. A second and perhaps more decisive argument against eq. 2 may be cited from crystal structure considerations. It was shown by Taylor[5] that his calcium silicate hydrate (I), or artificial tobermorite, was a layer crystal and that the structure of the layers did not change with increasing CaO/SiO_2 ratio. A hydrate with a molar CaO/SiO_2 ratio of 0.92 gave the same X-ray diffraction line pattern as a hydrate with a CaO/SiO_2 ratio of 1.41. This can be explained by assuming that the lime in excess of 1 mole per mole of SiO_2 was located between the layers, as was postulated by Bernal.[3] In this case, however, it is difficult to imagine the existence of unhydrated or incompletely hydrated CaO in an aqueous system between layers of hydrated calcium silicate. Bernal assumed layers of $Ca(OH)_2$ between the calcium silicate hydrate layers, which seems more reasonable, and which would lead to the stoichiometry represented by eq. 1.

Taylor arrived at the formula $Ca_3Si_2O_7 \cdot 2H_2O$ on the basis of dehydration experiments.[4] We conducted some dehydration experiments, which will be published in more detail in the future by Brunauer, Kantro and Weise. Tobermorites having CaO/SiO_2 ratios of 1.0 and 1.5 were prepared by the reaction of calcium hydroxide and hydrous silica at 23°. In the course of drying at a water vapor pressure of 5×10^{-4} mm., both hydrates lost approximately one-third of their water of hydration, one retaining only 0.65 mole of water, the other about 1 mole of water per mole of SiO_2. The tobermorite obtained in the paste hydration of Ca_3SiO_5 also lost roughly one-third of its water of hydration under the same drying conditions. On the other hand, when a less drastic drying agent was used, more of the water of hydration was retained. At a vapor pressure of 8×10^{-3} mm., produced by a mixture of magnesium perchlorate dihydrate and tetrahydrate, about 14% more water was retained by hydrated Ca_3SiO_5 pastes than at 5×10^{-4} mm. pressure.

On the basis of the above considerations, we conclude that eq. 2 does not represent the stoichiometry of the paste hydration of Ca_3SiO_5 in a saturated calcium hydroxide solution at room temperature.

Calcium Hydroxide.—We were unable to determine the calcium hydroxide content of paste-hydrated Ca_3SiO_5 by chemical means because the solvents used both in the Franke method[6] and the Lerch and Bogue method[7] removed some of the lime from the high-lime tobermorite.

The calcium hydroxide content of the hydrated paste was determined by X-ray line intensity measurements. The paste used in these determinations was prepared from Ca_3SiO_5(II). The lime was extracted from a portion of the paste by a

(4) H. F. W. Taylor, *J. Chem. Soc.*, 163 (1953).

(5) H. F. W. Taylor, *ibid.*, 3682 (1950).

(6) B. Franke, *Z. anorg. allgem. Chem.*, **247**, 180 (1941).

(7) W. Lerch and R. H. Bogue, *Ind. Eng. Chem., Anal. Ed.*, **2**, 296 (1930).

modification of the Franke method,[1] and a known quantity of calcium hydroxide (III) was added to the remaining tobermorite (mixture C). Comparison of the intensities of the two strongest calcium hydroxide lines obtained from the Ca_3SiO_5 paste and from mixture C gave the weight fraction of $Ca(OH)_2$ in the former.

We prepared X-ray diffractometer charts of six samples of the Ca_3SiO_5 paste, and six of mixture C. The results are shown in Table I.

TABLE I

INTENSITIES OF CALCIUM HYDROXIDE LINES

Chart No.	Mixture C $Ca(OH)_2$ lines 4.90 Å.	2.63 Å.	Chart No.	Ca_3SiO_5 Paste $Ca(OH)_2$ lines 4.90 Å.	2.63 Å.
1	557	848	1A	616	747
2	565	839	2A	411	748
3	..	847	3A	..	718
Av.	561	845		513	738
4	576	878	4A	411	788
5	644	876	5A	598	871
6	..	888	6A	..	777
Av.	610	881		505	812

Charts 1, 2, 3 and 1A, 2A, 3A were obtained on the same day, and the average intensity of each calcium hydroxide line obtained for one of the materials was compared with the average intensity of the same line obtained for the other material. Likewise, charts 4, 5, 6 and 4A, 5A, 6A were obtained on the same day, and the average intensities were compared in a similar manner. Such precautions are important because it is difficult to reproduce the voltage and current settings exactly from day to day. Mixture C contained 38.8% calcium hydroxide; the uncorrected percentage of calcium hydroxide in the Ca_3SiO_5 paste based on the intensities given in Table I was 34.1 ± 0.3%. Correction for the differences in mass absorption coefficients lowered this value to 33.9 ± 0.3%. (This result has since been confirmed using an internal standard, to be published by Copeland and Bragg.)

Dr. S. A. Greenberg of the Johns-Manville Research Center determined the calcium hydroxide content of our Ca_3SiO_5 paste by his Chevenard thermobalance and obtained a value of 34.7%. This is in good agreement with our X-ray value of 33.9%. The latter value corresponds to 85.4 ± 0.8% of the stoichiometric amount according to eq. 1. The missing 15% of calcium hydroxide may be ascribed to adsorption on the tobermorite surface. As will be seen later, the specific surface area of tobermorite is large; it can account for the adsorption of this amount of calcium hydroxide without difficulty. The adsorbed calcium hydroxide decomposes at lower temperatures than crystalline calcium hydroxide and, because of the heterogeneity of the surface, over a range of temperatures. This is the reason why the thermobalance results, giving the values for crystalline calcium hydroxide, checked the X-ray results so well.

In contrast with the finely divided tobermorite, the calcium hydroxide produced in the paste-hydration of Ca_3SiO_5 appeared in the form of relatively large crystals, easily visible under the microscope. The X-ray diffraction lines were sharp, indicating larger calcium hydroxide crystals than those produced in the ball-mill hydration of Ca_3SiO_5.[1]

The Extent of Hydration of Ca_3SiO_5.—The Ca_3SiO_5 paste, discussed in the previous section, contained 85.4 ± 0.8% of the stoichiometric amount of calcium hydroxide according to eq. 1. Earlier we discussed the two ways of calculating the water of hydration of Ca_3SiO_5 pastes. The values for this particular paste were 84.5 and 85.3%; the average was 84.9 ± 0.4% of the stoichiometric water of hydration according to eq. 1. Because these independent determinations showed such excellent agreement, we believed at first that the Ca_3SiO_5 paste was only 85% hydrated in 2.5 years. However, this did not turn out to be the case.

We were unable to detect more than a very small amount of unhydrated Ca_3SiO_5 in the above paste by means of our X-ray diffractometer. We determined the amount of unhydrated Ca_3SiO_5 in the paste by diluting samples of the paste with known quantities of Ca_3SiO_5 and comparing the mixtures with the undiluted paste. The result was 0.5% unhydrated Ca_3SiO_5 in the paste. Details of the method will be presented later by Copeland and Bragg.

Microscopic examination of the Ca_3SiO_5 paste confirmed the X-ray results; it indicated less than 1% unhydrated Ca_3SiO_5. We had to conclude, therefore, that the Ca_3SiO_5 paste was almost completely hydrated. As stated in the two previous sections, the deficiency in the water of hydration may be ascribed to partial decomposition of the tobermorite under our drying conditions, and the deficiency in calcium hydroxide to adsorption on the tobermorite surface. The fact that the deficiency was 15% in both cases is probably sheer coincidence; for the time being we have no other explanation for it.

Tobermorite.—1. On the basis of crystal structure and other considerations, Bernal[3] suggested that the tobermorite system of hydrates might be represented by the structural formula

$$Ca[SiO_2(OH)_2][Ca(OH)_2]_x[H_2O]_y$$

where x varies from 0 to 0.5 and y from 0 to 1.0. We shall disregard the $[H_2O]_y$ term, which represents adsorbed or zeolitic water. We cannot tell how much adsorbed water is attached to the surface of the hydrate in the saturated calcium hydroxide solution, and the hydrate dried under our drying conditions contains little or no adsorbed water.

The low-lime end-member of the tobermorite series would be the compound $Ca[SiO_2(OH)_2]$, in which two of the oxygen ions of the SiO_4 tetrahedron are replaced by hydroxyl ions. The compounds containing more lime, according to Bernal, "would represent an addition of epi-axially arranged $Ca(OH)_2$ layers, possibly on both sides of the calcium silicate layers. The spacings of the two are sufficiently alike to permit this."

Much has been written by different investigators on the question whether the lime in excess of a CaO/SiO_2 ratio of 1.0 is adsorbed or whether it is in solid solution. Steinour[8] pointed out that a zeolitic solid solution, the type that exists in the tober-

(8) H. H. Steinour, *Chem. Revs.*, **40**, 391 (1947).

morites, can be regarded as "a special kind of internal adsorptive system"; it does not make any difference, therefore, whether we call it one or the other. We share Steinour's point of view, and we add that if we call the zeolitic uptake of lime adsorption, it should be clear that it is *chemical adsorption*. The fact that the high-lime end-member of the tobermorite series has a definite composition clearly indicates that the phenomenon is not physical adsorption. If the extra lime were physically adsorbed on the monocalcium silicate hydrate, the uptake of lime would be a function of the specific surface area of the hydrate, and we would find that the CaO/SiO_2 ratio of the high-lime end-member of the series would vary with the specific surface area. However, there is no such variation. Greenberg[9] determined the CaO/SiO_2 ratio of the high-lime end-member of the series and obtained a value of 1.5 within his experimental error. He also measured the surface areas of some of his preparations by nitrogen adsorption, and the *largest* specific surface area he obtained was only about one-third as large as that of our tobermorite.

The tobermorite we obtained in the paste-hydration of Ca_3SiO_5 in a saturated calcium hydroxide solution at 23° was the high-lime end-member of the tobermorite series, having a CaO/SiO_2 ratio of 1.5. Bernal's structural formula for this compound may be written as $Ca_2[SiO_2(OH)_2]_2[Ca(OH)_2]$. Since we found nothing in our experiments that would contradict this formula, we tentatively accept it as the structural formula of our tobermorite.

2. Whereas the X-ray diffraction line pattern of artificial afwillite, produced in the ball-mill hydration of Ca_3SiO_5, was identical with that of the natural mineral afwillite,[1] the line pattern of our artificial tobermorite was far from being identical with that of the natural mineral tobermorite. Claringbull and Hey[10] listed 29 lines for the natural mineral from Tobermory pier and 32 lines for one of Taylor's artificial tobermorites; but our tobermorite showed only four lines on the diffractometer charts. These four lines, a very strong and very broad line with the peak at about 3.03 Å., and three much weaker lines with peaks at about 11, 2.82 and 1.82 Å., correspond to the four strongest lines of Taylor's artificial tobermorite, obtained from the hydration of Ca_3SiO_5.[5] The scarcity of lines indicates poor crystallization; the widths of the lines indicate fine subdivision.

The fact that Taylor's tobermorite was much better crystallized than ours suggests that his crystals were also larger than ours. Greenberg's[9] tobermorite, like Taylor's, gave a large number of X-ray lines and, as we stated before the surface area of his tobermorite was much smaller than that of ours. The smaller surface areas of Taylor's and Greenberg's crystals indicate a smaller adsorption of calcium hydroxide on the tobermorite surface, which would probably explain why the molar CaO/SiO_2 ratios of their hydrates were equal to 1.5 within their experimental errors.

(9) S. A. Greenberg, THIS JOURNAL, **58**, 362 (1954).

(10) G. F. Claringbull and M. H. Hey, *Mineral. Mag.*, **29**, 960 (1952).

Taylor[5] and Bernal[3] regard tobermorite as a layer crystal, with a variable distance between the layers, depending on the water content. Taylor obtained the value of 11 Å. for the distance between the calcium silicate hydrate layers, when the adsorbed (or zeolitic) water was removed. The X-ray diffractometer chart of our tobermorite showed a broad line with its peak at 11 Å. for the dry substance. On the other hand, Debye–Scherrer photographs, which were prepared by exposing the substance to laboratory air of about 40% relative humidity, showed a very broad line, extending from 11 to 15 Å. The broadening was, doubtless, caused by adsorbed water.

3. We determined the density of a Ca_3SiO_5 paste and obtained the value 2.406 ± 0.005 g./cc. The calculated density of the tobermorite in the paste, assuming additivity of the densities of the constituents of the paste, was 2.44 ± 0.01 g./cc. We may compare this value with that of Taylor's artificial tobermorite. He did not measure the density, but it can be calculated from his crystal structure data. Heller and Taylor[11] found that their artificial tobermorite had an orthorhombic unit cell, with $a = 5.62$ Å., $b = 3.66$ Å., and $c = 11.0$ Å. Assuming that the cell contains one molecule of $Ca_3Si_2O_7 \cdot 3H_2O$, the density of the substance is 2.514 g./cc. A change in the c spacing from 11.0 to 11.3 Å. would give an exact agreement with our density value of 2.44 g./cc. Taylor found values for the c spacing ranging from 11.0 to 11.5 Å., and Greenberg[9] obtained the value of 11.3 Å. for artificial tobermorite. Claringbull and Hey[10] reported values ranging from 11.2 to 11.4 Å. for natural tobermorite. Our own value of 11 Å. may easily be in error to the extent of 0.3 Å. Thus, the density of our calcium silicate hydrate also indicates that it is artificial tobermorite.

4. Similar conclusion was reached from measurement of the index of refraction. It was found that the average index of refraction of our calcium silicate hydrate was approximately the same as that of calcium hydroxide, 1.56 ± 0.015. Claringbull and Hey[10] reported the value of 1.558 ± 0.003 for the mean index of refraction of natural tobermorite, and Heller and Taylor[12] obtained a mean refractive index of about 1.56 for artificial tobermorite.

5. The specific surface area of our artificial tobermorite was 220 m.²/g. If we assume that the tobermorite particles were spherical and all the same size, the surface area leads to a particle diameter of 110 Å. We may compare this value with the average crystallite dimension, obtained from X-ray line broadening. Our tobermorite had only one strong line, with its peak at 3.03 Å. The half-intensity width of this line, corrected for instrumental broadening, gave an average crystallite dimension of 96 Å., which is in fair agreement with the nitrogen adsorption value. Electron micrographs, obtained by Swerdlow and Heckman,[13]

(11) L. Heller and H. F. W. Taylor, *J. Chem. Soc.*, 2397 (1951).

(12) L. Heller and H. F. W. Taylor, *ibid.*, 2535 (1952).

(13) M. Swerdlow, H. F. McMurdie and F. A. Heckman, "Proceedings of the International Conference on Electron Microscopy," London, 1954 *J. Roy. Microsc. Soc.* (in press).

likewise indicated particles of this order of magnitude.

Whereas the surface area values obtained for our artificial afwillite by nitrogen adsorption and by water vapor adsorption were the same, for our artificial tobermorite water vapor adsorption gave a larger surface than nitrogen adsorption. The surface available to water molecules was 320 $m.^2/g.$ The discrepancy may be explained by assuming that water molecules can penetrate, to some extent, between the calcium silicate hydrate layers in tobermorite, whereas nitrogen molecules cannot. Afwillite is not a layer crystal, which would explain the agreement between water and nitrogen adsorption surface area values.

6. The differential thermal analysis curve of our Ca_3SiO_5 paste, obtained by Greenberg, showed only two peaks: one strong endothermic peak at 550°, which corresponds to the dehydration of calcium hydroxide, and one exothermic peak around 900°, which may correspond to the formation of wollastonite, or possibly rankinite. Thus, the DTA curves of afwillite[1] and tobermorite are very different.

The DTA curve of paste-hydrated Ca_3SiO_5 gave no indication of the presence of afwillite, nor did the X-ray diffractometer charts. On the other hand, tobermorite obtained from the Ca_3SiO_5 paste after the hot extraction of calcium hydroxide, showed unmistakably the presence of afwillite. The strongest afwillite line, the one at 2.83 Å., was not definitely identifiable, because it coincided with a tobermorite line, but the afwillite lines at 3.18 and 2.73 Å. were clearly identifiable. We may guess roughly that this tobermorite contained 10 to 20% afwillite.

The Stoichiometry of Paste Hydration.—The question may be raised whether other reactions than that represented by eq. 1 would explain our experimental results.

Bessey[14] and Taylor[5] found evidence of the existence of a dicalcium silicate hydrate in a saturated calcium hydroxide solution at 17°. If we assume that such a hydrate does form in the hydration of Ca_3SiO_5 at 23°, the stoichiometry of the reaction may be represented by the equation

$$Ca_3SiO_5 + xH_2O = Ca_2SiO_4 \cdot (x - 1)H_2O + Ca(OH)_2 \quad (3)$$

The quantity of lime produced in these reactions is 66.7% of that indicated by eq. 1. The quantity of lime we obtained was 85.4%; eq. 3, therefore, cannot represent the hydration reaction. If, however, we assume that in the hydration of Ca_3SiO_5 two calcium silicate hydrates are produced, $Ca_2SiO_4 \cdot (x - 1)H_2O$ and $Ca_3Si_2O_7 \cdot 3H_2O$(T), in the proportion of two molecules of the former to one of the latter, we can account approximately for our experimental results. Nevertheless, we do not favor this explanation. Taylor's dicalcium silicate hydrate gave a pattern *very* similar to that of tobermorite. Our calcium silicate hydrate pattern resembled the latter more than the former. In addition, the DTA curves, the density and the average index of refraction indicated that the hydrate was tobermorite.

Another possible reaction that would give an approximate explanation for our results is

$$4Ca_3SiO_5 + 10H_2O = Ca_7Si_4O_{15} \cdot 5H_2O + 5Ca(OH)_2 \quad (4)$$

This reaction, at *complete* hydration, would indicate $^5/_6$ as much water of hydration and $^5/_6$ as much calcium hydroxide as eq. 1, which is not too far from the results we obtained. Nevertheless, we are reluctant to suggest this explanation. There are already two calcium silicate hydrates in the literature, having X-ray patterns practically indistinguishable from each other. It does not seem to us desirable to propose now the existence of a third hydrate, indistinguishable in X-ray pattern from tobermorite, and very similar to it in other properties.

All of our experimental results can be explained on the basis of the reaction represented by eq. 1, without the necessity of postulating new compounds or phenomena unfamiliar to the colloid chemist. Although the stoichiometry of the paste hydration of Ca_3SiO_5 is not as decisively settled as that of ball-mill hydration, the weight of evidence strongly favors the hydration reaction represented by eq. 1.

The lime is in two different forms in the calcium silicate hydrate; two-thirds of it is located in the calcium silicate hydrate layers, and one-third is in zeolitic solid solution or is adsorbed chemically. The calcium hydroxide is also in two different forms; under our experimental conditions 85% of it was in the crystalline form, and 15% was adsorbed on the tobermorite surface. Tobermorites, having smaller specific surface areas than ours, adsorb a smaller fraction of the calcium hydroxide. This appeared to be the case for the tobermorites of Taylor and Greenberg.

Acknowledgments.—We wish to express our great indebtedness to Mr. T. C. Powers and Dr. H. H. Steinour for many helpful discussions and valuable suggestions, to Mr. E. E. Pressler for all chemical analyses and extractions, to Dr. D. L. Kantro for preparing a part of the materials used by us, for the density determination and for a part of the surface area measurements, to Dr. L. S. Brown for the index of refraction determination and for the microscopic examination, and to Miss Edith Turtle for a part of the surface area measurements.

We also wish to express our sincere appreciation to Dr. S. A. Greenberg for the thermobalance and DTA measurements, and to Dr. A. B. Cummins, for permitting and encouraging the cooperation between the Johns-Manville Research Center and the Portland Cement Association Research and Development Laboratories.

(14) G. E. Bessey, "Proceedings of the Symposium on the Chemistry of Cements," Stockholm, 1938, p. 178.

NOTES

LIQUID AMMONIA AS A SOLVENT. XI. THE CONDUCTIVITY OF METAL-AMMONIA SOLUTIONS

By Philip Marshall and

Albion College, Albion, Michigan

Herschel Hunt

Purdue University, Lafayette, Indiana

Received June 29, 1955

The conductance measurements of Kraus and Lucasse[1] are frequently referred to as demonstrating that conduction is identical for concentrated solutions of the alkali metals in liquid ammonia. However, it should be noted that the atomic conductivities were not actually obtained since the densities of the solutions were not known.

The densities of these solutions were determined at a later date and sufficient data are now available in the literature to calculate the atomic conductivities for sodium and potassium solutions. The densities of sodium solutions at varying concentrations were determined by Kraus, Carney and Johnson[2] and the densities of the corresponding potassium solutions by Johnson and Meyer.[3] Combining the density and conductivity data we obtain the values

Table I

Volumes of Sodium and Potassium-Ammonia Solutions from Density Determinations[a]

d, g./ml.	n, moles NH_3	ΔV, ml.	N	V', l.
	A. Potassium			
0.6282	4.95	27.28	5.09	0.1966
.6351	7.03	29.00	4.00	.2503
.6433	9.65	29.67	3.16	.3162
.6483	11.20	29.20	2.82	.3547
.6522	13.20	29.36	2.47	.4049
.6583	16.22	28.30	2.06	.4797
.6598	17.75	28.44	1.93	.5179
.6659	23.18	26.91	1.54	.6514
.6685	26.76	26.15	1.35	.7402
	B. Sodium			
0.5782	5.48	40.96	4.96	0.2015
.5888	6.73	42.26	4.27	.2340
.6044	8.87	43.15	3.47	.2885
.6163	11.03	43.37	2.91	.3429
.6251	13.10	43.29	2.54	.3938
.6322	15.24	43.13	2.23	.4481
.6376	17.41	43.13	1.99	.5021
.6423	19.63	42.93	1.79	.5570
.6462	21.75	42.54	1.64	.6100
.6494	24.07	42.48	1.49	.6690

[a] Data from Kraus, Carney and Johnson[2] and Johnson and Meyer.[3]

(1) C. A. Kraus and W. W. Lucasse, *J. Am. Chem. Soc.*, **43**, 2529 (1921).

(2) C. A. Kraus, E. S. Carney and W. C. Johnson, *ibid.*, **49**, 2206 (1927).

(3) W. C. Johnson and A. W. Meyer, *ibid.*, **54**, 3621 (1932).

Table II

Atomic Conductivities of Concentrated Solutions of Sodium and Potassium in Liquid Ammonia[a]

V, l.	V', l.	N	l, ohm^{-1} cm.$^{-1}$	Λ, ohm^{-1} cm.^{2}
		A. Potassium		
0.1238 (sat. soln.)	0.197	5.09	4569	899,000
.1295	.203	4.93	4190	851.000
.1519	.226	4.43	3233	731,000
.1572	.231	4.33	2940	679,000
.1730	.247	4.05	2571	635,000
.2004	.275	3.64	1858	511,000
.2103	.285	3.51	1772	505,000
		B. Sodium		
0.1370 (sat. soln.)	0.202	4.96	5047	1,016,000
.1440	.209	4.78	4348	908,000
.1444	.209	4.78	4394	918,000
.1560	.222	4.51	3718	825,000
.1681	.233	4.29	3166	738,000
.1804	.246	4.07	2687	662,000
.1926	.258	3.88	2347	606,000
.2099	.276	3.63	1945	537,000

[a] Data from Table I, and Kraus and Lucasse.[1]

given in Tables I and II and plotted in Fig. 1.[4] In the tables n is the number of moles of ammonia per gram atom of metal; d is the observed density

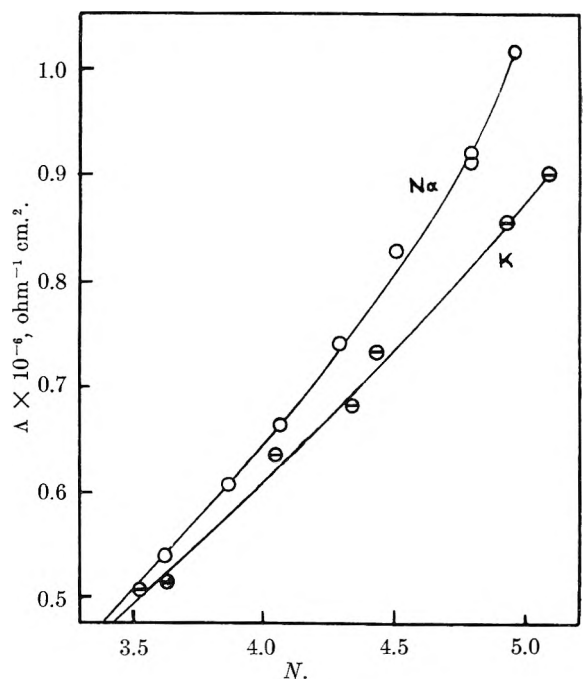

Fig. 1.—Atomic conductivities of concentrated solutions of sodium and potassium in liquid ammonia: atomic conductivity, Λ, *vs.* normality, N.

(4) The conductivity work was performed at −33.6°; the densities of the sodium solutions were determined at −33.8° and of the potassium solutions at −33.2°. The differences were assumed to be negligible.

of the solution; ΔV is the volume change per mole of metal above that to be expected from the sums of the metal and ammonia volumes; N is the normality; V is the observed volume of ammonia per gram atom of the metal; V' is the volume of the solution per gram atom of the metal; l is the specific conductance, and Λ is the equivalent or atomic conductance. The values of V' in Table II were obtained from a graph of V *vs.* V', constructed from the data of Table I.

From the graph it may be seen that the atomic conductance of sodium is about 20% greater than that of potassium when the two solutions are at a concentration of 4.96 moles per liter. In absolute magnitude this amounts to about 160,000 ohm^{-1} $cm.^2$, scarcely a negligible amount. It is evident that this variation is well outside the range of experimental error and we must conclude that the conductivities are not identical.

It seems evident that a successful theory regarding these solutions must be capable of offering a reasonable explanation for the observed variation in their atomic conductivities.

HEATS OF MICELLE FORMATION

By Eric Hutchinson and Lorraine Winslow

Department of Chemistry, Stanford University, Stanford, California

Received July 11, 1955

In a recent publication[1] we reported some observations on the calorimetrically determined heat effect associated with the formation of micelles in solutions of sodium decyl sulfate in water. This work has been extended to cover the case of sodium decyl sulfate in aqueous solutions of sodium chloride and the case of potassium laurate in pure water.

The results which we have obtained are shown in Figs. 1 and 2, in which the heat of solution (integral) per mole is plotted as a function of concentration. The results for sodium decyl sulfate in 0.1 M aqueous sodium chloride solutions indicate a break in the curve in the concentration range 0.010 to 0.011 mole detergent per liter. Associated with this break is the heat of micelle formation, which we estimate to be -0.288 ± 0.047 kcal. per mole. This may be compared with the value obtained in pure water,[1] namely, -0.21 kcal. per mole. The results obtained for potassium laurate in water indicate a break in the concentration range 0.019 to 0.020 mole soap per liter, and we estimate the heat of micelle formation to be -0.088 ± 0.002 kcal. per mole.

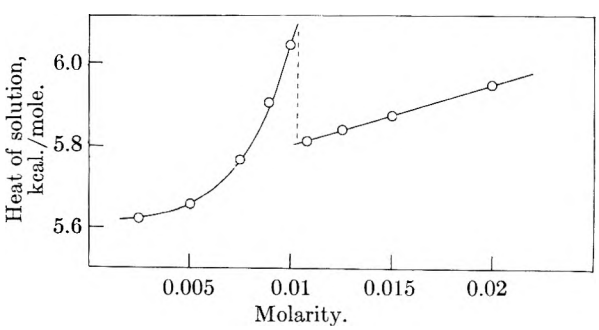

Fig. 1.—Plot of the heat of solution (integral) in kcal. per mole of sodium decyl sulfate in 0.1 M sodium chloride solution as a function of the concentration of sodium decyl sulfate.

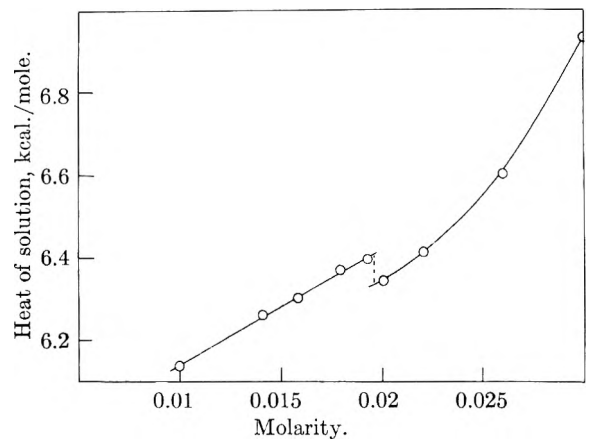

Fig. 2.—Plot of the heat of solution (integral) in kcal. per mole of potassium laurate in water as a function of the concentration of soap.

The effect of added sodium chloride on the heat of micelle formation in sodium decyl sulfate solutions appears to be quite small, despite the fact that it is known from light scattering measurements[2] that added salts have a considerable effect on the charge of the micelle. In the presence of added sodium chloride at concentrations as high as 0.1 M the micelle has a charge of only some 5 or 6 electronic charges per 50 or so units, and even so, according to our results, the process of micelle formation occurs with relatively small entropy and heat changes. This would seem to add further evidence to support the view that in the concentration ranges discussed here the principal type of micelle has a loose structure such as was suggested by Hartley,[3] even when carrying only a small charge.

The value for the heat of micelle formation in potassium laurate solutions is appreciably less than that for sodium decyl sulfate. This result is to some extent misleading, however, in that the micelle of potassium laurate contains some lauric acid formed by hydrolysis, and, as will be discussed in a forthcoming paper, the heats of solubilization of a variety of solubilizates are slightly positive. The true heat of micelle formation in this case, then, may be expected to be somewhat closer to that of sodium decyl sulfate when allowance is made for this fact.

The hydrolysis which occurs in the case of potassium laurate does not interfere with the ease of making the necessary experiments, but we have failed, after many experiments, to obtain corresponding heats of micelle formation for laurylamine hydrochloride. Hydrolysis, in this case, seems to lead to very erratic and irreproducible results.

This work was supported by the Office of Naval Research.

(1) E. Hutchinson, K. Manchester and L. Winslow, This Journal, **58**, 1125 (1954).

(2) E. Hutchinson and J. C. Melrose, *Z. physik. Chem.* (Neue Folge), **2**, 363 (1954).

(3) G. S. Hartley, "Aqueous Solutions of Paraffin-Chain Salts," Hermann et Cie, Paris, 1936.

INTERACTIONS IN POLYMER SOLUTIONS OBSERVED BY EQUILIBRATIONS ACROSS MEMBRANES[1]

By Doyle C. Udy and John D. Ferry

Department of Chemistry, University of Wisconsin, Madison, Wisconsin

Received July 29, 1955

In view of the continuing interest in interactions between macromolecules and small molecules in multicomponent systems,[2-5] especially as evidenced by equilibration across membranes, it may be appropriate to record briefly some equilibration studies made several years ago but not previously published because of their fragmentary and primarily negative nature.

The polymers used were polyvinyl acetate (M_n = 140,000) and styrene–maleic anhydride copolymer (M_n = 190,000) dissolved in dioxane, and approximately half-neutralized styrene–maleic acid copolymer (*i.e.*, the hydrolyzed anhydride) dissolved in water at *p*H 8.8, all at concentrations of about 5%. Added reagents tested for interaction were dimethyl phthalate and cyclohexanone, for polyvinyl acetate; 2-amino-5-azotoluene and phenylurea, for the anhydride copolymer; and urea, aniline and phenylglycine, for the acid copolymer. Concentrations of the added reagents ranged from 0.01 to 1%.

Equilibrations were made with the polymer solution in a cellophane tube (in the case of dioxane as solvent, previously treated with concentrated sodium hydroxide to increase porosity) immersed in an equal volume of solvent, slowly agitated at 25° for 1 to 5 days. The added reagent was introduced sometimes inside and sometimes outside the membrane. After equilibration, the internal and external solutions were weighed and analyzed for the added reagent, in some cases by spectrophotometry, in others by Kjeldahl nitrogen determination.

The effect of the polymer on the distribution of added reagent was expressed by the ratio $(\ln w_3/w_3')/w_2$, where w_2 is the concentration of polymer and w_3 and w_3' those of the reagent inside and outside the membrane, all expressed as g. per 1000 g. of solvent. This ratio was of the order of $\pm 1 \times 10^{-3}$ in all the above systems, much smaller than those derived from various equilibrations with proteins, nucleic acid and polyvinyl pyrrolidone—even though some of the reagents presumably provided opportunity for hydrogen bonding and fairly strong polarization forces.

After the above experiments were completed, however, another system was found which did exhibit strong interaction: methyl green added to solutions of one-third neutralized styrene–maleic acid copolymer in 0.1 *M* sodium chloride at *p*H 4.76. The ratio $(\ln w_3/w_3')/w_2$ varied from a limiting value of 0.39 at low w_2 (0.5 to 1.0) to 0.18 at w_2 = 6.0. If the interaction was interpreted as binding, the equilibrium constant for the first molecule bound was calculated to be about 4×10^5 (mole/l.)$^{-1}$, comparable in magnitude with those for binding of various dyes to serum albumin.[5] The equilibrations were not extended to dye concentrations high enough to estimate the number of binding sites; the maximum amount of dye bound was about 0.012 mole per monomer unit.

Methyl green is of course a considerably larger molecule than any of the other reagents, and from comparative studies on proteins[2,5] higher binding would be expected on this account. Moreover its two positive charges no doubt contribute some electrostatic interaction even in the presence of 0.1 *M* salt. But the enormous contrast between its behavior and that of the others suggests that quite specific configurations are needed for strong interactions, as others have concluded from studies on natural macromolecules.[2-5]

(1) Supported in part by the Research Committee of the Graduate School of the University of Wisconsin from funds supplied by the Wisconsin Alumni Research Foundation, and in part by a grant from Research Corporation.

(2) I. M. Klotz, in "The Proteins," Vol. I, H. Neurath and K. Bailey, Academic Press, Inc., New York, N. Y., 1953, Chapter 8.

(3) G. Oster, *J. Polymer Sci.*, **16**, 235 (1935).

(4) H. G. Heilweil and Q. Van Winkle, This Journal, **59**, 939 (1955).

(5) E. Fredericq, *Bull. soc. chim. Belg.*, **63**, 158 (1954).

CONFIGURATIONAL ENTROPY AND CHOICE OF STANDARD STATES, ENTROPIES OF FORMATION OF COMPLEX IONS, AND THE CHELATE EFFECT

By Henry A. Bent[1]

Department of Chemistry, University of Connecticut, Storrs, Connecticut

Received July 12, 1955

Entropies of reaction, measures of molecular motion,[2-4] often contain a sizable, usually physically irrelevant, configurational term. In Table I, for example, are listed standard $\Delta\bar{S}°$ values,[5] calculated originally from the equation

$$\Delta\bar{S}° = (\Delta\bar{H}° - \Delta\bar{F}°)/T = \Delta\bar{H}°/T + R \ln K_m \quad (1)$$

K_m the equilibrium constant, concentrations in molalities, $\Delta H°$ from direct calorimetry, or the temperature variation of K_m, for the formation of thirty-two complexes from cations and anions and twenty-eight complexes from cations and neutral molecules, all in water. "In all but four of the thirty-one examples in the first group $\Delta S°$ favors complex formation. In all but six of the twenty-eight reactions in the second group the entropy change does not favor the formation of the complex. Five of the unusual examples in the latter group are taken from one reference and it would appear to be advisable to check these data."[5]

If, however, solute concentrations were expressed in, say, moles per 1000 kg. of solvent, instead of moles per 1000 g.—which is physically quite arbitrary—$R \ln K$ would be smaller by multiples of $R \ln 10^3$, with nine more "exceptions" in the first group, but two less in the second.

Gurney appears to have been the first to clearly recognize this problem of "standard states." He suggests the term unitary entropy for the difference

(1) Department of Chemistry, University of Minnesota, Minneapolis 14, Minneapolis.

(2) H. S. Frank and M. W. Evans, *J. Chem. Phys.*, **13**, 507 (1945).

(3) A. A. Frost and R. G. Pearson, "Kinetics and Mechanism," John Wiley and Sons, Inc., New York, N. Y., 1952, Chapter 7.

(4) R. W. Gurney, "Ionic Processes in Solution," McGraw-Hill Book Co., New York, N. Y., 1953.

(5) R. J. P. Williams, This Journal, **58**, 121 (1954).

TABLE I

MOLAR ENTROPIES OF FORMATION OF COMPLEX IONS IN WATER[a]

Reaction		$\Delta\bar{S}°$	$\Delta\bar{S}°'$	Reaction		$\Delta\bar{S}°$	$\Delta\bar{S}°'$
Ag^{I}	Cl^-	+ 6.0	+14.0	Mg^{II}	$2NH_3$	− 3.0	+13.0
Ag^{I}	$2S_2O_3^{--}$	−26.0	−10.0	Zn^{II}	$4NH_3$	− 6.7	+25.3
Ag^{I}	$2CN^-$	+25.1	+41.0	Cu^{II}	$4NH_3$	−10.0	+22.0
Au^{I}	$2CN^-$	+17.0	+33.0	Ni^{II}	$6NH_3$	−25.7	+22.3
Mg^{II}	SO_4^{--}	+31.0	+39.0	Co^{II}	$6NH_3$	−17.0	+31.0
Mg^{II}	$CH_2(CO_2)_2^{--}$	+24.0	+32.0	Cd^{II}	$4NH_3$	−13.0	+19.0
Ba^{II}	$S_2O_3^{--}$	+19.0	+27.0	Hg^{II}	$4NH_3$	− 7.7	+24.3
Zn^{II}	$CH_2(CO_3)_3^{--}$	+27.0	+35.0	Cu^{I}	$2NH_3$	− 2.7	+13.3
Zn^{II}	$4CN^-$	− 7.3	+24.7	Ag^{I}	$2NH_3$	−11.0	+ 5.0
Cd^{II}	$2CN^-$	+30.0	+46.0	Co^{III}	$5NH_3$	−23.3	+16.7
Hg^{II}	$2Cl^-$	+16.0	+32.0	Cu^{II}	En	−15.0	− 7.0
Hg^{II}	$3Cl^-$	+13.7	+37.7	Cu^{II}	2En	+ 3.3	+19.3
Hg^{II}	$2Br^-$	+10.0	+26.0	Ni^{II}	En	−12.0	− 4.0
Hg^{II}	$4Br^-$	+10.3	+42.3	Co^{II}	En	− 7.0	+ 1.0
Hg^{II}	$4I^-$	−13.7	+18.3	Zn^{II}	En	− 7.0	+ 1.0
Hg^{II}	$4CN^-$	−15.3	+16.7	Cu^{II}	Trien	+22.0	+30.0
La^{III}	SO_4^{--}	+26.0	+34.0	Ni^{II}	Trien	+23.0	+31.0
Cr^{III}	OH^-	+43.3	+51.3	Co^{II}	Trien	+22.0	+30.0
Cr^{III}	Cl^-	+23.3	+31.3	Fe^{II}	Trien	+ 8.0	+16.0
Cr^{III}	$2Cl^-$	+40.2	+56.2	Mn^{II}	Trien	+12.0	+20.0
U^{IV}	OH^-	+50.5	+58.5	Fe^{II}	Dipy	0.0	+ 8.0
Fe^{III}	O_2H^-	+49.0	+57.0	Fe^{II}	3Dipy	0.0	+24.0
Fe^{III}	OH^-	+50.0	+58.0	Ag^{I}	Pyridine	− 6.3	+ 1.7
Fe^{III}	F^-	+49.0	+57.0	Ag^{I}	α-Picoline	− 3.7	+ 4.3
Fe^{III}	Cl^-	+35.0	+43.0	Ag^{I}	γ-Picoline	− 3.7	+ 4.3
Fe^{III}	Br^-	+23.0	+31.0	Ag^{I}	$C_4H_9NH_2$	− 5.3	+ 2.7
Fe^{III}	N_3^-	+ 5.0	+13.0	Ag^{I}	$C_2H_5NH_2$	− 5.3	+ 2.7
Fe^{III}	$C_2O_4^{--}$	+43.0	+51.0	Ag^{I}	Tolylamine	− 5.8	+ 2.2
Sn^{II}	OH^-	+23.0	+31.0				
Sn^{II}	Cl^-	+14.0	+22.0				
Sn^{II}	Br^-	+ 8.0	+16.0				
Cd^{II}	Cl^-	+ 8.0	+16.0				

[a] $\Delta\bar{F}°' = \Delta\bar{H}°' - T\Delta\bar{S}°'$, where $\Delta\bar{H}°' = \Delta\bar{H}°$ and $\Delta\bar{S}°' = \Delta\bar{S}° - \Delta n \cdot 8$. Hence, in water, $\Delta\bar{F}°' = \Delta\bar{F}° + T(\Delta n.8) = \Delta\bar{F}° + 2380\Delta n$ cal. (at 25°). $K_m = \exp(-\Delta\bar{F}°/RT)$; $K_N = \exp(-\Delta\bar{F}°'/RT)$.

between the partial molal entropy $\bar{S}_i$ and the absolute value of the partial molal configurational entropy ($-R \ln N_i$ in dilute solutions, according to the simple lattice model).[6] More precisely, $\bar{S}_i°' = \lim_{N_i \to 0}(\bar{S}_i + R \ln N_i)$; whereas the usual standard partial molal entropy, $\bar{S}_i = \lim_{m_i \to 0}(\bar{S}_i + R \ln m_i)$. Hence, in water, $\bar{S}_i°' = \bar{S}_i° - R \ln 55.5 = \bar{S}_i° - 8$ e.u., and

$$\Delta\bar{S}°' = \Delta\bar{S}° - \Delta n \cdot 8 \qquad (1')^{7}$$

where Δn = change in number of moles of solute (for the reactions in Table I, $-\Delta n$ = number of ligands).

Unitary values, calculated according to equation 1′, are listed in the third column of Table I. For simple structures, these values represent changes in the intrinsic, thermal part of the entropy. All of the values are positive, with three exceptions: the silver(I) bisthiosulfate complex in the first group, and the simple ethylenediamine complexes of Cu(II) and Ni(II) in the second. Recent data suggest that the latter values are probably positive also (Table II).

(6) Reference 3, p. 88ff. Following Adamson (see ref. 12), we shall designate the unitary entropy by the symbol $\bar{S}_i^{\dagger}$.

(7) Alternatively, at equilibrium $\Delta\bar{S} = \Delta\bar{H}/T$, with $\Delta\bar{S} = \Delta\bar{S}°'$ + $\Delta\bar{S}^{cf}$ (cf for configurational), where $\Delta\bar{S}^{cf} = \Sigma\nu_i\bar{S}_i^{cf} = \Sigma\nu_i(-R \ln N_i^{eq.}) = -R \ln k_N$. Hence in water, where $K_N = K_m(55.5)^{-\Delta n}$, $\Delta\bar{S}°' = \Delta\bar{H}/T + R \ln K_m - \Delta n(R \ln 55.5)$.

Table II also lists data of Spike and Parry, from which changes in unitary entropy in the exchange

$$M(NH_3)_2 + en = M(en) + 2NH_3 \qquad (2)$$

for M = Cd(II), Zn(II) and Cu(II) are found to

TABLE II

MOLAR HEATS AND ENTROPIES OF FORMATION OF SOME METAL AMINE COMPLEX IONS

Reaction	$\Delta\bar{F}°$, kcal.	$\Delta\bar{H}°$, kcal.	$\Delta\bar{S}°$, cal./°C.	$\Delta\bar{S}°'$, cal./°C.	Ref.
Cu^{II} En	−14.2	− 8.6	+21	+28	8
	−14.3	−11.6	+ 9	+17	9
	−15.0	−14.6	+ 1.3	+ 9.3	10
	−14.2	−18.9	−15.0	− 7.0	5
Ni^{II} En	− 9.9	− 4.8	+19	+27	8
	−10.1	− 8.8	+ 4	+12	9
	− 9.9	−12.6	−12.0	− 4.0	5
Cd^{II} En	− 7.96	− 7.0	+ 3.1	+11.1	11
Cd^{II} $2NH_3$	− 6.75	− 7.1	− 1.2	+14.8	11
Zn^{II} En	− 8.39	− 6.6	+ 6.0	+14.0	10
Zn^{II} $2NH_3$	− 6.84	− 6.7	+ 0.3	+16.3	10
Cu^{II} En	−15.0	−14.6	+ 1.3	+ 9.3	10
Cu^{II} $2NH_3$	−10.7	−12.0	− 4.4	+11.6	10

(8) F. Basolo and R. K. Murmann, *J. Am. Chem. Soc.*, **74**, 2373 (1952).

(9) G. H. McIntyre, Jr., Thesis, Penn. State Coll., 1953.

(10) C. G. Spike and R. W. Parry, *J. Am. Chem. Soc.*, **75**, 3770 (1953).

(11) C. G. Spike and R. W. Parry, *ibid.*, **76**, 2726 (1953).

be, respectively, −3.7, −2.3 and −2.3 e.u., similar to values given recently by Adamson[12a] (under the heading $\Delta S^{0\prime}$).[12b]

Negative values such as these might arise from a loss on chelation in chain-configurational entropy[13] of the flexible ethylenediamine molecule; for the subtraction ($S_i - R \ln N_i$) sorts out only first-segment configurational contributions, leaving in the difference ($\bar{S}_i$(unitary)) entropy arising from orientation of successive segments. For ethylenediamine (number of segments $x = 4$) in the water lattice (coördination number $z = 4$), this chain-orientation entropy should probably amount to roughly $R \ln (z)(z-1)^{x-2}$, or 7.1 e.u. *at infinite dilution*. In more concentrated solutions, allowance should be made for (1) a decrease in chain entropy, from sites blocked by neighboring chains, and (2) an increase in first-segment entropy, from the contribution of polymer segments to the total number of lattice sites. Using Flory's[13] expression for the configurational entropy of a lattice, coordination number z, occupied by n_1 simple monomeric molecules (the solvent), and n_2 flexible polymer molecules, each with x segments (altogether $n_0 \equiv n_1 + xn_2$ lattice sites)

$$S^{cf} = k \ln \left(\frac{1}{n_2!}\right) \underbrace{\prod_{i=0}^{n_2-1} (n_0 - xi)}_{\text{I}} \underbrace{(z-1)}_{\text{IIa}} \underbrace{\left(\frac{n_0 - xi}{n_0}\right)^{x-1}}_{\text{IIb}}$$

one finds, on differentiating factor by factor, that

$$\bar{S}_2^{cf} = \underbrace{-R \ln \frac{n_2}{n_0}}_{\text{I}} + \underbrace{R(x-1)\ln(z-1)}_{\text{IIa}} \underbrace{- Rv_2(x-1)}_{\text{IIb}}$$

In the limit $\lim_{n_2 \to 0}(\bar{S}_2 - \bar{S}_2^{cf})$, term I approaches $-R \ln N_2$ and IIb vanishes.[14] In slightly more concentrated solutions, however, the first-segment entropy, term I, is greater than the ideal value $-R \ln N_2$ by an amount $RN_2(x-1)$, about 0.1 e.u. for a 1 molal aqueous solution of ethylenediamine, with term IIb four times greater. These corrections[15] are not overwhelming, and judging from the figure 7.1 e.u., compared to 2.3 − 3.7 e.u., it would appear that chelation does not tie down the ethylenediamine molecule entirely; which is to suggest that the entropy of M(en) is greater than that of $M(NH_3)_2$ by more than their masses alone would indicate.

Configurational effects may also explain, in part, the negative "unitary" entropy of formation of the silver(I) bisthiosulfate complex (−10 e.u.). On association, the thiosulfate ion, like ethylenediamine, stands to lose configurational entropy, perhaps (monosubstituted tetrahedral ion[17]) the full amount, $R \ln 4$; *i.e.*, about 3 e.u.; this, incidentally, is nearly the difference in the entropies of $S_2O_3^{--}$ and SO_4^{--} (8 and 4.1 e.u., respectively[18]), when one allows for their difference in mass.[19] The complexed thiosulfate ion also probably loses librational entropy not possessed by simple atomic ions, like the halogens—perhaps 5 e.u., totaling altogether 3 + 5 = 8 e.u.,[20] or 16 e.u. per two ions coördinated.

One more comparison like (2) on a more highly coördinated ion may be mentioned. ΔS^0 for the reaction

$$Ni(NH_3)_6^{++} + 3en = Ni(en)_3^{++} + 6NH_3 \qquad (2')$$

is given[21] as +24 e.u., with $\Delta S^0 - \Delta n \cdot 8 = 0$.

These examples are not to deny the chelate effect, or that it is primarily an entropy effect. Ethylenediamine coördinates copper or nickel or cadmium or zinc ions more tightly than does ammonia. In large part this is a concentration effect that shows up primarily in the configurational entropy, and ΔS^0, rather than in the unitary entropy (or the enthalpy).

The author wishes to acknowledge many discussions on the subject of complex ions with Dr. R. Kent Murmann.

(12) (a) A. W. Adamson, *J. Am. Chem. Soc.*, **76**, 1578 (1954); (b) Adamson discusses the −8 e.u. addition to $\bar{S}_i$ (applicable at all temperatures) in terms of hypothetical one molal and mole fraction unity states, and states of "minimum translational entropy." The former refer to the mathematical limits already cited, the latter to the entropy arising from the geometrical configurations accessible to localized systems of distinguishable particles.

(13) P. J. Flory, *J. Chem. Phys.*, **10**, 51 (1942); *Ann. Rev. Phys. Chem.*, **2**, 383 (1951).

(14) Because the concentration of occupied sites near polymer molecule $i + 1$ has been taken equal to the average concentration, $(n_0 - xi)/n_0$.

(15) Even for simple monomeric structures a correction of similar magnitude should be made in the computation of ΔS(unitary) from K_m when the latter is not extrapolated to infinite dilution; for in such cases the recorded entropy change is essentially defined by the equation $\Delta\bar{S}^0 = \Delta\bar{H}/T + R \ln K_m$, whereas for simple structures $\Delta S^{0\prime} = \Delta\bar{H}/T + R \ln K_N$, $N_i = m_i/(55.5 \times \Sigma m_i)$ (counting all lattice configurations as equally probable). Hence (to this approximation), $\Delta\bar{S}^{un} - \Delta\bar{S}^0 = R \ln (K_N/K_m) = -\Delta n \times R \ln (55.5 + \Sigma m_i)$, which in dilute solutions differs from the quantity $-\Delta n \cdot 8$ e.u. by the amount $\Delta n(R\Sigma m_i/55.5)$, or about 0.14 e.u. in one of the cases studied by Spike and Parry.[16]

(16) See ref. 11 (solution D).

(17) D. M. Yost and H. Russell, "Systematic Inorganic Chemistry," Prentice–Hall, Inc., New York, N. Y., 1946, p. 388.

(18) W. M. Latimer, "Oxidation Potentials," Prentice–Hall, Inc., New York, N. Y., 1952, p. 72.

(19) $(3/2)R \ln (\text{M.W. } S_2O_3)/(\text{M.W. } SO_4) = 0.5$ e.u. The justification for the use of a three-halves-R-log-mol. wt. term here for motion that is more vibrational than translational in character is this. For one degree of freedom, $S^{vib} = Rx/(e^x - 1) - R \ln (1 - e^{-x})$, $x = h\nu/kT$, and where classically $\nu = (1/2\pi)(K/m)^{1/2}$. Hence when $h\nu << kT$, $S^3_{vib} = (3/2)R \ln (m) + 3R + 3R \ln T - R \ln (K_1K_2K_3)^{1/2} + 3R \ln (2\pi k/h)$. Thus the term $(3/2)R \ln (m)$ that appears in the Sackur–Tetrode equation for the translation entropy of a gas also describes the mass-dependence of classically excited vibratory motion in solids and liquids (*cf.* Latimer, ref. 18, p. 359).

(20) Gurney, ref. 4, p. 182.

(21) A. E. Martell and M. Calvin, "Chemistry of the Metal Chelate Compounds," Prentice–Hall, Inc., New York, N. Y., 1952, p. 150.

THE ELECTRIC MOMENTS OF SOME DERIVATIVES OF PYRIDINE AND QUINOLINE

BY MAX T. ROGERS

Contribution from the Kedzie Chemical Laboratory, Michigan State University, East Lansing, Michigan

Received August 12, 1955

The observed electric moments of various pyridine and quinoline derivatives have been compared with the values calculated by vector addition of the group moments (found from an analysis of data for benzene derivatives) and the moments of the heter-

TABLE I

EMPIRICAL CONSTANTS, MOLAR REFRACTIONS, MOLAR POLARIZATIONS AND DIPOLE MOMENTS AT 25°

Compound	ϵ_1	a	v_1	b	P_1	MR_D	μ Obsd.	μ Calcd.
2-Aminopyridine	2.2730	6.180	1.14460	−0.315	115.5	28.34	2.06	2.11
4-Aminopyridine	2.2725	22.40	1.14478	− .450	350.8	28.34	3.97	3.78
2-Nitropyridine	2.2726	36.20	1.14484	− .867	554.1	29.61	5.06	5.32
4-Nitropyridine	2.2731	3.917	1.14478	− .750	82.41	29.61	1.61	1.62
1-Methyl-2-quinolone	2.2731	19.88	1.14468	− .706	329.9	45.97	3.72	3.71
2-Hydroxyquinoline (benzene)	2.2743	4.550	1.14490	− .665	100.9	44.27	1.66	2.62
2-Hydroxyquinoline (dioxane)	2.2100	17.67	0.97283	− .333	288.5	44.27	3.45	2.62

ocycles themselves.[1-3] The agreement is usually rather good but there is some evidence that the resonance structures in which electrons are transferred to the nitrogen atom from the group are of considerable importance.[2] To investigate further the effect of good electron donor and acceptor groups the electric moments of 2- and 4-aminopyridine, 2- and 4-nitropyridine and 2-hydroxyquinoline have been measured. Since 2-hydroxyquinoline appeared to be in the keto form in dioxane solution the moment of 1-methyl-2-quinoline was also determined. The only compounds for which values (in D) have been reported previously are 2-aminopyridine[1] (2.17) and 4-aminopyridine (3.79 in benzene[1] and 4.36 in dioxane solution[2]). Our values agree with these within the limits of experimental error.

The electric moment of 1-methyl-2-quinolone in benzene solution is in good agreement with the value computed from bond moments (C–N, 0.4; C=O, 3.1 as in tetraphenylcyclopentadienone). However, the observed moment of 2-hydroxyquinoline in dioxane (3.45) is higher than the value calculated for 2-hydroxyquinoline assuming free rotation about the C–O bond (2.66); it is also somewhat higher than that calculated for 2-quinolone (3.12). The data indicate that this substance exists largely in the keto form in dioxane. The value of the moment of 2-hydroxyquinoline in benzene solution is much lower (1.66) than expected. This substance is presumably in the enol form and the low value may result from a field effect which tends to favor the positions of the (positively charged) hydroxyl hydrogen atom nearest the (negatively charged) nitrogen atom. The moment calculated for 2-hydroxyquinoline when the hydroxyl hydrogen is in the position closest to the nitrogen atom is 1.69. Curran[2] reported the value 6.0 for the electric moment of 4-pyridone in dioxane which is somewhat larger than the moment (4.90) found by use of the bond moments employed in the above calculation.

The agreement is good between the observed and calculated values for 2- and 4-nitropyridine and for 2- and 4-aminopyridine. These results do not suggest any large enhancement of resonance when either electron donor or electron acceptor groups are substituted in the pyridine or quinoline ring. A similar conclusion was reached from a study of the electric moments of methyl and chloro derivatives.[3]

Experimental

Materials. Benzene and Dioxane.—These were purified as described previously.[4]

2-Aminopyridine, 2-Hydroxyquinoline and 1-Methyl-2-quinolone.—These were Eastman Kodak Co. materials which were purified by several recrystallizations from appropriate solvents; 2-aminopyridine, m.p. 57°; 2-hydroxyquinoline, m.p. 194°; 1-methyl-2-quinolone, m.p. 72°.

4-Aminopyridine.—Material supplied by Bios Laboratories was recrystallized from alcohol, m.p. 157.2°.

2-Nitropyridine and 4-Nitropyridine.—These were prepared by the method of Kirpal and Bohm[5]; m.p. 68° (2-nitropyridine) and 48° (4-nitropyridine).

Apparatus and Method.—The dielectric constants and densities of six solutions, ranging in mole fraction from 0.002 to 0.020, were measured at 25°. The apparatus, technique and method of calculation have been described.[4] The constants ϵ, a, v_1 and b of the Halverstadt–Kumler[6] equation are shown in Table I for each compound. The molar polarization at infinite dilution P_2, the molar refraction (calculated from empirical constants) and the dipole moment of each substance is also shown. The probable error in the dipole moments is about ±0.10 D. Calculated values of the electric moments were obtained by vector addition of the observed heterocycle moment to group moments employed previously for benzene derivatives.[7]

(1) C. A. Goethals, *Rec. trav. chim.*, **54**, 299 (1935).
(2) B. C. Curran, *J. Am. Chem. Soc.*, **67**, 1835 (1945).
(3) M. T. Rogers and T. W. Campbell, *ibid.*, **75**, 1209 (1953).
(4) M. T. Rogers, *ibid.*, **77**, 3681 (1955).
(5) A. Kirpal and W. Bohm, *Ber.*, **65**, 680 (1932).
(6) I. F. Halverstadt and W. D. Kumler, *J. Am. Chem. Soc.*, **64**, 2988 (1942).
(7) M. T. Rogers, unpublished results.

DENSITY OF DIBUTYL PHTHALATE

BY A. I. KEMPPINEN AND N. A. GOKCEN

Department of Metallurgical Engineering, Michigan College of Mining & Technology, Houghton, Michigan

Received August 29, 1955

Dibutyl phthalate, also known as *n*-butyl phthalate or dibutyl 1,2-benzenedicarboxylate,[1] has a vapor pressure of 3×10^{-5} mm. at room temperature,[2] and a relatively high boiling point of 340°.[2,3] These properties make it a suitable fluid for diffusion pumps, accurate flowmeters and vacuum manometers. Such uses occasionally require data on the variation of its density with temperature,[4] heretofore not available in the literature. The purpose of this paper was, therefore, to determine the density of dibutyl phthalate from 2.4 to 64.7°.

Experimental Procedure

The procedure consisted of accurate determinations of the weight and volume of the liquid at constant temperature. For this purpose a special Pyrex density bulb was made as follows: A Pyrex tube 15 cm. long and a uniform inside diameter of approximately 0.38 cm. was calibrated for volume per unit length by weighing it when empty and full

(1) Name approved by the International Union of Chemistry.
(2) S. Dushman, "Scientific Foundations of Vacuum Technique," John Wiley and Sons, Inc., New York, N. Y., 1949, p. 222.
(3) C. D. Hodgman, "Handbook of Chemistry and Physics," Chemical Rubber Publishing Co., Sandusky, Ohio, 1952–1953, pp. 1070–71.
(4) N. A. Gokcen, "Improved Vacuum-Fusion Method for Determination of Oxygen and Nitrogen in Metals," *J. Metals* in press.

of mercury. A millimeter scale was attached to this tube after joining it to a Pyrex bulb. The volume of this bulb up to zero point on the millimeter scale was determined within 59.127 ± 0.002 ml. by weighing the contained mercury or water.

Dibutyl phthalate obtained from the Central Scientific Company was boiled under vacuum and then poured into the density bulb with a special funnel in order not to wet the stem above the liquid level. Vacuum was applied in order to remove any trapped bubbles. The liquid was weighed and correction for the displacement of air from the bulb was made. The bulb was enclosed in a glass tube with a stopper through which a standardized thermometer was inserted and the entire assembly was then placed in a water thermostat controlled within ±0.1° or better. After half hour the volume of liquid was determined by reading the level in the stem within ±0.2 mm. and correcting for the expansion of the bulb. The density was then calculated in the usual manner, by dividing the weight in grams by the volume in milliliters.

Results

The results are shown in Table I.

TABLE I

Temp., °C.	Density, g./ml.	Temp., °C.	Density, g./ml.
2.4	1.0595	28.9	1.0392
2.7	1.0591	31.1	1.0379
4.8	1.0588	47.8	1.0243
6.3	1.0576	54.0	1.0177
7.7	1.0552	63.0	1.0110
27.9	1.0394	64.7	1.0089

A large scale plot of density *versus* temperature yielded a straight line with a maximum scatter of ±0.0008, and an average scatter of less than ±0.0005. Results are summarized as follow: density, g./ml. (±0.0005) = $1.0619 - 0.000801t$, where t = °C. The coefficient of linear expansion = 0.000265 mm./mm. °C. The coefficient of cubic expansion = 0.000796 ml./ml. °C. The density at 20° which is 1.0459 agrees well with the only reliable published value[3] of 1.0465.

THE USE OF C-14 LABELED PERFLUOROOCTANOIC ACID IN THE STUDY OF ADHESION AND OTHER SURFACE PHENOMENA

BY J. W. SHEPARD AND JOHN P. RYAN

Contribution No. 102 from the Central Research Department, Minnesota Mining & Manufacturing Company, St. Paul, Minn.

Received September 12, 1955

A number of workers in recent years have demonstrated the value of radioactive tracer techniques in studying surface phenomena.[1-5] One technique uses a system consisting of a long-chain fatty acid deposited on a substrate. The acid is labeled with C-14 and thus various chemical reactions at the surface, surface diffusion, transfer phenomenon, etc., can be conveniently measured. The monolayer is usually deposited on the substrate by one of three techniques: (1) the Langmuir–Blodgett procedure; (2) adsorption from solution, or (3) the retraction method.[6]

The second method was chosen for our work because of the analogy to an adhesive system which consists of a mixture of compounds free to migrate to an interface. Initially we worked with a benzene solution of C-14 labeled stearic acid. The panels (glass and aluminum) used in the study "carried out" some of the solution when removed from the adsorption cell. This necessitated a rinse step which was undesirable since it also removed some of the adsorbed acid. Smith and Allen[7] in their work with the C-14 labeled *n*-nonadecanoic acid—cyclohexane system, eliminated the rinse step by using an adsorption solution of low concentration and correcting for the "carry-out." In view of the difficulties encountered with a hydrocarbon acid, we decided to change to a system which would eliminate the "carry-out" problem. Zisman and coworkers have described techniques for forming monolayers of long-chain polar compounds from hydrocarbon solutions which are not wet by the solution once the monolayer has formed.[8] A surface composed of closely packed, oriented CF_3 groups was found to produce the most non-wetting surface of those studied. Solution "carry-out" on such surfaces is negligible. The system we selected was an *n*-decane solution of perfluoroöctanoic acid labeled with C-14 in the carboxyl group.[9]

Our initial work with this system has been designed primarily to develop a simple reproducible technique for adsorbing a monolayer of C-14 tagged perfluoro acid on surfaces such as glass and aluminum. In addition to giving us a system for further study of adhesive forces, this technique also allows us to measure the surface area—an important parameter in any surface study. Quantita-

TABLE I

ROUGHNESS FACTORS FOR ALUMINUM AND GLASS SURFACES

Sample	Side	Surface condition	Roughness factor[a]
Aluminum #16	A	Slight trisodium phos-	5.5
	B	phate etch	4.5
Aluminum #17	A	Slight trisodium phos-	11
	B	phate etch	5.9
Aluminum #36	A	"B" Side electropolished	2.6
	B		1.3
Aluminum #37	A	"B" Side electropolished	2.6
	B		1.5
Glass #34	A	Microscope slides	2.3
	B		1.6
Glass #35	A	Microscope slides	2.1
	B		1.7
Glass #38	A	Microscope slides	2.3
	B		2.0
Glass #39	A	Microscope slides	2.3
	B		2.1

[a] The samples were counted to a $^9/_{10}$ statistical error of 5%.

(1) J. E. Young, *Austr. J. Chem.*, **8**, 173 (1955).

(2) D. E. Beischer, THIS JOURNAL, **57**, 134 (1953).

(3) F. P. Bowden and A. C. Moore, *Trans. Faraday Soc.*, **47**, 900 (1951).

(4) E. Rideal and J. Tadayon, *Proc. Roy. Soc. (London)*, **A225**, 346 (1954).

(5) J. E. Willard, THIS JOURNAL, **57**, 129 (1953).

(6) W. A. Zisman, W. C. Bigelow and D. L. Pickett, *J. Colloid Sci.*, **1**, 513 (1946).

(7) H. A. Smith and K. A. Allen, THIS JOURNAL, **58**, 449 (1954).

(8) W. A. Zisman and F. Schulman, NRL Report 3950, "Spreading of Liquids on Low Energy Surfaces."

(9) We are indebted to the Fluorochemical Division of our Company, who kindly furnished us with the radioactive acid.

tive methods for measuring areas of plane surfaces are lacking. We have found that using a fluorinated acid eliminates "carry-out" and gives reasonable values for surface areas of plane surfaces.

Experimental

The concentration of the perfluoro acid solution was 0.005 *M* and the usual dip-time was one hour. We found that a complete monolayer was formed in less than a minute. A five-minute dip with agitation in *n*-decane did not remove any of the adsorbed acid. This observation indicates that solution "carry-out" is negligible and the monolayer is not readily desorbed by the solvent.

The usual manner of expressing surface areas of plane surfaces is in terms of a "roughness factor"—ratio of the true surface area to the geometrical area. To convert the radioactive count to roughness factor requires a knowledge of: (1) the area occupied by the perfluoroöctanoic acid molecule, (2) the specific activity of the radioactive acid, (3) the counting efficiency of the counter, and (4) the area of the sample counted. The value for the molecular area of the perfluoro acid, 24 Å.^{2}, was taken from Zisman's report.[8] The specific activity of the radioactive acid was 0.12 millicurie per gram. The counting efficiency of the Q-gas flow counter was calculated using a 50% geometry correction and a 23% backscattering factor.[10] The samples were masked for counting to insure constant area. The unmasked area was 2.45 cm.^{2}. Some typical roughness factors obtained with the perfluoroöctanoic acid are shown in Table I. Autoradiographs of the surfaces showed a uniform deposit of the adsorbed acid. The relative values for the various samples seem reasonable in view of the different surface conditions. A variation in the roughness factor between two sides of the same sample might be expected because of differences in their previous histories. The twofold difference between the sides of sample #17 was found to be quite reproducible. Smith and Allen[7] report roughness factors of less than unity for Ni, Al and Fe and a value of 1.2 for Cu using a tagged *n*-nonadecanoic acid film. They used a value of 20.5 Å.^{2} for the molecular area of the acid.

We intend to extend our study of various surface phenomena using the perfluoro acid–*n*-decane system and to publish the results and a more detailed description of the experimental work.

(10) H. Sobotka, "Monomolecular Layers," Am. Assn. Adv. Sci., Washington, D. C., 1954, p. 113.

COMMUNICATION TO THE EDITOR

VAPOR PRESSURE OF POTASSIUM

Sir:

Experimental data on the vapor pressure of potassium in the pressure range 0.162 to 6.529 atm. absolute have been obtained with an apparatus described previously.[1] The results, which are shown in Table I, were fitted by linear least squares correlation of log P *vs.* $1/T$, yielding the following equation:

$$\log P = (-4207/T) + 4.096$$

where P is in atm. abs. and T is in degrees Kelvin (°C. + 273.2). The normal boiling point, as calculated from this equation, is 753.8°.

The standard error of the pressure in this equation, as computed from the variance of the data, is 1.1% of the pressure. The largest possible systematic error is believed to have been in the relation of thermocouple e.m.f. with temperature. A platinum–10% rhodium thermocouple was employed, which was calibrated against a similar couple standardized by the National Bureau of Standards and certified correct to ± 0.25%.

(1) M. M. Makansi, C. H. Muendel and W. A. Selke, *J. Phys. Chem.*, **59**, 40 (1955).

TABLE I

VAPOR PRESSURE OF POTASSIUM

Temp., °K.	Obs. press., atm. abs.	Temp., °K.	Obs. press., atm. abs.	Temp., °K.	Obs. press., atm. abs.
859.9	0.162	1105.9	1.965	1226.7	4.651
919.6	.334	1119.4	2.128	1238.5	5.051
959.0	.516	1147.1	2.712	1240.0	5.051
1018.9	.934	1166.4	3.053	1245.5	5.250
1036.1	1.092	1175.2	3.293	1258.7	5.690
1036.7	1.061	1184.2	3.452	1263.0	5.850
1060.0	1.314	1198.9	3.852	1270.4	6.129
1088.6	1.713	1206.3	4.092	1280.8	6.529
1091.3	1.751	1212.5	4.251		

DEPARTMENT OF CHEMICAL ENGINEERING
COLUMBIA UNIVERSITY
NEW YORK 27, N. Y.

M. M. MAKANSI
M. MADSEN
W. A. SELKE
C. F. BONILLA

RECEIVED NOVEMBER 28, 1955

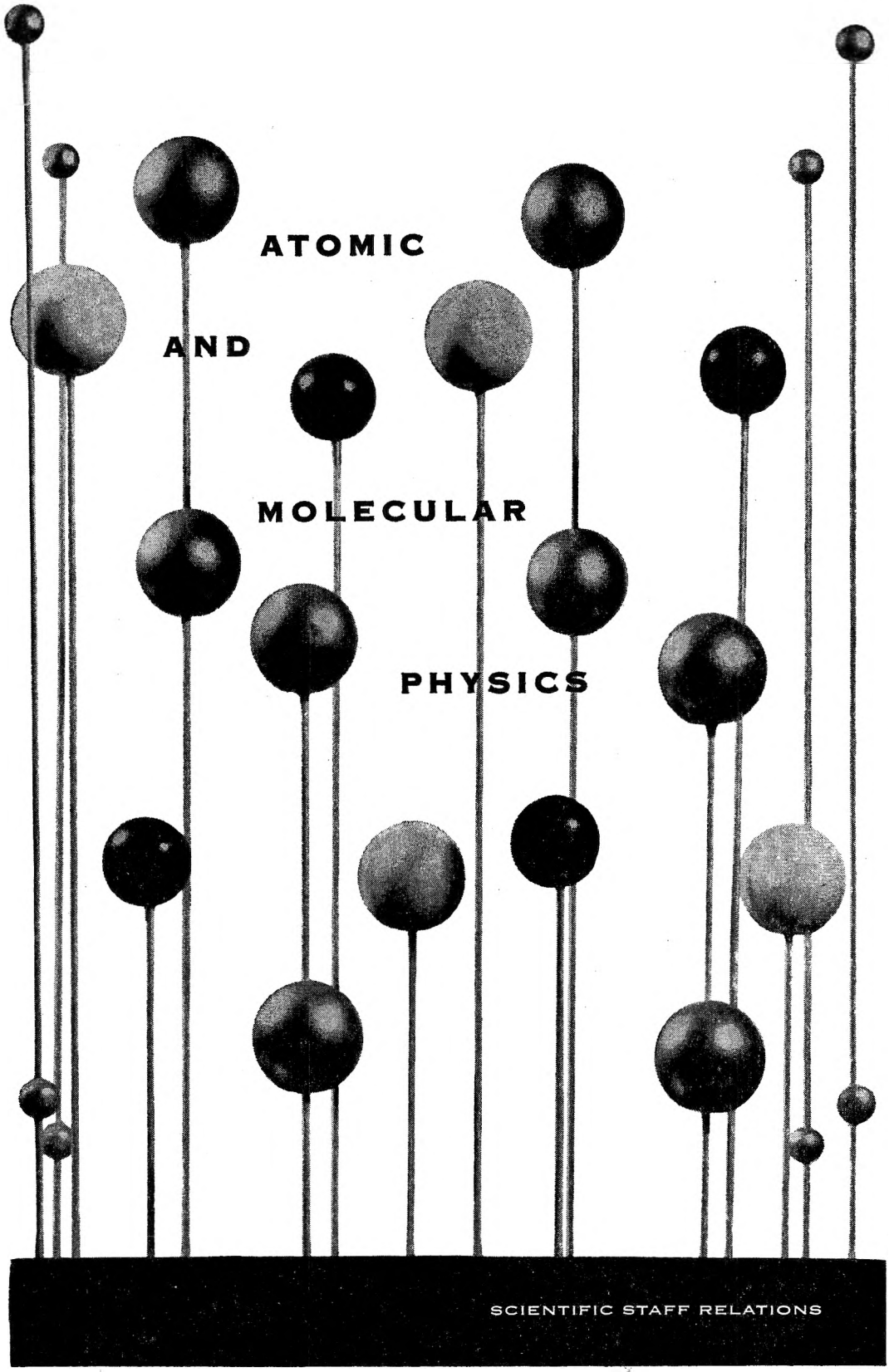

Molecular structure model, courtesy
California Institute of Technology

The Hughes Research Laboratory is pioneering in long-range fundamental research in the field of radio, microwave, and millimeter spectroscopy, atomic clocks, atomic and molecular amplifiers, and frequency standards. Techniques using gases, liquids, and solids are employed.

Those who would qualify for work in this field should have the Doctorate Degree, with course activity and experience in one or more of the following areas:

RADIO AND MICROWAVE SPECTROSCOPY
Gases, liquids and solids.

ATOMIC AND MOLECULAR BEAM SPECTROSCOPY

NUCLEAR RESONANCE

PARAMAGNETIC AND FERROMAGNETIC RESONANCE

ATOMIC SPECTRA WITH EMPHASIS ON HYPERFINE STRUCTURE
Knowledge of quantum mechanics and noise theory is desirable.

The Hughes program will be concerned with investigation of atomic frequency and time control devices of unprecedented accuracy, and with atomic amplifiers of unprecedented low noise.

HUGHES

RESEARCH
AND DEVELOPMENT
LABORATORIES

Culver City,
Los Angeles
County,
California